



HAL
open science

Novel di(N-heterocyclic carbene) ligands and related transition metal complexes

Marco Monticelli

► **To cite this version:**

Marco Monticelli. Novel di(N-heterocyclic carbene) ligands and related transition metal complexes. Other. Université de Strasbourg; Università degli studi (Padoue, Italie), 2017. English. NNT : 2017STRAE051 . tel-02918137

HAL Id: tel-02918137

<https://theses.hal.science/tel-02918137>

Submitted on 20 Aug 2020

HAL is a multi-disciplinary open access archive for the deposit and dissemination of scientific research documents, whether they are published or not. The documents may come from teaching and research institutions in France or abroad, or from public or private research centers.

L'archive ouverte pluridisciplinaire **HAL**, est destinée au dépôt et à la diffusion de documents scientifiques de niveau recherche, publiés ou non, émanant des établissements d'enseignement et de recherche français ou étrangers, des laboratoires publics ou privés.



UNIVERSITÉ DE STRASBOURG



École doctorale de Physique et Chimie physique ED 182

Institut de Physique et Chimie des Matériaux de
Strasbourg UMR 7504

THÈSE présentée par:
Marco MONTICELLI

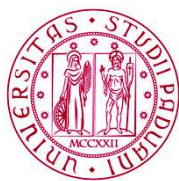
pour obtenir le grade de: **Docteur de l'université de Strasbourg**

Novel di(N-heterocyclic carbene) ligands and related transition metal complexes

Membres du jury:

Dr. BELLEMIN-LAPONNAZ Stéphane	directeur de thèse	Université	de Strasbourg
Pr. TUBARO Cristina (IT)	directeur de thèse	Université de Padova	
Pr. ZANOTTI Valerio Bologna (IT)	rapporteur	Université	de
Dr. CÉSAR Vincent Toulouse	rapporteur	CNRS-Université	de

Discipline : chimie



UNIVERSITÀ
DEGLI STUDI
DI PADOVA



Sede Amministrativa: Università degli Studi di Padova (IT)
 Université de Strasbourg (FR)

Dipartimento di Scienze Chimiche

Département de Matériaux Organiques, Institut de Physique et Chimie des Matériaux de
Strasbourg (IPCMS)

CORSO DI DOTTORATO DI RICERCA IN: SCIENZE MOLECOLARI

CURRICOLO: SCIENZE CHIMICHE

CICLO XXIX

ECOLE DOCTORALE DE PHYSIQUE ET CHIMIE-PHYSIQUE (ED 182)

NOVEL DI(N-HETEROCYCLIC CARBENE) LIGANDS AND RELATED TRANSITION METAL COMPLEXES

Tesi redatta con il contributo finanziario della Fondazione Cariparo

Coordinatore del corso:

Ch.mo Prof. Antonino Polimeno

Supervisore:

Prof. Cristina Tubaro

Directeur de l'Ecole doctorale

Prof. Jean-Pierre Bucher

Co-Directeur de Thèse:

Dr. Stéphane Bellemin-Laponnaz

PhD candidate : Marco Monticelli

ABSTRACT	1
SOMMARIO	7
RÉSUMÉ	13
CHAPTER 1: INTRODUCTION	19
1.1 HISTORY	19
1.2 FISCHER, SCHROCK AND NHC CARBENE COMPLEXES	20
1.3 DI(N-HETEROCYCLIC CARBENE) LIGANDS	26
1.4 FORMATION OF AZOLIUM SALTS	29
1.5 SYNTHESIS OF NHC-METAL COMPLEXES	30
1.6 APPLICATIONS OF NHC-METAL COMPLEXES	36
1.6.1 <i>Metallophilic interaction</i>	36
1.6.2 <i>Luminescence application</i>	39
1.6.3 <i>Anti-tumoral applications</i>	44
CHAPTER 2: RESULTS AND DISCUSSION	
METAL COMPLEXES WITH DI(N-HETEROCYCLIC CARBENE) LIGANDS	
BEARING A RIGID PHENYLENE BRIDGE	53
2.1 INTRODUCTION	53
2.2 SYNTHESSES AND CHARACTERIZATION OF THE AZOLIUM PROLIGANDS	57
2.3 SYNTHESSES AND CHARACTERIZATION OF SILVER(I) COMPLEXES	58
2.4 SYNTHESSES AND CHARACTERIZATION OF GOLD(I) COMPLEXES AND PHOTOPHYSICAL	
PROPERTIES	63
2.4 SYNTHESSES OF COPPER(I) COMPLEXES	72
2.5 SYNTHESSES OF IRIDIUM(III) AND RUTHENIUM(II) COMPLEX	74
CHAPTER 3: RESULTS AND DISCUSSION	
METAL COMPLEXES WITH AN IMIDAZOLE-BASED NHC LIGAND	
FUNCTIONALIZED WITH A TRIAZOLE IN THE 5 POSITION OF THE	
BACKBONE	79
3.1 INTRODUCTION	79
3.2 SYNTHESSES OF THE PROLIGANDS	84
3.3 SYNTHESSES OF TRANSITION METAL COMPLEXES	88
3.4 BIOLOGICAL TESTS	99
CHAPTER 4: RESULTS AND DISCUSSION	
METAL COMPLEXES WITH HETERODITOPIC LIGANDS BASED ON	
IMIDAZOL-2-YLIDENE AND 1,2,3-TRIAZOL-5-YLIDENE MOIETIES	
CONNECTED WITH A PROPYLENE BRIDGE	105

4.1	INTRODUCTION	105	
4.2	SYNTHESES OF THE PROLIGANDS.....	110	
4.3	SYNTHESES OF SILVER(I) COMPLEXES.....	111	
4.4	SYNTHESES OF GOLD(I) COMPLEXES	114	
4.5	SYNTHESES OF PALLADIUM(II) COMPLEXES.....	119	
CHAPTER 5: RESULTS AND DISCUSSION			
BIS(BENZOXAZOLIUM) PROLIGANDS AND ATTEMPTED SYNTHESIS OF RELATED TRANSITION METAL COMPLEXES			125
5.1	INTRODUCTION	125	
5.2	SYNTHESIS AND CHARACTERIZATION OF THE OXAZOLIUM PROLIGANDS	129	
5.3	ATTEMPTS TO SYNTHESIZE TRANSITION METAL COMPLEXES BEARING BIS(BENZOXAZOL-2-YLIDENE) LIGANDS	133	
CHAPTER 6: CONCLUSIONS			137
CHAPTER 7: EXPERIMENTAL SECTION.....			141
7.1	MATERIALS AND METHODS	141	
7.2	METAL COMPLEXES WITH DI(N-HETEROCYCLIC CARBENE) LIGANDS BEARING A RIGID PHENYLENE BRIDGE	144	
7.2.1	<i>General procedure for the synthesis of 1,1'-dimethyl-3,3'-phenylene- bis(imidazolium) diiodide a - c</i>	144	
7.2.2	<i>General procedure for the synthesis of the 1,1'-dimethyl-3,3'-phenylene bis(imidazolium) bis(hexafluorophosphate) salts d - f</i>	145	
7.2.3	<i>General procedure for the syntheses of the silver(I) complexes 1 - 3</i>	146	
7.2.4	<i>General procedure for the syntheses of gold(I) complexes 4 - 6</i>	147	
7.2.5	<i>General procedure for the syntheses of the copper(I) complexes 8 - 9</i>	149	
7.2.6	<i>In situ synthesis of the copper complex 7</i>	150	
7.2.7	<i>Synthesis of the iridium(III) complex 10 and characterization of the species 10*</i>	151	
7.2.8	<i>Synthesis of the ruthenium(II) complex 11</i>	152	
7.2.9	<i>X-ray crystal structure details of compounds 1, [Ag₂(ortho- diNHC)(CH₃CO₂)](PF₆), 2, 4, 5 and 11</i>	154	
7.3	METAL COMPLEXES WITH AN IMIDAZOLE BASED NHC LIGAND FUNCTIONALISED WITH A TRIAZOLE IN THE 5 POSITION OF THE BACKBONE.....	156	
7.3.1	<i>Synthesis of halogen - functionalized imidazoles</i>	156	
7.3.2	<i>Attempts for the synthesis of different (ethynyl)imidazoles</i>	156	
7.3.3	<i>Synthesis of 5-ethynyl-1-methylimidazole g</i>	157	
7.3.4	<i>Syntheses of h</i>	158	

7.3.5	<i>Synthesis of the proligand i</i>	158
7.3.6	<i>Synthesis of the proligand l</i>	159
7.3.7	<i>Synthesis of the proligand m</i>	160
7.3.8	<i>Synthesis of the silver(I) complex 12</i>	160
7.3.9	<i>Synthesis of the silver(I) complex 13</i>	161
7.3.10	<i>Synthesis of the silver(I) complex 14</i>	162
7.3.11	<i>Synthesis of the gold(I) complex 15</i>	162
7.3.12	<i>Synthesis of gold(I) complex 16 via post-methylation of complex 15 and conversion to complex 17</i>	163
7.3.13	<i>Synthesis of copper(I) complex 18</i>	164
7.3.14	<i>Synthesis of ruthenium(II) complex 19</i>	165
7.3.15	<i>X-ray crystal structure details of complexes 12 and 15</i>	166
7.4	METAL COMPLEXES WITH HETERODITOPIC LIGANDS BASED ON IMIDAZOL-2-YLIDENE AND 1,2,3-TRIAZOL-5-YLIDENE MOIETIES CONNECTED WITH A PROPYLENE BRIDGE	167
7.4.1	<i>Synthesis of 4-[3-(1H-imidazol-1-yl)propyl]-1-benzyl-1H-1,2,3-triazole</i>	167
7.4.2	<i>Synthesis of 4-[3-(1H-Imidazol-1-yl)propyl]-1-phenyl-1H-1,2,3-triazole n</i>	167
7.4.3	<i>Synthesis of 3-(benzyl)-1-methyl-5-[3-(3-methyl-1H-imidazol-3-ium-1-yl)propyl]-3H-1,2,3-triazol-1-ium diiodide and 3-(phenyl)-1-methyl-5-[3-(3-methyl-1H-imidazol-3-ium-1-yl)propyl]-3H-1,2,3-triazol-1-ium diiodide o</i>	168
7.4.4	<i>General synthesis of 3-(substituted)-1-methyl-5-[3-(3-methyl-1H-imidazol-3-ium-1-yl)propyl]-3H-1,2,3-triazol-1-ium bis(hexafluorophosphate) p and q</i>	169
7.4.5	<i>Synthesis of silver(I) complex 20</i>	170
7.4.6	<i>Synthesis of silver(I) complex 21</i>	171
7.4.7	<i>Synthesis of gold(I) complexes 22 and 22'</i>	172
7.4.8	<i>Synthesis of gold(I) complexes 23 and 23'</i>	173
7.4.9	<i>Synthesis of palladium(II) complexes 24 and 24'</i>	174
7.4.10	<i>X-ray crystal structure details of complex 23 and 24</i>	176
7.5	BIS(BENZOXAZOLE) PROLIGANDS AND ATTEMPTS FOR THE SYNTHESIS OF TRANSITION METAL COMPLEXES.....	177
7.5.1	<i>Syntheses of the precursors N,N'-bis(3,5-di-tert-butyl-2-hydroxyphenyl)-(substituted)diamine</i>	177
7.5.2	<i>Syntheses of N,N'-(substituted)bis(5,7-di-tert-butyl-3H-benzooxazol-1-ium) bis(tetrafluoroborate)</i>	178
7.5.3	<i>Attempts for the syntheses of metal complexes with 3,3'-(substituted)bis(5,7-di-tert-butyl-3H-benzooxazol-1-ium)bistetrafluoroborate proligands</i>	181
	PUBLICATIONS AND COMMUNICATIONS TO CONGRESSES	183

Abstract

In the last decades, N-heterocyclic carbenes (NHC) ligands have been studied by many groups due to their peculiarity in terms of major stability and versatility with respect to other type of ligands based on nitrogen (amines, imines, etc.) or phosphorous (phosphines, phosphites, etc.) donor atoms.

Nowadays, the role of these ligands in the chemistry of transition metal complexes is pivotal, and the applications of the resulting compounds span from catalysis to luminescence to bioinorganic chemistry.

This PhD, a collaboration between the University of Padova and the University of Strasbourg, is focused on the chemistry of di(N-heterocyclic carbene) ligands and can be divided in four families of ligands that constitute the four chapters:

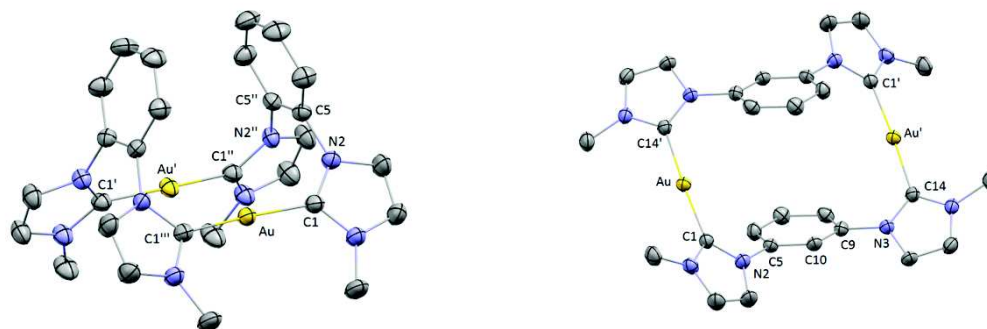
- i)* metal complexes with di(N-heterocyclic carbene) ligands bearing a rigid phenylene bridge between the carbene units;
- ii)* metal complexes combining an imidazole-based NHC ligand functionalized with a triazole in the 5 position of the backbone;
- iii)* metal complexes with heteroditopic ligands based on imidazol-2-ylidene and 1,2,3-triazol-5-ylidene moieties connected with a propylene bridge;
- iv)* bis(benzoxazolium) proligands and attempted synthesis of related transition metal complexes.

i) Metal complexes with di(N-heterocyclic carbene) ligands bearing a rigid phenylene bridge between the carbene units.

Ortho- meta- and para-phenylene bis(imidazolium) salts have been used as proligands for the syntheses of various silver(I) complexes. These compounds, with general formula $[\text{Ag}_2\text{L}_2](\text{PF}_6)_2$ (L=di(N-heterocyclic carbene) ligand), have been used as transmetalating agents for the formation of the corresponding gold(I) and copper(I) complexes. These compounds maintain the same dinuclear dicationic molecular structure as for the silver(I) precursors, as confirmed by the resolved solid state crystal structures.

The photoluminescence properties of the synthesized complexes have been studied and

are strongly influenced by the structure of the di(NHC) ligand employed. In particular, the gold(I) complexes show interesting quantum yields of emission modulated by the geometry of the complex (distance between the two metal centers) and also by the packing of the complexes in solid state, as shown below.

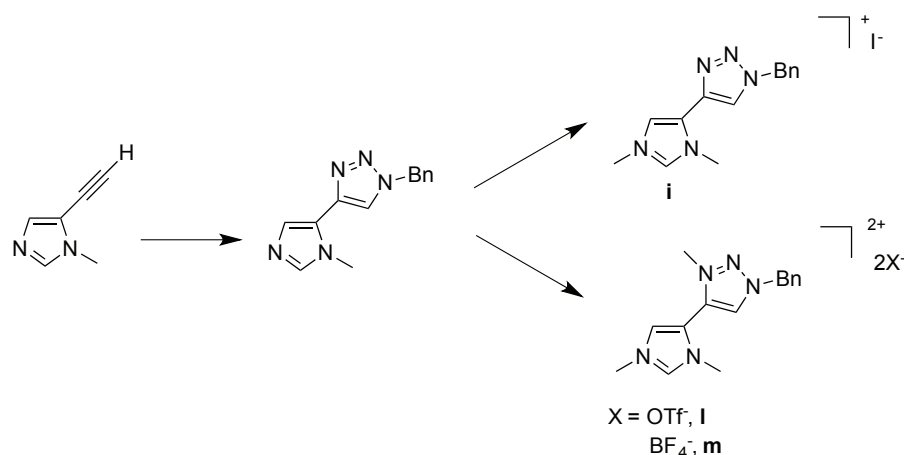


Complex	λ_{\max} (nm)	Φ (%)	τ (ms)	M···M distance (Å)
<i>ortho</i> -phenylene gold(I) complex	380	1.0	1.1	3.657
<i>meta</i> -phenylene gold(I) complex	450	5.7	0.4	7.140
<i>para</i> -phenylene gold(I) complex	478	2.8	22 – 140	7.213

With the *ortho*-phenylene silver(I) diNHC complex, the transmetalation was also successful for the access to mononuclear ruthenium(II) and iridium(III) complexes that show a chelate coordination of the ligand on the metal center.

ii) metal complexes combining an imidazole-based NHC ligand functionalized with a triazole in the 5 position of the backbone.

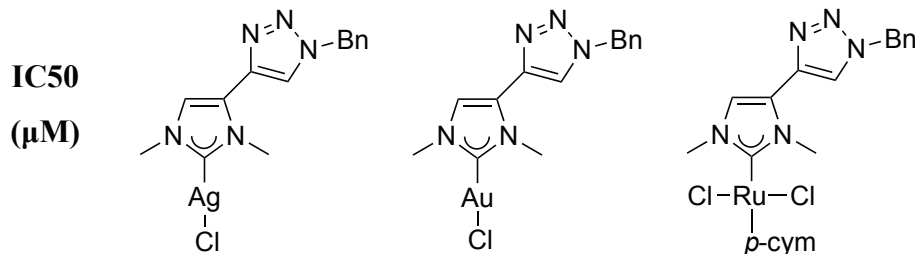
The copper catalyzed azide alkyne cycloaddition reaction (CuAAC) also called “click reaction” has been used for the functionalization of the [5-(trimethylsilyl)ethynyl]-1-methylimidazole with a 1,2,3-triazole ring. As function of the methylating agents, it was possible to alkylate only the nitrogen on the imidazole ring (proligand **i**) or both on imidazole and triazole rings (proligands **l** and **m**).



Starting from the proligands **l** and **m**, silver(I) complexes of stoichiometry Ag:L 1:1 (L= di(N-heterocyclic carbene) ligand) have been obtained, albeit with poor purity due to the oily nature of the products.

Using the proligand **i** it has been possible to isolate a silver(I) complex of formula AgCl(NHC), which has been successively employed for the synthesis of gold(I), copper(I) and ruthenium(II) complexes.

The *in vitro* cytotoxic activities of these compounds have been evaluated and in these preliminary results the silver(I) complex appears the most active and selective.



HCT116	1.38 \pm 0.36	6.4 \pm 0.8	40 \pm 1
MCF7	2.0 \pm 0.2	7 \pm 1	11.6 \pm 0.5
PC3	0.3 \pm 0.1	6 \pm 1	25 \pm 2

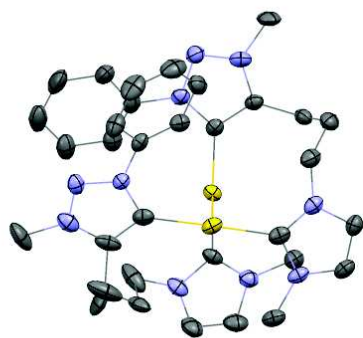
iii) metal complexes with heteroditopic ligands based on imidazol-2-ylidene and 1,2,3-triazol-5-ylidene moieties connected with a propylene bridge.

Heteroditopic proligands have been successfully synthesized using the CuAAC click reaction followed by methylation and anion exchange.

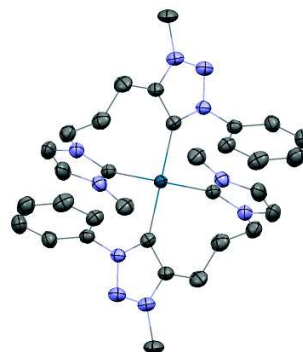
A series of novel di-NHC gold(I) complexes, having general formula [Au₂L₂](PF₆)₂, have been synthesized and fully characterized through the transmetalation of the di-NHC moiety from pre-formed silver(I) complexes. The same pathway has been adopted

for the synthesis of palladium(II) complexes that show the chelation of two ligands on the same metal center (i.e. homoleptic complexes).

Due to the presence of two different carbene units (imidazole-2-ylidene and triazol-5-ylidene), it is possible to obtain a mixture of isomers which has been investigated by NMR and mass analyses.



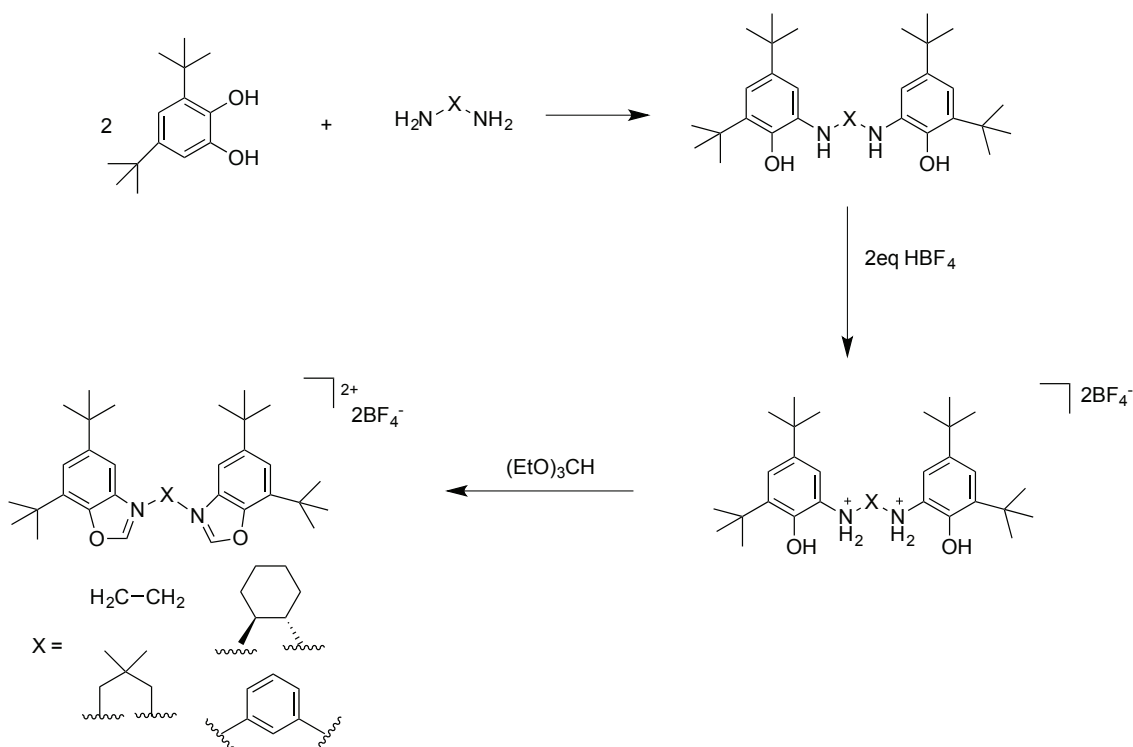
gold(I) complex



palladium(II) complex

iv) *bis(benzoxazolium) prolignands and attempted synthesis of related transition metal complexes.*

Finally the chemistry of benzoxazole has been investigated. Different prolignands containing benzoxazole rings have been synthesized starting from the corresponding diamine, as shown below.



These organic scaffolds have been used as proligands for the synthesis of metal complexes. Unfortunately, despite the various reaction conditions adopted (deprotonating agent, solvent, temperature, time...), the results obtained in this regard are not satisfactory, probably for the intrinsic instability of the ligand precursors and/or of the corresponding free carbenes.

Sommario

Nelle ultime decadi, i leganti carbenici N-eterociclici sono stati studiati da numerosi gruppi in virtù delle loro peculiarità, quali maggiore stabilità e versatilità rispetto a leganti con atomi donatori all'azoto (ammine, immine etc.) o al fosforo (come per esempio fosfine, fosfiti ed altri).

Attualmente, il ruolo di questi leganti nella sintesi di complessi con metalli di transizione è essenziale e le applicazioni dei corrispondenti complessi spaziano dalla catalisi alla luminescenza fino alla chimica bioinorganica.

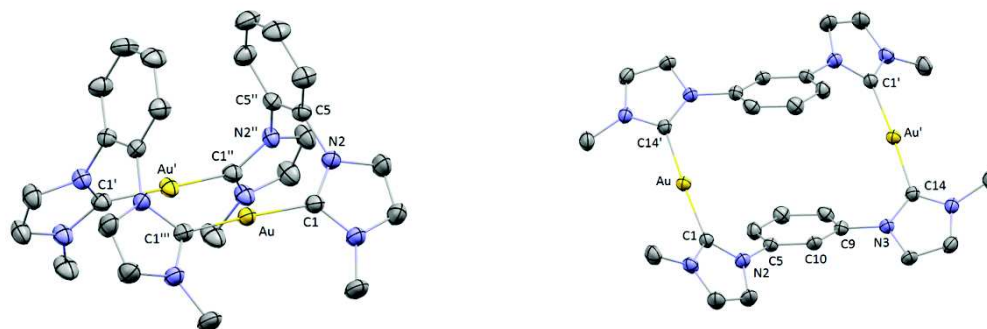
Questo dottorato, effettuato in collaborazione tra l'Università degli Studi di Padova e l'Università di Strasburgo, è focalizzato sulla chimica dei carbeni N-eterociclici e può essere diviso in quattro differenti capitoli:

- i)* complessi metallici con leganti dicarbenici N-eterociclici legati da ponte fenilene rigido;
- ii)* complessi metallici con legante carbenico N-eterociclico funzionalizzato con un triazolo in posizione 5 del backbone;
- iii)* complessi metallici con leganti eteroditopici basati su unità imidazol-2-ilideniche e triazol-5-ilideniche legate tra loro mediante ponte propilenico;
- iv)* leganti bis(benzossazolici) e tentativi di sintesi dei corrispondenti complessi con metalli di transizione.

i) complessi metallici con leganti dicarbenici N-eterociclici legati da ponte fenilene rigido.

Complessi di argento(I) sono stati sintetizzati partendo dai sali precursori dei leganti bisimidazolici con ponte *orto- meta- e para-*fenilenico. Tali complessi, con formula generale $[\text{Ag}_2\text{L}_2](\text{PF}_6)_2$ (L = legante dicarbenico N-eterociclico), sono stati usati come agenti di transmetallazione per l'ottenimento dei complessi di oro(I) e rame(I) corrispondenti; questi composti mantengono la medesima natura dinucleare dicationica dei precursori di argento, confermata dalla risoluzione delle strutture mediante diffrazione ai raggi X.

Le proprietà di luminescenza dei complessi sintetizzati sono state studiate e sono fortemente influenzate dalla struttura del legante dicarbenico N-eterociclico utilizzato. In particolare i complessi di oro(I) presentano interessanti rese quantiche di emissione che variano a seconda della geometria del complesso (in termini di distanza tra i centri metallici) e soprattutto per il packing dei complessi allo stato solido.

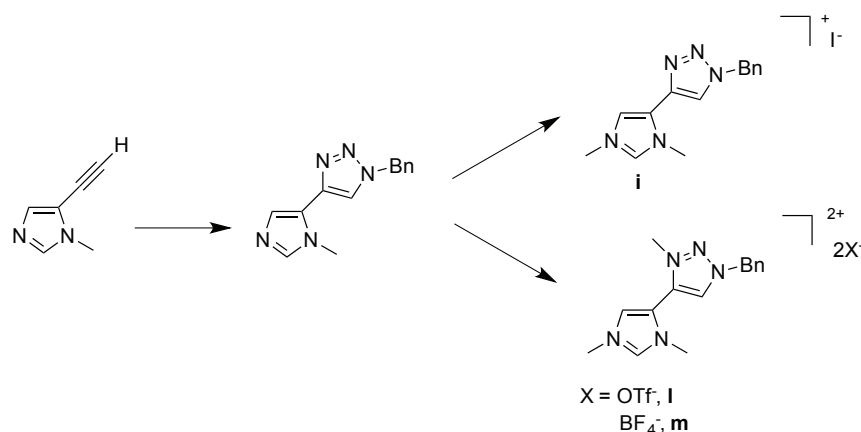


Complessi di oro(I) con legante diNHC a ponte	λ_{\max} (nm)	Φ (%)	τ (ms)	Distanza M...M (Å)
<i>orto</i> -fenilene	380	1.0	1.1	3.657
<i>meta</i> -fenilene	450	5.7	0.4	7.140
<i>para</i> -fenilene	478	2.8	22 – 140	7.213

A partire dal complesso di argento con legante dicarbenico a ponte *orto*-fenilene, la reazione di transmetallazione è stata utilizzata per la sintesi di complessi mononucleari di rutenio(II) e iridio(III) che mostrano la chelazione dell'unità dicarbenica al centro metallico.

ii) complessi metallici con legante carbenico N-eterociclico funzionalizzato con un triazolo in posizione 5 del backbone.

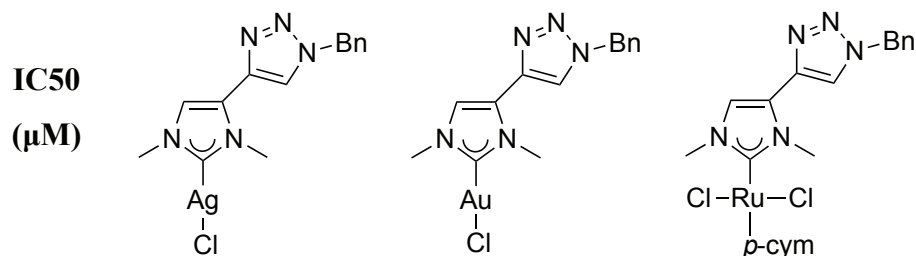
La reazione di cicloadizione azide alchino rame catalizzata (CuAAC) comunemente chiamata "reazione di click" è stata utilizzata per la funzionalizzazione del composto [5-(trimetilsilil)etynil]-1-metilimidazolo con un anello 1,2,3-triazolo. Utilizzando differenti agenti metilanti è possibile metilare solamente l'azoto dell'anello imidazolico (precursore del legante, **i**) o entrambi gli anelli imidazolico e triazolico (precursori dei leganti, **l** e **m**).



Partendo dai precursori dei leganti, **i** e **m**, sono stati ottenuti complessi di argento(I) con rapporto Ag:L 1:1 (L = dicarbene N-eterociclico), anche se con bassa purezza a causa della natura oleosa dei prodotti.

Utilizzando il precursore **i** è stato possibile isolare il complesso di argento(I) con formula AgCl(NHC), che è stato successivamente impiegato per la sintesi dei complessi di oro(I), rame(I) e rutenio(II).

L'attività citotossica in vitro di tali composti è stata valutata e risultati preliminari mostrano un'attività e selettività maggiore per il complesso di argento(I) rispetto agli altri complessi metallici studiati.



HCT116	1.38 ± 0.36	6.4 ± 0.8	40 ± 1
MCF7	2.0 ± 0.2	7 ± 1	11.6 ± 0.5
PC3	0.3 ± 0.1	6 ± 1	25 ± 2

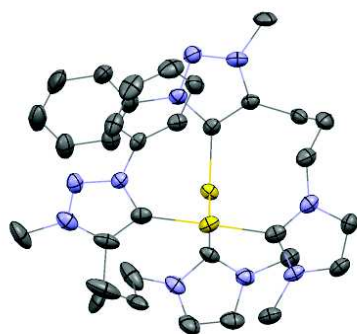
iii) complessi metallici con leganti eteroditopici basati su unità imidazol-2-ilideniche e triazol-5-ilideniche legate tra loro mediante ponte propilenico.

Precursori dei leganti eteroditopici sono stati sintetizzati mediante reazione di click CuAAC, seguita da metilazione e scambio di anione.

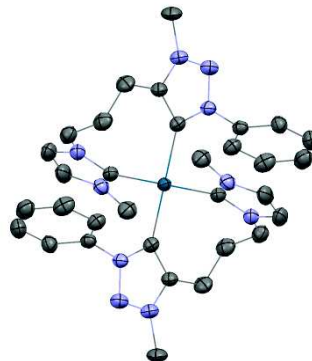
Una nuova serie di complessi di oro(I), con formula generale $[\text{Au}_2\text{L}_2](\text{PF}_6)_2$, è stata ottenuta mediante reazione di transmetallazione dell'unità dicarbena N-eterociclica a partire dal complesso di argento(I) preformato.

La medesima via sintetica è stata utilizzata per la sintesi di un complesso di palladio(II) che mostra la chelazione di due unità dicarbeniche allo stesso centro metallico.

A causa della presenza di due diverse unità carbeniche (imidazol-2-ilidene e triazol-5-ilidene) è possibile ottenere una miscela di isomeri la cui composizione è stata analizzata mediante spettri NMR e tecniche di massa.



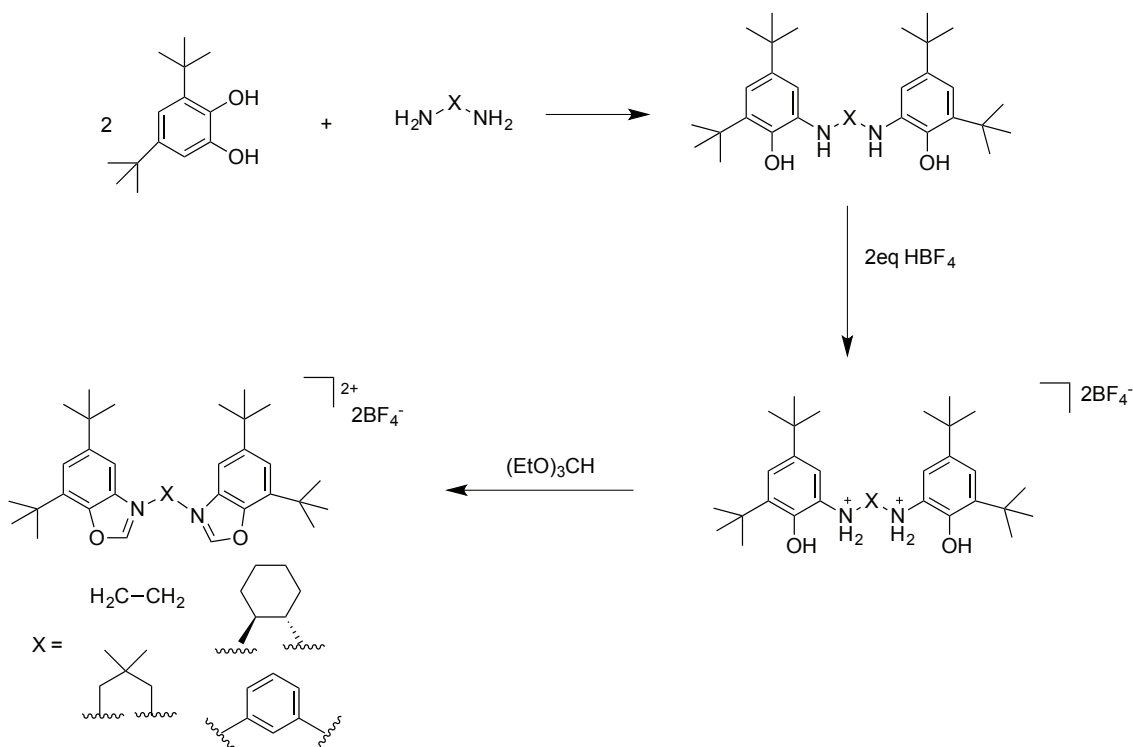
Complesso di oro(I)



Complesso di palladio(II)

iv) leganti bis(benzossazolic) e tentativi di sintesi dei corrispondenti complessi con metalli di transizione.

Precursori dei leganti con anello benzossazolic sono stati sintetizzati a partire dalla relativa diammina, mediante gli step riportati nello schema seguente.



Queste molecole organiche sono state utilizzate come precursori dei leganti per la sintesi di diversi complessi con metalli di transizione. Sfortunatamente, nonostante le differenti condizioni di reazione utilizzate (agente deprotonante, solvente, temperatura, tempo...), i risultati ottenuti non sono soddisfacenti, probabilmente a causa dell'instabilità intrinseca dei precursori e/o dei relativi carbeni.

Résumé

Dans les dernières décennies, les ligands carbènes N-hétérocycliques (NHC) ont été étudiés par de nombreux groupes en raison de leur propriétés particulières en termes de stabilité et de polyvalence par rapport à d'autres types de ligands à base d'azote (amines, imines, etc.) ou de phosphore (phosphines, phosphites, etc.).

Ainsi de nos jours, le rôle de ces ligands dans la chimie des complexes de métaux de transition est essentielle, de même que leurs applications allant de la catalyse à la luminescence en passant par la chimie bio-inorganique.

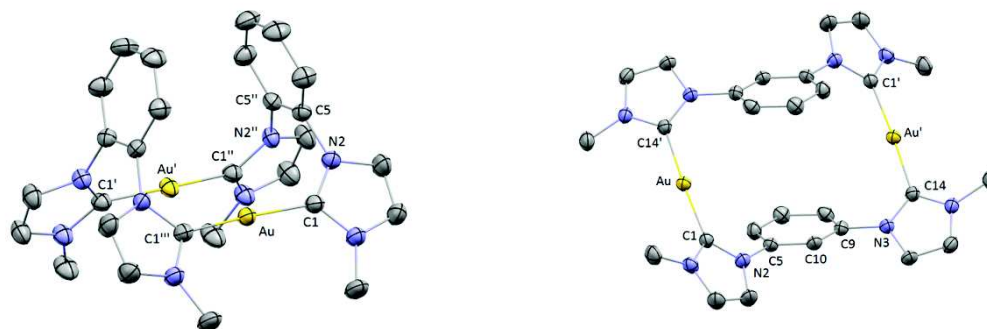
Ce travail de thèse, en co-tutelle entre l'Université de Padoue et l'Université de Strasbourg, se concentre sur la chimie des carbènes bis-(N-hétérocycliques) et peut être divisé en quatre familles de ligands qui constituent les quatre chapitres du manuscrit:

- i) complexes métalliques avec des ligands di(carbène N-hétérocyclique) portant un pont phénylène rigide entre les unités carbéniques;
- ii) complexes métalliques combinant un ligand NHC fonctionnalisé avec un triazole dans la position 5 du squelette;
- iii) complexes métalliques avec des ligands hétéroditopiques à base d'un imidazol-2-ylidène et d'un 1,2,3-triazol-5-ylidène reliés par un pont propylène;
- iv) proligands bis (benzoxazoles) et les tentatives de complexation sur des métaux de transition.

i) Complexes métalliques avec des ligands di(carbène N-hétérocyclique) portant un pont phénylène rigide entre les unités carbéniques.

Des sels de bis (imidazolium) *ortho-* *meta-* et *para*-phénylène ont été utilisés comme précurseurs des ligands carbènes pour la synthèse de complexes d'argent(I). Ces composés, de formule générale $[Ag_2L_2](PF_6)_2$ (L = ligand di(NHC)), ont été utilisés comme agents de transmétallation pour l'obtention des complexes d'or(I) et de cuivre (I) correspondants. Ces composés conservent la même structure moléculaire dicationique dinucléaire des précurseurs d'argent(I), comme le confirment les structures cristallines résolues à l'état solide.

Les propriétés de photoluminescence des complexes synthétisés ont été étudiées et sont fortement influencées par la structure moléculaire du ligand di(NHC) employé. En particulier, les complexes d'or(I) présentent des rendements quantiques d'émission intéressants qui sont modulés par la géométrie du complexe (distances inter-métalliques) et également par l'empilement cristallin des complexes à l'état solide.



Complex d'or(I) avec le ligand diNHC a pont	λ_{\max} (nm)	Φ (%)	t (ms)	distance M...M (Å)
<i>orto</i> -phenylene	380	1.0	1.1	3.657
<i>meta</i> -phenylene	450	5.7	0.4	7.140
<i>para</i> -phenylene	478	2.8	22 – 140	7.213

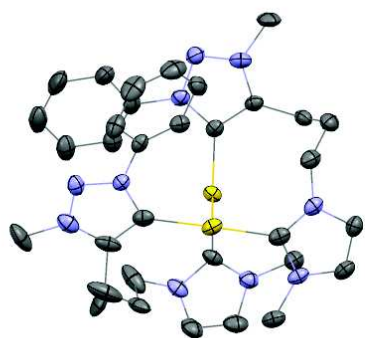
En utilisant les complexes d'argent (I) contenant le pont *orto*-phénylène, la transmétallation a abouti à la synthèse de complexes mononucléaires de ruthénium(II) et d'iridium(III). L'analyse structurale de ces composés confirme la coordination bidente du ligand sur le centre métallique.

ii) Complexes métalliques avec un ligand NHC fonctionnalisé avec un triazole en position 5 du squelette.

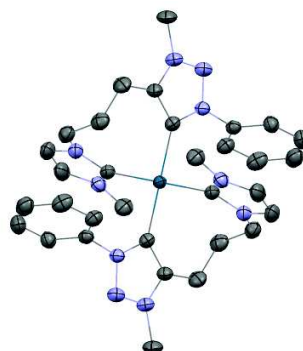
Le réaction de cycloaddition entre un azide et un alcyne catalysée au cuivre (CuAAC), également appelé "réaction de type clic" a été utilisée pour la fonctionnalisation du [5-(triméthylsilyl) éthynyl]-1-méthylimidazole. En adaptant le bon agent de méthylation, il était possible d'alkyler uniquement l'azote sur le cycle imidazole (précurseur de ligand, **i**) ou les deux atomes d'azote sur l'imidazole et le triazole (précurseurs des ligands, **l** et **m**).

d'argent(I) préformés. La même voie a été adoptée pour la synthèse du complexe de palladium(II), qui contient deux ligands sur le même centre métallique.

En raison de la présence de deux unités carbéniques différentes, il est possible d'obtenir un mélange d'isomères : les géométries possibles ont été étudiées par RMN et analyse de masse.



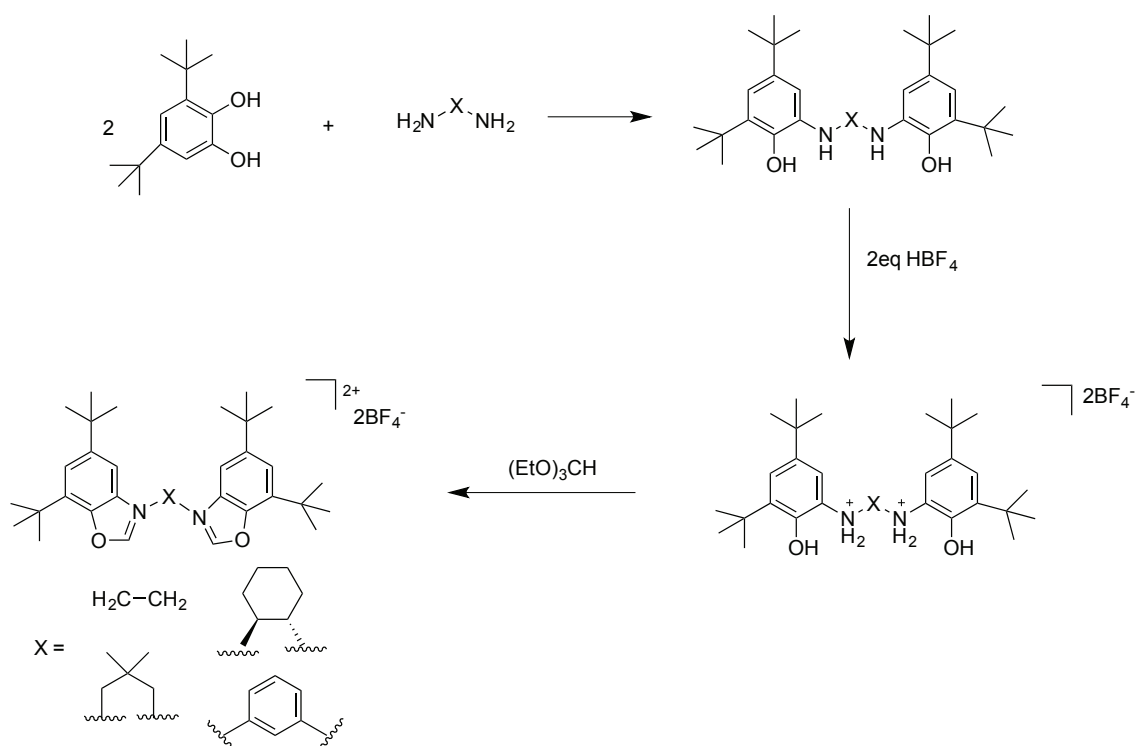
complexe d'or(I)



complexe de palladium(II)

iv) proligands bis-(benzoxazoles) et tentatives de synthèse de complexes de métaux de transition.

Différents précurseurs de ligands avec des cycles benzoxazoles ont été synthétisés à partir de la diamine correspondante suivant le schéma ci-dessous.



Ces benzoxazoliums ont été utilisés comme précurseurs de ligands carbènes pour la synthèse de complexes métalliques. Malheureusement, en dépit des diverses conditions

de réactions adoptées (agent de déprotonation, solvant, température, temps, etc.), les résultats obtenus à cet égard n'ont pas été satisfaisants, probablement dû à l'instabilité intrinsèque des précurseurs de ligands et/ou des carbènes libres correspondants.

Chapter 1: INTRODUCTION

N-heterocyclic carbene ligands and transition metal complexes

1.1 History

In the last decades, N-heterocyclic carbenes (NHCs) have become one of the most studied class of ligands for the syntheses of transition metal complexes.^{1,2} Moreover, the azolium salt, proligands of the NHCs, are interesting by themselves since they can be also used as ionic liquids,³ as liquid crystals⁴ or as building blocks in the syntheses of macromolecules for different applications.⁵

Since from their discovery in 1968 by Öfele and Wanzlick,⁶ NHCs have been studied by several groups and, thanks to Arduengo *et al.*⁷ who first isolated a stable free N-heterocyclic carbene (Figure 1.1), the interest of the scientific community towards these ligands has afterward continuously increased.

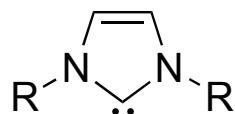


Figure 1.1: generic structure of a N-heterocyclic carbene (NHC)

The synthesis of the free NHC was achieved by direct deprotonation of 1,3-diadamantylimidazolium iodide salt with a strong base; in particular, the presence of two sterically encumbered adamantyl nitrogen substituents stabilizes the carbene preventing the coupling of two carbene moieties.

After this pioneering study, the majority of the research activity concerning NHCs has been dedicated to the synthesis and catalytic applications of metal complexes with these ligands.⁸ In this field, it is worth to mention in particular the ruthenium(II)-carbene complexes reported in Figure 1.2 and their application in olefin metathesis, which earned their inventor, prof. R. Grubbs, the Nobel Prize in 2005.⁹

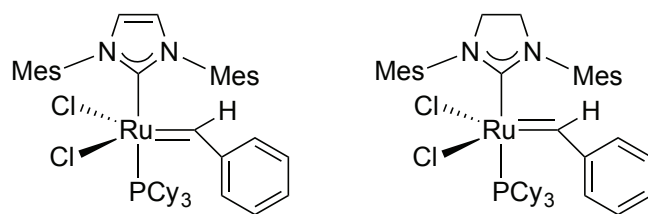


Figure 1.2: “second generation” Grubbs catalysts

1.2 Fischer, Schrock and NHC carbene complexes

Carbene as ligands are usually classified in two different categories, which are Schrock- or Fischer-type carbenes, depending on the nature of the carbene-metal bond.

In Schrock-type carbene complexes the metal-carbene bond is covalent and derives from the interaction between a carbene in triplet state electronic configuration (due to the low energy separation between the σ and the p_{π} -orbitals) and a metal fragment. The HOMO orbital of the resulting complex has more ligand character and the LUMO has more metal character. Schrock carbenes are considered nucleophiles and they usually bind to early transition metals in high oxidation state such as Ti(IV), Mo(VI), W(VI) or Ta(V).¹⁰

On the other hand, the metal-carbene bond in Fischer-type carbene complexes results from a σ -donation of electron density from the carbene (singlet state electronic configuration) to the metal center accompanied by a π -backdonation from the metal to the carbene carbon atom. The HOMO orbital of the relative complex has more metal character whereas the LUMO has more ligand character. The carbene fragment acts as an electrophile and it is usually strongly bonded to late transition metal centers in low or medium oxidation state. Concerning the nature of the bond, the Fischer-carbene carbon atom has an empty p_{π} -orbital that can be useful in the stabilization of the species by the π -backdonation from a d_{π} -orbital of the metal (Figure 1.3).^{11,12}

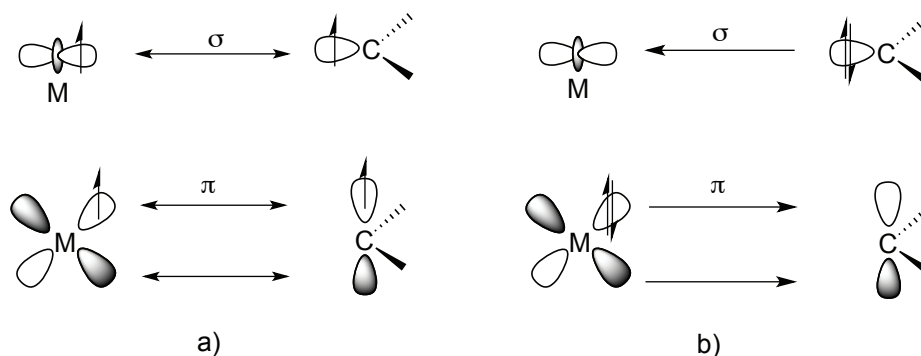


Figure 1.3: metal-carbon bond interactions in Schrock a) and Fischer b) type carbene complexes

Taking into consideration the substituents to the carbene carbon, NHCs are singlet carbenes and therefore, N-heterocyclic carbene complexes may be classified as Fischer-type compounds. However, NHCs do not present the same reactivity as Fischer-type carbenes (they are in fact rather inert species, they do not present an electrophilic character) and most importantly, they bind to the metal centers via σ -donation and the π -backdonation from the metal is usually negligible. This can be easily explained, considering that the energy of the vacant p_π orbital in the NHC is too high and so this orbital cannot receive electron density from the metal center; this enhancement in energy is a consequence of strong $N \rightarrow C$ π -donation in this type of carbenes (vide infra).

Two important contributions are in fact fundamental in the stabilization of the carbene carbon atom in a NHC species: the *inductive* and the *mesomeric* effect.¹¹

- The *inductive effect* is due to the different electronegativity between the nitrogen atoms and the carbon in position 2; in fact, the nitrogen atoms reduce the electron density on the carbene center by σ -withdrawing effect (Figure 1.4 in red).
- The *mesomeric (or resonance) effect* is due to the interaction between the p_π occupied orbitals of the nitrogen atoms (that are π -donors) and the same symmetry orbital of the carbon (Figure 1.4 in grey).

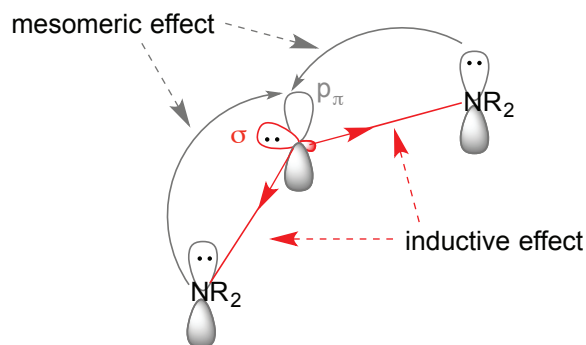


Figure 1.4: inductive and mesomeric effect in N-heterocyclic carbene

These two effects at the same time induce an increase of the energy level of the p_{π} orbital and stabilize the *sigma* orbital due to the enhanced *s* character of the carbene carbon atom. As the results, the gap between the σ and p_{π} orbitals is higher and a single ground state electronic configuration is favored (Figure 1.5).

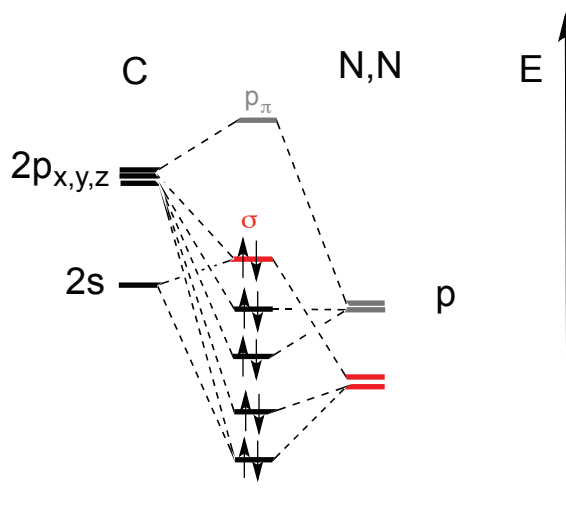
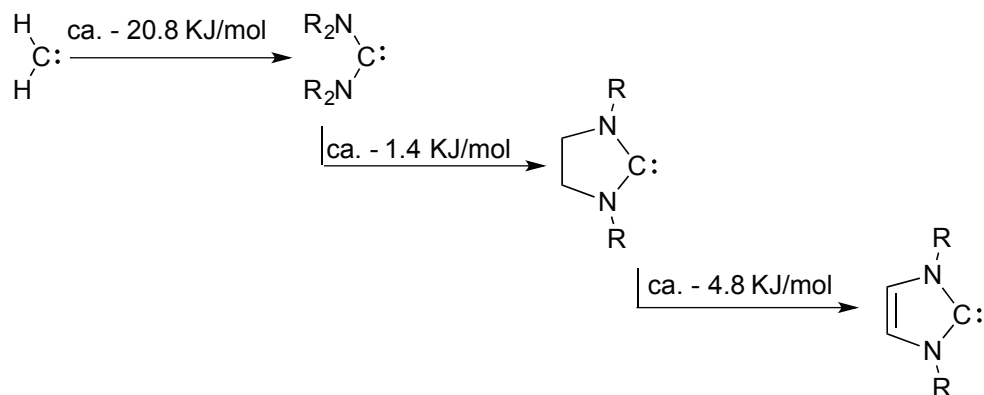


Figure 1.5: qualitative orbital diagram of the N-C-N fragment

Contrary to what usually reported in the literature, recently some authors^{13,14,15} explained that the contribution of π -backdonation in NHC metal complexes is important in the stabilization on the M-C bond, as observed in the Fischer-type carbenes metal complexes. Using energy decomposition analysis (EDA) it is possible to obtain data concerning the different contributions of σ -donation, $\pi_{\text{in plane}}$ and $\pi_{\text{out of plane}}$ -backdonation. The largest contribution is observed for the σ -donation, but a non-negligible effect is also observed for the π -backdonation, which is correlated to the presence of donating groups as substituents on the N atoms.

The NCN carbene fragment can be further stabilized by ring closure and by the introduction of a double bond between the position 4 and 5 on the backbone of the ring (from imidazolin-2-ylidene to imidazol-2-ylidene) (Scheme 1.1).¹⁶



Scheme 1.1: stabilization of the H-C-H fragment by ring closure and unsaturation

As described before, NHCs are good σ -donor ligands, stronger than other classes of two-electron donor species like phosphine, amine and ether ligands.

Their corresponding organometallic complexes are characterized by very high stability in different conditions (like for example high temperature and oxidative environment) and this is mainly attributed to the strong metal-carbene carbon bond. Furthermore, it is possible to tune different parameters on the ligands (like for example nitrogen wingtip substituents, heterocyclic ring) and consequently modify the stereo-electronic properties of the complexes.

For example, using bulky or long alkyl chain¹⁷ substituents at the nitrogen atoms or adding a polar group on the nitrogen wingtip¹⁸ it is possible to change both the steric hindrance and the solubility properties of the ligands (Figure 1.6) and, as consequence, of the related complexes.

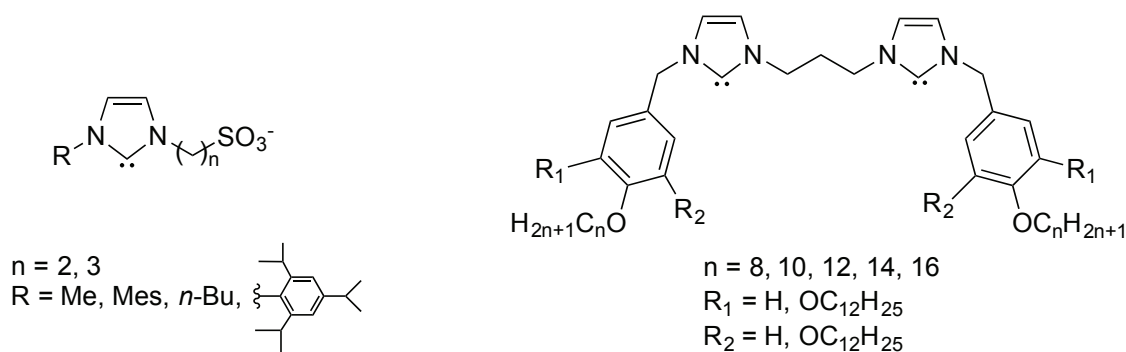


Figure 1.6: selected example of different substituents of the nitrogen atoms

Interesting examples can be obtained if the substituent on the nitrogen atom contains a second donor atom that can act as ligand. As depicted in Figure 1.7, the ligand can coordinate the same metal in a chelate fashion via carbene carbon and the second donor atom (C or N) or can bridge two metal centers.^{19,20,21}

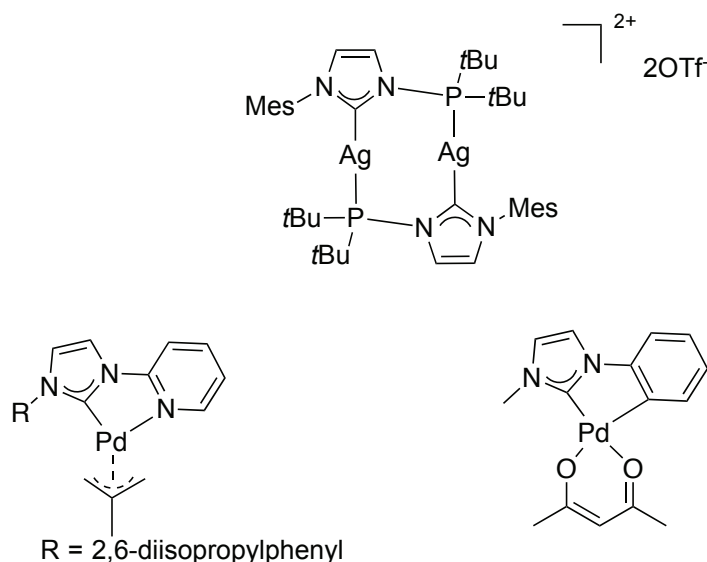


Figure 1.7: some examples of NHC-metal complexes functionalized with different coordinating groups, such as a phosphine (top), pyridine (bottom left) or *ortho*-metalated phenyl ring (bottom left).

There are different parameters that can be modified on the N-heterocyclic carbene scaffold in order to change the electronic and steric properties of the ligand:

- the position of the carbene donor atom;
- the substituents on the backbone and on the nitrogen wingtip atom;
- the nature of the ring (in terms of number of atoms and unsaturation).

The majority of NHCs reported in the literature involves NHCs derived from the imidazole ring. Two different carbons can be the candidates for the formation of a carbene species: the carbon in position 2 of the ring, that allows to obtain the so-called *normal* carbene and the carbon in position 4/5, giving instead the so called *abnormal* carbene.

The acidity of the two protons (C2-H vs C4/5-H) is very different (pK_a 24 vs 31)²² so that in order to obtain an *abnormal* carbene usually the C2 position should be protected (by an organic framework as alkyl or aryl group or by the coordination to another metal). The stability of the carbene in position 4/5 is lower with respect to the carbene

in position 2 and the donating properties of the *abnormal* carbene are generally superior to those of *n*NHC.²³

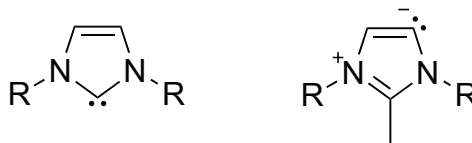


Figure 1.8: *normal*-NHC (left) and *abnormal*-NHC (right)

The modification of the substituents and the presence of a double bond between the carbons in position 4 and 5 can be another important parameter to change the electronic properties of the ligand. For example moving from the unsaturated NHC (imidazol-2-ylidene) to the saturated 5-member ring (imidazolin-2-ylidene) the electron donor capability is increased (Figure 1.9).^{24,25}

Also the variation of the imidazole moiety (moving from the imidazole ring to the benzimidazole one) or the presence of halogens in position 4 and/or 5 of the ring can have an important role on the electronic properties of the ligands and, as a consequences, of the metal.²⁶

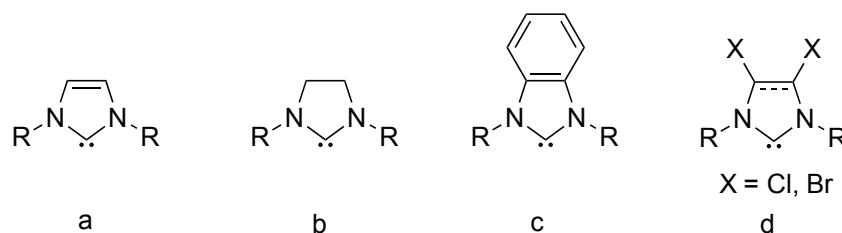


Figure 1.9: unsaturated NHC (a) and saturated one (b), benzimidazole ring (c) and halogenated NHC (d)

Different heterocyclic scaffolds are available for the obtainment of heterocyclic carbenes spanning from the “classical” imidazole-, imidazoline- or benzimidazole-2-ylidene to other five-member rings, like pyrazol-, triazole- or tetrazole-ylidene, to six-, seven- or four-member rings or to more “exotic” ones. Some of them are depicted in Figure 1.10 and Figure 1.12.

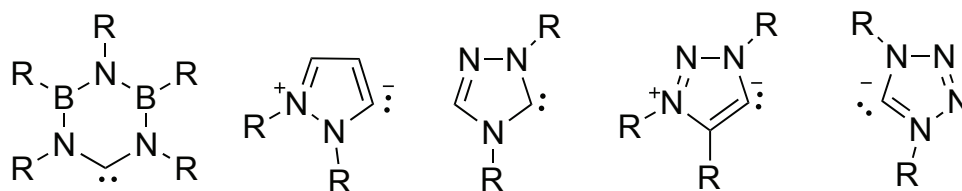


Figure 1.10: NHC based on different heterocycles

Among them, it is interesting to mention the 1,3,4-trisubstituted-1,2,3-triazol-5-ylidene compounds (that will be discussed in more details in Chapters 3 and 4) (Figure 1.11).

The triazolium salts can be easily synthesized via copper catalyzed alkyne azide cycloaddition (CuAAC) followed by the alkylation or arylation of the nitrogen in position 3.²⁷

Different experimental results have demonstrated the strong σ -donor nature of this type of ligands, which lies in between to that shown by the imidazole-2-ylidene and the imidazole-4/5-ylidene. These compounds are usually called *mesoionic carbenes* (MIC), due to their persistent zwitterionic nature: in fact, it is not possible to write a neutral resonance structure (Figure 1.11).²⁸

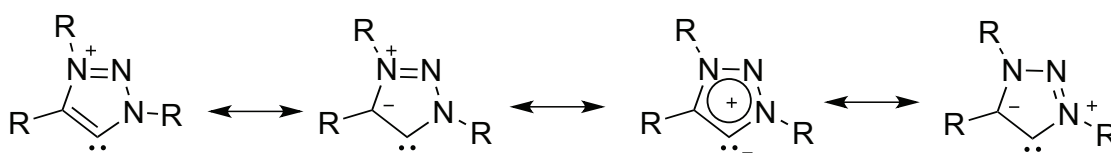


Figure 1.11: resonance structure for the free 1,3,4-trisubstituted-1,2,3-triazole-5-ylidene

Finally, another class of compounds is the so-called *expanded ring carbenes*, i.e. carbenes in which the number of carbon atoms of the heterocyclic ring spans from six to eight. The basicity is superior with respect to the classical imidazole-based carbenes and also the steric properties are modified. Due to the wider N-C_{carbene}-N angle (in some case higher than 120°), a twisting of the N-substituents toward the metal atom is observed, thus resulting in a steric protection of the metal center (Figure 1.12).²⁹

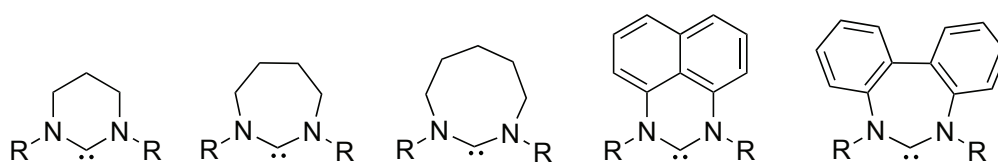


Figure 1.12: different examples of expanded ring NHCs

1.3 Di(N-heterocyclic carbene) ligands

An interesting aspect in the functionalization of a NHC is the possibility to connect different azole moieties in order to generate poly-NHC ligands.

In this case, together with the R₁ groups on the position 4 or 5 of the imidazole ring (peripheral functions) and the wingtip substituents R, it is possible to act also on the bridge Y between the two carbene moieties (see Figure 1.13).

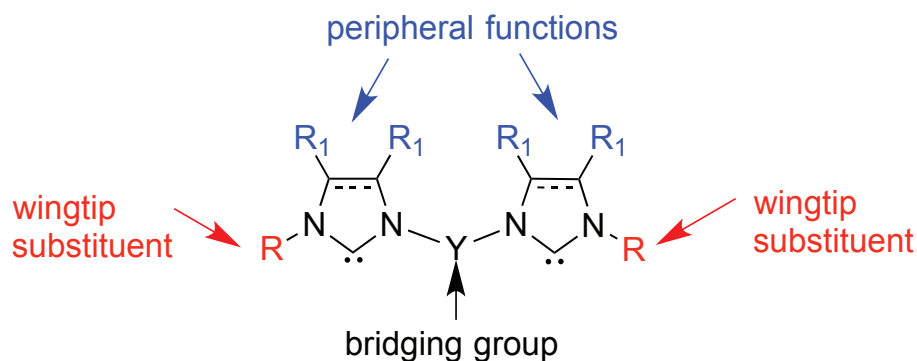
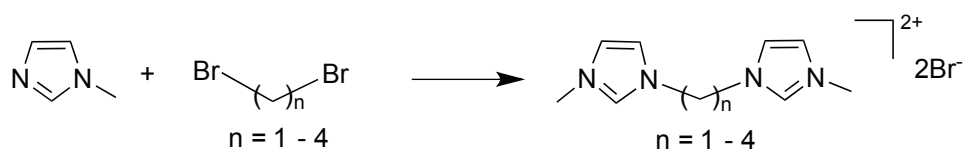


Figure 1.13: general representation of di(N-heterocyclic carbene) ligand

Concerning the R substituents on the imidazole moieties and the peripheral functions, the same considerations reported for mono NHCs can be applied also for the di(N-heterocyclic carbene) ligands.

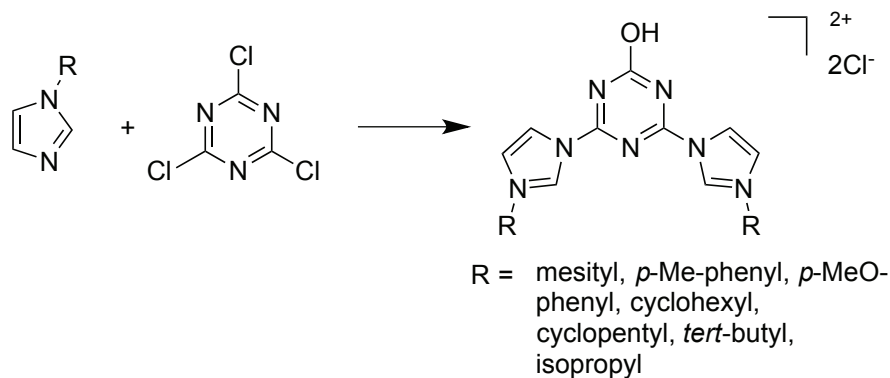
The nature of the bridge Y between the heterocyclic moieties is a key element in influencing the coordination mode of the ligand on the metal center/s: with short or constrained linkers a bridging coordination of the ligand between different metals giving polynuclear structures can be observed, while with more flexible bridges, the chelating coordination occurs preferentially.³⁰

The diazolium salts, precursors of the di(N-heterocyclic carbene) ligands are easily obtained, starting for example from 1-methylimidazole and an alkyl dihalide (Scheme 1.2).³¹



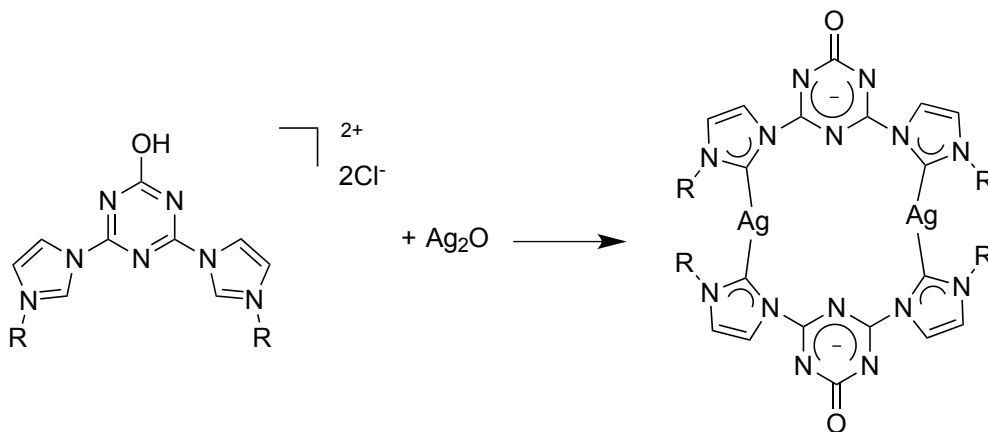
Scheme 1.2: synthesis of di(N-heterocyclic carbene) proligands with alkyl bridges

Strassner *et al.*³² synthesized different di(NHC) proligands with triazynonide bridge reacting 1-alkylimidazole and cyanuric chloride in acetonitrile under reflux (Scheme 1.3).



Scheme 1.3: synthesis of diimidazolium salts by in situ hydrolysis of the first chlorine atom

An interesting feature with this type of proligands is that, once deprotonated (for example by reaction with silver(I) oxide), they generate anionic di(N-heterocyclic carbene), that can give neutral dinuclear complexes (Scheme 1.4).

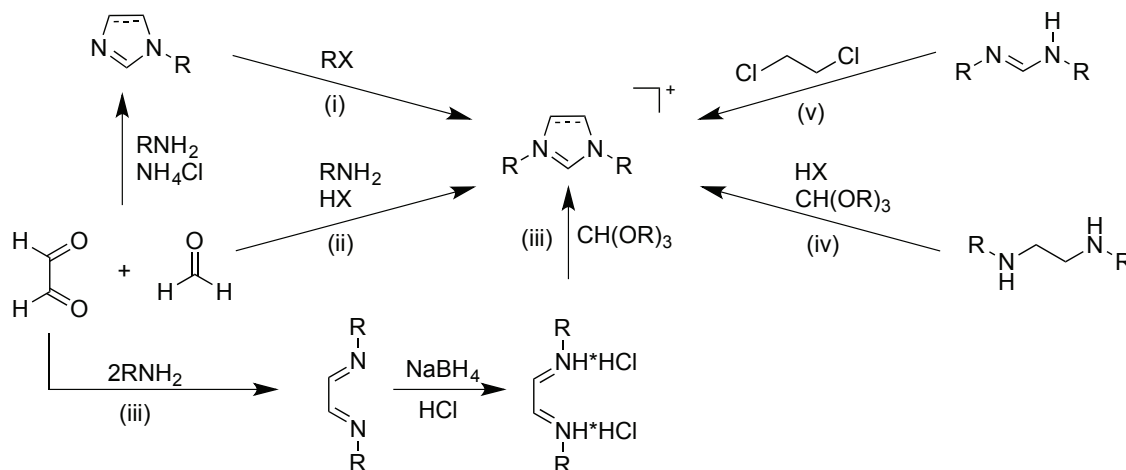


Scheme 1.4: formation of neutral di(NHC) silver(I) complexes

The biggest advantage to work with di(N-heterocyclic carbene) moieties with respect to the mono(NHC) ones is the possibility to optimize the molecular structure in order to fulfill the desired parameters to afford better performances in catalysis as well as in other fields of application.

1.4 Formation of azolium salts

In this section, the synthetic pathways for the imidazolium salts will be briefly described.



Scheme 1.5: different pathways for the syntheses of imidazolium derivatives

The first way of synthesis (i) is the most used one and involves the functionalization with different alkyl or aryl substituents on the nitrogen atom of the imidazole. This reaction can be achieved using different type of alkylating or arylating agents starting from milder ones (like CH_3I ³¹ or benzylbromide²⁶) to stronger ones (like methyl triflate or R_3OBF_4 ³³) and working in various solvents (spanning from polar to non-polar ones like DMSO, methanol or dichloromethane) and reaction conditions (temperature and time).

The second way of synthesis (ii) is the “one pot” condensation of glyoxal, paraformaldehyde and primary amines to form the imidazolium salts.³⁴

With the other pathways (iii and iv), diamine or diimine compounds can be used as scaffold for the syntheses of NHCs by ring closure using *ortho*-formate species (usually triethyl *ortho*-formate).

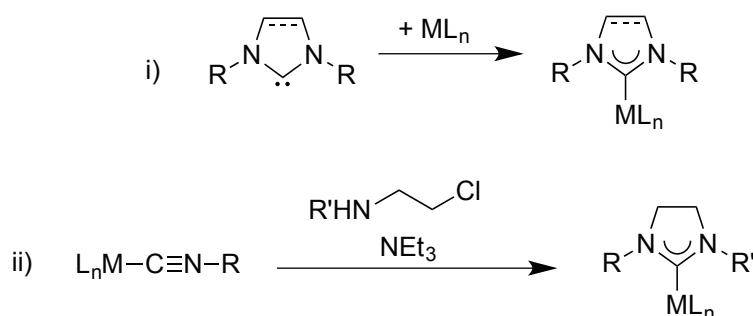
Finally (v) the syntheses of imidazoles can be achieved by reaction of formamidine with dichloroethane and a base under solvent-free reaction conditions. This pathway implies usually harsh conditions (high temperature and long time) and in some cases, a mixture of products can be observed.³⁵

The reaction conditions for the syntheses of imidazolium derivatives with the pathways ii, iii, iv and v are harsher than the ones used in the functionalization at the nitrogen atom. In this thesis, this reaction pathway (i) will be the most used (Chapter 2, 3 and 4) with respect to the other pathways.

1.5 Synthesis of NHC-metal complexes

In this section, the different ways to synthesize transition metal complexes with N-heterocyclic carbene ligands will be described.

In general two different approaches can be envisaged for the synthesis of N-heterocyclic carbene complexes: i) the preformed carbene (isolated or generated *in situ* as described below) can bind the metal center or ii) an isocyanide, activated towards nucleophilic attack by coordination to the metal center, reacts with an amine to form the NHC complex (Scheme 1.6).³⁶



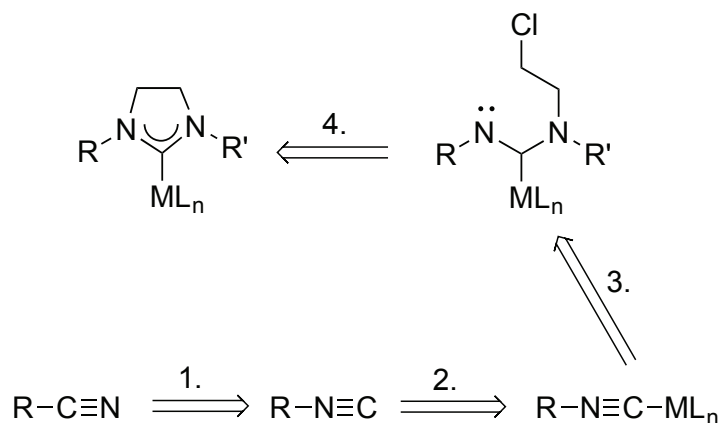
Scheme 1.6: different pathways for the synthesis of NHC transition metal complexes

As described previously, the imidazolium salts, precursor of the NHC ligands, are very easy to synthesize. The isocyanide are not very stable species, sometimes they are not easy to prepare and, in general, is it easier to functionalize the NHC scaffold with respect to the isocyanide one. Finally, the “preformed” NHCs can react with a wide range of metal centers, both in high or low oxidation state. By contrast, the reaction of the isocyanide with the amines to give the coordinated carbene, strongly depends on the nature of the metal center, that should be electron poor. For all these reasons, the first approach is preferred to the second one.

In any case, the syntheses of transition metal complexes via nucleophilic attack of an amine to a functionalized isonitrile ligand coordinated to the metal center, followed by

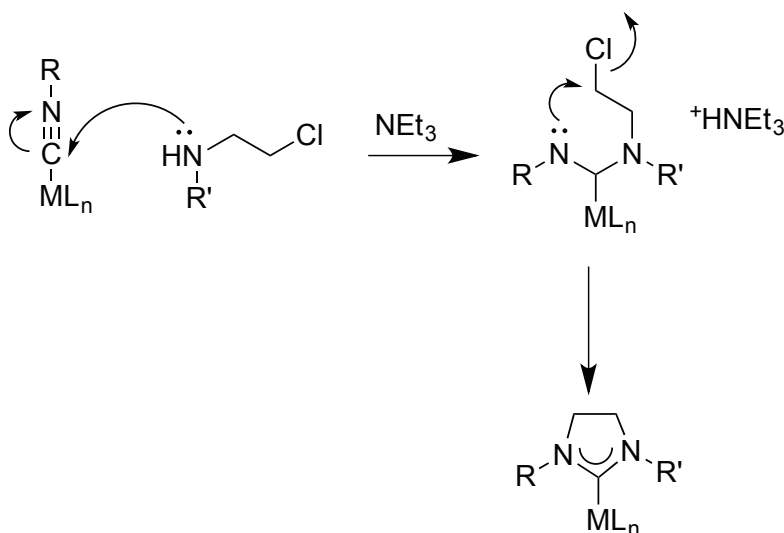
intramolecular cyclization and consequent formation of the NHC (Scheme 1.6, ii) is a procedure that requires various synthetic steps (Scheme 1.7):

1. syntheses of the isonitrile compound;
2. coordination of the isonitrile to a metal precursor;
3. reaction with the amine;
4. ring closure.



Scheme 1.7: retrosynthetic pathway for the syntheses of NHC-metal complex starting from isonitriles

The most important step is the nucleophilic attack of the nitrogen of an amine to the isonitrile carbon, following the procedure reported in Scheme 1.8.^{37,38}

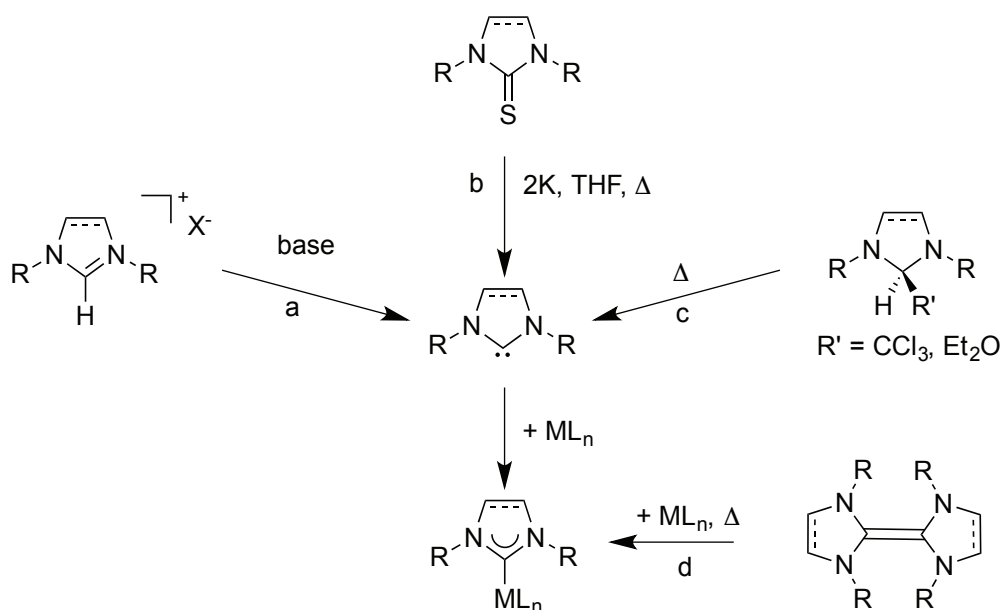


Scheme 1.8: formation of NHC complexes

As regards, the first approach to the synthesis of NHC-complexes, there are different reactions that can afford the formation of the carbene fragment (Scheme 1.9):

- a) treatment of the preformed carbene proligand with a base in order to deprotonate the position 2 of the NHC;

- b) treatment of an imidazole-2-thione with potassium;
 c) thermal treatment of an imidazole proligand bearing a good leaving group in position 2 of the NHC scaffold.³⁹

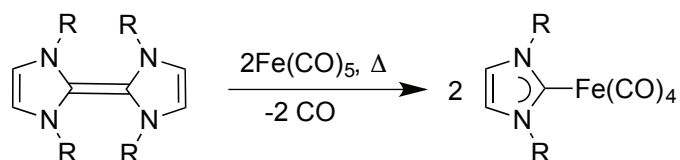


Scheme 1.9: different pathways for the synthesis of free carbene and transition metal complexes

In pathway *a*, different bases can be used, starting from really strong ones to milder ones and with different nucleophilic properties (KO^tBu, BuLi, NaH, NaOAc, K₂CO₃ and others, under various reaction conditions and solvents).

Due to the instability of the free carbene in solution and in air, it is important to work in inert and dry conditions.

Depending on the N-substituents, the free carbenes may dimerize, giving an olefin; these formed organic species can be considered good candidates as precursor for the synthesis of transition metal complexes (Scheme 1.9 pathway *d*). In order to obtain a metal compound, the thermal treatment of an electron rich olefin in presence of an electron poor metal precursor allows to obtain the opportune metal complex⁴⁰ (Scheme 1.9 and example Scheme 1.10).

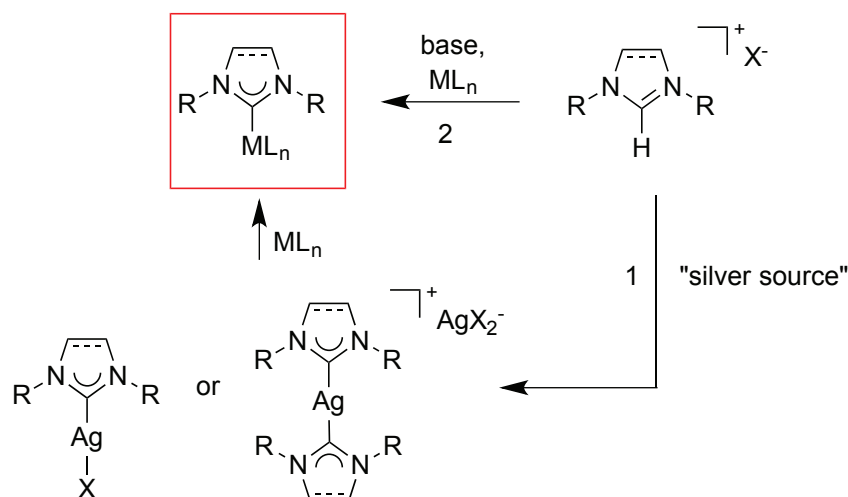


Scheme 1.10: formation of Fe(0) complex starting from an olefin and a Fe(0) metal precursor by thermal cleavage treatment

Another approach for the synthesis of transition metal complexes is the transmetalation of the NHC ligand from a silver(I) NHC complex to a second metal center. The synthesis of the silver(I) complex belongs to the first approach, i.e. to the deprotonation of the azolium salt to give the carbene ligand. This reaction occurs in fact between the azolium salt and usually silver(I) oxide, which acts both as a base, to give the free carbene *in situ*, and as metal precursor forming the complex.

In Scheme 1.11 the two different procedures to obtain a metal complex starting from the azolium salt are depicted:

- *transmetalation* of the NHC ligand from the preformed silver(I) complex (Scheme 1.11, pathway 1);
- *in-situ* deprotonation of the proligand with a base in presence of an opportune metallic precursor to obtain the metal complex (Scheme 1.11, pathway 2).



Scheme 1.11: syntheses of metal complexes via 1) silver(I) complex or 2) deprotonation in presence of a metal

Concerning the *transmetalation*, different silver(I) compounds can be used to form the silver(I) NHC complexes, like for example Ag_2O , Ag_2CO_3 , $AgNO_3$ and $AgOAc$. Generally, the reaction conditions are very mild (room temperature), the scope of used solvent is very large (also water can be employed); furthermore it is not strictly necessary to adopt an inert atmosphere and generally the required purifications of the product are simple.⁴¹ It is interesting to underline that the nature of the counterion of the proligands is important in determining the structures of the obtained products (Figure 1.14).^{1b}

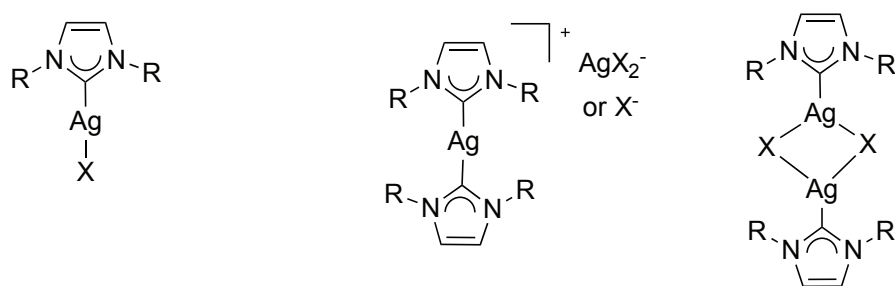
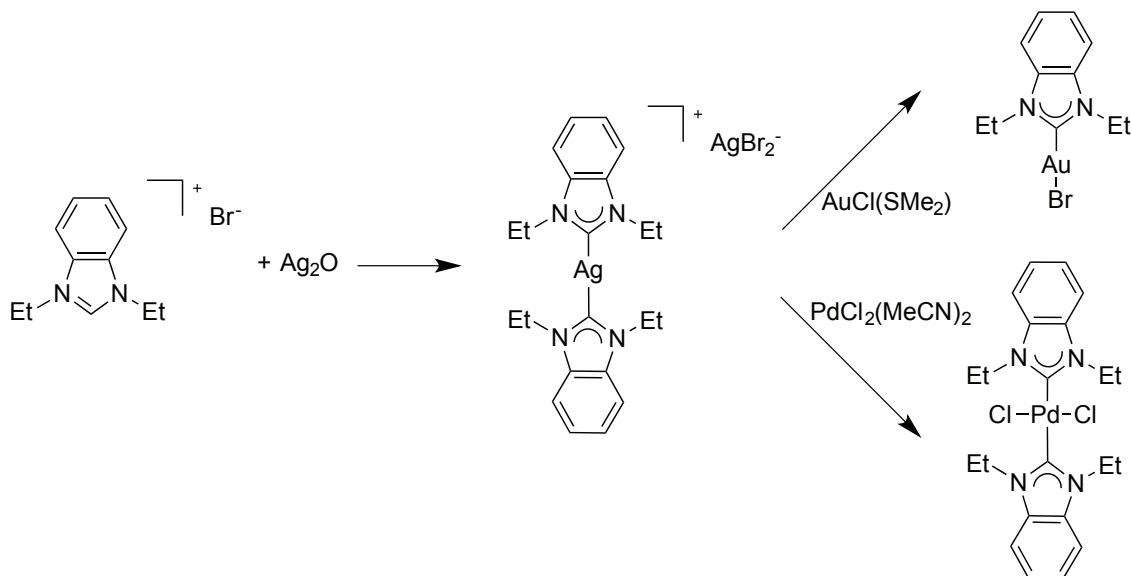


Figure 1.14: examples of silver(I) complexes with different structures

The second step, i.e the *transmetalation* of the carbene ligand to another metal center, can be facilitated with the employment of a metal halide precursor: the formation of silver(I) halide, that is insoluble in most organic solvents, provides the driving force for the formation of metal-NHC complexes. The biggest advantage of this procedure is the possibility to work in really mild conditions, so that the possibility of side reactions is minimized.

For example, Lin *et al.*⁴² adopted this procedure to transmetalate the NHC scaffold to gold(I) or palladium(II) centers using really mild condition (room temperature for a short period), obtaining the complexes in good yields and purities (Scheme 1.12).

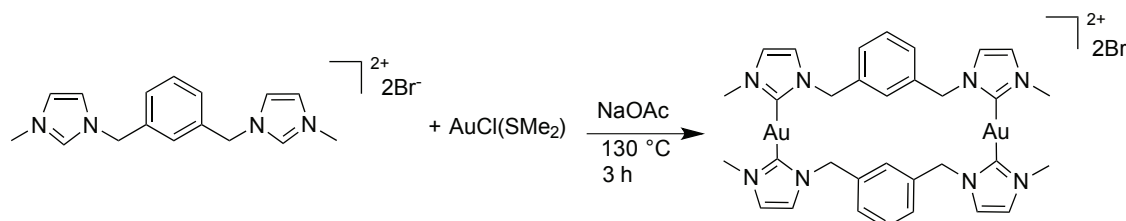


Scheme 1.12: transmetalation of the carbene ligand to gold(I) or palladium(II) centers

Concerning the deprotonation pathway, as described before, the free carbene may be unstable so usually the base and the metal precursor are added together in the reaction

mixture, in order to coordinate the NHC as formed and thus avoiding other decomposition or evolution pathways.

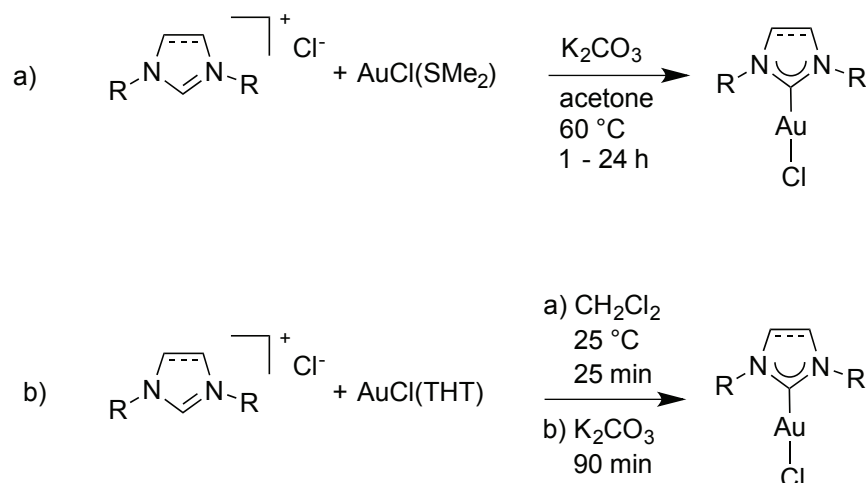
One of the most used procedures for the syntheses of gold(I) complexes is the treatment of the precursor of the ligand with a mild base (usually NaOAc) in presence of the proper gold(I) precursor in DMF at high temperature (130 °C) (Scheme 1.13).⁴³



Scheme 1.13: in situ deprotonation of the azolium salt and synthesis of gold(I) complex

This procedure cannot be adopted for all the azolium salts, since some substituents to the heterocyclic ring cannot tolerate the harsh reaction conditions (like for example alkynyl substituents).

For this purpose, Nolan⁴⁴ and Gimeno⁴⁵ developed a similar strategy but using really mild conditions (Scheme 1.14).



Scheme 1.14: procedure reported by Nolan a) and Gimeno b) for the synthesis of metal complexes using mild conditions

1.6 Applications of NHC-metal complexes

NHC-metal complexes are a versatile class of compound that can be used for different applications, spanning from luminescence to catalysis or to medicinal chemistry.⁴⁶

The widest field of application for NHC-transition metal complexes is surely the field of catalysis and it is difficult to summarize this topic in few pages due to the high number of different metal centers that can be adopted and the several reactions that can be catalyzed by the various metal complexes. In this regard there are several reviews that summarize the use of each metal center in several catalytic reactions or describe the different metal complexes employed to catalyze the same reaction.⁴⁷

Two different metal centers can be connected via the same poly-NHC ligand, thus giving different heterobimetallic complexes. Also in this field, several reaction can be catalyzed and the cooperativity effect can be the added value for the syntheses of the desired compound.⁴⁸

In the next paragraphs we would like to briefly describe the state of the art on the applications of NHC complexes as luminescent compounds and as therapeutic agents in medicinal chemistry; these fields of research will be analysed because the complexes synthesized and described in this thesis will be used in these regards.

First of all it is important to introduce the concept of “metallophilic interaction” because of the luminescence applications, especially for the gold(I) complexes.

1.6.1 Metallophilic interaction

The metallophilic interaction is a weak *intra* or *inter*-molecular interaction between heavy metal centers that is usually associated to the luminescence properties of the complexes.⁴⁹

This property is observed with different heavy metal centers but with gold(I) (d^{10} configuration) this interaction is more important and it is named “*aurophilic interaction*” or “*aurophilicity*”.

In most cases the aurophilic interaction is present between linearly dicoordinated gold(I) (d^{10} close shell electronic configuration) centers. The low coordination number is an important parameter due to the minimization of the steric repulsions between the ligands in the aggregates.

In terms of energies, the interactions between different gold centers are weak, in the range of 7 – 12 Kcal/mol,⁵⁰ comparable to the energy of the H-bond interaction but stronger than the van der Waals interactions.

Concerning the number of gold(I) centers involved in this interaction, each metal can be involved in one or more aurophilic contacts that are generally present perpendicularly to the axis defined by the metal centers and the two coordinated ancillary ligands. The distance between the metal centers spans in the range 2.5 - 3.5 Å and is lower than the sum of the van der Waals radii (for two gold(I) centers 3.7 Å).

The aurophilic interaction may be reversible and depends on several factors, like for example the presence of bulky ligands, steric hindrance around the metal centers, reticular forces in crystal and solvation energies in solution. Other parameters, such as temperature or complex concentration in solution, can modify the effects related to this interaction.

As stated above, the presence of metallophilic interaction is usually coupled with solid state photoluminescence in UV-Vis region. The presence of heavy metal center, like gold, enhances the spin-orbit coupling of the system, thus increasing the probability to reach a triplet excited state via intersystem crossing (ISC) and to have a radiative decay via phosphorescence with large Stock shift.⁵¹

It is not always easy to attribute the emission properties to a specific electronic transition but there are many cases in which the metal-metal interaction shows a fundamental role in these transitions.⁵²

In addition with the aurophilic or generally the metallophilic interaction, there is another effect, called *relativistic effect*, that can contribute in modifying the electronic structure of the system and can be important to understand the photochemical properties of species.

Due to the high-speed of the electrons when they move near heavy nuclei, a resulting mass increase is observed and leads to an energetic stabilization and radial contraction, especially for the s and p orbitals. This contraction has, as consequence, a stronger shielding of the nuclear charge, that is reflected in a destabilization and expansion for the d and f orbitals. These effects are maximized in the case of gold, since it presents a maximum relativistic effect among all its local neighbours in the periodic table.

In the case of polynuclear gold complexes, molecular orbitals based on 5d occupied orbitals are destabilized, while molecular orbitals based on empty 5s and 5p orbitals are stabilized. As a consequence, the HOMO-LUMO gap is decreased and at the same time the excited states are stabilized, so the probability of electronic transition is enhanced.

Different groups used theoretical methods to quantify the aurophilic interaction. Pyykkö *et al.* shows that aurophilic interaction has a dispersive (van der Waals) nature.⁵³ Two equations have been obtained and, in general, the D_e (aurophilic interaction energy) is a function of the equilibrium distances R_e (in pm) and take into account different other parameters as n (free parameters, 3.95 in Pyykkö studies), a and b (the so-called Hershbach-Laurie parameters, which can be obtained from Raman spectroscopy combined with crystallography).⁵³

$$D_e [KJ/mol] = \left(\frac{R_e b}{n}\right) * (6.022 * 10^{-2}) e^{(R_e - a)/b}$$
$$D_e [J] = \left(\frac{R_e b}{n}\right) [10^2 Nm^{-1}] * e^{(R_e - a)/b}$$

Equations 1.1: equation for the calculation of the aurophilic interaction energy D_e reported by Pyykkö

Schwerdtferger *et al.*⁵⁴ proposed another simpler equation that take into account the equilibrium distance R_e (Equation 1.2).

$$D_e [KJ/mol] = \left(\frac{R_e b}{n}\right) * (1.27 * 10^6) e^{(-0.035 R_e)}$$

Equation 1.2: equation for the calculation of the aurophilic interaction energy D_e reported by Schwerdtferger

With both equations it is possible to estimate the energy associated with the aurophilic interaction and the obtained values are in agreement with the experimental ones. Furthermore, Pyykkö has also studied the influence of the ligands coordinated to the gold(I) centers in determining the force of these interaction and NHCs appears as the ligands able to promote the stronger aurophilicity.

1.6.2 Luminescence application

$[\text{Ru}(\text{bpy})_3]^{2+}$ and $[\text{Ru}(\text{tpy})_2]^{2+}$ complexes and functionalized derivatives have received considerable attention as potential chromophoric species and can be used in various research fields as light emitting devices, sensors or photosensitizers in the artificial photosynthesis (Figure 1.15).⁵⁵

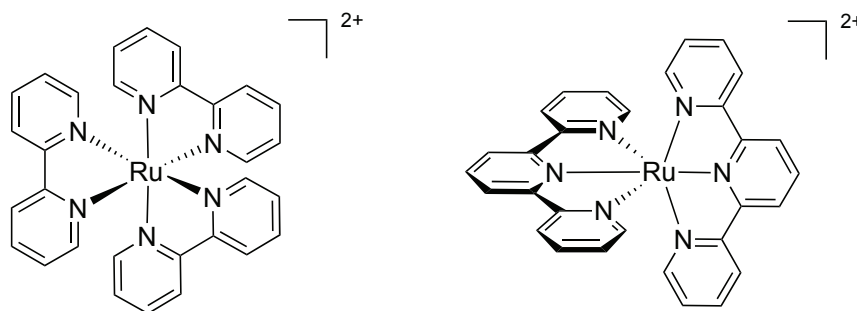


Figure 1.15: general structure of $[\text{Ru}(\text{bpy})_3]^{2+}$ (left) and $[\text{Ru}(\text{tpy})_2]^{2+}$ (right)

The possibility to introduce one or more NHC moiety instead of the pyridine one could change and modulate the electron properties of the complexes and, as a consequence, of the absorption-emission parameters.

Chung *et al.*⁵⁶ synthesized complexes similar to $[\text{Ru}(\text{bpy})_3]^{2+}$ and $[\text{Ru}(\text{tpy})_2]^{2+}$ changing the number of imidazole-2-ylidene moieties and compared the luminescence properties of the synthesized compounds with the ruthenium(II) complexes mentioned above (Figure 1.16).

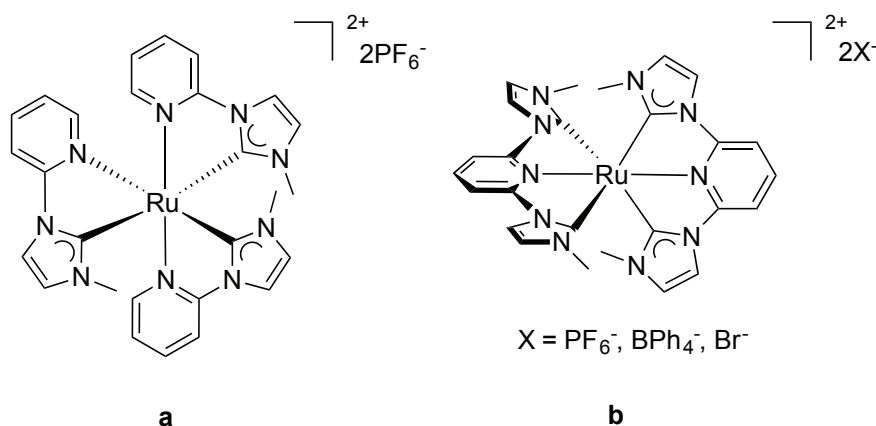


Figure 1.16: ruthenium(II) complexes synthesized by Chung

Interestingly, complex **a** shows a blue shift with respect to $[\text{Ru}(\text{bpy})_3]^{2+}$ in the absorption spectrum probably due to the more electron donating properties of the NHC. Concerning the emissive properties, the complex is completely nonemissive in solution.

The complexes of type **b** (with different counterions) show a blue shift in the absorption spectra and an interesting emissive behavior has been observed, due to the modification of the scaffold (pyridine/NHC exchange).

Table 1.1 it is possible to observe that the novel complexes have an impressive emission compared with the complex with tpy ligand, due to the modification of the scaffold (pyridine/NHC exchange).

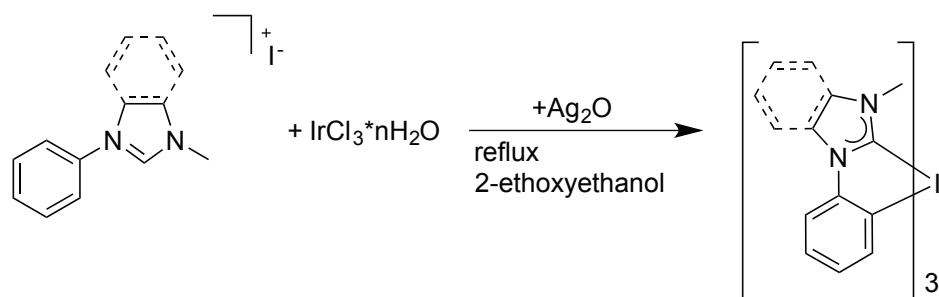
Table 1.1: spectroscopic properties of Ru(II) complexes^a

Complex	λ_{max}^{abs} [nm]	ϵ [$10^3 M^{-1} cm^{-1}$]	λ_{max}^{em} [nm]	Rel em int ^b	Decay time [ns]
[Ru(bpy) ₃] ²⁺	450	14.3	597	3.83	860 ⁵⁵
[Ru(tpy) ₂] ²⁺	474	17.2			0.25 ^c
a	368	11.7			
b(PF₆⁻)	343, 382	11.6, 15.2	532	1.04	820
b(BPh₄⁻)	343, 382	15.6, 20.1	532	0.39	490
b(Br⁻)	343, 382	13.0, 16.8	532	1.10	600
b(Br⁻) (H₂O)	341, 381	13.8, 17.3	532	9.90	3100

^a 2.33*10⁻⁵ M in acetonitrile (if not differently specified) at room temperature. ^b relative maximum intensity at emission. ^c ref 57

In particular, the counter-ions show an important role in influencing the emission properties: the complexes with PF₆⁻ and Br⁻ (especially in water) have a very high decay time, if compared with the [Ru(tpy)₂]²⁺. This is probably due to a different charge redistribution (that change with the solvent) that can quench the luminescence of the complex.

Thompson and coworkers⁵⁸ used functionalized imidazolium salts as proligands for the synthesis of iridium(III) complexes with the procedure reported in Scheme 1.15, it was possible to obtain pure iridium(III) complexes in *fac* and *mer* configuration.

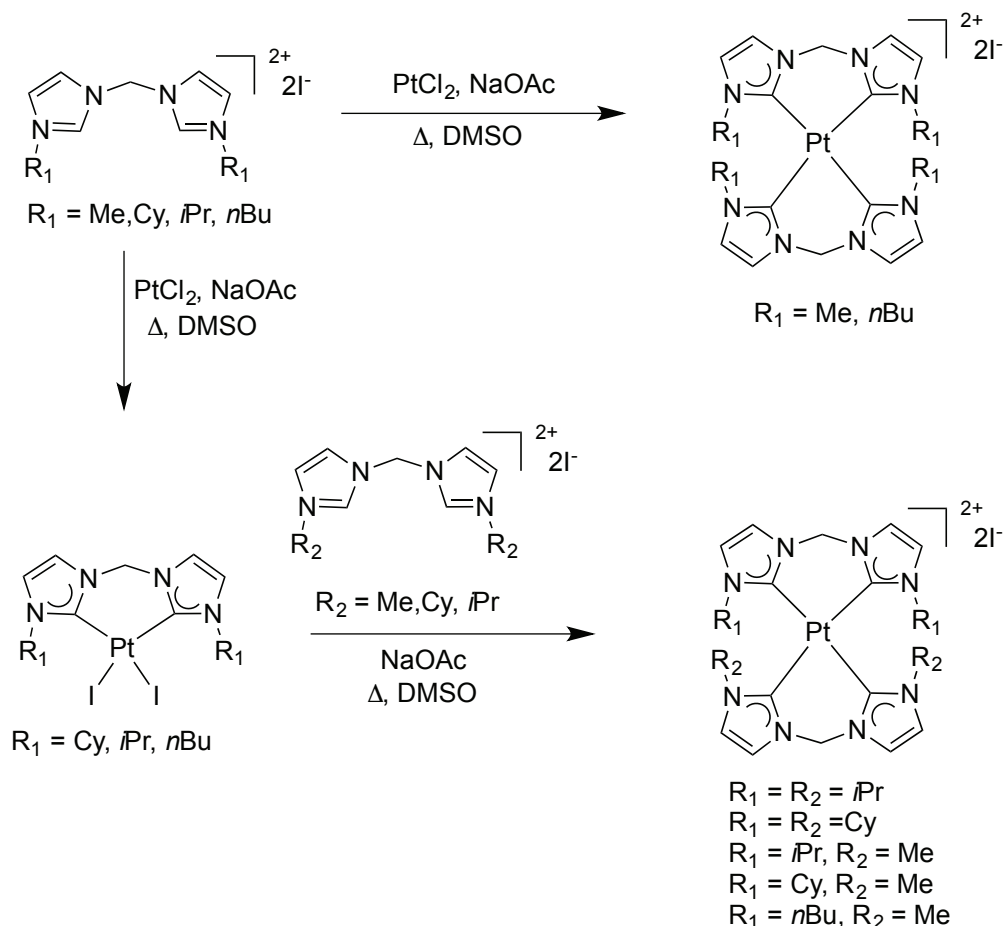


Scheme 1.15: synthesis of iridium(III) complexes

The *fac*- and *mer*-isomers have similar absorption band shapes. The Ir(III) complexes display intense emission at 77 K in the near-UV spectrum and, notably, also luminesce at room temperature in solution is observed. The complexes exhibit higher luminescent quantum yields than related pyrazolyl-based systems.

The fact that near-UV emission is observed at room temperature for the $[\text{Ir}(\text{NHCs})_3]$ complexes suggests that the non-emissive excited state for these complexes has been significantly destabilized with respect to the corresponding excited state in related pyrazolyl-based complexes due to the different electronical features of the two classes of complexes.

The group of Strassner⁵⁹ is very active in the field of luminescent NHC complexes mostly with platinum(II). Working with bis(imidazolium) salts with methylene bridge between the imidazole moieties and the opportune Pt(II) precursor, they obtained the bischelate complexes of platinum(II) of general formula $[\text{Pt}(\text{L})_2]\text{I}_2$ with two different procedures (Scheme 1.16).

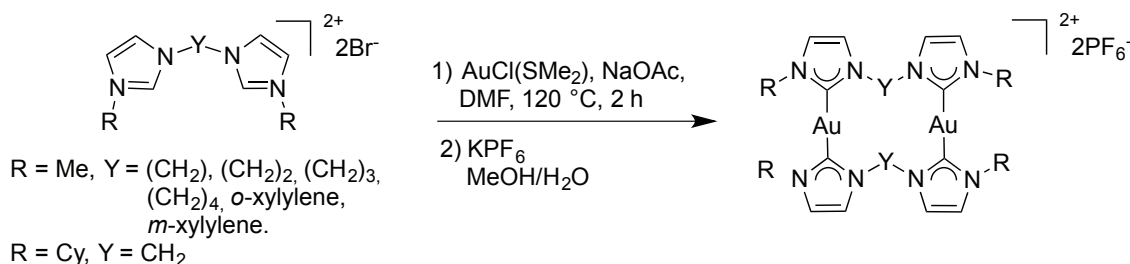


Scheme 1.16: reaction pathways for the syntheses of platinum(II) complexes

The absorption spectra of the different complexes show the same shapes and maxima. Concerning the emission spectra, the maxima wavelengths are independent from the substituents, but the quantum yields differ significantly.

Concerning gold(I) complexes, the group of Tubaro³¹ reported the synthesis and luminescence properties of dinuclear gold(I) complexes in which the aurophilic interaction is the key element for the comprehension of the high quantum yield.

Different gold(I) complexes have been synthesized using the procedure in which the proligands react with gold(I) precursor in presence of a mild base, followed by anion exchange from Br^- to PF_6^- (Scheme 1.17).



Scheme 1.17: synthesis of different gold(I) complexes

The photophysical properties of these gold(I) complexes have been investigated both in solution and in solid at 77 K and room temperature. All the absorption maxima are centered in the near UV region (220 - 330 nm) and can be attributed to a $\pi-\pi^*$ ligand centered transition. In solution, all the complexes are stable but they are weak emitters (Φ_{em} up to 0.4 %). In solid state, the complexes reported in Figure 1.17 are relatively strong emitters, especially the gold(I) complex with propylene bridge between the two carbene units.

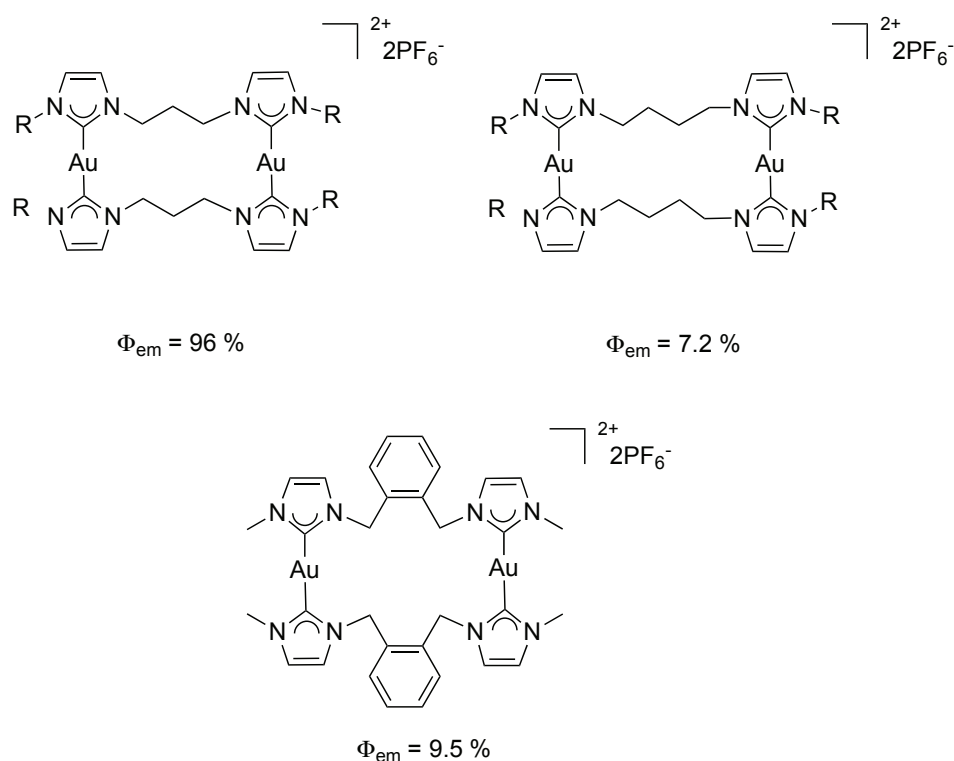


Figure 1.17: gold(I) complexes that show important quantum yield

It is interesting to note that in the crystal structure, the complex with propylene bridge shows a gold-gold distance of 3.2722(5) Å, that is indicative of the presence of aurophilic interactions. Notably, the Au \cdots Au distance is significantly shorter than the

one observed for complex bearing the methylene bridge (3.5425(6) Å): this is due to the fact that the propylene linkers of the two bridging dicarbene ligands are arranged on the same side with respect to the mean plane defined by the gold and the carbene carbon atoms. This particular arrangement of the structure allows to bring the gold(I) centers very closed (Figure 1.18).

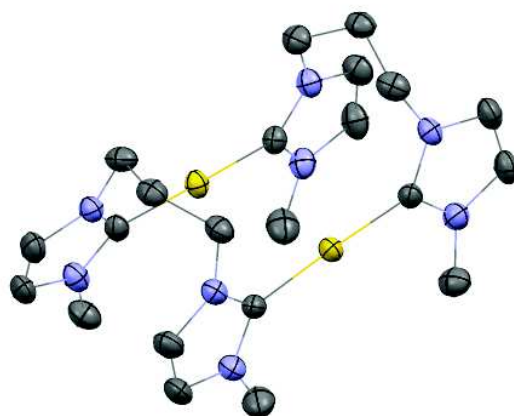


Figure 1.18: ORTEP view of the cationic gold(I) complex with propylene bridge (hydrogens and PF_6^- are omitted for clarity). Gold atoms in yellow, carbon atoms in grey and nitrogen atoms in lilac

The high quantum yield in the solid state can be attributed to the peculiar arrangement of the complex molecules in the solid state, both in crystals and in powder. The excellent luminescence properties of gold(I) complex with propylene bridge in terms of color and intensity make it appealing for electroluminescent devices.

1.6.3 *Anti-tumoral applications*

Transition metal complexes have been discovered to be important compounds in biological applications especially in the treatment of tumors.

Among them, *cis*-platin, discovered by Rosenberg in 60's,⁶⁰ is a highly active compound against different cancer cell lines, effecting cures for 70 – 90 % of testicular cancer, but also is highly effective against ovarian cell lines, head and neck cancers, bladder cancers and different lymphomas.⁶¹

However, this compound presents undesirable side effects as neurotoxicity and nephrotoxicity so different metal complexes have been studied as alternative anticancer agents and this field is still an highly active field with the purpose of finding more

effective anti-tumor agents with less side effects.⁶²

Modification on the substituents on the platinum center (Figure 1.19) allows to decrease the collateral effect of the treatments of cancers and significant research has regarded the possibility to find complexes which are active against cancer cells and inactive with non-cancer cells.

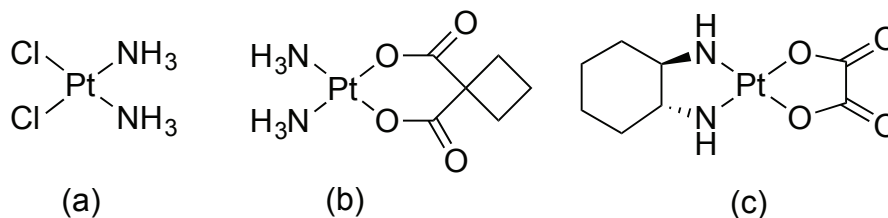


Figure 1.19: examples of different Pt(II) compounds: *cisplatin* (a), *carboplatin* (b) and *oxaliplatin* (c)

Interestingly, metal–NHC complexes display promising pharmacological properties as novel antitumor drugs and some NHC complexes exhibit cytotoxic effects comparable to *cis-platin*.⁶³ In addition, some of them (e.g. with Ag, Au, Pt, Ru metal) have shown to be efficient also *in vivo*. Regarding their mode of action, the choice of the coordinated metal most probably determines the main biological target.

Pt–NHC complexes have been highlighted as a promising and original platform for building new cytotoxic drugs of the *cis-platin* series.

Different NHC–Pt–amine compounds have been synthesized and show lower IC_{50} compared to *cis-platin* and interesting selectivity (Figure 1.20).⁶⁴ It is important to underline that the modulability of the NHC scaffold is an important point on the possibility to optimize the structure of the complex and find the most active species.

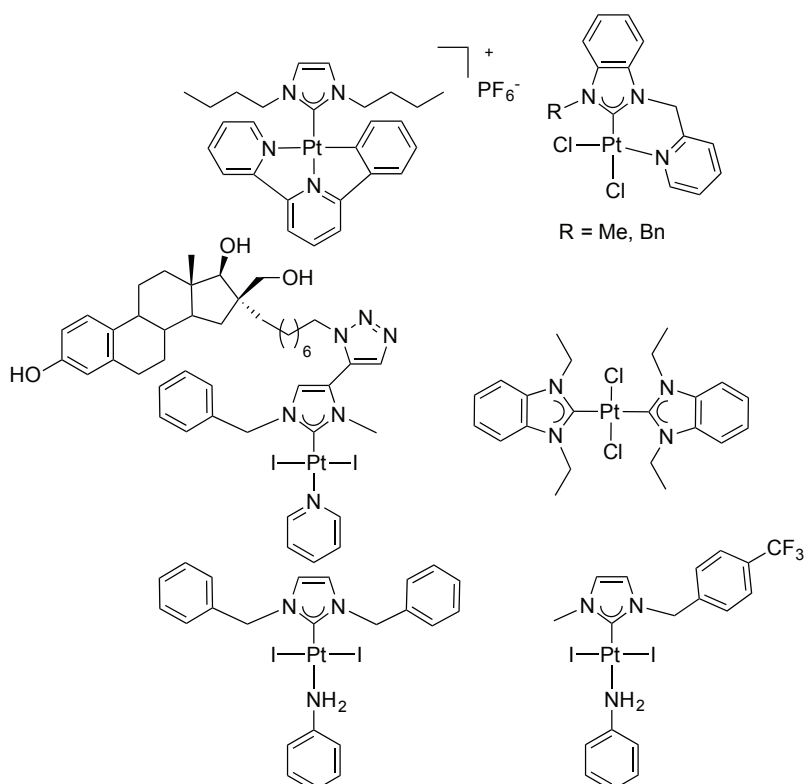


Figure 1.20: some Pt(II)-NHC complexes that have been studied for their antitumoral properties

Other strategies have focused on applying Pt(IV) complexes that are more reactive, less toxic than Pt(II) complexes and more soluble in water. Bellemin-Laponnaz *et al.*⁶⁵ made a screening of several platinum(IV) NHC complexes and found that there is a correlation between the stability of the complexes and their antiproliferative activities (Figure 1.21).

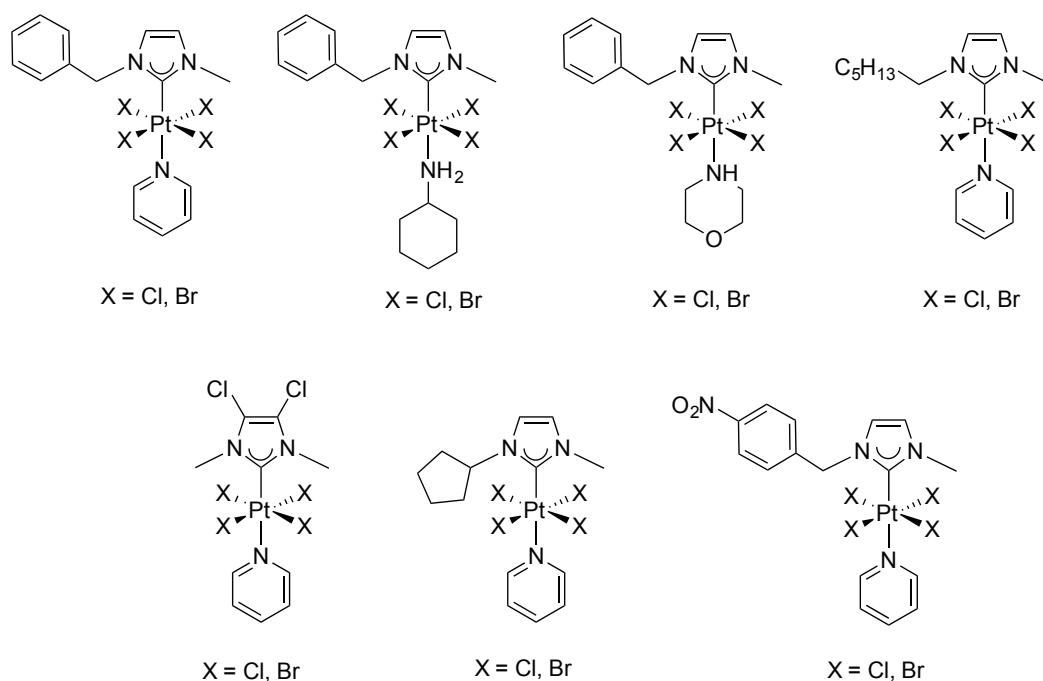
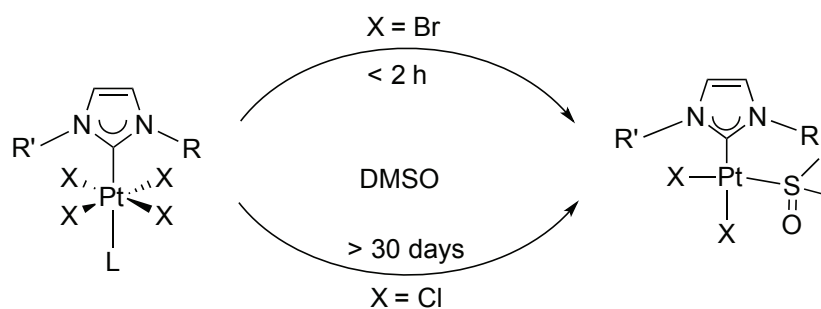


Figure 1.21: examples of Pt(IV) complexes

The results are really promising: the observed IC_{50} values are lower than those obtained using the corresponding Pt(II) complexes. Another point that should be taken into account is the stability of the complexes in the reaction media (usually DMSO/water): during the time needed for the IC_{50} experiments the complexes are stable but, using lower concentrations, a decomposition via reduction to the Pt(II) complex can be observed. This behavior can be important in influencing the mechanism of action of these complexes.



Scheme 1.18: decomposition pathway from Pt(IV) to Pt(II) complexes

Silver(I) complexes are usually used as antimicrobial species and recently they found application as antiseptics.⁶⁶ Nowadays different silver(I) NHC complexes have been studied against different cancer cell lines. It is difficult to find a correlation between apoptosis of the cells and the structure of the carbenes but it seems that the metal-

carbene carbon bond has an important role in the possibility to release the metal in the cell media. In Figure 1.22 different silver(I) complexes have been proposed; the modulability of the system can be useful for changing the lipophilic properties and the stability of the complexes in the cellular media.⁶⁷

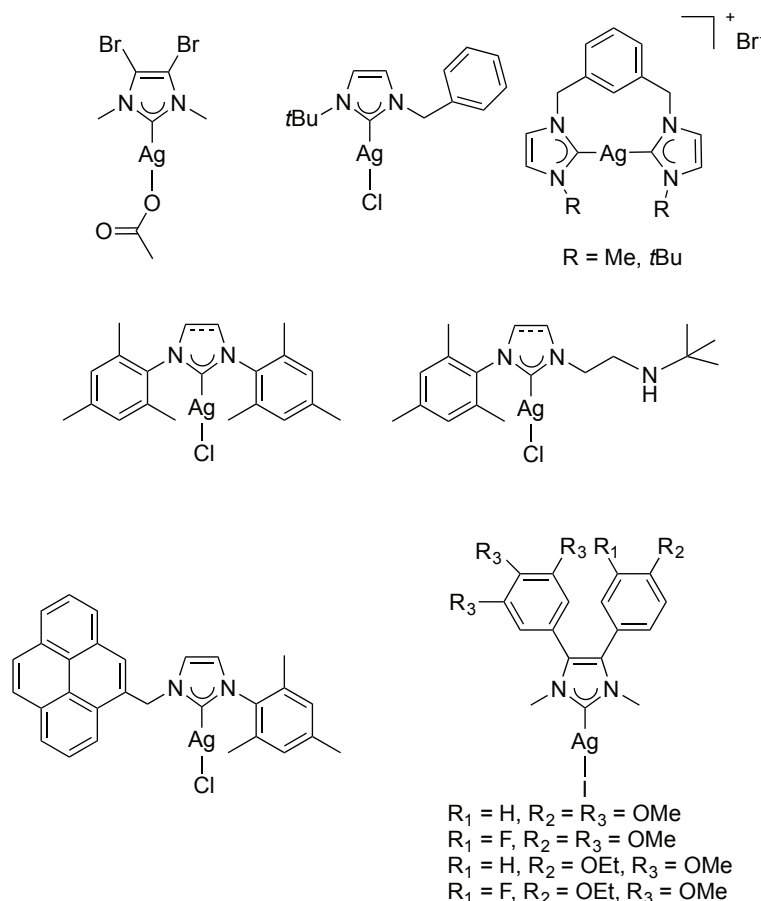


Figure 1.22: different silver(I) complexes used for antitumoral application

Moving to gold(I) complexes, the first species used in medicinal chemistry were the Aurophin and Et_3PAuCl ; their efficiency is associated to the inhibition of the TrxR enzyme (thioredoxin reductase), important for the control of mitochondrial function and the intracellular redox activity (Figure 1.23).⁶⁸

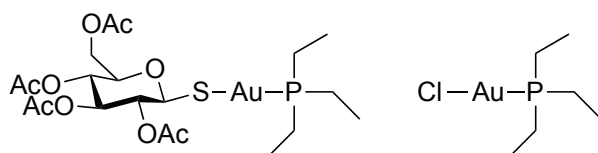


Figure 1.23: structure of aurophin (left) and Et_3PAuCl (right)

The number of gold complexes that can be synthesized is very large and based on the structural variety of the used ligands, a unique mode of action or pharmacological

profile is unlikely to exist.

As discussed for the previous NHC compounds, different modifications on the scaffold of the carbene can be done in order to modify different parameters (lipophilicity, logP, steric hindrance,...) and increase the performances of the complexes.

Some of the most interesting gold(I) NHC complexes are reported in Figure 1.24^{69,17} but other complexes with different groups bonded directly to the gold(I) center (especially thiol functions) and different substituents on the backbone or on the nitrogen wingtip atom on the NHC have been also employed with interesting results.

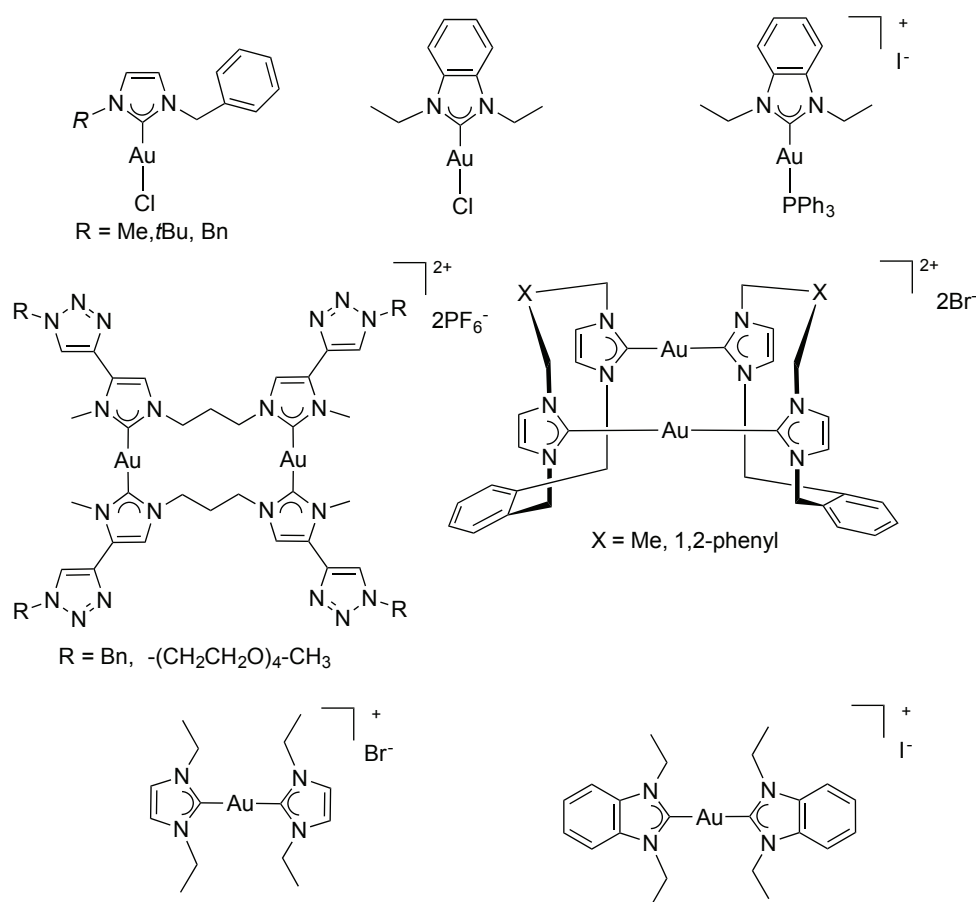


Figure 1.24: some structures of Au(I) NHC complexes

Some dicarbene complexes are also reported and the presence of more than one gold(I) atom could suggest the presence of a cooperative effect, important in the apoptosis.

Besides the mentioned silver, gold and platinum derivatives, NHC complexes with palladium and copper have also been recently reported to exhibit antiproliferative properties.

Palladium(II) complexes are studied because of the analogous electronic structure and

geometry to platinum(II) complexes; they present higher cytotoxicity with respect to gold(I), platinum(II) and silver(I) complexes bearing the same NHC ligands.⁷⁰ These interesting results could be attributed to the possibility of Pd(II) complexes to interact with DNA, thus enabling cross bindings, inhibiting the synthesis of damaged DNA as well as inducing apoptosis.

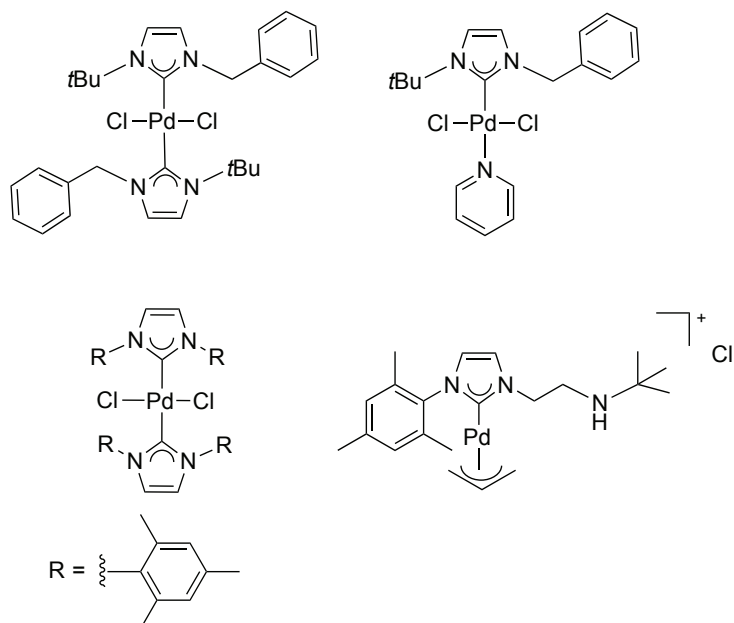


Figure 1.25: examples of palladium(II) metal complexes

Concerning copper(I,II)⁷¹ metal centers, they are important for the function of several enzymes and proteins and are involved in a lot of physiological processes and for these reasons, they may be less toxic than non-essential metals, such as platinum. For this purpose, recently different copper metal complexes (examples depicted in Figure 1.26) were studied. These compounds have shown relatively high stability in different media, that might allow them to reach biological targets inside the cell; this evidence is reflected with high cytotoxicity against different cancer cell lines.

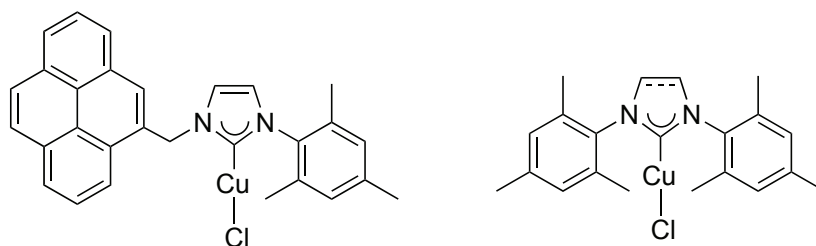


Figure 1.26: examples of copper metal complexes

Finally, nickel(II) and ruthenium in different oxidation states can be used as metal centers for the syntheses of NHC transition metal complexes with antitumoral applications.

It is important to underline that it is fundamental to synthesize nickel complexes with intrinsic low toxicity: a drastic reduction in the cytotoxic activity of nickel was successfully achieved by encapsulation of the metal center in Ni–NHC complexes by employing a new class of tightly binding NHC ligand. The number of examples is not as wide as for other metal centers due to the intrinsic toxicity of the metal that is difficult to modulate and decrease “with” the organic scaffold (Figure 1.27).⁷²

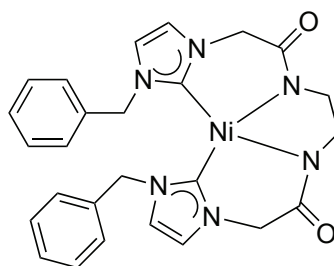


Figure 1.27: example of nickel(II) complex

Ruthenium-based drugs are much less toxic than platinum based drugs and capable of overcoming the resistance induced by platinum drugs in cancer cells. The activity of ruthenium complexes was attributed to the ability of this metal to mime iron in binding to biological molecules. A problem that can be observed with ruthenium complexes is the low stability and solubility in the biological media; it is therefore necessary to functionalize the organic ligand, for example with a peptide conjugated species, in order to improve the solubility of the complex in the cellular environment.⁷³

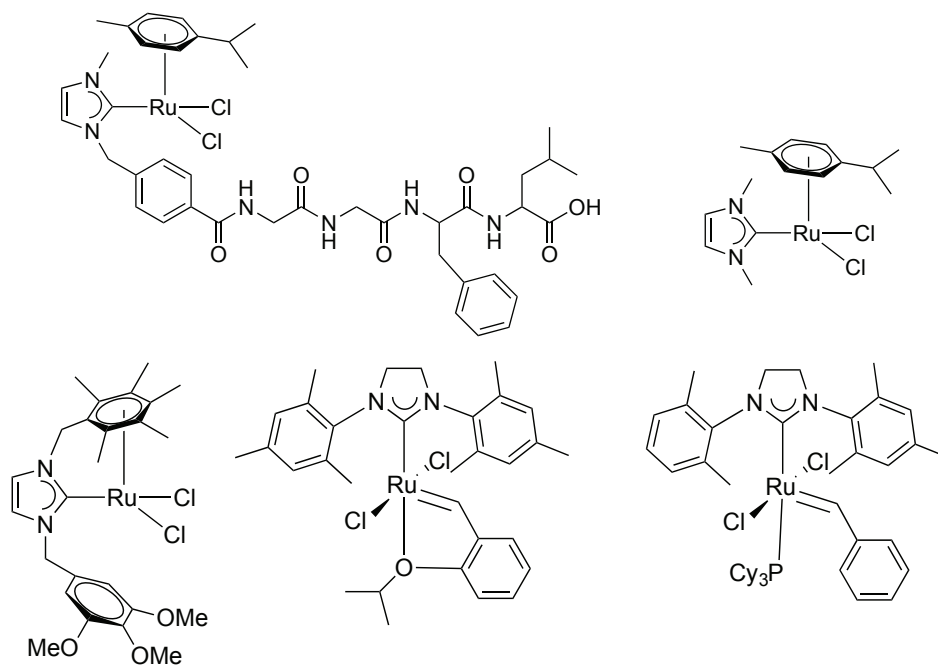


Figure 1.28: examples of ruthenium(II) NHC complexes

In conclusion, although *cis*-platin has achieved significant clinical benefit for some tumours, its effectiveness has been limited by toxic side effects and development of drug resistance.

Metal–NHC complexes display promising pharmacological properties as novel antitumor drugs. Each metal has important peculiarities and it is difficult to understand or predict the mechanism of action of each complex, considering that it can change moving from different ligands and metals.⁶³ An important point is that *in vitro* (most common analysis) and *in vivo* assays (closer to the real application with patients) could give really different results (the best *in vitro* results in IC₅₀ values are not always coherent with good results when conducted in *in vivo*) so it is not always easy to compare the behavior of the complexes.

Chapter 2: RESULTS AND DISCUSSION

Metal complexes with di(N-heterocyclic carbene) ligands bearing a rigid phenylene bridge

2.1 Introduction

In Chapter 1, different dicarbene proligands and the syntheses of the corresponding transition metal complexes were considered and described. The majority of these reported examples contains an aliphatic bridge between the two imidazole moieties; it is well known, that the flexibility of the bridge plays an important role in determining the chelating rather than bridging coordination of the di(N-heterocyclic carbene) ligand on the metal center/s.

In this Chapter, we describe the syntheses of metal complexes with di(N-heterocyclic carbene) ligands that contain a rigid phenylene bridge connecting the two carbene moieties.

Three phenylene bis(imidazolium) proligands have been studied (Figure 2.1). They are characterized by the different substitution of the aromatic bridge (*ortho*, *meta* or *para*).

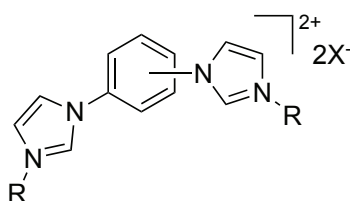


Figure 2.1: *ortho*-, *meta*- and *para*-phenylene bis(imidazolium) salts employed in this study

A limited number of examples has been reported in the literature^{74,75,76,77,78,79} with this type of ligands and most of them involves the *meta*-phenylene bridge between the imidazole moieties. In this particular case, the ligand can easily behave as *CCC*-pincer, as a consequence of metalation of the carbon in position 2 of the phenylene bridge.

Examples in the literature involve various metal centers, like for example titanium(IV),^{74e} ruthenium(II),⁸⁰ rhodium(III),⁸¹ iridium(III)^{76d} palladium(II)⁸² and platinum(II)^{74d,83} (Figure 2.2).

As it is evident from the examples displayed in Figure 2.2, and as already outlined above, with the *para*-ligand and especially with the *meta*-phenylene bis(imidazole) ligands, it is possible to have, in addition to the coordination of the two carbene carbons, the metalation of a phenylene ring giving *CCC*-pincer ligands.

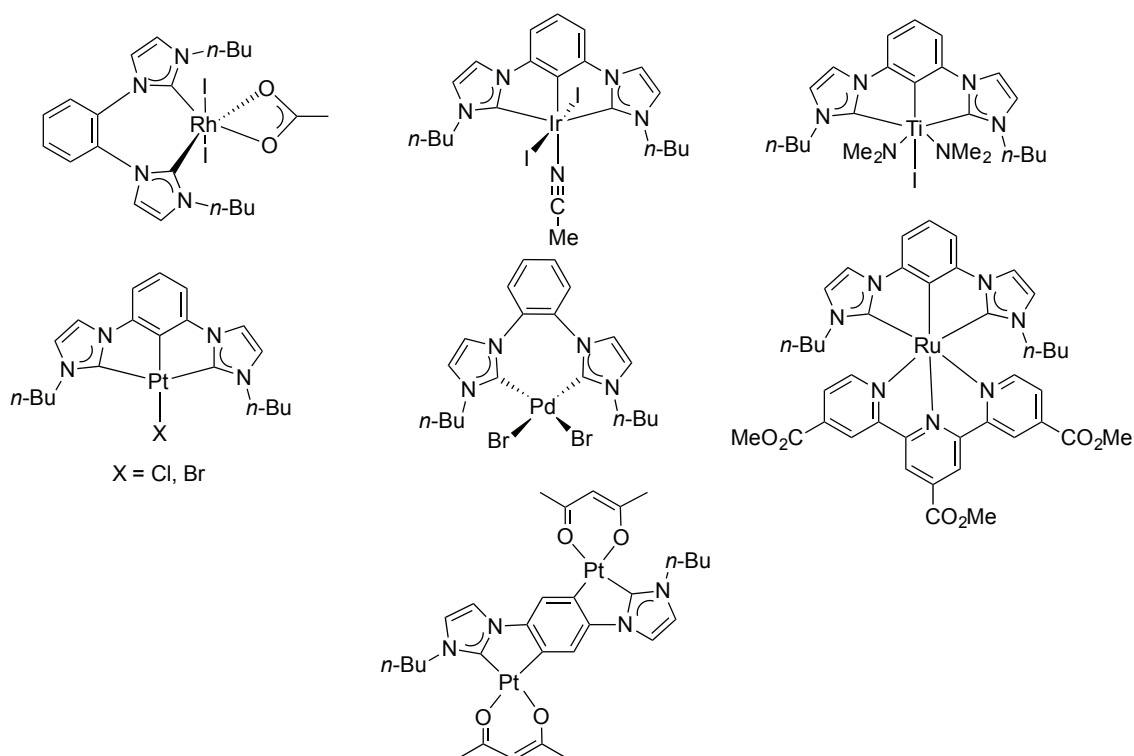
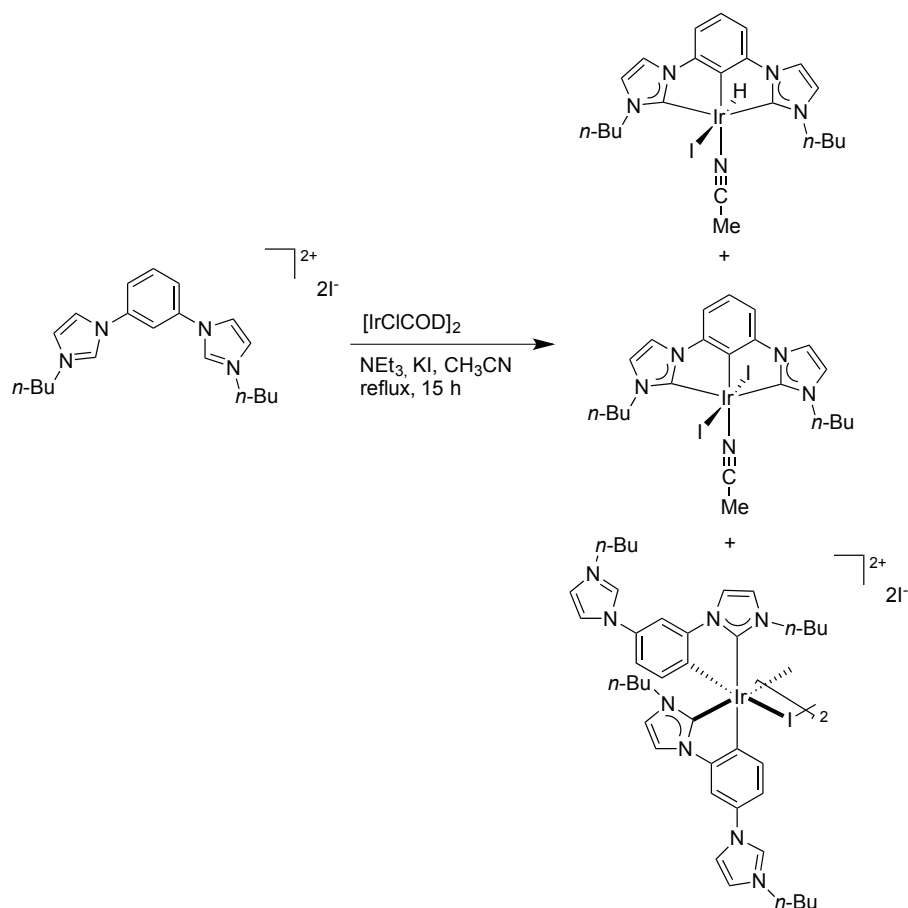


Figure 2.2: examples of metal complexes with di(NHC) bearing a phenylene bridge between the carbene units

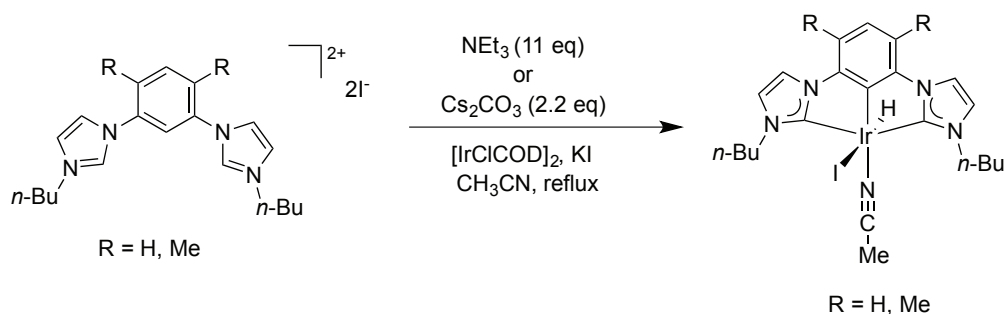
These transition metal complexes are usually obtained via deprotonation of the bis(imidazolium) proligand with an external base (such as NEt_3 , K_2CO_3 , Cs_2CO_3 or $\text{KO}t\text{Bu}$) in the presence of the metal precursor.

The group of Braunstein is very active in this field especially in the syntheses of iridium(III) complexes and in their post-functionalization.^{76d,77a-b} By reacting the *meta*-phenylene bis(imidazolium) proligand in acetonitrile with NEt_3 as base and the proper Ir(I) precursor (i.e. $[\text{IrClCOD}]_2$), a mixture of complexes has been obtained (Scheme 2.1).



Scheme 2.1: syntheses of different iridium(III) complexes

The output of the reaction could be optimized by changing the base and/or the molar ratio between the proligand and the base; in this way only the iridium pincer hydride/iodide complex has been obtained.

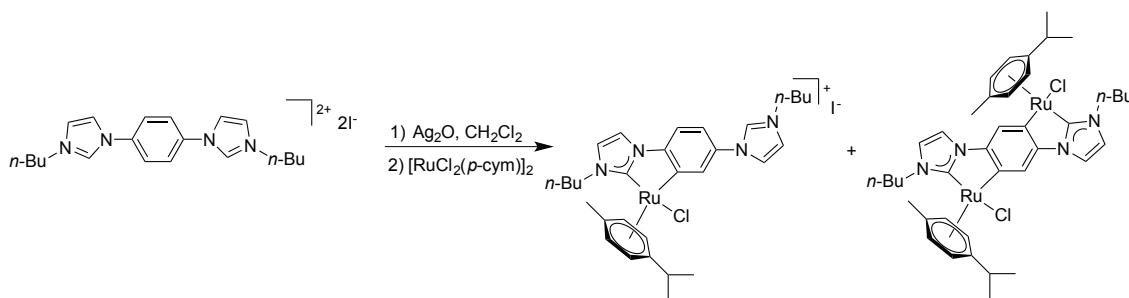


Scheme 2.2: syntheses of an iridium(III) hydride complexes

A different strategy that can be used is the transmetalation of the dicarbene ligand from the preformed corresponding silver(I) complex.

This procedure has been used for example by Albrecht *et al.*⁸⁴ for the syntheses of ruthenium(II) complexes with a *para*-phenylene dicarbene; in this case also the *ortho*-metalation of the proton in *alpha*-position to the CN bond is observed (Scheme 2.3).

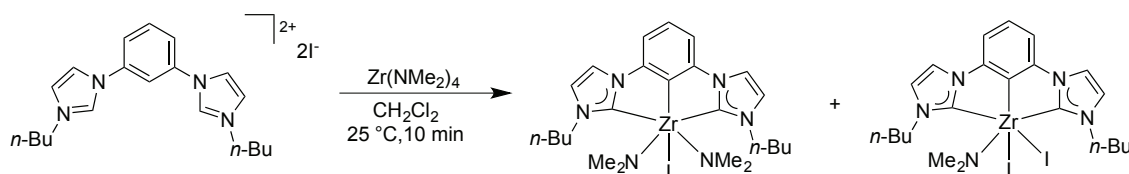
The silver(I) complex is not isolated but a solution of ruthenium(II) precursor is added directly to the reaction mixture, giving a mixture of two products (Scheme 2.3): a dinuclear complex and a mononuclear one, in which one imidazolium moiety has not been deprotonated.



Scheme 2.3: synthesis of ruthenium(II) complexes with a *para*-phenylene dicarbene via transmetalation of the ligand from the corresponding silver(I) complexes

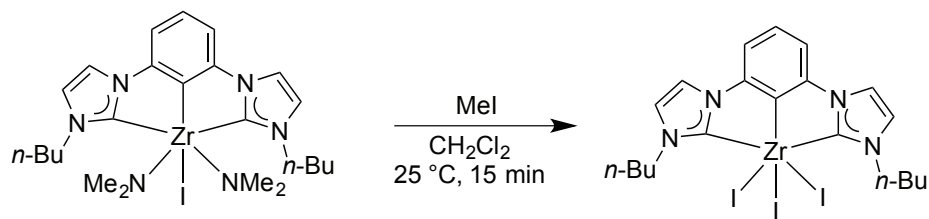
A synthetic alternative approach consists in the deprotonation of the azolium salt using a base already coordinated to the metal.

The reaction with the zirconium precursor $Zr(NMe_2)_4$ under very mild conditions gives a mixture of two complexes: each of them has a dicarbene that act as *CCC*-pincer ligand, and a different number of iodide and dimethylamine ligands (Scheme 2.4). This is one of the first reported examples in which also the carbon in position 2 of the phenylene bridge acts as donor atom to bond the metal center.^{74a-b,74d,74i}



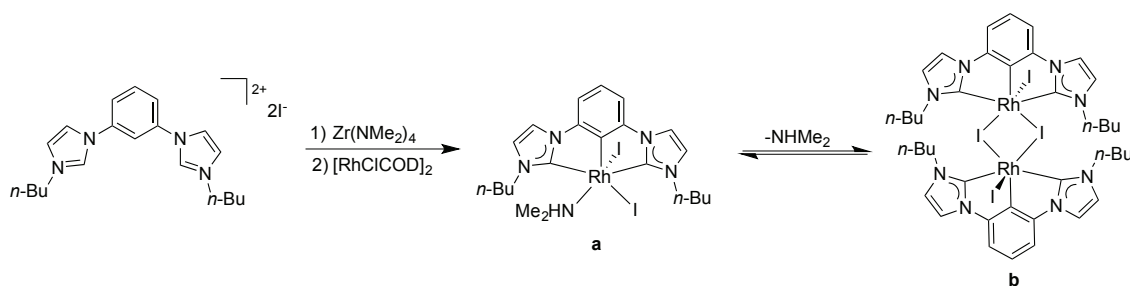
Scheme 2.4: syntheses of zirconium(IV) complexes (the complex on the right is identified in the X-Ray crystal structure and occupies 9 % of the crystal sites)

It is interesting to underline that in the presence of an excess of methyl iodide it is possible to coordinate three I^- groups on the metal center (Scheme 2.5).



Scheme 2.5: ligand exchange

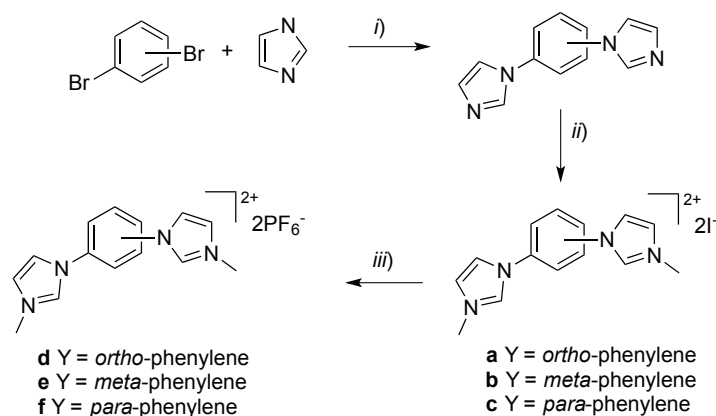
Finally, starting from the described zirconium(IV) diNHC complex it is possible to selectively transfer the pincer ligand to other metal centers, like for example rhodium(III) (Scheme 2.6).



Scheme 2.6: reaction to obtain a rhodium(III) complex (a) and dirhodium(III) complex (b)

2.2 Syntheses and characterization of the azolium proligands

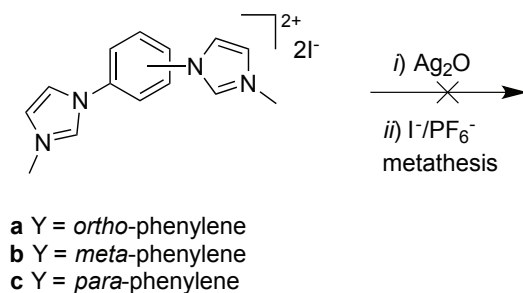
The phenylene bis(imidazole)⁸⁵ precursors were prepared starting from *ortho*-, *meta*- or *para*-dibromobenzene and imidazole using copper catalyzed Ullmann-type coupling procedure (Scheme 2.7). The diimidazolium cations were prepared in a subsequent step, by direct alkylation of the phenylene bis(imidazole) compounds with methyl iodide in dimethylsulfoxide at room temperature. In this way the bis(imidazolium) diiodide salts were isolated and their solubility in the most common organic solvents could be improved via anion I⁻/PF₆⁻ exchange, yielding bis(hexafluorophosphate) salts.



Scheme 2.7: Preparation of diimidazolium salts. Experimental details: *i*) imidazole, dibromobenzene, CuO, K₂CO₃, DMSO, 150 °C, 48 h. *ii*) MeI, DMSO, room temperature, 12 h; *iii*) NH₄PF₆, methanol

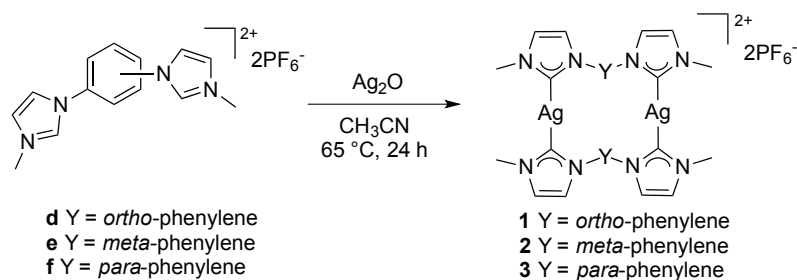
2.3 Syntheses and characterization of silver(I) complexes

The syntheses of the silver complexes were initially attempted using the procedure already reported by Tubaro *et al.*⁸⁶ for similar di(imidazolium) salts, in which the chosen diimidazolium diiodide salt reacts with Ag₂O in water for 24 hours at room temperature, followed by anion I⁻/PF₆⁻ metathesis. Unfortunately, a mixture of products has been obtained with an appreciable quantity of the starting diimidazolium salt, as indicated in the ¹H-NMR spectra by the signal at ca. 9 - 10 ppm due to the proton in position 2 of the imidazole ring (Scheme 2.8).



Scheme 2.8: unsuccessful attempts to synthesize the silver(I) complexes. Experimental details: *i*) silver(I) oxide (2.5 eq), water, 25 °C, 24 h, *ii*) KPF₆, water, 25 °C, 30 min

The successful syntheses of the complexes was finally performed by reacting the diimidazolium bis(hexafluorophosphate) salt with excess silver(I) oxide in acetonitrile as solvent, for 24 hours at 65 °C (Scheme 2.9).



Scheme 2.9: Syntheses of silver(I) complexes **1**, **2** and **3**

The complexes are light grey solids, soluble in polar organic solvents like acetonitrile or DMSO. They have been characterized by different techniques in order to confirm their purity and structure; the data suggested a dinuclear dicationic structure of the type $[\text{Ag}_2\text{L}_2](\text{PF}_6)_2$ with two di(N-heterocyclic carbene) ligands L bridging the two silver centers. The ^1H -NMR spectra confirmed the deprotonation of the proligands, due to the absence of a signal at ca. 9.5 - 10 ppm associated to the protons in position 2 of the imidazole rings. The formation of the silver(I) complexes is also supported by the presence of the carbene carbon signal in the $^{13}\text{C}\{^1\text{H}\}$ -NMR spectra deshielded at ca. δ 180 - 185 ppm, in the typical range of carbene carbons coordinated to a silver(I) center.⁸⁶

The dinuclear dicationic nature of the complexes with the two dicarbene ligands bridging the two metal centers has been then further established by the ESI-MS spectra, which show peaks corresponding to $[\text{Ag}_2\text{L}_2\text{PF}_6]^+$, $[\text{Ag}_2\text{L}_2]^+$ and $[\text{Ag}_2\text{L}_2]^{2+}$ fragments. Hahn *et al.* have reported similar results⁸⁷ with a *para*-phenylene ligand with ethyl groups at the N-atoms in position 1 of the heterocyclic ring.

Single crystals of complexes **1** and **2** have been obtained by slow diffusion of diethyl ether in an acetonitrile solution of the complexes and were studied by X-ray diffraction (Figure 2.3 and Figure 2.4).

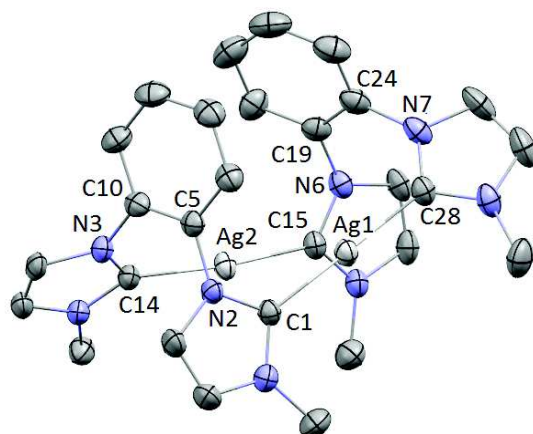


Figure 2.3: ORTEP view of one of the two cationic units of complex **1**. Ellipsoids are drawn at their 30 % probability. Hydrogen atoms and PF_6^- anions have been omitted for clarity. Selected bond distances (\AA) and angles (deg) (data in squared parentheses are referred to the second cationic unit): C1-Ag1 2.076(5) [2.092(5)], C28-Ag1 2.076(5) [2.085(5)], C14-Ag2 2.088(5) [2.091(5)], C15-Ag2 2.088(5) [2.094(5)], C1-N2 1.345(7) [1.346(6)], C5-N2 1.430(7) [1.427(7)], C5-C10 1.387(8) [1.379(7)], C10-N3 1.414(7) [1.433(7)], C14-N3 1.347(7) [1.356(6)], C15-N6 1.360(6) [1.346(7)], C19-N6 1.410(7) [1.428(7)], C19-C24 1.383(7) [1.390(8)], C24-N7 1.422(7) [1.434(8)], C28-N7 1.346(6) [1.356(7)], Ag1...Ag2 3.289(2) [3.265(1)]; C1-Ag1-C28 175.8(2) [176.7(2)], C15-Ag2-C14 170.7(2) [171.5(2)]

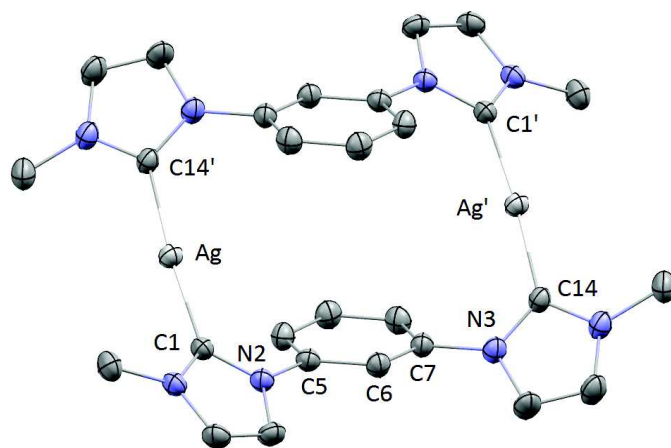


Figure 2.4: ORTEP view of the cationic part of complex **2**. Ellipsoids are drawn at their 30 % probability. Hydrogen atoms and PF_6^- anions have been omitted for clarity. Selected bond distances (\AA) and angles (deg): C1-Ag 2.092(4), C14'-Ag 2.086(4), C1-N2 1.350(5), C5-N2 1.431(4), C5-C6 1.392(5), C6-C7 1.383(5), C7-N3 1.437(4), C14-N3 1.352(5); C14'-Ag-C1 175.16(13). Symmetry code for equivalent atoms: ' = 1-x, -y, -z

The unit cells contain cationic complexes with PF_6^- anions. The X-ray diffraction analyses confirm that the metal complexes are dinuclear dicationic species with two dicarbene ligands bridging the two silver atoms. In the complex **1**, the bridging ligands form a 14-member ring while in **2** the *meta*-isomers of the bridging phenylene cause the formation of a 16-member ring. As reported in Figure 2.3 and Figure 2.4 the conformation of the ligands with respect to the plane passing through the $\text{C}_{\text{carbene}}\text{-Ag-Ag-C}_{\text{carbene}}$ bonds is different: in the silver(I) complex with *ortho*-phenylene ligands the cationic moieties show a *syn* conformation while for the *meta*-phenylene one an *anti*-conformation is observed; the centrosymmetric nature of the complex **2**, with an inversion center located in the middle of the 16-membered ring forces this conformation.⁸⁸ In the silver(I) complex with the *meta*-phenylene ligands the $\text{Ag}\cdots\text{Ag}$ distance is 7.165(2) Å, while for the *ortho*- isomer the distances are 3.289(2) Å and 3.265(1) Å (these different distances are due to the fact that the two independent cationic complexes are present in the unit cell); interestingly, the $\text{Ag}\cdots\text{Ag}$ interatomic separation observed with complex **1** is slightly shorter than the sum of the Van der Waals radii for silver, thus suggesting the presence of argentophilic interaction between the two metals. The $\text{Ag-C}_{\text{carbene}}$ bond lengths span from 2.076(5) to 2.094(5) Å in **1** and from 2.086(4) to 2.092(4) Å in **2** and fall in the typical range observed for $[\text{Ag}(\text{NHC})_2]^+$ complexes; the $\text{C}_{\text{carbene}}\text{-Ag-C}_{\text{carbene}}$ angles slightly deviate from the linearity. Finally, the mean planes of the phenyl rings in complex **2** are parallel and at a distance of 4.306(2) Å (centroid-to-centroid separation of 4.409(2) Å). Considering the crystal packing, it is evident that in this complex other $\pi\cdots\pi$ interactions are present, in particular between the phenyl rings of adjacent molecules (centroid to centroid distance of 4.803(2) Å) and between the phenyl ring and the imidazole one of faced molecules (centroid to centroid distance of 4.299(2) Å) (Figure 2.5).

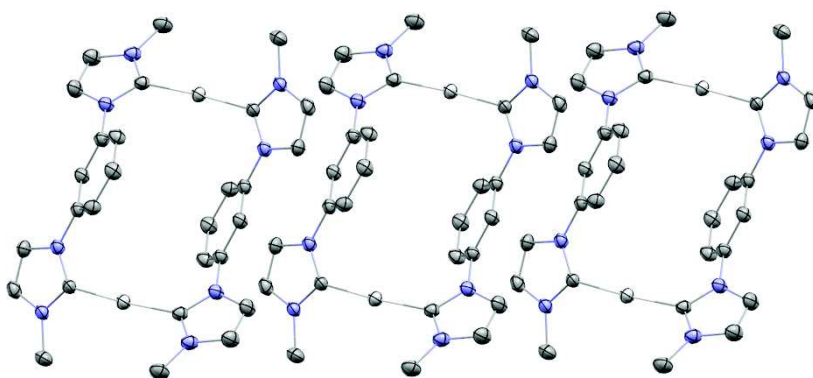


Figure 2.5: Packing diagram of cationic complexes in **2** evidencing the stacking of adjacent molecules

Interestingly, during the crystallization of the complex **1**, few crystals of a different species have been obtained and isolated. In Figure 2.6 it is reported the ORTEP view of a cationic coordination metallopolymer in which one di(N-heterocyclic carbene) ligand has been substituted by an acetate anion.

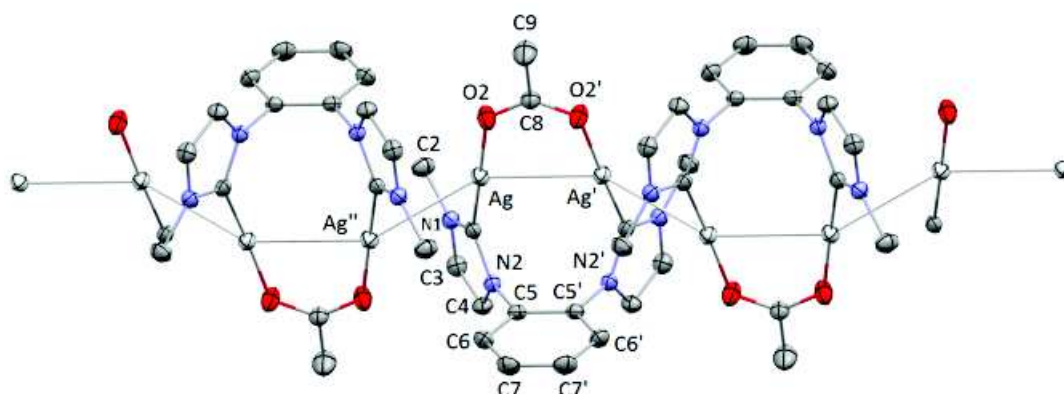


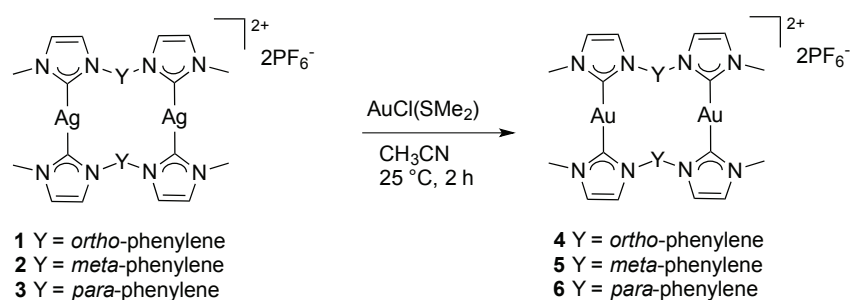
Figure 2.6: ORTEP view of the polymeric structure of complex $[\text{Ag}_2(\text{CH}_3\text{COO})(\text{ortho-diNHC})](\text{PF}_6)$. Ellipsoids are drawn at their 30 % probability. Hydrogen atoms have been omitted for clarity. Selected bond distances (Å) and angles (deg): C1-N1 1.348(5), C1-N2 1.352(5), C1-Ag 2.067(4), C2-N1 1.462(5), C3-C4 1.340(6), C3-N1 1.378(5), C4-N2 1.382(5), C5-C6 1.379(5), C5-C5' 1.383(7), C5-N2 1.436(5), Ag-O2 2.111(3), Ag \cdots Ag' 2.9279(8), Ag \cdots Ag'' 3.0462(7); N1-C1-N2 104.6(3), N1-C1-Ag 128.8(3), N2-C1-Ag 126.6(3), C5'-C5-N2 119.73(18), C1-Ag-O2 176.63(14), C1-N1-C3 110.8(3), C1-N1-C2 124.1(3), C3-N1-C2 125.0(3), C1-N2-C4 111.1(3), C1-N2-C5 122.9(3), C4-N2-C5 126.0(3), C8-O2-Ag 126.6(3), Ag' \cdots Ag \cdots Ag'' 148.51(1). Symmetry code for equivalent atoms: ' = $\frac{1}{2}-x, y, z$; '' = $-x, 1-y, -z$

The complex $[\text{Ag}_2(\text{CH}_3\text{COO})(\text{ortho-diNHC})](\text{PF}_6)$ is a cationic coordination polymer formed by infinite chains of dimers $[\text{Ag}_2(\text{CH}_3\text{COO})(\text{ortho-diNHC})]$ connected by Ag \cdots Ag Van der Waals interactions. The symmetric dinuclear complex is formed by two silver atoms bridged by the diNHC ligand and by an acetate anion. The polymeric

structure develops along the a axis of the cell. The diNHC ligand and the metal atoms form an eight membered ring with a boat conformation. The Ag atom is bonded to a carbene carbon atom (C1-Ag 2.067(4) Å), and an oxygen atom of an acetate anion (Ag-O2 2.111(3) Å) in a nearly linear arrangement (C1-Ag-O2 176.63(14)°). The mean planes of the imidazole rings of the bridging diNHC ligand form a dihedral angle of 64.01(2)°. The Ag'...Ag and Ag...Ag'' separations are 2.9279(8) and 3.0462(7) Å. The polymeric structure develops in a zig zag chain with an Ag'...Ag...Ag'' angle of 148.51(1)°. In the crystals of the metallopolymer, PF₆⁻ anions are also present to neutralize the positive charges. The process leading to the formation of complex [Ag₂(CH₃COO)(*ortho*-diNHC)](PF₆) should involve the hydrolysis of acetonitrile solvent to ammonium acetate.

2.4 Syntheses and characterization of gold(I) complexes and photophysical properties

Gold(I) complexes have been synthesized via transmetalation of the dicarbene ligand from the corresponding silver(I) complexes [Ag₂L₂](PF₆)₂. The experiments have been performed using Schlenk techniques under an inert atmosphere of argon, using acetonitrile as solvent, for two hours at room temperature. After filtration through a plug of Celite in order to remove the AgCl salts, the solution was concentrated and the product precipitated with diethyl ether in order to obtain off-white solids (Scheme 2.10), which are soluble in acetonitrile and dimethylsulfoxide.



Scheme 2.10: syntheses of the gold(I) complexes **4**, **5** and **6**

The symmetric dinuclear structure of the silver(I) precursors is maintained upon transmetalation of the ligand to the gold(I) centers and this is confirmed by different techniques. In particular, the ¹H-NMR spectra are very similar to those of the silver(I) complexes in terms of number and pattern of signals, thus suggesting the same

symmetric structures. The signals in the aromatic region are slightly shifted downfield in comparison to the corresponding silver(I) complexes; the same shift has been observed in the $^{13}\text{C}\{^1\text{H}\}$ -NMR spectra for the signals concerning the C4 and C5 carbons. As regards the carbene carbon signal, it is slightly upfield shifted or remains unchanged with respect to the one of the silver(I) complex due to the higher Lewis acidity of the gold(I) center with respect to the silver(I) one.⁸⁹

The ESI-MS spectra and the simulation of the isotopic pattern support the formation of dinuclear dicationic complexes, in fact peaks of the fragments $[\text{Au}_2\text{L}_2\text{PF}_6]^+$ and $[\text{Au}_2\text{L}_2]^{2+}$ are present (at m/z 1015.08 and 435.42) (Figure 2.7).

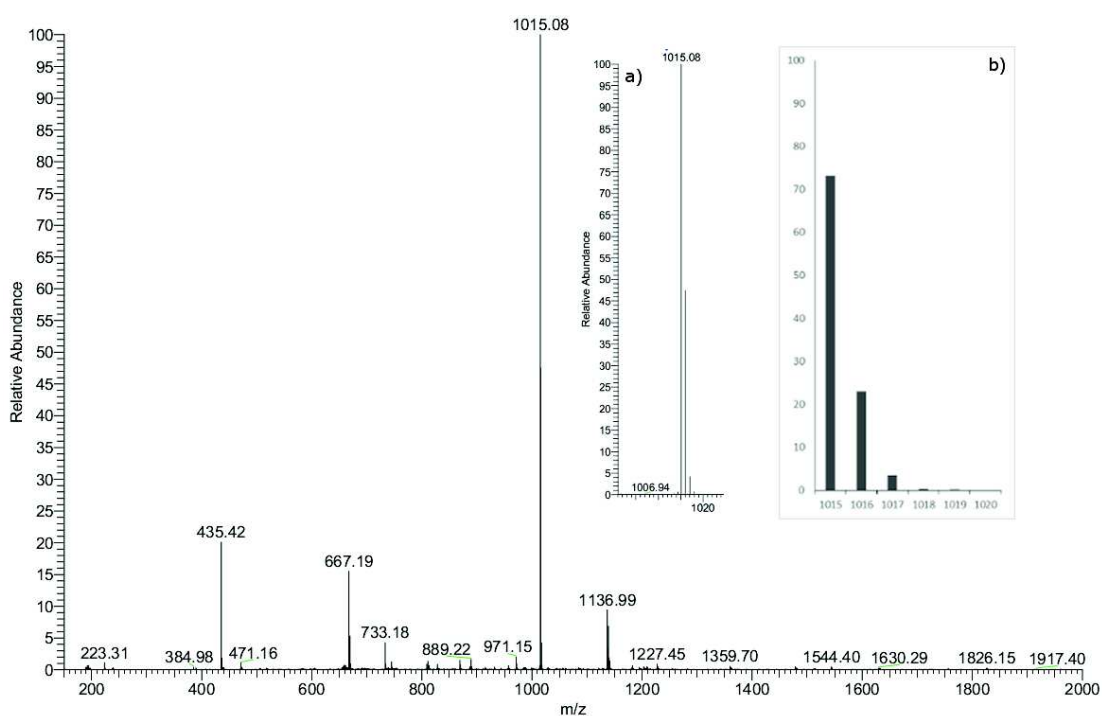


Figure 2.7: ESI-MS spectra of the complex **4** and in the inset simulation of the isotopic pattern for the signal at m/z 1015.09 associated to the fragment $[\text{Au}_2\text{L}_2\text{PF}_6]^+$

By slow diffusion of diethyl ether into a solution of the complexes **4** and **5**, some single crystals have been obtained and the crystal structure was solved by X-ray diffraction studies (Figure 2.8 and Figure 2.9).

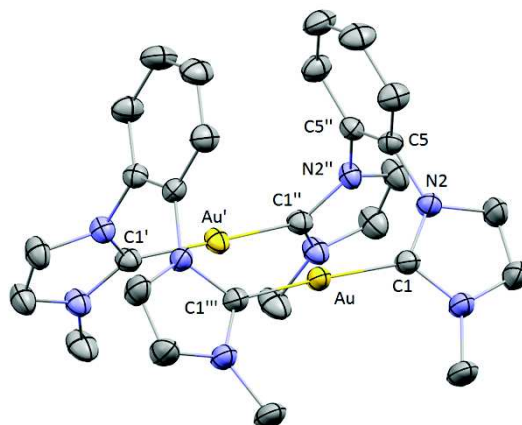


Figure 2.8: ORTEP view of the cationic complex **4**. Ellipsoids are drawn at their 30 % probability. Hydrogen atoms, PF_6^- anions and acetonitrile solvent molecule have been omitted for clarity. Selected bond distances (\AA) and angles (deg): C1-Au 2.013(5), C1-N2 1.363(5), C5-N2 1.434(4), C5-C5'' 1.392(7); C1-Au-C1''' 174.1(2). Symmetry code for equivalent atoms: ' = 1-x, y, $\frac{1}{2}$ -z; '' = x, y, $\frac{1}{2}$ -z; ''' = 1-x, y, z

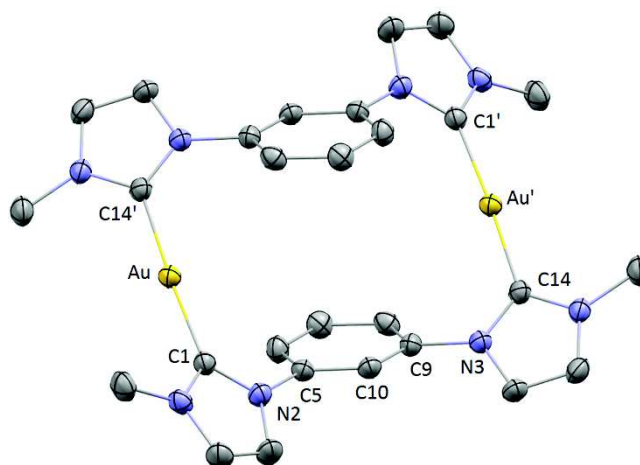


Figure 2.9: ORTEP view of the cationic complex **5**. Ellipsoids are drawn at their 30 % probability. Hydrogen atoms, PF_6^- anions and acetonitrile solvent molecule have been omitted for clarity. Selected bond distances (\AA) and angles (deg): C1-Au 2.021(5), C14'-Au 2.025(5), C1-N2 1.359(6), C5-N2 1.437(6), C5-C10 1.392(6), C10-C9 1.388(6), C9-N3 1.447(6), C14-N3 1.343(6); C14'-Ag-C1 175.7(2). Symmetry code for equivalent atoms: ' = -x, -y, 1-z

The structures of the gold(I) complexes are very similar to those obtained for the silver(I) ones.

These compounds present a dinuclear dication structure, with the dicarbene moieties coordinated in a bridging way to two gold(I) centers and two PF_6^- anions are present to neutralize the positive charge.

The structure of **4** shows the two bridging ligands in a 14-membered ring adopting a boat conformation. The complex is highly symmetric, with a *syn* conformation⁸⁸ of the two phenylene rings (considering a plane generated by the C-Au-Au-C bounds). The Au...Au distance is 3.656(2) Å and the Au-C_{carbene} bond is 2.013(5) Å, in the typical range for analogous NHC-Au(I) complexes; the angle between the two carbene carbons and the gold(I) (C_{carbene}-Au(I)-C_{carbene}) is slightly deviate from the linearity (174.1(2)°). The gold(I) complex with *meta*-phenylene bridge is isostructural with the silver(I) complex **2**, forming a symmetric 16-member ring with an *anti* conformation of the diNHC. The Au...Au distance is 7.140(2) Å; the Au-C_{carbene} bond lengths are 2.021(5) and 2.025(5) Å and, also in this case, the C_{carbene}-Au-C_{carbene} angle shows a slight deviation from linearity (175.68(16)°). As mentioned for the corresponding silver(I) complex, due to the centrosymmetry of the system, the mean planes of the phenyl rings are parallels and at a distance of 4.416(2) Å (considering centroid to centroid separation).

As already observed in the silver(I) complex **1**, the gold(I) complex **4** does not present $\pi\cdots\pi$ inter-molecular stacking between adjacent moieties.

A different behavior has been observed for the gold(I) complex with *meta*-phenylene bridge in which strong $\pi\cdots\pi$ interactions between the phenyl rings and between a phenyl ring and an imidazole of faced molecules have been observed (Figure 2.10). The first interaction (adjacent phenyl rings) is confirmed by a distances between the two phenyl rings of 4.775(2) Å (considering the separation between the two centroids); the distance between the imidazole ring and the adjacent phenyl one is instead 4.423(2) Å.

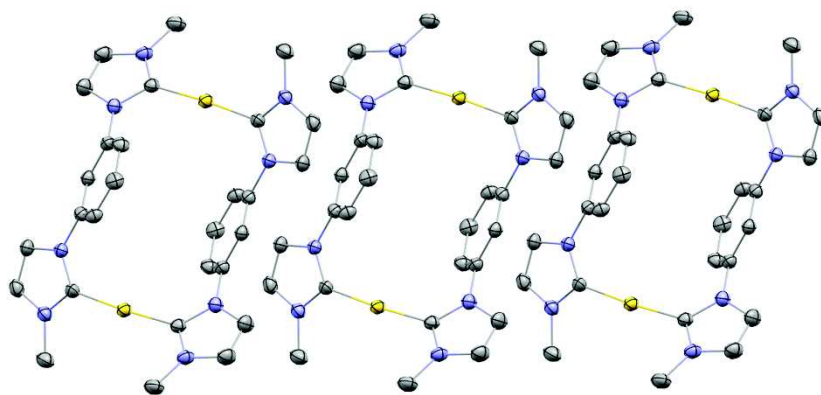
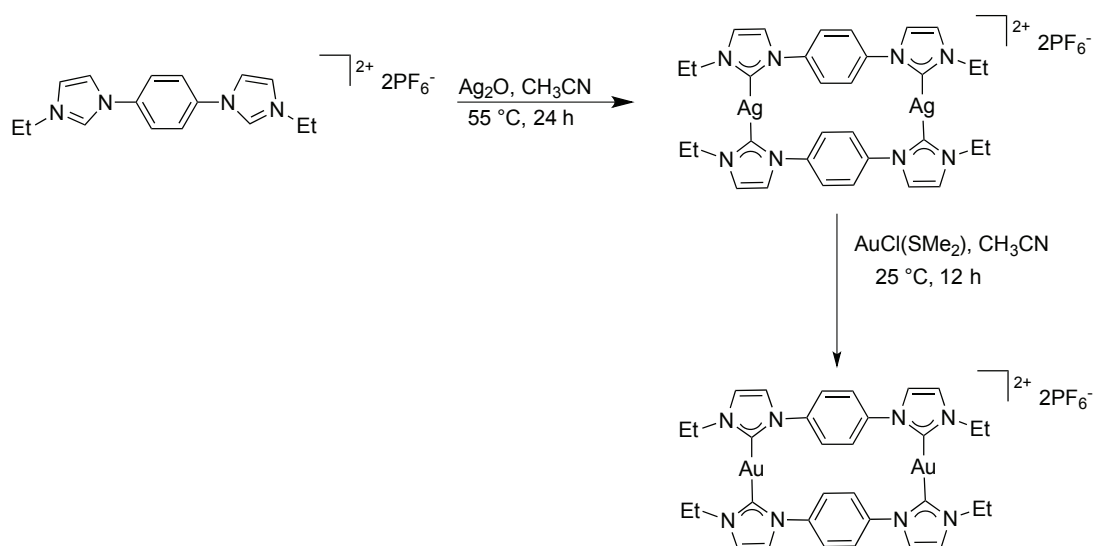


Figure 2.10: packing diagram of cationic complexes in **5** evidencing the stacking of adjacent molecules

The structures of the silver(I) and gold(I) complexes with the *para*-phenylene have not been solved, however Hahn reported very similar compounds having an ethyl nitrogen wingtip substituent instead of a methyl one.⁸⁷ The same procedure adopted in this work, has been used for the syntheses of the silver(I) and gold(I) complex reported in Scheme 2.11.



Scheme 2.11: synthesis of the gold(I) complex reported by Hahn *et al.*

The structure of the gold(I) complex has been reported by Hahn in ref. 87, but it will be discussed also here for completeness and comparison with the *ortho*- and *meta*-compounds. The structure (Figure 2.11) shows the two bridging ligand in a 18-membered ring in a very symmetric conformation. The $Au\cdots Au$ distance is $7.213(2)\text{ \AA}$ and the $Au-C_{\text{carbene}}$ distances span from $2.015(7)$ to $2.041(8)\text{ \AA}$, in the typical range for analogous NHC-Au(I) complexes; the angle between the two carbene carbons and the gold(I) ($C_{\text{carbene}}-Au(I)-C_{\text{carbene}}$) is slightly deviate from the linearity ($173.6(3)^\circ$ and $171.8(3)^\circ$). The dihedral angle between the two imidazole rings bonded to the same gold(I) atom are 9.81° and 6.34° . Only few examples are reported in the literature with these features.⁹⁰

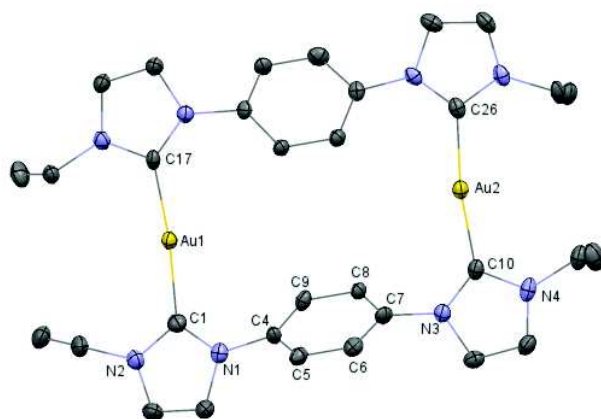


Figure 2.11: ORTEP view of the gold(I) complex with *meta*-phenylene bridge reported by Hahn *et al.*. Ellipsoids are drawn at their 50 % probability. Hydrogen atoms, PF_6^- anions have been omitted for clarity. Selected bond distances (Å) and angles (deg): Au1-C1 2.034(8), Au1-C17 2.015(7), Au2-C10 2.026(8), Au2-C26 2.041(8); C1-Au1-C17 173.6(3), C10-Au2-C26 171.8(3)

Looking more closely to the structure, it is possible to find a intramolecular interaction between the two phenyl rings (C8-C9 close to C24-C25) as a consequence of their different orientation in the space (Figure 2.12).

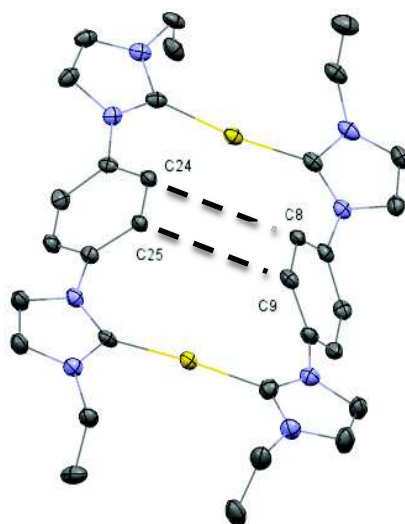


Figure 2.12: intramolecular interaction between carbons of phenylene rings: C24-C8 = 3.882 Å, C25-C9 = 3.853 Å

Looking for the packing of different molecules, it can be observed a nonclassical hydrogen bonds between the hexafluorophosphate (present as counterion) and the cations that allow to obtain an infinite layered structure.

More interestingly, $\pi\cdots\pi$ inter-molecular stacking between phenyl rings of different molecules have been observed. In this packed structure, the two different phenyl rings of two unities $[\text{Ag}_2(\text{L})_2]^{2+}$ are arranged in a coplanar fashion with a centroid-centroid distance of 4.005 Å.

Unfortunately, no luminescence studies have been done for this molecule in order to compare the different experimental features.

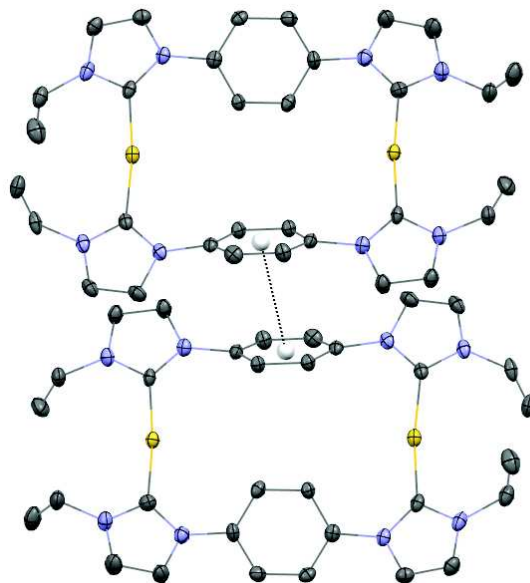


Figure 2.13: packing diagram of cationic complex previously described evidencing the stacking of adjacent molecules

Comparing all the structures obtained and those cited and reported in the literature, it is evident that the different isomers of the phenylene ring are the key element that induces the different packing and structure of the complexes, which are not significantly affected by the different metal centers.

In particular, in the case of di(N-heterocyclic carbene) ligands bearing a 1,3-disubstituted arene linker, two possible structures are reported in the literature: (i) open ring stretched out conformation characterized by a long intramolecular $\text{Au}\cdots\text{Au}$ distance and by intermolecular $\pi\cdots\pi$ interactions and (ii) a twisted conformation with a short intramolecular $\text{Au}\cdots\text{Au}$ distance. Examples of both type (i)⁹¹ and type (ii)^{92,93} have been recently reported in the literature with silver(I), gold(I) and mercury(II) metal centers.

The interatomic interaction between different moieties have been demonstrated to play an important role in influencing the luminescence properties of the silver(I) and gold(I) complexes.

The photophysical properties of both gold(I) and silver(I) complexes have been investigated at room temperature in the solid state as powder. The excitation profiles reported in Figure 2.14 and recorded by monitoring the emission maxima are centered in the UV region (below 400 nm) and can be attributed to the $\pi-\pi^*$ ligand centered (LC) transitions.³¹

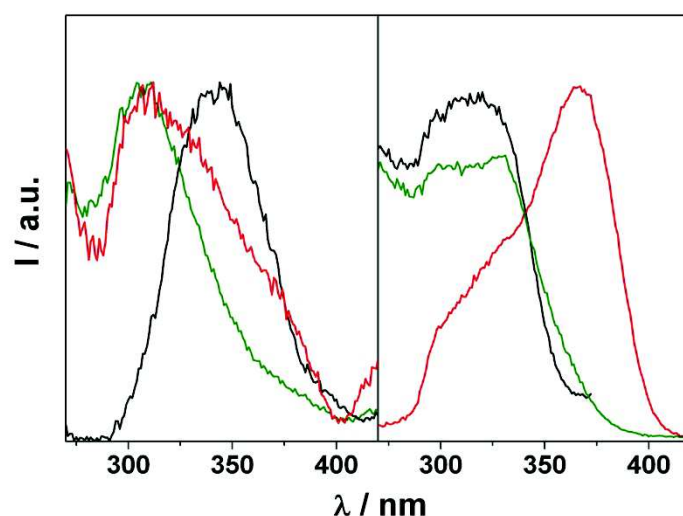


Figure 2.14: Excitation spectra ($\lambda_{em} = \lambda_{max}$) in the solid state as powder at 298 K. Left window: **1** (black), **2** (red) and **3** (green). Right window: **4** (black), **5** (red) and **6** (green)

In the emission spectra (Figure 2.15), all the maxima are centered between 410 and 480 nm (blue region). The gold(I) complexes show a discrete PLQY (maximum value of 5.7 %) while the corresponding silver(I) complexes are weaker emitters (Table 2.1).

The shape profiles and the lifetime decays of the reported compounds suggest the presence of two types of emitting states. In particular, the complexes with *para*-phenylene ring show longer lifetime (that follow a biexponential decay) and red shifted maxima. All these informations suggest that for the complexes with *ortho*- and *meta*-phenylene bridge the emissions are ligand centered (LC) while for the complexes with *para*-phenylene bridge the character of the emission is predominantly metal centered (MC).⁹³

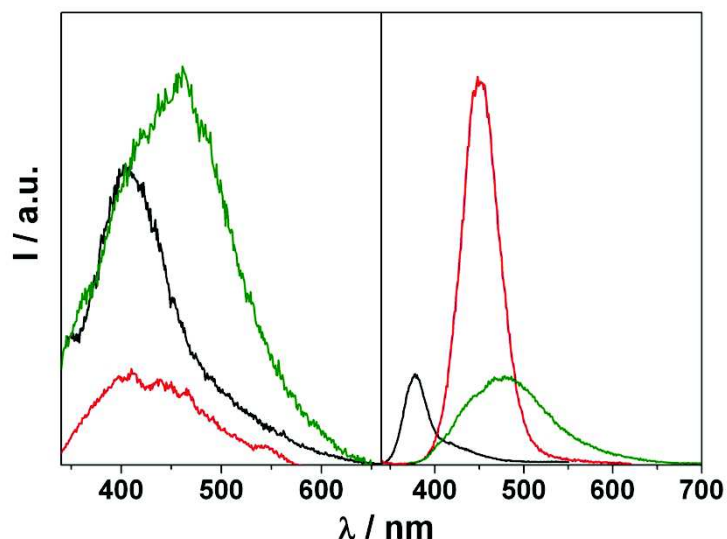


Figure 2.15: Emission spectra ($\lambda_{\text{exc}} = 300$ or 330 nm) in the solid state as powder at 298 K. Left window: **1** (black), **2** (red) and **3** (green). Right window: **4** (black), **5** (red) and **6** (green). For each window, the profile intensities have been normalized according to the corresponding quantum efficiencies.

Table 2.1: Photophysical data of the investigated complexes in the solid state (as powder) at room temperature

Complex	λ_{max} (nm) ^a	Φ (%) ^a	τ (μs) ^b	M···M distance (\AA)
1	410	< 1%	^c	3.266
2	420	< 1%	^c	7.165
3	460	< 1%	15.0 - 234	-
4	380	1.0	1.1	3.657
5	450	5.7	0.4	7.140
6	478	2.8	22 - 140	7.213 ^d

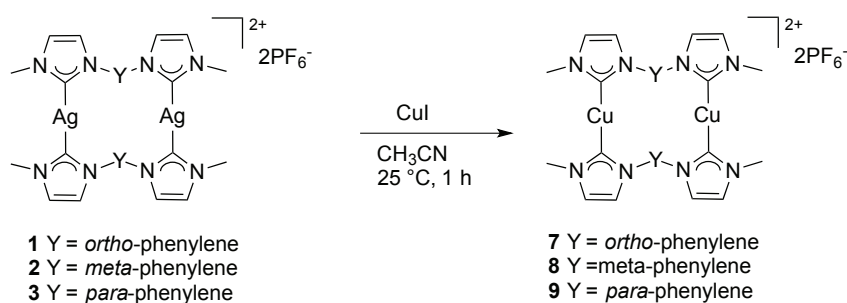
^a $\lambda_{\text{exc}} = 300$ or 330 nm; ^b $\lambda_{\text{exc}} = 330$ nm; ^c Not detected due to the weakness of the signal. ^d From Ref. 87,94

In order to find a correlation between the PL performances and the geometrical factors of the complexes, initially the aurophilic interaction model⁵³ was taken into account; in this model, the luminescence properties of a complex are mainly influenced by the metal-metal distance. Unfortunately, in the present case, the samples have different emitting states (MC and LC) and it is not possible to find a simple relation between the metal-metal distance and the emitting properties (in particular PLQY). For example, comparing the complexes **4** and **5**, the higher PLQY is observed for the complex with the *meta*-phenylene bridge, which however present the longer distance between the two gold(I) centers.

These results suggest that with these complexes additional factors, rather than the solely distance between metals, such as sample geometry and $\pi\cdots\pi$ crystal stacking, influence the optical properties of the dinuclear gold(I) complexes.

2.4 Syntheses of copper(I) complexes

The copper(I) complexes have been synthesized using the transmetalation route already adopted for the gold(I) complexes, working in acetonitrile at room temperature for one hour and using copper(I) iodide as copper source (Scheme 2.12).



Scheme 2.12: syntheses of copper(I) complexes **7**, **8** and **9**

The complexes are not very stable in ambient atmosphere, especially copper(I) complexes with *ortho*-phenylene bridge **7**, which evolves in solution after a couple of minutes (see further in the text).

Concerning the characterization by NMR, they all present the same pattern of signals described for the silver(I) and gold(I) complexes. Small differences in terms of chemical shift can be observed especially for the carbene carbon signal, which is shifted at lower ppm with respect to the silver(I) and gold(I) ones, due to the lower Lewis acidity of the copper(I) compared to the other metals. Also the ESI-MS analysis confirm the dinuclear dicationic structure of the compounds, as indicated by the presence of the peaks associable to the fragments $[\text{Cu}_2\text{L}_2\text{PF}_6]^+$, $[\text{Cu}_2\text{L}_2]^+$ and $[\text{Cu}_2\text{L}_2]^{2+}$.

As already stated above, the copper(I) complexes are stable under strictly anaerobic conditions, while they tend to evolve when exposed to air and moisture. This behavior is particularly evident for the complex with the *ortho*-phenylene bridge: for example the colorless NMR solution, when exposed to air becomes yellow and a formation of a yellow/green solid has been observed. The NMR analysis of the evolved solution reveals the presence of only one species, characterized by a new set of signals, very similar as regards the pattern although deshielded of ca. 0.5 ppm with respect to the pristine copper(I) complex (Figure 2.16).

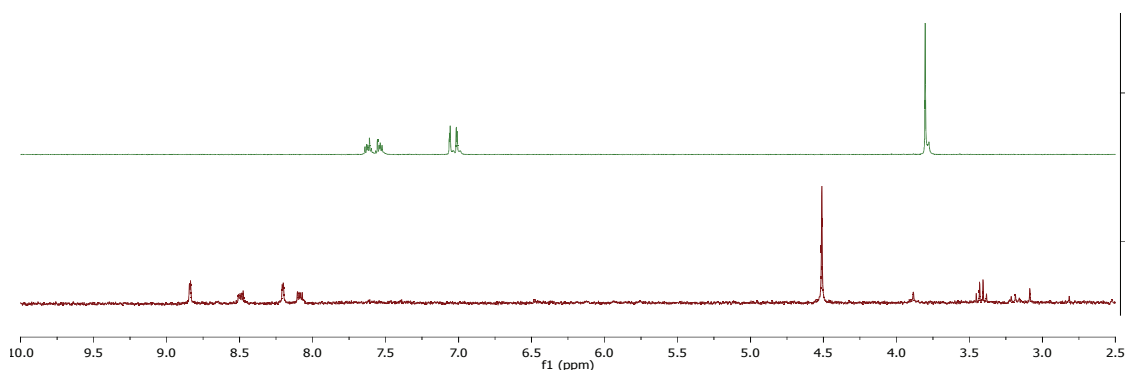


Figure 2.16: ^1H -NMR spectra of the copper(I) complex **7** (top) and the evolved compound (bottom) (in DMSO-d_6)

In the $^{13}\text{C}\{^1\text{H}\}$ -NMR spectrum, no signal has been detected in the proper region of carbene carbon atoms bonded to a copper(I) center; by means of 2D experiments, it was possible to associate the carbon in position 2 of the imidazole ring to a signal at 127.4 ppm.

Different attempts to crystallize this evolved compound have been performed by slow diffusion of diethyl ether into the acetonitrile solution of the evolved copper complex, but it was possible to obtain only crystals of $[\text{Cu}(\text{CH}_3\text{CN})_4](\text{PF}_6)$.

The whole of this results suggest that the copper(I) complex quickly decomposes giving evolution products such as $[\text{Cu}(\text{CH}_3\text{CN})_4]^+$ and organic species, which present the same functional groups of the phenylenebis(imidazole) ligand.

Some of the possible structures proposed for the obtained organic species are reported in Figure 2.17.

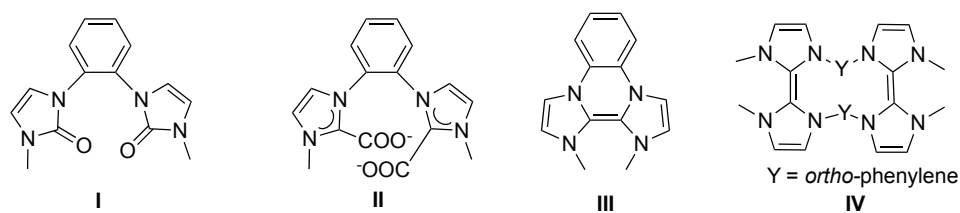


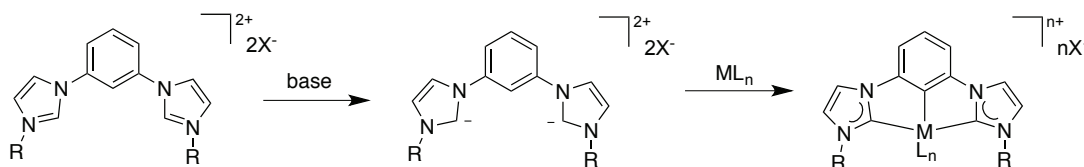
Figure 2.17: possible structures of decomposition compounds from complex **7**

The first two structures (**I** and **II**) are not coherent with the NMR data, since no signals associable to CO or acetate groups have been observed. Structure **III**, deriving from the coupling between two imidazoles of the same molecule (Figure 2.17) appears the more feasible. In particular, this hypothesis is supported by the C2 chemical shift at 127.4 ppm, which indicates an aromatic type carbon, and by the presence of a NOESY peak between the methyl protons of the molecule and the CH in position 5 on the backbone,

and between the CH protons in position 4 of the heterocyclic ring and the CH of the phenyl bridge.⁹⁵ Finally, also the ESI-MS spectra seem to support this hypothesis, since the main peaks are characterized by m/z lower than 385.

2.5 Syntheses of iridium(III) and ruthenium(II) complex

Ruthenium(II) and iridium(III) metal complexes with phenylene bridge di(N-heterocyclic carbene) ligands have been mainly obtained via direct deprotonation of the proligand using an external base, followed by the addition of a proper metal source; this procedure, as reported in Section 2.1, allows to obtain the proper complex, often characterized also by the metalation of the phenylene bridging group (Scheme 2.13).

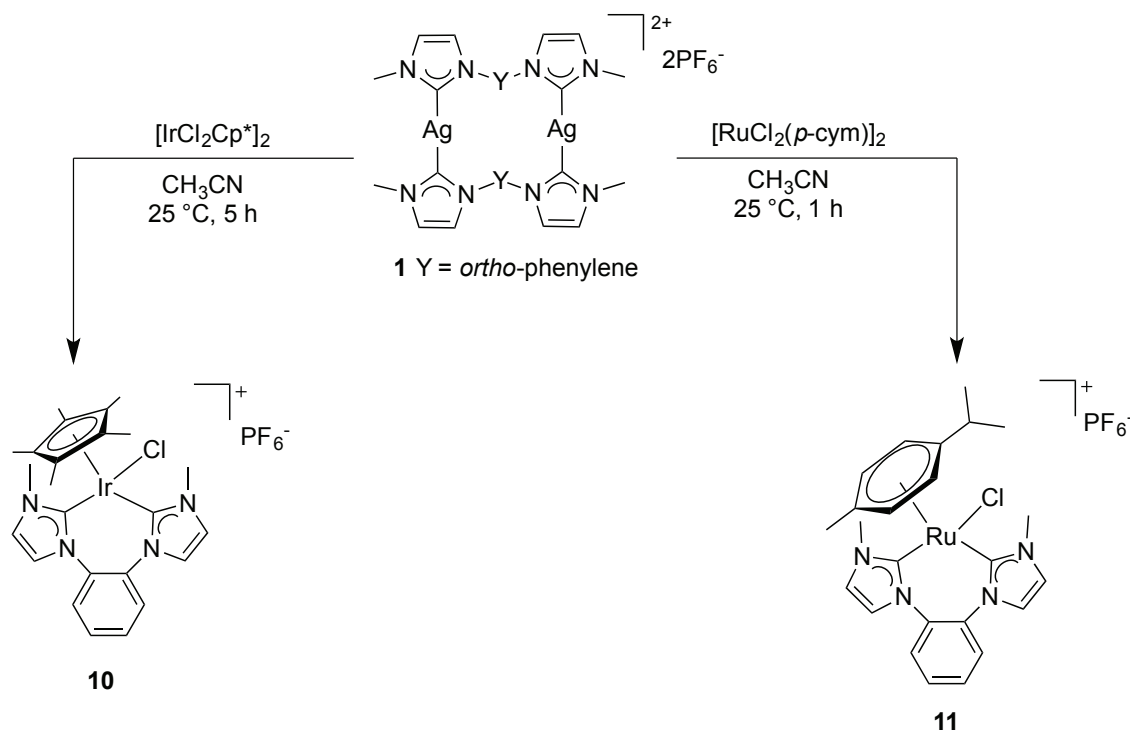


Scheme 2.13: general reaction pathway for the syntheses of CCC-pincer complexes

In this work, a different reaction procedure, i.e. the transmetalation, has been employed, with the aim of understanding if there is an influence of the procedure on the reaction outcome.

The transmetalation has been successful only in the case of the ligand with the *ortho*-phenylene bridging group. Despite using several different reaction conditions, changing the temperature, the time and the ratio Ag:M, it was not possible to synthesize complexes with *meta* and *para*-phenylene ligands. In all cases a certain quantity of reprotonated ligand has been observed. The reaction of the silver(I) complex **1** at room temperature in acetonitrile, with different ratio Ag:M (1:1 for Ir and 1:2 for Ru) affords the complexes **10** and **11**.

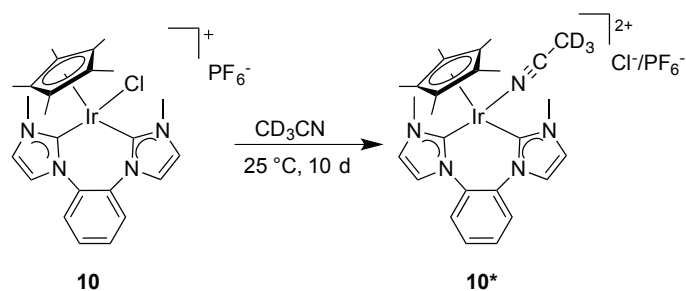
In both cases monocationic complexes are obtained, in which one di(N-heterocyclic carbene) ligand is chelating the metal center; the coordination sphere is completed by one chloride ligand and by an aromatic ring (Cp^* for the iridium(III) and *p*-cymene for the ruthenium(II) complex), present in the precursor of the metal centers.



Scheme 2.14: syntheses of iridium(III) and ruthenium(II) complexes **10** and **11**

The proposed structures are supported by ESI-MS spectra, in which the signal attributed to the fragment $[\text{IrClCp}^*(\textit{ortho}\text{-diNHC})]^+$ or $[\text{RuCl}(\textit{ortho}\text{-diNHC})(\textit{p}\text{-cym})]^+$ is observed. The coordination of the carbene carbon atom to the metal is confirmed by the ^{13}C -NMR spectra, which show a signal at 157.0 ($\text{C}_{\text{carbene}}\text{-Ir}$) and 179.5 ($\text{C}_{\text{carbene}}\text{-Ru}$), in the typical range of carbene carbon coordinated to iridium(III) or ruthenium(II) centres respectively. The ^1H -NMR analysis also supports the proposed structure with the presence of all the expected signals (Cp^* and \textit{p} -cymene for the iridium(III) and ruthenium(II) respectively).

Interestingly, the iridium(III) complex tends to evolve in solution and after ca. 10 days a new set of signals appears in the ^1H -NMR spectra. This new species, namely **10*** is formed by the replacement of a chloride ligand with a deuterated acetonitrile solvent molecule (Scheme 2.15).



Scheme 2.15: evolution of iridium(III) complex **10** to obtain **10***

The formation of the dicationic complex $[\text{IrCp}^*(\text{ortho-diNHC})(\text{CD}_3\text{CN})]^{2+}$ is supported by a qualitative test, i.e. by addition of AgPF_6 to a freshly prepared solution of the iridium(III) complex; a new set of NMR signals emerge and coincides with that observed on analyzing a standing solution of complex **10**. The changes observed in the ^1H and $^{13}\text{C}\{^1\text{H}\}$ -NMR spectra further point to the formation of a dicationic complex: in particular, the signals of the dicarbene ligand move downfield, as a consequence of the increased positive charge on the complex, with the exception of the carbene carbon, which instead moves upfield (150.3 for **10*** and 157.0 for **10**); this is a consequence of the higher Lewis acidity of the metal center and a similar behavior has been already reported for other iridium(III) or palladium(II) complexes.^{96,97}

By slow diffusion of diethyl ether into a solution of acetonitrile of the complex **11**, some crystals of the ruthenium(II) complex have been obtained and were analyzed by X-ray diffraction (Figure 2.18).

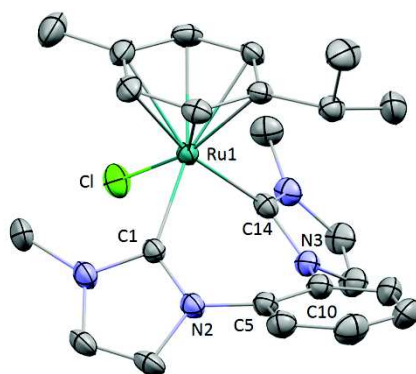


Figure 2.18: ORTEP view of the cationic complex in **11**. Ellipsoids are drawn at their 30 % probability.

Hydrogen atoms, PF_6^- anions and acetonitrile molecules have been omitted for clarity. Selected bond distances (Å) and angles (deg): C1-Ru1 2.051(5), C1-N2 1.353(7), C5-N2 1.428(7), C5-C10 1.396(7), C10-N3 1.424(7), C14-N3 1.381(7), C14-Ru1 2.035(5), Cl-Ru1 2.4182(13), Ru1-CT 1.734(5); CT-Ru1-

Cl 126.7(2), CT-Ru1-Cl 128.2(2), CT-Ru1-C14 128.9(2), C14-Ru1-Cl 88.4(2), C14-Ru1-Cl 84.4(2), C1-Ru1-Cl 85.4(2). CT is the centroid of the *p*-cymene ligand

The obtained molecular structure confirms our experimental characterizations: a monocationic complex with a PF₆⁻ counter-ion can be observed.

The ruthenium center shows a distorted tetrahedral coordination environment considering the two carbene carbon atoms of the chelating ligand, the chlorine atom and the centroid of the *p*-cymene molecule. The chelating ligand forms a 7-member coordination ring with a boat conformation. The C_{carbene}-Ru-C_{carbene} bond angle is 88.4(2)°, and the C_{carbene}-Ru-Cl bond angles are 84.4(2)° and 85.4(2)° while the bond angles at the ruthenium atom involving the centroid of the *p*-cymene ligand are wider spanning from 126.7(2)° to 128.9(2)° as usually observed in other ruthenium (arene) NHC complexes in the literature.^{98,99} The C_{carbene}-Ru, Ru-Cl and Ru-C bond distances for the *p*-cymene ligand lie in the usual range.

Chapter 3: RESULTS AND DISCUSSION

Metal complexes with an imidazole-based NHC ligand functionalized with a triazole in the 5 position of the backbone

3.1 Introduction

In this Chapter, the synthesis of functionalized imidazoles with a triazole on the backbone and synthesis of the corresponding transition metal complexes will be described.

Firstly the methodologies to build up the triazole moiety on the imidazole rings will be discussed and some examples regarding the synthesis of related transition metal complexes will be depicted.

A classical reaction for the syntheses of 1,2,3-triazoles is the Huisgen 1,3-dipolar cycloaddition,¹⁰⁰ which involves the condensation of an alkyne with an azide.¹⁰¹ The reaction at high temperature gives a mixture of 1,4- and 1,5-regioisomers in usually 1:1 ratio (Figure 3.1).¹⁰²

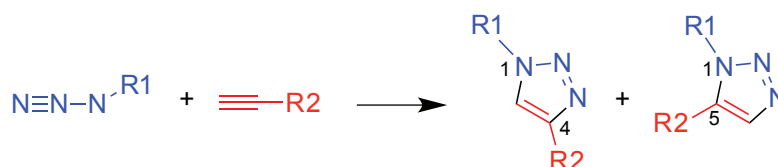


Figure 3.1: synthesis of 1,4- and 1,5-regioisomers

Sharpless *et al.*¹⁰³ and Meldal *et al.*¹⁰⁴ developed independently the highly regioselective syntheses of 1,4-triazoles using copper(I) as catalyst for the reaction. This procedure is usually called as CuAAC, i.e. Copper Azido-Alkyne Cycloaddition. Copper(I) salts like CuI, CuOTf · C₆H₆ and [Cu(NCCH₃)₄](PF₆) (in presence of a nitrogen base such as for example 2,6-lutidine, triethylamine or diisopropylamine) or a copper(II) salt and a reducing agent, which *in situ* generates a copper(I) active species, can be used as catalysts. In this regard, the most common precursors are CuSO₄ · 5H₂O and ascorbic acid or sodium ascorbate as reducing agent. The classical solvent system is a mixture of water and *t*BuOH but other solvents (like H₂O/THF, MeOH and CH₃CN) can be employed.¹⁰⁴

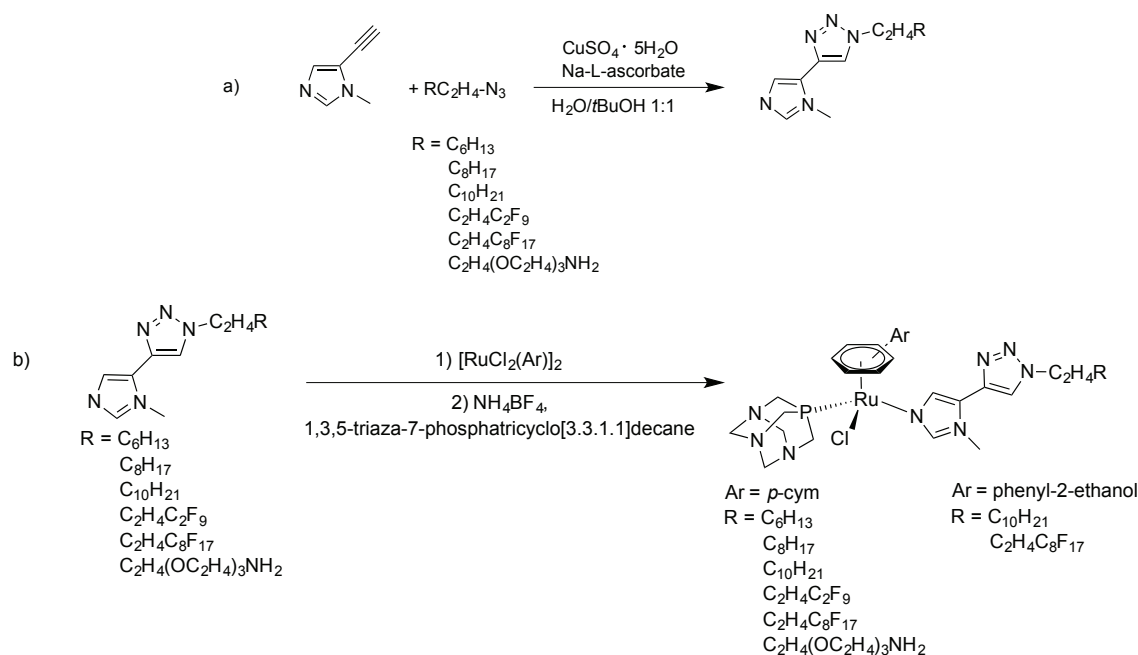
Several examples are reported in the literature in which the CuAAC reaction is used for the functionalization of an imidazole with triazole rings.¹⁰⁵

Ligand functionalization via click reaction and metal complex formation are separated events, so that it is possible to functionalize the ligand after the formation of the complex or vice versa the functionalization of the ligand can occur before complexation.

The group of Dyson has been very active in the syntheses of ruthenium complexes for antiproliferative applications. It can be anticipated that the presence of the triazole unit accompanied by the presence of long alkyl chains influence the cytotoxicity against different tumoral cell lines.

Different approaches^{106,107} were adopted for the syntheses of such complexes:

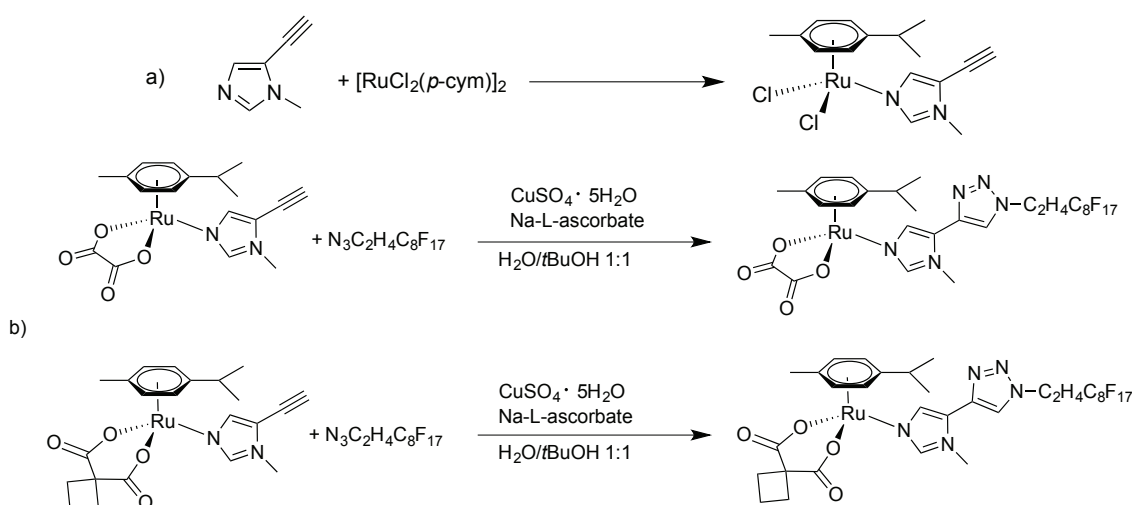
- 1) a) functionalization with a triazole ring of an imidazole followed by b) reaction with the opportune metal precursor;



Scheme 3.1: syntheses of ruthenium(II) complexes via direct reaction between the functionalized ligand and the metal source

- 2) a) syntheses of metal complexes with unfunctionalized imidazole ligand and b)

reaction with the azide to add the triazole moiety.

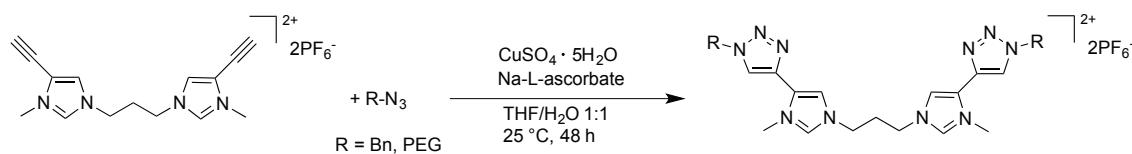


Scheme 3.2: syntheses of ruthenium(II) complexes via post-functionalization of the complexes

It is interesting to underline that with both procedures the classical CuAAC reaction affords the expected products in good yields and high purities and the presence of the ruthenium(II) metal center does not interfere with the cyclization pathway.

The antiproliferative activity of these complexes was tested against ovarian cancer cell line and cisplatin-resistant strain A2780cisR, using the MTT assay that measures the metabolic activity of viable cells. In general, the cytotoxicities of the complexes may be correlated to their lipophilicity. As the length of the alkyl chain increases, the lipophilicity increases and the cytotoxicity is greater.

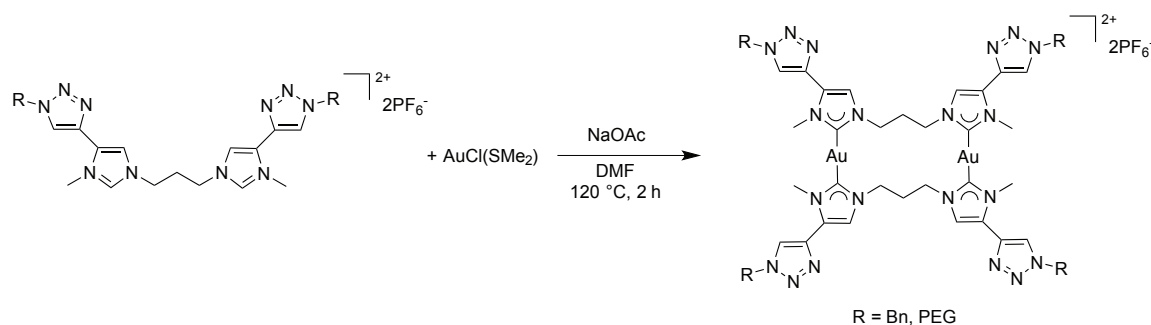
As regards the second approach described before, Baron *et al.*¹⁰⁸ reported the synthesis of functionalized dicarbene proligands (Scheme 3.3), successively employed for the obtainment of gold(I) and gold(III) complexes of interest in bioinorganic chemistry.



Scheme 3.3: syntheses of functionalized dicarbene proligands

The synthesis of the proligands was performed under very mild conditions (room temperature, 2 days) and the products were obtained in good yields and in pure form (as solid with benzyl group or liquid with PEG chains) by simple extraction from the water phase with a halogenated solvent.

The transition metal complexes were prepared by reaction of the proligands with a gold(I) precursor ($\text{AuCl}(\text{SMe}_2)$) in the presence of a base in order to deprotonate the position 2 of the imidazole moieties (Scheme 3.4).



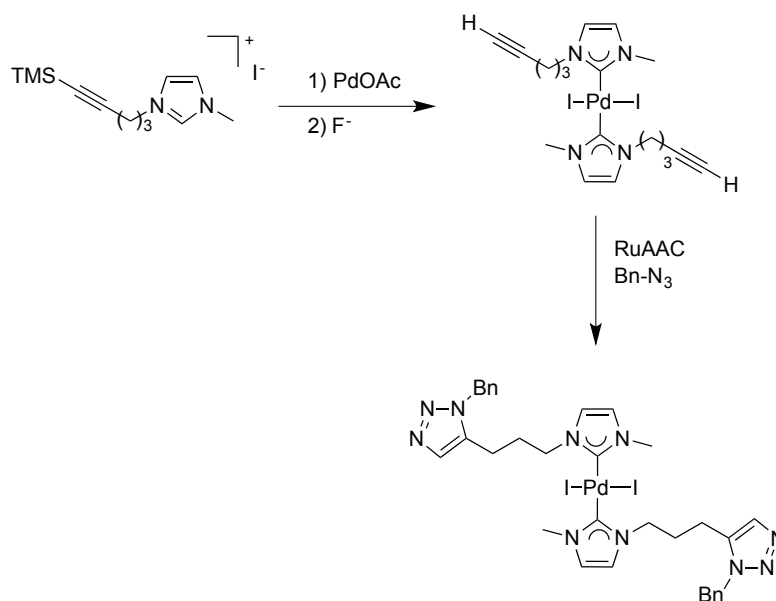
Scheme 3.4: syntheses of gold(I) complexes with triazole-functionalized bisimidazol-2-ylidene ligands

After this step, the oxidative addition of iodide to the gold(I) complexes was performed. All the gold(I) and gold(III) complexes were tested against both tumoral cell and healthy cell lines and demonstrated that their antiproliferative properties are generally very good and positively influenced by the functionalization of the di(N-heterocyclic carbene) ligand. In particular the complexes bearing the PEG chain are the best performers both in terms of activity and selectivity towards the cancer and healthy cell lines.

Chardon *et al.*¹⁰⁵ proposed another pathway for the syntheses of palladium(II) and platinum(II) complexes bearing triazole-functionalized imidazole-2-ylidene ligands.

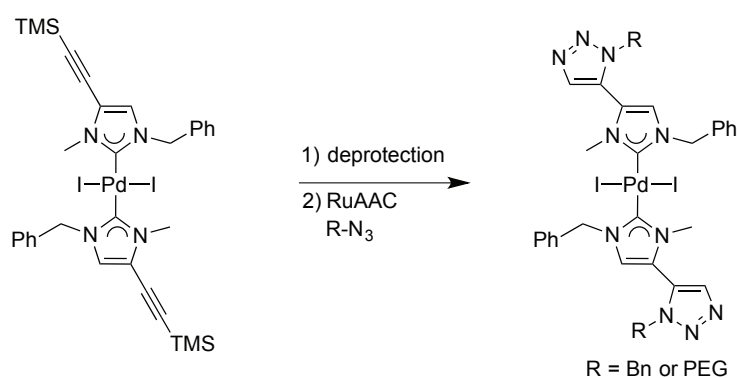
Starting from a proligand with an alkyne substituent on the nitrogen wingtip position, the first step was the synthesis of the palladium complex and the subsequent step was the CuAAC reaction for the functionalization of the imidazoles.

Interestingly, the CuAAC cycloaddition was not efficient for the formation of the triazole ring but a similar pathway, using a ruthenium complex as a catalyst (reaction named RuAAC cycloaddition),¹⁰⁹ allows the formation of the 1,5-regioisomer of the triazole ring (Scheme 3.5).

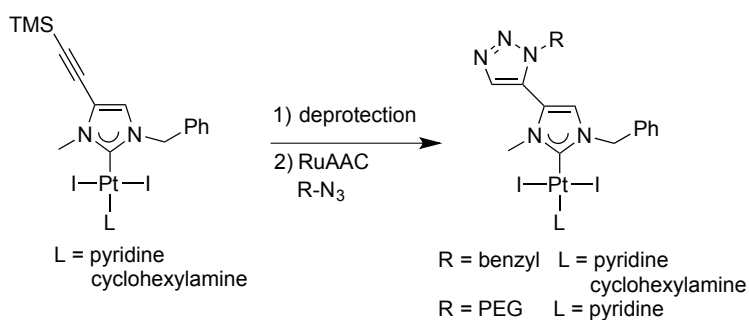


Scheme 3.5: synthesis of palladium(II) complex

The same synthetic strategy can be applied also to palladium(II) or platinum(II) complexes with an alkyne in position 5 of the imidazole moiety (Scheme 3.6 and Scheme 3.7).



Scheme 3.6: functionalization of the imidazole moieties to obtain a triazole-functionalized imidazole-2-ylidene complex



Scheme 3.7: syntheses of platinum(II) complexes with triazole-functionalized imidazole-2-ylidene ligands

For these complexes the CuAAC cycloaddition is not compatible with the presence of palladium metals, but the RuAAC cycloaddition is very useful for such modification.

3.2. Syntheses of the proligands

Different compounds were initially designed as azolium proligands for the subsequent synthesis of NHC metal complexes (Figure 3.2).

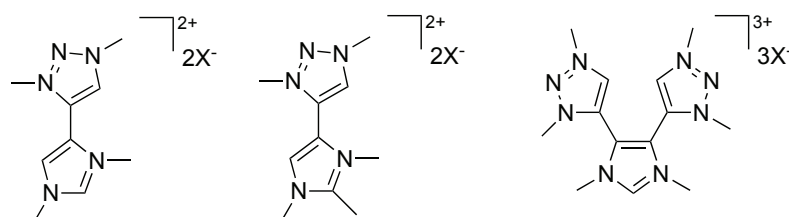


Figure 3.2: different proligand designed

With these different scaffolds it could be possible to obtain complexes with different nuclearity and different ways of coordination of the ligands (via C2 of the imidazole or C5 of the triazole moiety) to the metal center/s, like in the examples reported in Figure 3.3.

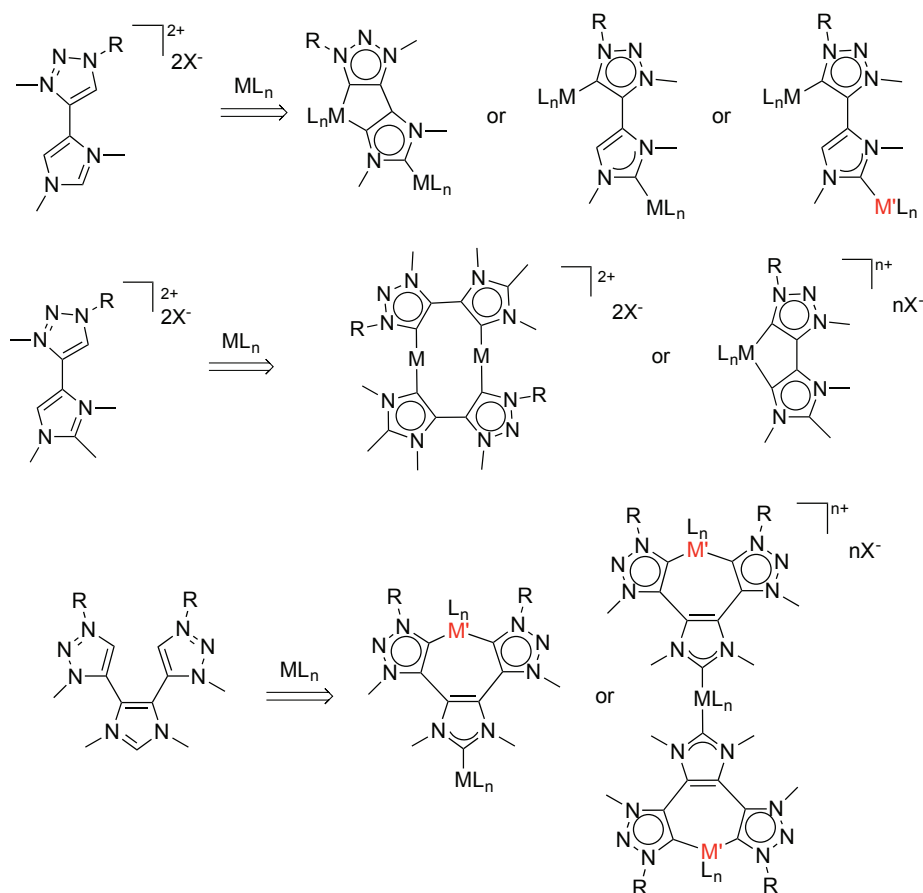


Figure 3.3: design of different metal complexes

The synthetic procedure for all these three proligands implies: 1) syntheses of the imidazole derivatives with iodide substituents in position 4 and/or 5 of the imidazole rings, 2) Sonogashira coupling with a terminal alkyne for the syntheses of the imidazoles with an alkyne group on the backbone; 3) CuAAC reaction for the functionalization of the imidazole rings with the triazole one and 4) quaternization of the nitrogen atom on the imidazole and/or triazole moiety with an alkyl group (Figure 3.4).

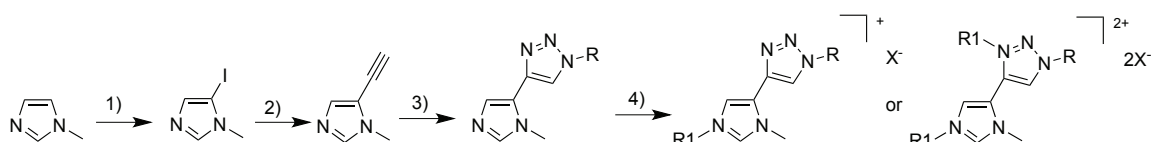


Figure 3.4: general procedure for the syntheses of functionalized imidazolium salts

Using the classical procedure reported in the literature,¹¹⁰ different imidazoles bearing one or two iodide in position 4 and/or 5 were synthesized with good yields and purities (Figure 3.5).

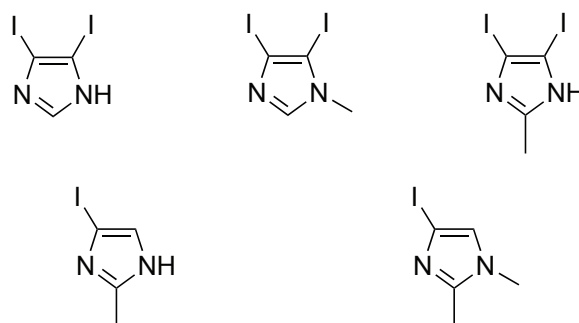
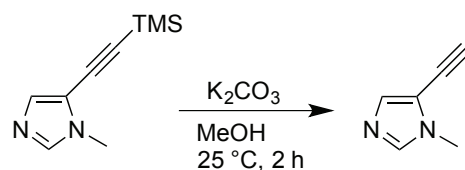


Figure 3.5: imidazoles bearing iodide on the backbone

The second step, i.e. the Sonogashira coupling,¹¹¹ was unfortunately unsuccessful (although reported), despite the different catalyst, solvent, temperature and time employed. In all the cases, the dark crude product shows the presence of a high number of signals and even after purification by column chromatography, it was not possible to isolate a pure species.

So we decided to move to the synthesis of this type of proligands starting from the commercially available 5-[(trimethylsilyl)ethynyl]-1-methylimidazole. The first step was the deprotection of the alkyne group: by treatment with potassium carbonate and

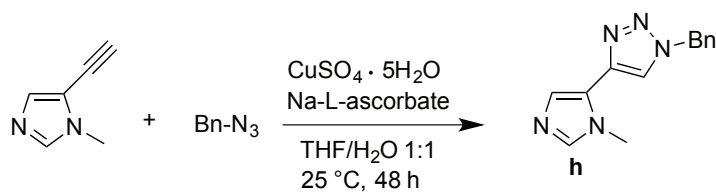
subsequent filtration of the crude solution, the desired product was obtained in excellent yield and purity (Scheme 3.8).



Scheme 3.8: deprotection of 5-[(trimethylsilyl)ethynyl]-1-methylimidazole

The NMR spectra confirm the deprotection of the alkyne, as indicated by the presence of a new signal concerning the C-H alkynyl hydrogen at δ 3.46 ppm.

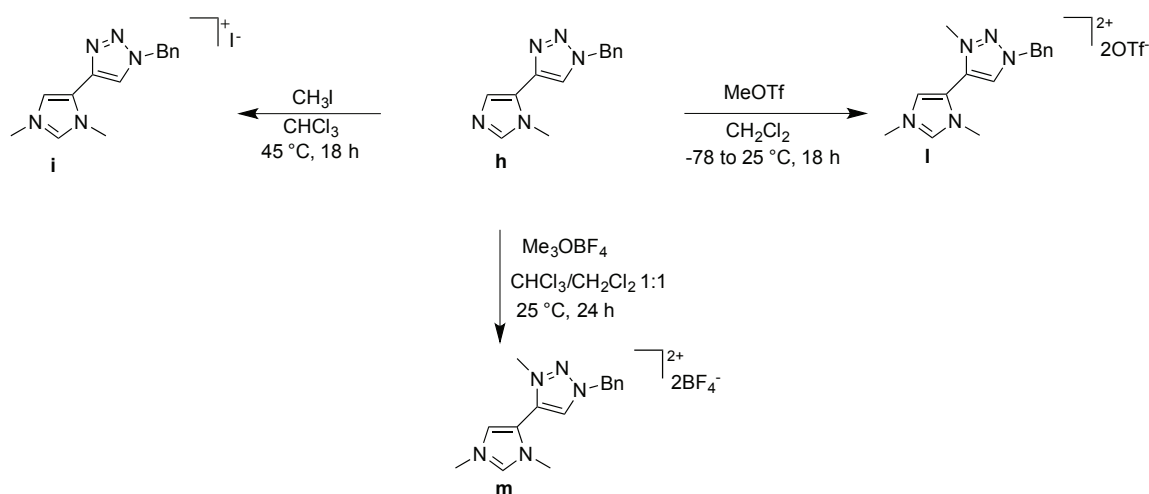
The click reaction with benzyl azide¹⁰⁸ allows the obtainment of the triazole-functionalized imidazole (compound **h**) in discrete yield and good purity. The product is isolated as oil, which has been used without further purification (Scheme 3.9).



Scheme 3.9: synthesis of compound **h**

The ¹H-NMR spectrum confirms the formation of the triazole moiety; in particular, the signal at 3.46 ppm, concerning the proton bonded to the alkyne, is substituted by the CH proton in position 5 of the triazole ring at ca. 7.4 ppm. Also a multiplet at 7.41 ppm, as indication of the presence of a phenyl ring, and a singlet at 5.54 ppm for a CH₂ group, confirm of the presence of the benzyl group bonded to the nitrogen in position 1 of the triazole ring.

The last step is the methylation of the imidazole ring and/or of the triazole one. Different syntheses have been performed using several methylating agents (Scheme 3.10).



Scheme 3.10: reaction pathways for the synthesis of proligands **i**, **l** and **m**

The reaction of the precursor **h** with methyl iodide affords compound **i**, which was simply isolated as a solid by adding diethyl ether to the reaction mixture. The $^1\text{H-NMR}$ spectrum confirms the methylation of the sole imidazole moiety, as indicated by the presence of two signals in the methyl region at 4.04 and 4.14 ppm. The signals of the CH_3 protons are deshielded with respect to the parent reagent, due to the positive charge of the obtained compound. The cationic structure of the proligand is confirmed by the ESI-MS spectra, which present one signal at m/z 254.07 associable to the lost iodide counteranion.

In accordance with data reported in the literature,^{33,112} the methylation of the triazole ring requires the use of stronger methylating agents than methyl iodide (like methyl triflate or trimethyloxonium tetrafluoroborate).

The proligands **l** and **m** were obtained by using stronger methylating agents, respectively MeOTf or Me_3OBF_4 , in chlorinated solvents. In these cases, after removal of the solvent, proligand **m** was isolated as a solid, while proligand **l** has an oily nature. For both compounds the dicationic nature was confirmed by ESI-MS analysis: the mass spectra present in fact the signals concerning the species $[\text{M-anion}]^+$ in which the proligands **l** and **m** have lost respectively one triflate or one tetrafluoroborate anion. The $^1\text{H-NMR}$ spectra confirm the methylation of the nitrogen atoms of both the imidazole and triazole rings; three singlets in the range 3.7 – 4.2 ppm are in fact

detected. All the other signals, predictable on the basis of the proposed structures, are present in the expected range of chemical shift.

In Figure 3.6 a comparison between the ^1H -NMR spectra of the precursor **h** and the proligands **i**, **l** and **m** is shown.

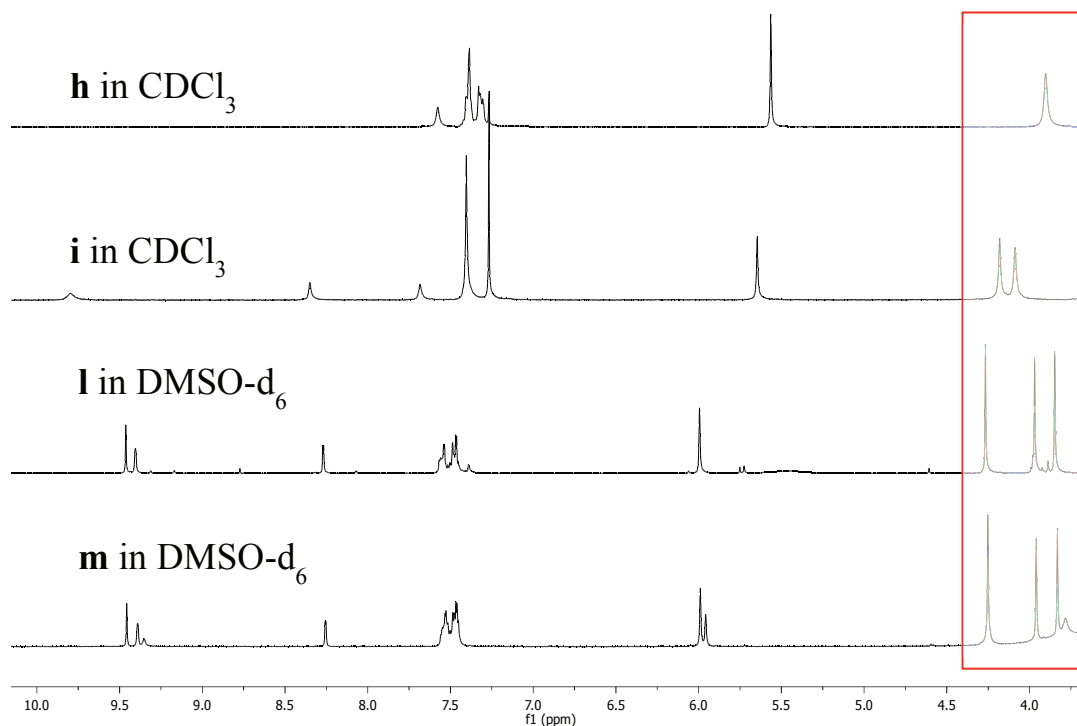


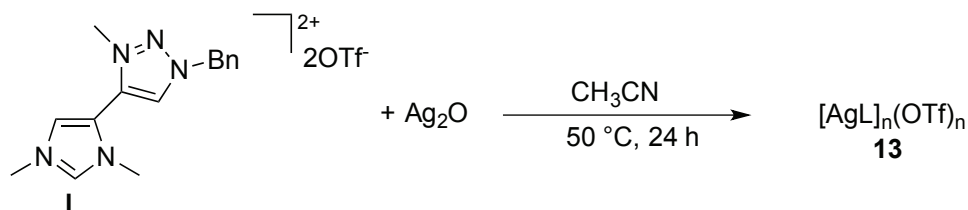
Figure 3.6: ^1H -NMR comparison for the compounds **h**, **i**, **l** and **m**

The qualitative comparison (due to the different deuterated solvents used for the characterization) shows the different degree of methylation. As can be seen in Figure 3.6 the precursor **h** shows only one signal for the methyl protons, the proligand **i** shows two singlets concerning the methyl groups bonded to the N position of the imidazole otherwise the proligands **l** and **m** show the presence of three signals, due to the fully methylated system.

3.3 Syntheses of transition metal complexes

The transmetalation route was chosen as procedure for the syntheses of different transition metal complexes. First of all, it was necessary to synthesize the silver(I) complexes and then use these compounds as reagents for the transmetalation of the imidazole-2-ylidene moiety to different metal centers.

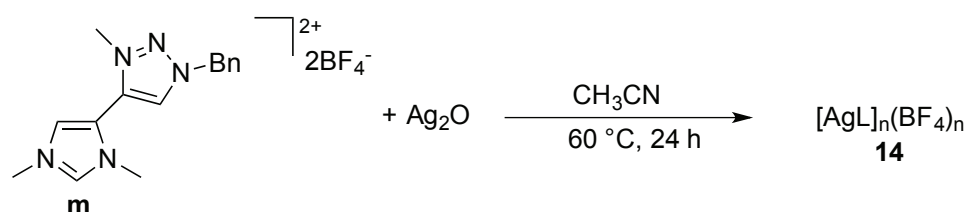
The reaction of proligand **1** with excess Ag_2O in acetonitrile at $50\text{ }^\circ\text{C}$ affords compound **13** as a brown oil (Scheme 3.11).



Scheme 3.11: synthesis of complex **13**

The ^1H -NMR of the residue shows the disappearance of the signals relative to the protons in position 2 of the imidazole ring and in position 5 of the triazole, thus suggesting that the deprotonation of the ligand has occurred in both positions; furthermore in the 2D HMBC and $^{13}\text{C}\{^1\text{H}\}$ -NMR, two signals attributable to the two carbene moieties are observed at δ 184.5 ppm (imidazolylidene) and 168.6 ppm (triazolylidene). The MALDI-TOF spectrum suggests a dinuclear nature for the compound, with the presence of two signals at m/z 899.173 and 1049.088, referred respectively to the fragments $[\text{Ag}_2\text{L}_2\text{OTf}]^+$ and $[\text{Ag}_2\text{L}_2(\text{OTf})_2\text{H}]^+$ with $\text{L} = n\text{NHC}/tz\text{NHC}$ dicarbene ligand (Figure 3.7).

The reaction was performed in similar conditions ($60\text{ }^\circ\text{C}$ for 24 hours) using proligand **m**, obtaining, also in this case, an oily product (complex **14**, Scheme 3.12). The NMR characterization data are very similar to those described for complex **13**, but this complex resulted to be less stable in solution than complex **13**; for example, the solubilization of the complex in deuterated solvent was accompanied by slow formation of a dark solid. This instability also did not allow a characterization of the product by ESI-MS or MALDI techniques, which showed only several fragments without the presence of the molecular peak.



Scheme 3.12: synthesis of complex **14**

For both complexes, the proposed structure is $[\text{AgL}]_n(\text{X})_n$ with a Ag:dicarbene ligand ratio 1:1; on the basis of the MALDI-TOF experiments with complex **13**, they are most likely dinuclear, but it is very difficult to propose a reasonable structure; in fact, a bridging coordination of the dicarbene ligand between two metal centers, would imply a highly tensioned structure. On the other hand, the oily nature of the compounds and the low stability in solution did not allow the obtainment of single crystals, necessary to clarify their structures. For this reason, the subsequent transmetalation reactions have not been studied.

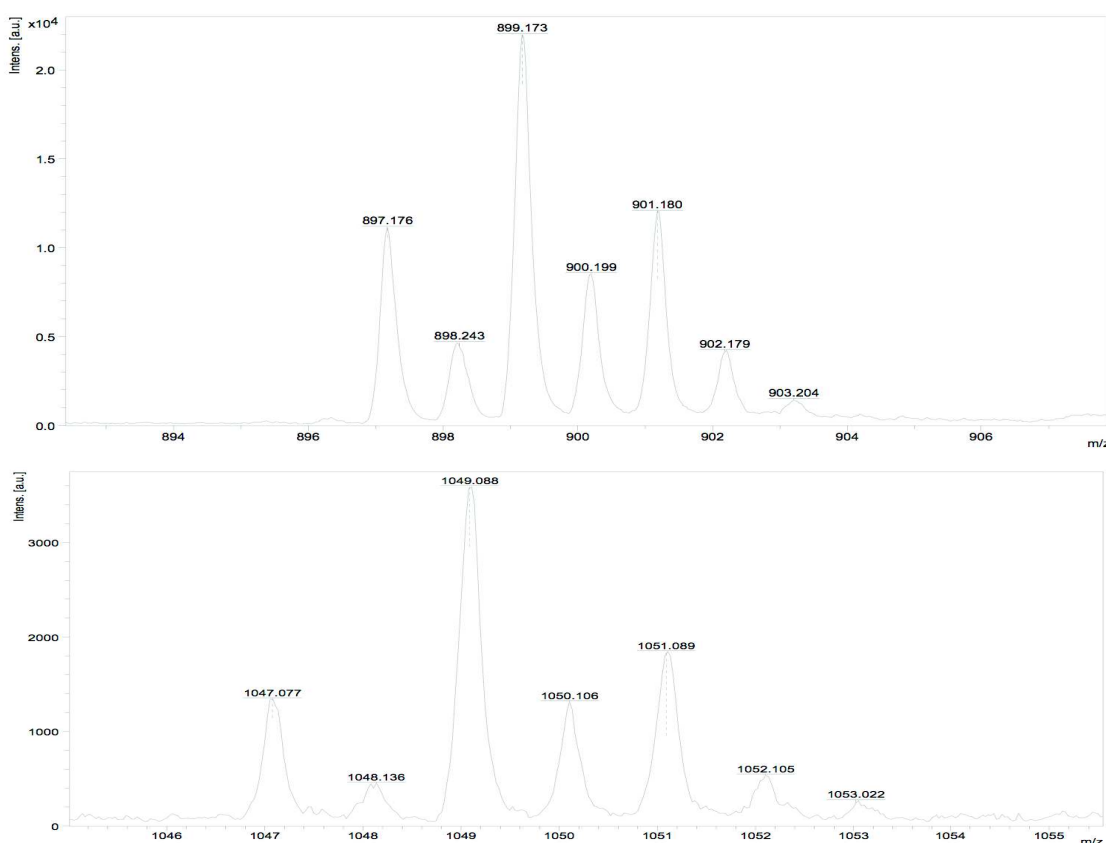
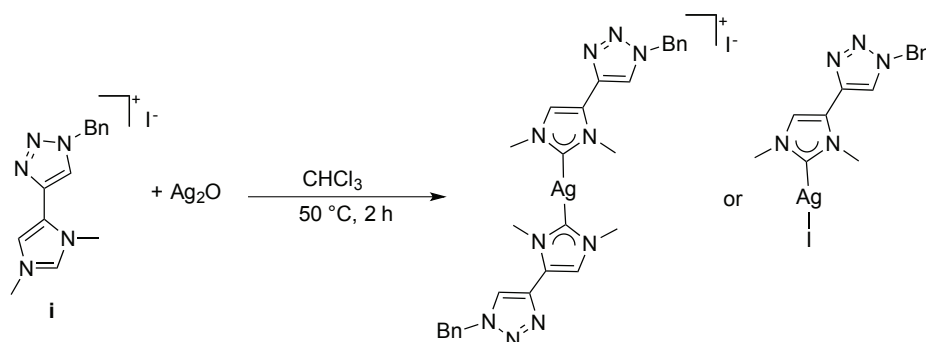


Figure 3.7: MALDI-TOF spectrum of complex **13**. On the top the signal concerning the fragment $[\text{Ag}_2\text{L}_2\text{OTf}]^+$ and on the bottom the signal concerning the fragment $[\text{Ag}_2\text{L}_2(\text{OTf})_2\text{H}]^+$

More attention was focused on proligand **i**. The reaction with excess Ag_2O in chloroform for 2 hours, followed by filtration through Celite, concentration and precipitation with diethyl ether, affords complex **12** as yellow solid soluble in classical chlorinated solvents (CHCl_3 , CH_2Cl_2).

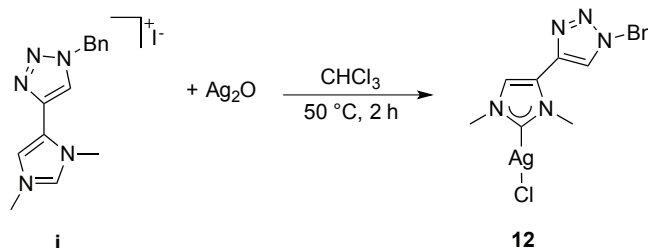
In the ^1H -NMR spectra the signal relative to the C2-H is absent confirming the deprotonation of the imidazolium salt. The formation of the silver(I) complex was assessed via $^{13}\text{C}\{^1\text{H}\}$ -NMR spectra that show a signal at δ 182.0 ppm relative to the C2

carbon, in the typical range of carbene carbon atoms coordinated to an Ag(I) center.¹¹³ The ESI-MS analysis presents a peak relative to the fragment $[\text{AgL}_2]^+$ at m/z 613.13. The two possible products are depicted in Scheme 3.13.



Scheme 3.13: possible complexes for the synthesis of silver(I) complexes

By slow diffusion of diethyl ether into a chloroform solution of the silver(I) complex, single crystals have been obtained and the structure has been elucidated by X-ray diffraction analysis. The silver(I) atom binds one NHC ligand and one chlorine ligand, probably deriving from the solvent used in the synthetic procedure.



Scheme 3.14: synthesis of the silver(I) complex **12**

In literature,¹¹⁴ several examples on similar exchange processes with the chlorinated solvent used during the synthesis are reported, especially with dichloromethane or 1,2-dichloroethane. It is interesting to underline that the same behaviour was reported in the literature for analogous silver(I) complexes of structure $\text{Ag}(\text{NHC})\text{X}$. The ESI-MS experiments present a signal concerning the species $[\text{Ag}(\text{NHC})_2]^+$ and this is in contrast with the solid state characterization, that shows the coordination of only one ligand on the metal center.

The crystal structure is reported in Figure 3.8.

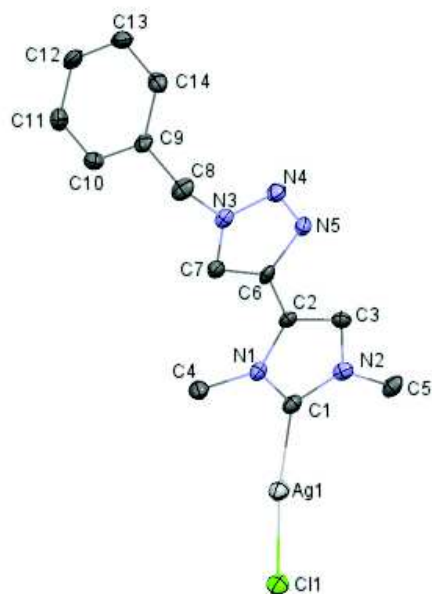


Figure 3.8: ORTEP view of complex **12**. Ellipsoids are drawn at their 30 % probability. Hydrogen atoms have been omitted for clarity. Selected bond distances (Å) and angles (deg): Ag1-Cl1 2.350(14), C1-Ag1 2.072(5), C1-N1 1.366(6), C1-N2 1.356(7), C2-C6 1.442(7), Cl1-Ag1-C1 170.07(14), N1-C1-N2 103.7(4)

The crystal structure is characterized by a non linear coordination of the ligands on the silver(I) atom ($C_{\text{carbene}}\text{-Ag-Cl } 170.07(14)^\circ$) and the Ag- C_{carbene} distance is 2.072(5) Å, coherent with the literature.

A careful observation of the structure and a comparison with the literature,^{114,115} allows to conclude that the correct structure can be described as dimeric with formula $\text{Ag}_2\text{Cl}_2\text{L}_2$ (Figure 3.9). It is interesting to underline that the Ag_2Cl_2 four member ring is planar with Ag...Ag distance of 3.85 Å. The two bridging chlorides are asymmetrically bound with Ag-Cl distances of 2.350(14) Å and 3.11 Å.¹¹⁶

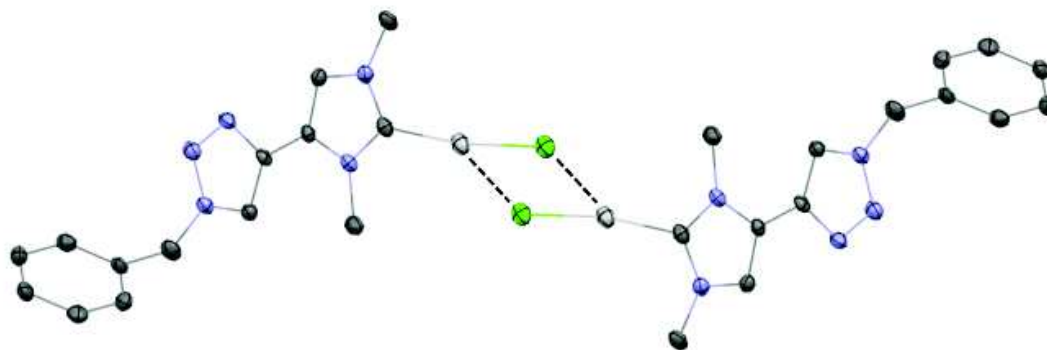
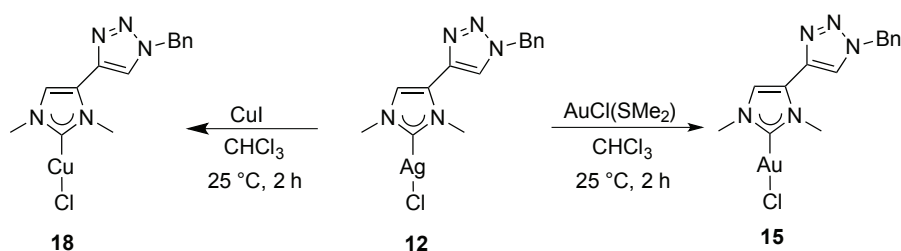


Figure 3.9: dimeric structure of the complex **12**

Gold(I) and copper(I) complexes have been synthesized adding a solution of a gold(I) or copper(I) precursor ($\text{AuCl}(\text{SMe}_2)$ or CuI) into a solution of the silver(I) complex **12**. The precipitation of AgX ($\text{X} = \text{Cl}^-$, I^-) confirms the successful transmetalation of the ligand. After filtration on Celite to remove the silver(I) salts, concentration of the reaction mixture and precipitation with diethyl ether, off-white solids were obtained.



Scheme 3.15: procedures for the syntheses of gold(I) and copper(I) complexes

The $^1\text{H-NMR}$ spectra of the silver(I), gold(I) and copper(I) complexes, **12**, **15** and **18** respectively, are very similar in terms of number, pattern and position of the signals (Figure 3.10). This suggests that the structure of the complex is maintained upon transmetalation; as a proof, the ESI-MS spectra of the gold(I) complex **15** show signals for the fragments $[\text{AuLCH}_3\text{CN}]^+$ and $[\text{AuCl}(\text{L}(\text{CH}_3\text{CN})\text{Na})]^+$ at m/z respectively 491.1280 and 549.0839, adducts with acetonitrile and Na^+ formed during the analysis.

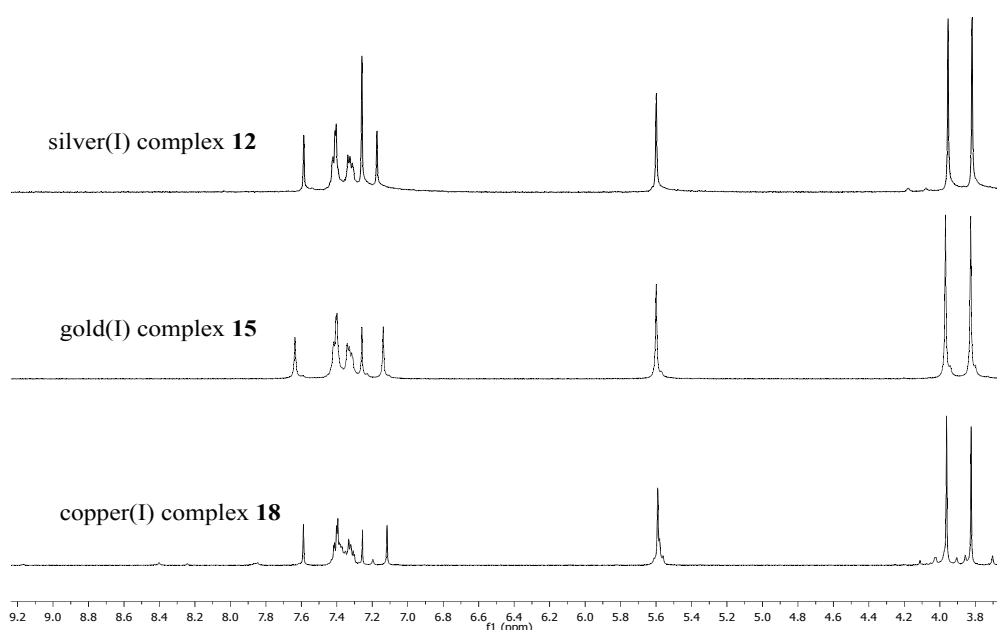


Figure 3.10: $^1\text{H-NMR}$ spectra of complexes **12**, **15**, **18** (in CDCl_3)

A further indication of the successful transmetalation is provided by the $^{13}\text{C}\{^1\text{H}\}$ -NMR spectra: the carbene carbon signals, at δ 173.2 ppm for the gold(I) complex **15** and at δ 179.8 ppm for the copper(I) complex **18**, are shifted compared with the same signal of the silver(I) complex (δ 182.0 ppm). The chemical shifts are coherent with the literature values¹¹⁷ and the observed differences can be attributed to the different Lewis acidity of the metal centers.

The copper(I) complex **18** is rather unstable and tends to decompose both in the solid state and in solution. After one week, it is possible to observe by ^1H -NMR the presence of a signal at ca. δ 10 ppm suggesting the proton in position 2 of the imidazolium ring, clear indication of the re-protonation of the ligand. Working in drybox to synthesize the complex and to stock it, no decomposition phenomena are observed.

By slow diffusion of diethyl ether into a chloroform solution of the gold(I) complex, single crystals of complex **15** have been obtained and the structure has been elucidated by X-ray diffraction analysis. The gold(I) atom coordinates one NHC ligand and one chlorine ligand and maintain the same structure observed for the silver(I) complex **12**.

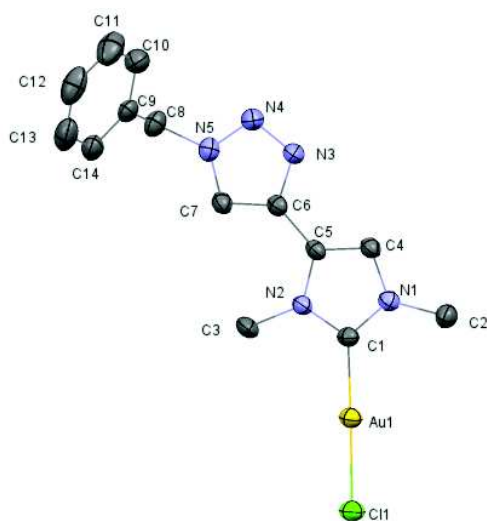


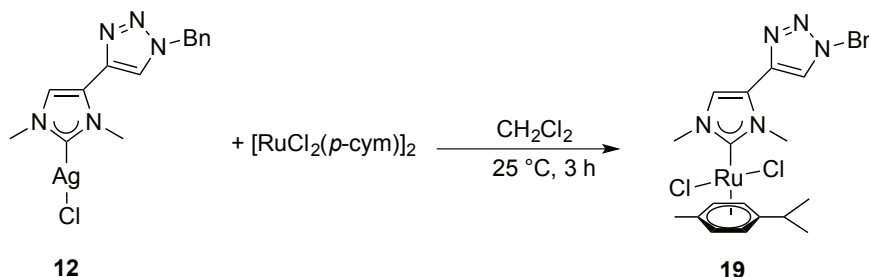
Figure 3.11: ORTEP view of complex **15**. Ellipsoids are drawn at their 30 % probability. Hydrogen atoms have been omitted for clarity. Selected bond distances (\AA) and angles (deg): Au1-Cl1 2.2828(13), C1-Au1 1.977(5), C1-N1 1.366(6), C1-N2 1.345(7), C5-C6 1.436(7), Cl1-Au1-C1 178.14(17), N1-C1-N2 104.6(4)

The crystal structure is characterized by a linear coordination of the ligands on the gold(I) center ($C_{\text{carbene}}\text{-Au-Cl}$ 178.14(17) $^\circ$), the Au- C_{carbene} bond length is 1.977(5) \AA , coherent with the literature.¹²⁶

The sum of the individual covalent radii of Au and C (Au-C) 2.108 Å). The Au-C_{carbene} bond length in **15** is shorter than the Ag-C_{carbene} bond distance [2.072(5) Å] in **12**; this can be explained with a smaller covalent radius of Au than Ag, and with a stronger bond in the case of gold, due to the higher p-backdonation in Au-NHC complexes than Ag-NHC ones. The strong Au-NHC interaction is also confirmed by the fact that the Au-C_{carbene} bond distance is shorter than the sum of the individual covalent radii of Au and C (Au-C) 2.108 Å.

In conclusion, the transmetalation route afforded gold(I) and copper(I) complexes, that maintain the same geometry and set of ligands on the metal center of the silver complex, as expected considering the similar chemical behavior of these three metals.

The transmetalation reaction was adopted also for the synthesis of the ruthenium(II) complex **19**. Using the dimer [RuCl₂(*p*-cymene)]₂ as ruthenium source in dry CH₂Cl₂ as solvent, the ruthenium(II)-NHC complex **19** has been obtained as brown-orange solid (Scheme 3.16).



Scheme 3.16: synthesis of ruthenium(II) complex **19**

All the characterizations confirm the proposed structure. The MS spectrum presents a fragment at m/z 524.1148 associable to the species [RuCl(*p*-cym)]⁺ (Figure 3.12), derived from the starting complex by a simple loss of a chloride ligand; the simulated pattern perfectly fits the experimental one.

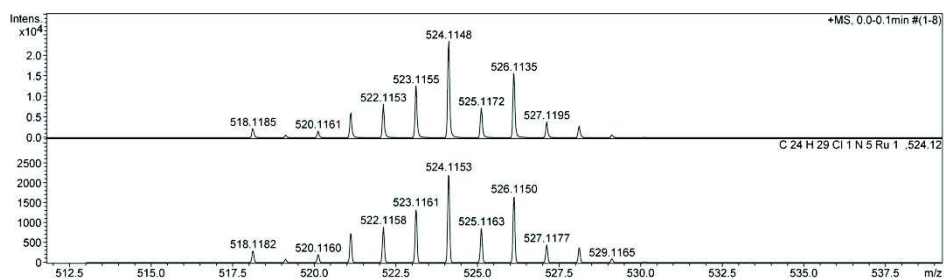


Figure 3.12: MS-spectrum of complex **19**. On the top the experimental signal concerning the fragment $[\text{RuCIL}(p\text{-cym})]^+$ and on the bottom the simulated isotopic pattern

The NMR spectra are coherent with the coordination to the ruthenium(II) center (in an octahedral geometry) of a carbene ligand and a *para*-cymene ring; in the $^{13}\text{C}\{^1\text{H}\}$ -NMR the carbene carbon signal at δ 175.7 ppm confirms the coordination of the NHC unity to a ruthenium(II) metal.¹¹⁸ The coordination sphere of the metal is completed by two chloride anions.

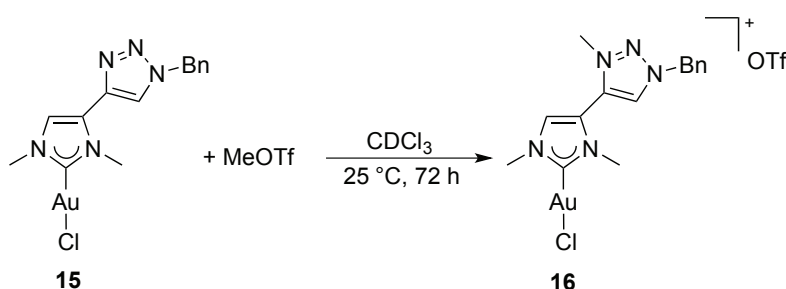
The stability of the gold(I) complex **15** obtained in this way prompted us to investigate a different approach for the obtainment of dinuclear complexes with *n*NHC/*tz*NHC mixed dicarbene ligands. This different synthetic procedure implies: i) methylation of the triazole ring of complex **15**, followed by ii) deprotonation of the triazole ring by reaction with silver(I) oxide. This two-step strategy is interesting because, in principle, it might allow the synthesis of homo- and heterobimetallic carbene complexes and has been already employed in the literature with simple di(*n*NHC) ligands.¹¹⁹

As regards the first step, different methylating agents have been tested (MeI , Me_3OBF_4), however the best results have been obtained with MeOTf in CHCl_3 as solvent. The addition of MeOTf to a solution of complex **15** in CDCl_3 causes a change in the colour of the reaction mixture; the reaction was followed via ^1H -NMR, observing the progressive disappearance of the signals related to complex **15** and the concomitant formation of some crystals. The completeness of the reaction was reached after three days at room temperature. The crystals were separated from the reaction mixture and dissolved in CD_3CN .

The ^1H -NMR spectrum confirms the methylation of the N3 nitrogen atom of the triazole ring and the obtainment of the cationic compound **16** (Scheme 3.17). The presence of a new singlet at 4.12 ppm in the ^1H -NMR spectrum and at 39.7 ppm in the ^{13}C -NMR one confirms the methylation of the nitrogen in position 3 of the triazole moiety. An

interesting evidence in the ^1H and ^{13}C -NMR spectra is the shift (ca. 1 ppm in the ^1H -NMR and ca. 10 ppm in the ^{13}C -NMR spectrum) of the signals associated to the CH group in position 5 of the triazole ring. This is probably due to the methylation of the nitrogen in position 3 that changes the electronic properties of the ring that could be reflected in this experimental feature.

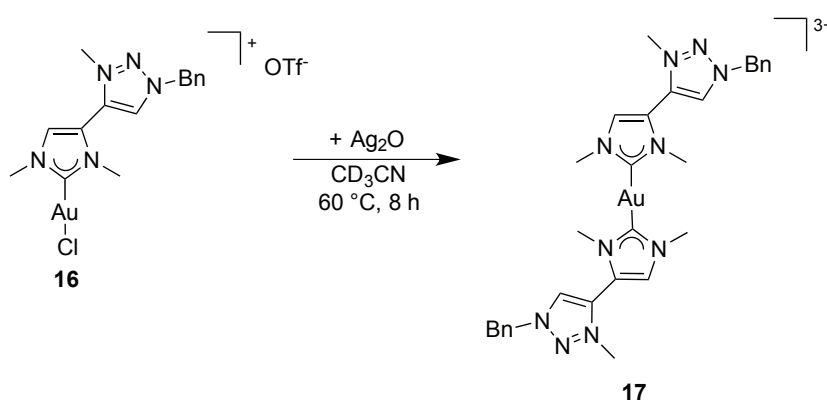
The position of the carbene carbon signal does not change significantly going from complex **15** to **16** (173.2 and 175.8 ppm, respectively), suggesting that the coordination sphere around the gold(I) center has not been affected by the reaction with MeOTf.



Scheme 3.17: synthesis of complex **16** via methylation of the complex **15**

The cationic nature of complex **16** was assessed also by ESI-MS spectrometry. The spectra displays a signal at m/z 500.00 representative of the fragment $[\text{AuLCl}]^+$.

Interestingly, complex **16** tends to evolve in acetonitrile solution at room temperature, as indicated by the appearance of a new set of signals in the ^1H -NMR spectra. The conversion is slow at room temperature and can be accelerated by adding Ag_2O (3 eq.) and heating the NMR tube at $60\text{ }^\circ\text{C}$ for 8 hours (Scheme 3.18).



Scheme 3.18: reaction procedure from the complex **16** to the complex **17**

The signals of the new species can be attributed to complex **17**, which is formed by a gold(I) center coordinated to two *n*NHC ligands. In the ESI-MS spectra the fragments $[\text{AuClL}_2\text{Na}]^+$ and $[\text{AuL}_2(\text{OTf})_2]^+$ confirm the coordination of two carbene moieties to the metal center. The proposed reaction is further supported by the shift of all the signals in the ^1H - (Figure 3.13) and ^{13}C -NMR spectra; in particular in the ^{13}C -NMR spectrum, the carbene carbon shifts from δ 175 ppm to 188 ppm, in the typical range of carbene carbons coordinated to a gold(I) center and having respectively in *trans* a halide ligand or a carbene ligand.¹²⁰

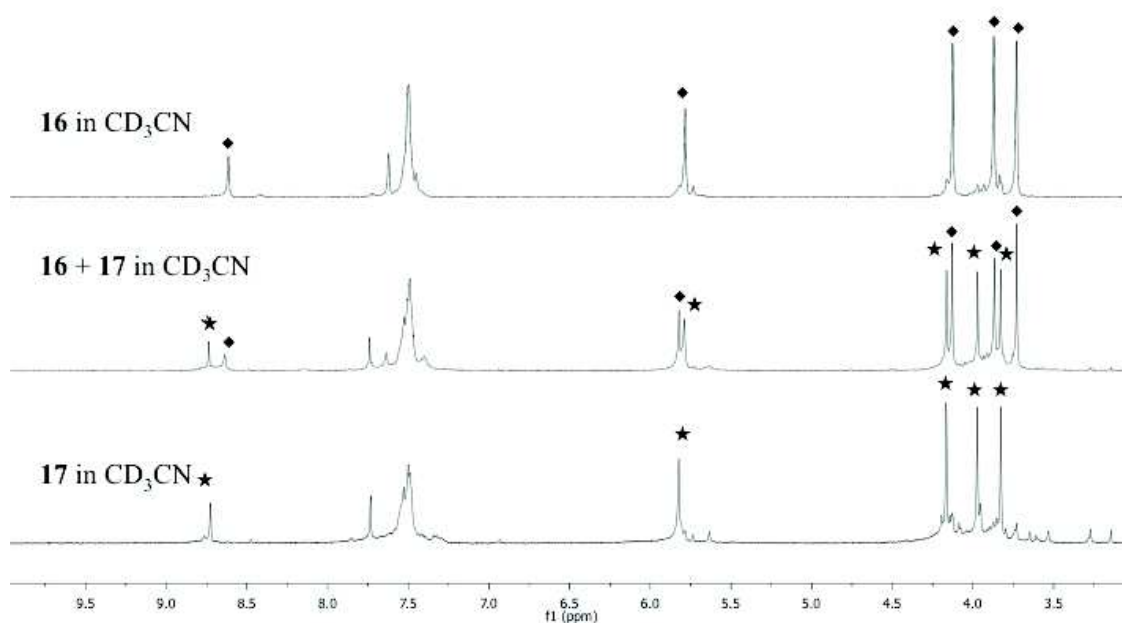
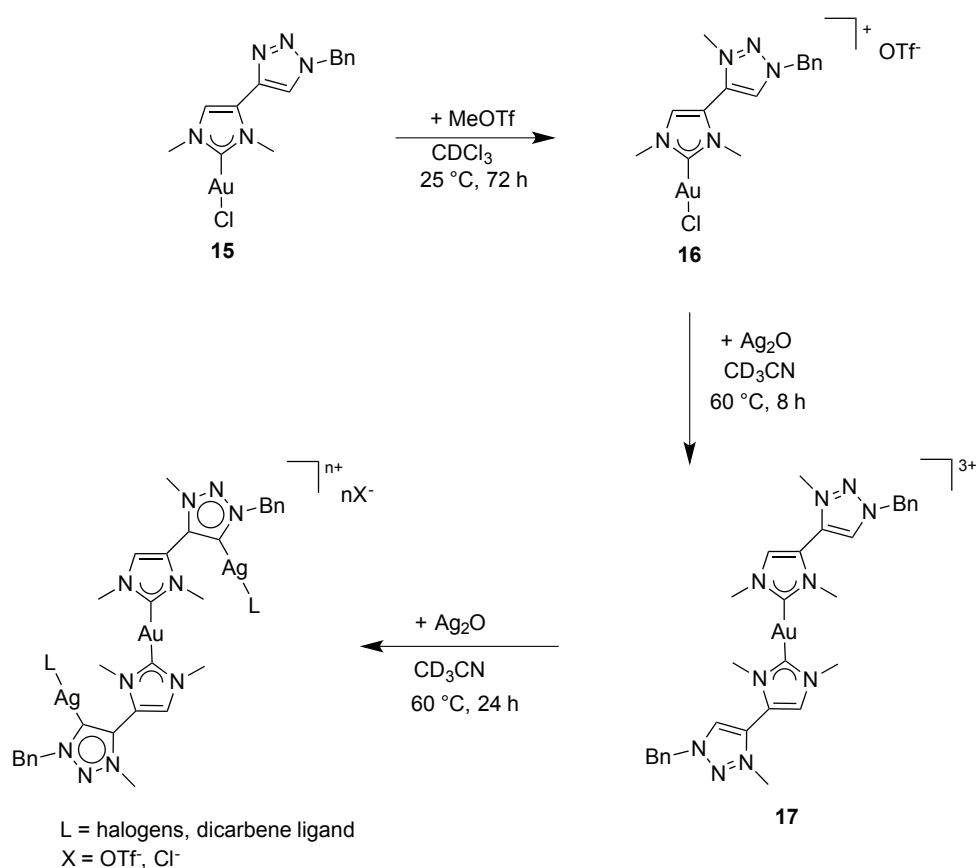


Figure 3.13: ^1H -NMR spectra showing the evolution of complex **16** into complex **17**

The counterion of the tricationic complex is not clear, due to the presence in solution of both triflate and chloride species.

A preliminary test was performed for the obtainment of a heterobimetallic complex of gold(I)/silver(I). Starting from complex **15**, the methylation with MeOTf afforded complex **16**. The subsequent addition of Ag_2O in excess (three equivalents with respect to complex **15**) for eight hours at 60 °C allows to convert complex **16** in the gold(I) complex **17** as described before.

An additional treatment (60 °C) of this resulting mixture (complex **17** and Ag_2O) for 24 hours showed the disappearance of the C5-H signal of the triazole (Scheme 3.19). The nature of this product has not been further investigated.



Scheme 3.19: reaction pathway for the synthesis of heterobimetallic complex

3.4 Biological tests

N-heterocyclic carbene complexes can be used as anticancer molecules for bioinorganic applications.^{108,121,122} *Cis*-platin is the mostly important coordination compound and it is active against different tumor cell lines but it presents undesirable side effects as neurotoxicity¹²³ and nephrotoxicity.¹²⁴ Different metal complexes are studied as alternative anticancer agents; in particular, gold(I) or gold(III) complexes bearing different type of ligands (porphyrins, dithiocarbamate and N-heterocyclic carbenes) show better performances than *cis*-platin and also reduced toxicity towards healthy cell lines.¹²⁵

The anti-cancer potential of gold(I) is widely studied starting from the use of Aurofin and analogous complexes in which one phosphine can be replaced with an NHC (Figure 3.14).¹²⁶

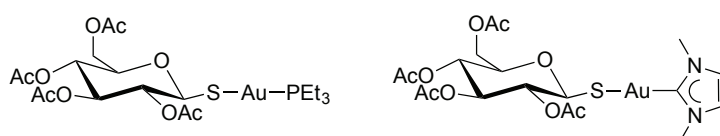


Figure 3.14: Aurofin and related NHC complex

Concerning silver(I) complexes they are usually used as antimicrobial agents and they have been proved to exhibit low toxicity towards humans,¹²⁷ furthermore some examples are present concerning the use complexes with this metal as anticancer compounds.¹²⁸ Also ruthenium compounds in different oxidation states (+II or +III) exhibit interesting properties in this regard.¹²⁹

Looking for transition metal complexes bearing NHC ligands, some comparisons between different IC₅₀ (in μM) of silver(I) complexes bearing imidazolin-2-ylidene and imidazol-2-ylidene ligands¹²³ can be done (Figure 3.15).

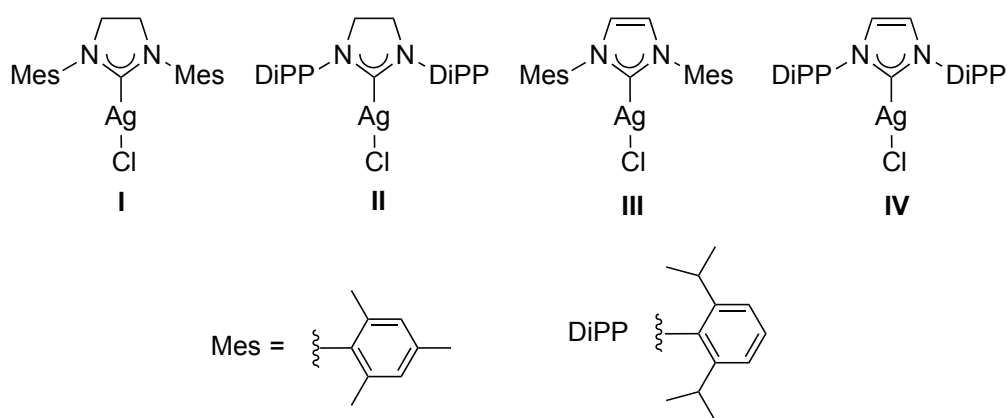


Figure 3.15: examples of different silver(I) complexes that have been tested as antitumoral agents against MCF7 cell line

Table 3.1: IC₅₀ (in μM) values for silver(I) complexes with MCF7 (breast cancer) cell line

Cis-platin	I	II	III	IV
10.4 \pm 0.01	0.25 \pm 0.01	0.06 \pm 0.01	0.08 \pm 0.01	0.03 \pm 0.01

Silver(I) complexes **I - IV**, bearing a imidazoline- or imidazole-2-ylidene ligand, are more active than *cis*-platin (Table 3.1). Concerning the nature of the ring, it is evident that the antiproliferative activity can be increased by working with more hindered substituents on the nitrogen wingtip atoms (Mes vs. DiPP) or by replacing the imidazoline-2-ylidene ligand with a more stable imidazole-2-ylidene.

Comparing the results obtained with the silver(I) complex **I** (Figure 3.16) and those of the corresponding gold(I) complex **V**, it can be observed that the IC₅₀ value for the gold(I) complex¹³⁰ is higher than that of the silver(I) complex and one order of magnitude lower with respect to that of *cis*-platin. This is somehow surprising

considering that in general gold(I) complexes have been assessed as less toxic (as a consequence of a lower IC_{50} value) than analogous silver(I) ones.

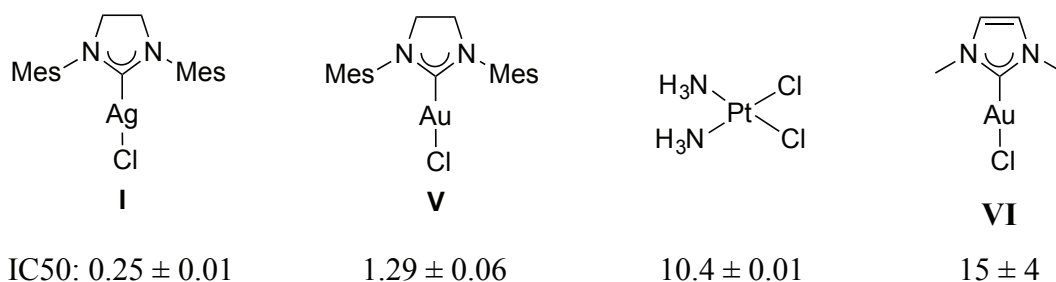


Figure 3.16: comparison between IC_{50} of silver(I), gold(I) and platinum(II) complexes with MCF7 cell line

In another study,¹³⁰ the gold(I) complex VI,¹³¹ smaller R groups on the nitrogen atoms and insaturation on the backbone, shows an IC_{50} (in μM) of 15 ± 4 with the MCF7 cell line. This suggests the importance of the steric hindrance of the nitrogen wingtip substituents in determining the stability and biological activity of the gold(I) complexes.

Ruthenium(II) complexes bearing a N-heterocyclic carbene ligand (Figure 3.17),¹³² show almost no activity with MCF7 cell line.

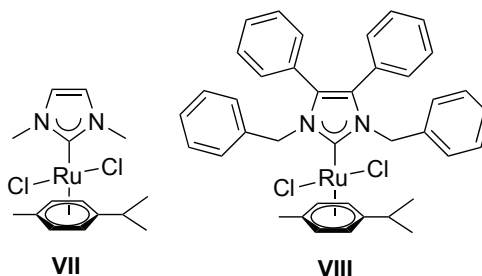


Figure 3.17: ruthenium(II) NHC complexes with almost no anticancer activity

The stable synthesized complexes of silver(I) **12**, gold(I) **15**, and ruthenium(II) **19** were tested with different tumoral cells: HCT116 (human colorectal carcinoma cell line), the MCF7 (a breast cancer cell line) and the PC3 (human prostat cancer cell line).

In Table 3.2 are reported the half inhibitory concentration (IC_{50} in μM) values for these complexes and the value for the *cis*-platin, taken as reference complex.

Table 3.2: IC₅₀ in (μM) values for complexes **12**, **15**, **19**

	HCT116	MCF7	PC3
12	1.38 ± 0.36	2.0 ± 0.2	0.3 ± 0.1
15	6.4 ± 0.8	7 ± 1	6 ± 1
19	40 ± 1	11.6 ± 0.5	25 ± 2
<i>cis-platin</i>	3.6 ± 0.1	4.2 ± 0.7	3.1 ± 0.2

After 72h of incubation; stock solutions in DMSO for all complexes; stock solutions in H₂O for cisplatin. MCF7 (breast carcinoma), HCT116 (colon cancer cells), PC3 (prostateadenocarcinoma). These tests were performed at Institut de Chimie des Substances Naturelles CNRS – UPR2301, Gif-Sur-Yvette, France.

The bio-activity of a complex is generally related to the release of the metal within the cell and may also be influenced by the stability of the complex itself: the best performances are obtained with metal complexes which are neither too inert (no release of metal) nor too labile (metal released in a very short period).¹³¹

In our case, the best performances have been obtained with the silver(I) complex **12** that shows better results than *cis-platin* (ten times more active in the case of PC3) and an interesting selectivity within the different analysed cell lines: the silver(I) complex **12** expresses in fact the cytotoxicity preferentially against the prostate cancer cell line.

Also the gold(I) complex **15** shows good IC₅₀ values, comparable to those of *cis-platin*, but with no selectivity between the different cell lines.

The results with the ruthenium(II) complex are less interesting, since high values of IC₅₀ have been obtained; nonetheless, these values are comparable or superior with the examples reported before with this metal.

These preliminary results indicate a trend between the different metal centers, already observed in the literature: moving from ruthenium(II) to gold(I) and silver(I) complexes, the performances in terms of activity against the different cancer cell lines (lower IC₅₀) are increased.

Regarding the functionalization of the imidazole-2-ylidene ligands with the 1,2,3-triazole ring, the effects are different with the different metals.

For the ruthenium(II) complexes, the presence of the triazole ring allows to increase the performances (comparison of the activities towards MCF7 shown by complex **19** and the complexes reported in Figure 3.17), which however still remain lower than those of the other metal complexes.

Concerning gold(I) complexes, the IC_{50} towards cancer cells MCF7 decreases of ca. one order of magnitude moving from the not functionalized complex **VI** to the functionalized one **15**; these data are in agreement with the same conclusions reached by Baron *et al.* regarding dinuclear gold(I) complexes with functionalized diNHC.¹⁰⁸ Finally, considering silver(I) complex **12**, a direct parallelism with the literature cannot be done, because the reported complexes (**II** and **IV** of Table 3.1) have different substituents on the nitrogen atoms of the imidazole rings. Anyway, it seems that the presence of a triazole ring on the backbone of the imidazole moiety decrease the performances of the compounds (higher IC_{50} values), probably due to the different interaction (hydrogen bonds, $\pi \cdots \pi$ or Van Der Waals interaction) of the molecule with the cells.

It will be interesting to extend the library of complexes in order to better compare the results and find more correlations between the anticancer activity of the metal complex and the structure of the NHC ligand (effect of the nature of the ring, substituents on the nitrogen atoms, substituents on the triazole ring). Furthermore, also the mechanism of action of the different complexes could be investigated in the future. On the basis of the literature, the mechanism of action of the silver(I) and gold(I) complexes should be similar, and in particular it should involve the substitution of the ancillary ligand (most probably the chloride) with sulfur containing biomolecules.^{133,134}

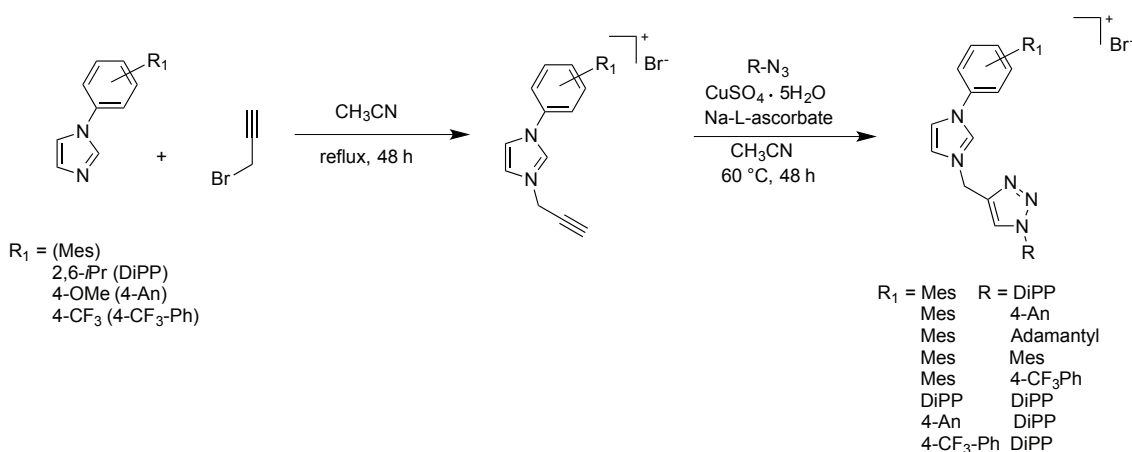
Chapter 4: RESULTS AND DISCUSSION

Metal complexes with heteroditopic ligands based on imidazol-2-ylidene and 1,2,3-triazol-5-ylidene moieties connected with a propylene bridge

4.1 Introduction

In Chapter 3, the general way to synthesize triazole rings, the possible modification of the imidazole backbone introducing a triazole substituent, and the synthesis of the corresponding metal complexes have been described. In this chapter, we will focus on a different approach, i.e. the introduction of the triazole functionality in the nitrogen wingtip substituent.¹³⁵

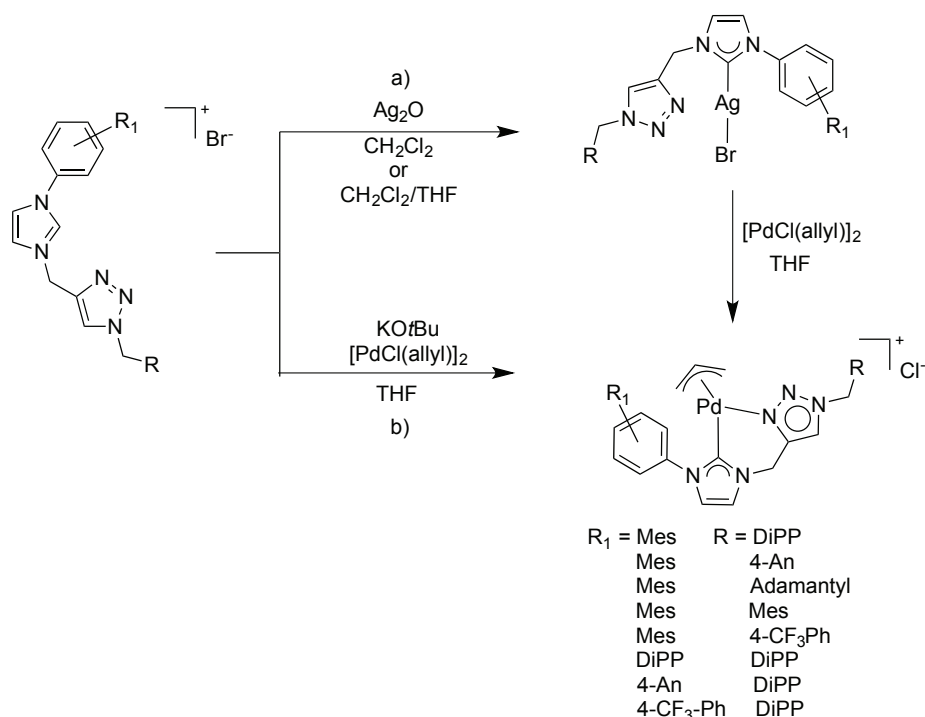
In this frame, the group of prof. Elsevier reported the synthesis of imidazolium salts with 1,2,3-triazoles on the substituent of the nitrogen atom in position 3 of the imidazole.¹³⁶ The first step of the synthetic procedure is the alkylation of the N-substituted imidazole with propargyl bromide (Scheme 4.1) followed by the CuAAC reaction to build the 1,2,3-triazole ring.



Scheme 4.1: syntheses of N-(prop-2-ynyl) imidazolium salts and subsequent Cu-catalyzed cycloaddition to introduce the 1,2,3-triazole moieties

Starting from these proligands, silver(I) and palladium(II) complexes were synthesized, with the procedures reported in Scheme 4.2. The silver(I) complexes are stable only in solution and the palladium(II) complexes can be obtained *via* transmetalation of the

NHC ligand (Scheme 4.2 a). Alternatively the synthesis of the Pd(II) complexes can be performed via deprotonation of the azolium salt with a strong base followed by the addition of the palladium(II) precursor (Scheme 4.2 b).



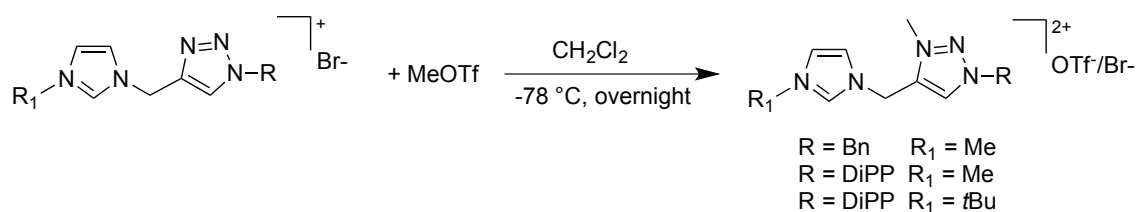
Scheme 4.2: syntheses of different metal complexes starting from functionalized *n*NHC proligands

It is important to underline that the triazole ring could act as a nitrogen donor ligand toward the metal center via the free nitrogen in position 3, as demonstrated in the case of palladium.

Only the quaternization of this position with an alkyl or aryl group provides 1,2,3-triazolium rings, which upon deprotonation of the CH group in position 5 of the triazolium ring, generate a second carbene ligand.

Cowie *et al.*⁴⁸ described the synthesis of unsymmetrical dicarbenes based on one N-heterocyclic carbene and one mesoionic carbene and the related homo- or hetero-bimetallic complexes.

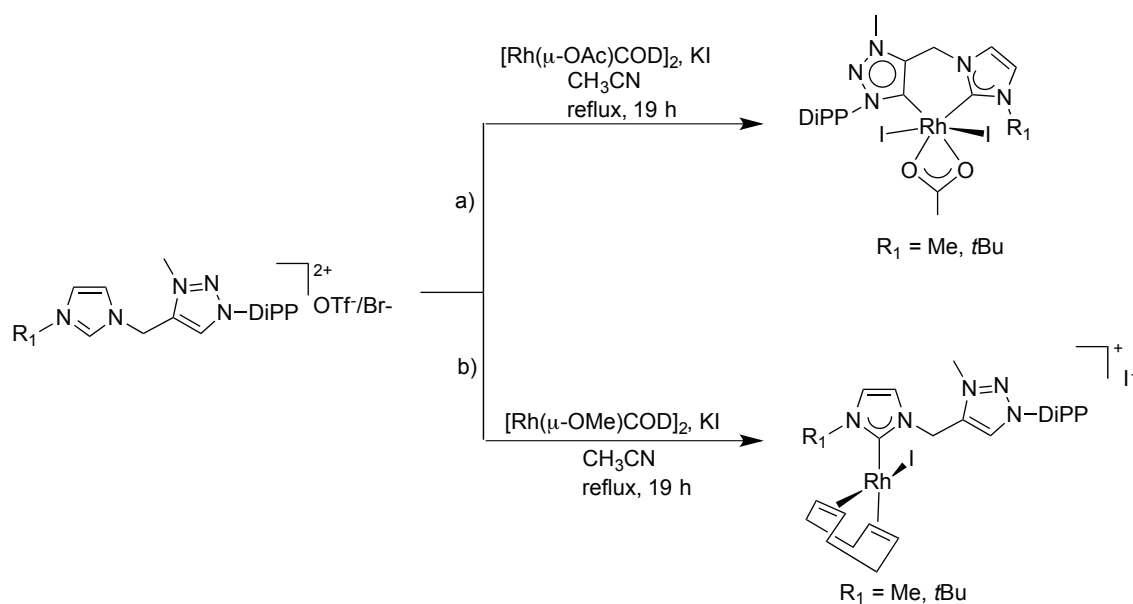
The proligands were obtained by using the same synthetic procedure reported in, followed by methylation of the N3-position of the triazole moiety with methyl triflate as alkylating agent (Scheme 4.3).



Scheme 4.3: methylation of N3-position of the triazole moiety

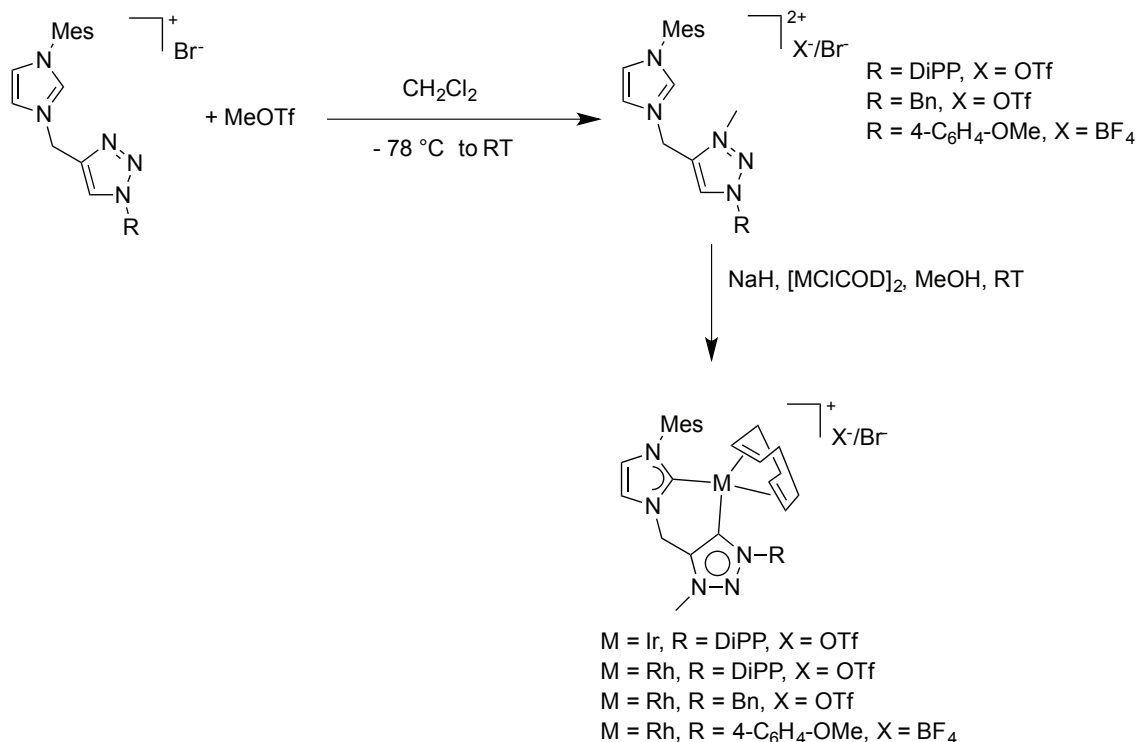
Different NHC metal complexes can be synthesized starting from these proligands. First of all, using $[\text{Rh}(\mu\text{-OAc})\text{COD}]_2$ in acetonitrile at reflux, rhodium(III) complexes have been isolated; the metal center is coordinated by one chelating *n*NHC/*tz*NHC dicarbene ligand, a chelating acetate anion and two iodides (Scheme 4.4 a).

Changing the nature of the metal precursor ($[\text{Rh}(\mu\text{-OMe})\text{COD}]_2$) a rhodium(I) complex was obtained, in which only the *n*NHC is ligated to the metal center, while the triazolium ring has not been deprotonated (Scheme 4.4 b).



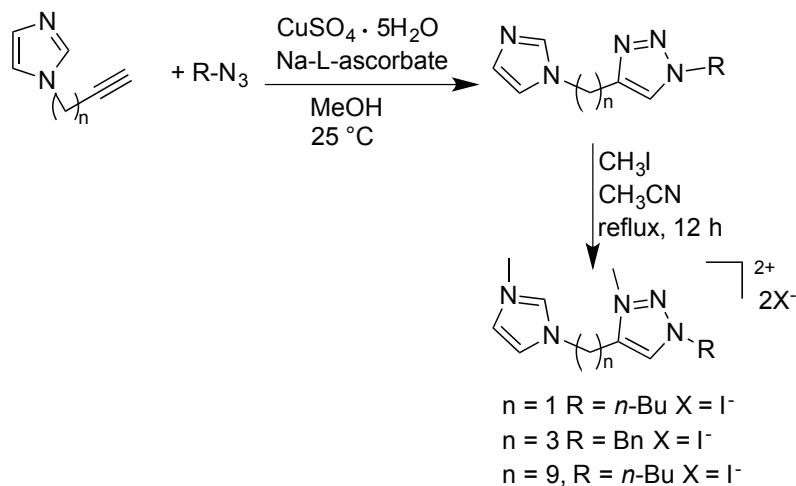
Scheme 4.4: syntheses of a) rhodium(III) or b) rhodium(I) complexes

A similar behavior has been observed also for palladium(II) complexes: by using palladium acetate as metal precursor, only coordination of the *n*NHC-C2 to the metal center has been detected; in this case the C5H of the *tz*NHC ring remains indeed untouched (Scheme 4.5).



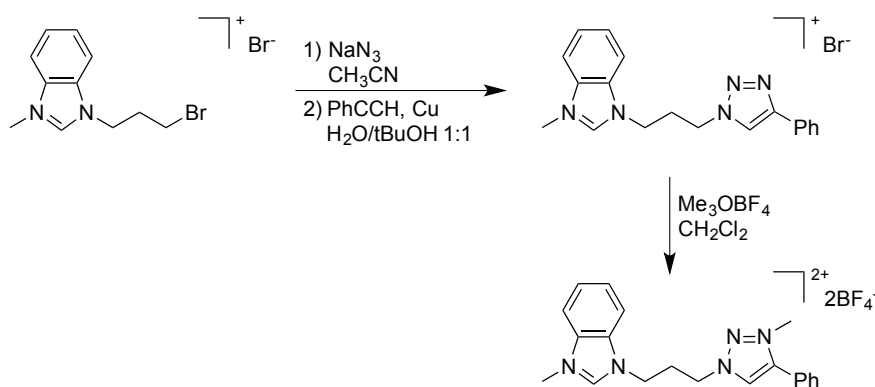
Scheme 4.8: syntheses of imidazole/1,2,3-triazole proligands and related transition metal complexes

Liebscher and co-workers¹³⁷ changed the length of the bridge between the imidazole and the triazole moieties; the proligands were obtained in two steps: click reaction to obtain the functionalized imidazoles, followed by alkylation with MeI (Scheme 4.9).¹³⁸



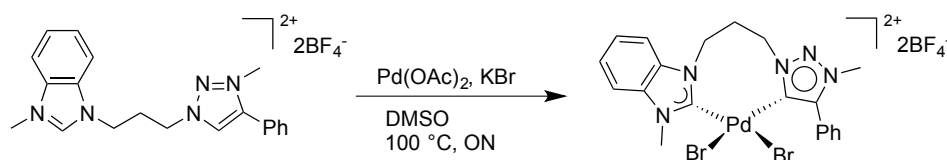
Scheme 4.9: syntheses of mixed imidazolium/triazolium proligands with different bridges

Huynh *et al.*^{135c} adopted another procedure for the synthesis of a proligand with propylene bridge: the treatment of a bromo-substituted imidazolium salt with sodium azide and phenyl acetylene in presence of copper powder affords the formation of the triazole ring that can be successively methylated with Me_3OBF_4 (Scheme 4.10).



Scheme 4.10: synthesis of mixed imidazolium/1,2,3-triazolium salt

The synthesis of a palladium(II) complex was possible by treatment of the proligand in the presence of palladium(II) acetate in DMSO at 100 °C (Scheme 4.11).

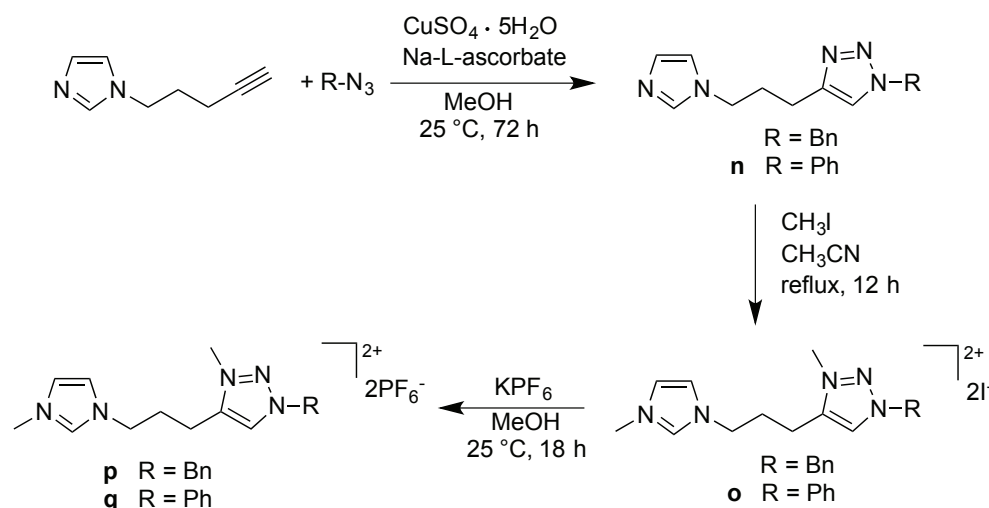


Scheme 4.11: synthesis of palladium(II) complex with chelation of the diNHC units to the metal center

In this Chapter, the syntheses of mixed proligands with imidazolium and 1,2,3-triazolium rings bridged by a propylene unit and the syntheses of the corresponding transition metal complexes will be described. The choice of a propylene bridge between the two heterocyclic rings was due to the finding that a dinuclear gold(I) complex with a propylene bridged di(imidazol-2-ylidene) ligand showed almost a unitary quantum yield of emission in the blue region.³¹ We thus are expecting to generate similar dinuclear gold(I) complexes with a mixed ligand.

4.2 Syntheses of the proligands

Following the procedure reported by Liebscher,¹³⁷ two different proligands with a propylene bridge between the two rings were successfully synthesized (Scheme 4.12).



Scheme 4.12: reaction pathway for the syntheses of the proligands **p** and **q**

The last step of the procedure, i.e. the anion exchange between I^- and PF_6^- was performed in order to increase the solubility of the proligands in polar solvents (DMSO and mostly CH_3CN), giving proligands **p** and **q**.

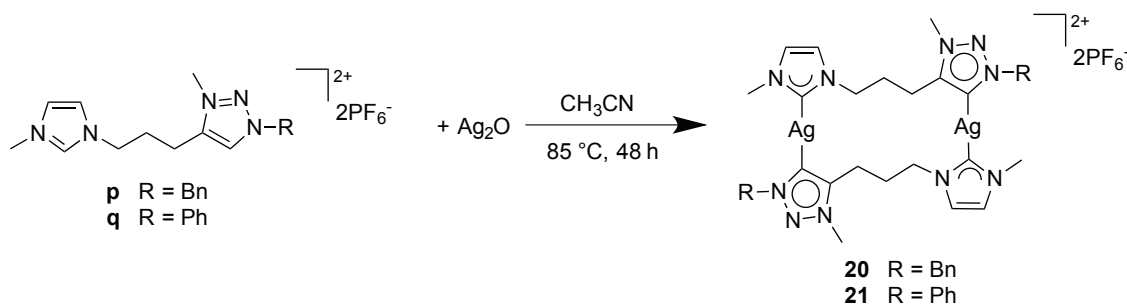
The NMR characterizations confirm the proposed structure: in particular, two different signals at δ 8.0 – 8.5 ppm are attributable to the protons in position 2 of the imidazolium moiety and in position 5 of the triazolium moiety. All the signals in the $^{13}C\{^1H\}$ -NMR spectra are in the proper range of ppm and coherent with the proposed structure; finally, the presence of a heptet at -144.6 ppm in the $^{31}P\{^1H\}$ -NMR confirms the successful anion exchange in the last step of the reaction.

4.3 Syntheses of silver(I) complexes

Some NMR tests were firstly made in order to find the best conditions for the syntheses of silver(I) complexes starting from the proligands **p** and **q**. Working with five equivalents of silver(I) oxide in deuterated acetonitrile at $85^\circ C$ for 48 hours, the complete disappearance of the signals of the protons in position 2 of the imidazolium and in position 5 of the triazolium was observed.

These reaction conditions were therefore adopted for the syntheses of the complexes in larger scale: the reactions were performed in acetonitrile as solvent, with an excess of Ag_2O at $85^\circ C$ in a close Schlenk tube under inert atmosphere (Scheme 4.13). After filtration on a Celite plug to remove the silver salts and addition of diethyl ether, an oil

or a white solid were obtained, respectively for the complex with benzyl (**20**) or phenyl (**21**) substituent on the nitrogen position of the *tz*NHC ring.



Scheme 4.13: syntheses of silver(I) complexes **20** and **21**

The complexes have been characterized by different techniques in order to confirm their structures and purities.

The disappearance of the deshielded signals at ca. 8 - 9 ppm in the ^1H -NMR spectra is consistent with the deprotonation at the positions C2-H of the imidazole moiety and C5-H of the triazole ring. The $^{13}\text{C}\{^1\text{H}\}$ -NMR spectra confirm the coordination of the ligand to the metal center: two different signals are in fact present at δ ca. 165 ppm and ca. 180 ppm, attributable to the coordinate carbene carbons of the *tz*NHC and *n*NHC moieties. The position of these signals is in the range of chemical shift reported in the literature for imidazole-2-ylidene or triazol-5-ylidene silver(I) complexes.¹³⁹

Finally, the presence of signals due to the species $[\text{Ag}_2\text{L}_2\text{PF}_6]^+$ in the ESI-MS spectra confirm the dinuclear dicationic structure of the complexes. The experimental isotopic distribution is in agreement with the simulated one for this fragment, as it can be observed from Figure 4.1 for complex **21**.

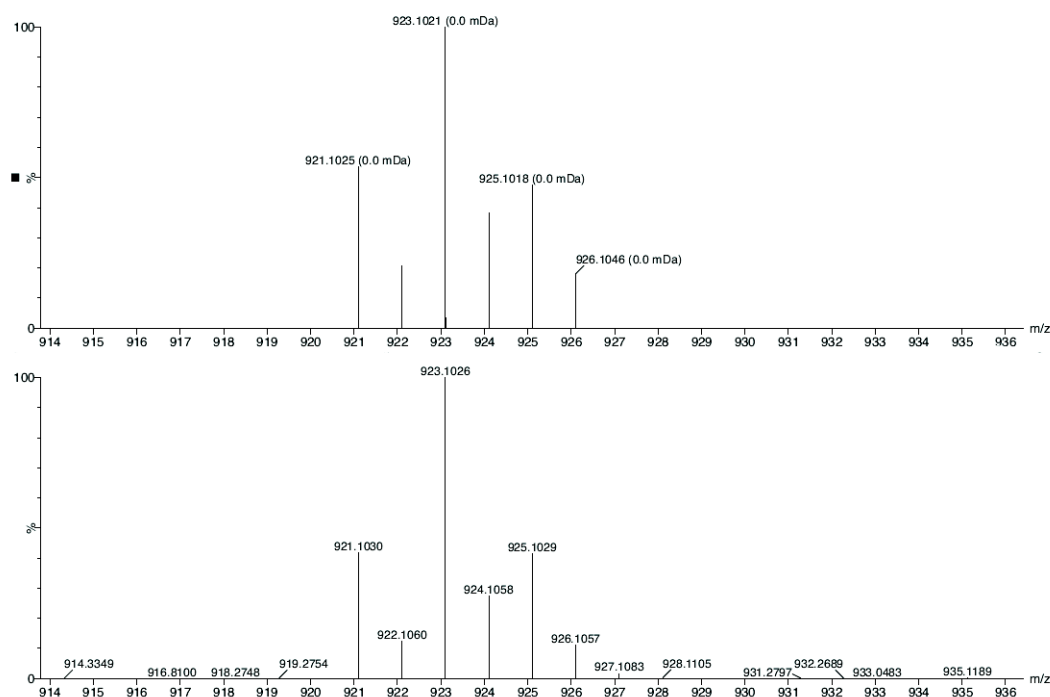


Figure 4.1: comparison between the experimental (top) and calculated (bottom) peak concerning the fragment $[Ag_2L_2PF_6]^+$ for complex **21**

All these data support the proposed structure for the silver complexes, with the coordination of two ligands in a bridging fashion between two different silver(I) centers. Unfortunately, no single crystals were obtained so it was impossible to confirm how these two ligands bridge the two metal centers. Due to the intrinsic ditopic nature of the ligands, two different isomers could be obtained: one with each silver(I) center coordinated by one *n*NHC and one *tz*NHC (Figure 4.2 left) and one isomer in which one silver(I) coordinates two *n*NHC and the other one binds the two *tz*NHC (Figure 4.2 right). Importantly, our investigations clearly show that only one single isomer is formed.

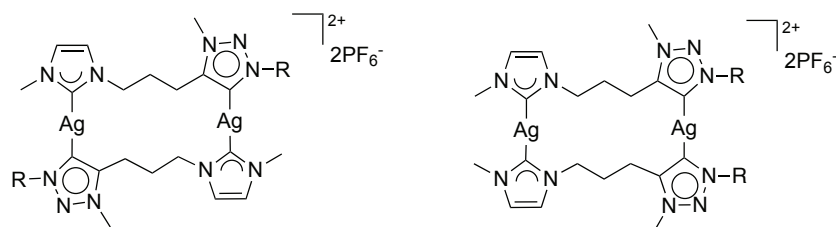


Figure 4.2: two possible isomers of silver(I) complexes

Nevertheless, VT NMR spectra were recorded in order to verify if an equilibrium may exist between the two species, but also at -75 °C the ¹H-NMR spectra present only one set of signals.

The proposed structure on the left of the Figure 4.2, with an *n*NHC faced to a *tz*NHC, appears the most probable for steric hindrance reasons and for similarity with analogues complexes reported in the literature.¹⁴⁰

Complex **20** (R = benzyl as substituent on the triazole ring) is an analytically pure compound with an oily nature: different recrystallization procedures have been checked in order to obtain a solid although crystals with no appreciable results. Furthermore, the compound is not very stable: for example its ¹H-NMR spectra in CD₃CN registered after one day shows a partial protonation of the dicarbene ligand accompanied by the formation of a black solid. For these reasons the direct transmetalation of the dicarbene ligand to gold(I) was carried out without isolation of the silver(I) complex.

On the other hand, complex **21** instead is more stable and its solid nature allows to isolate and then use it as precursor for the transmetalation of the dicarbene ligand to different metal centers.

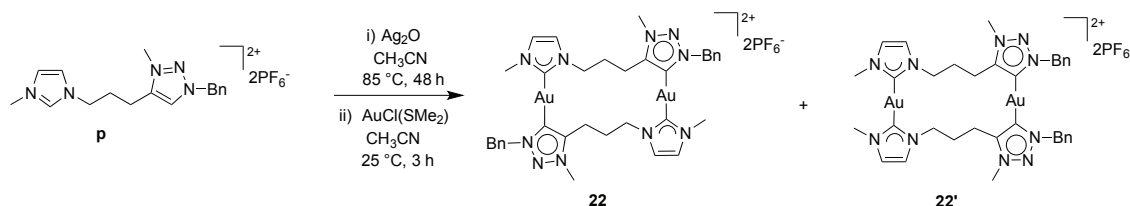
4.4 Syntheses of gold(I) complexes

The reaction procedure adopted for the syntheses of gold(I) complexes was the transmetalation reaction, i.e. starting from the silver(I) complexes, the dicarbene ligands are transferred to different metal centers.

As anticipated in the previous section, due to the different physical state of the silver(I) complexes **20** and **21**, oily and solid respectively, two slightly different synthetic procedures were adopted.

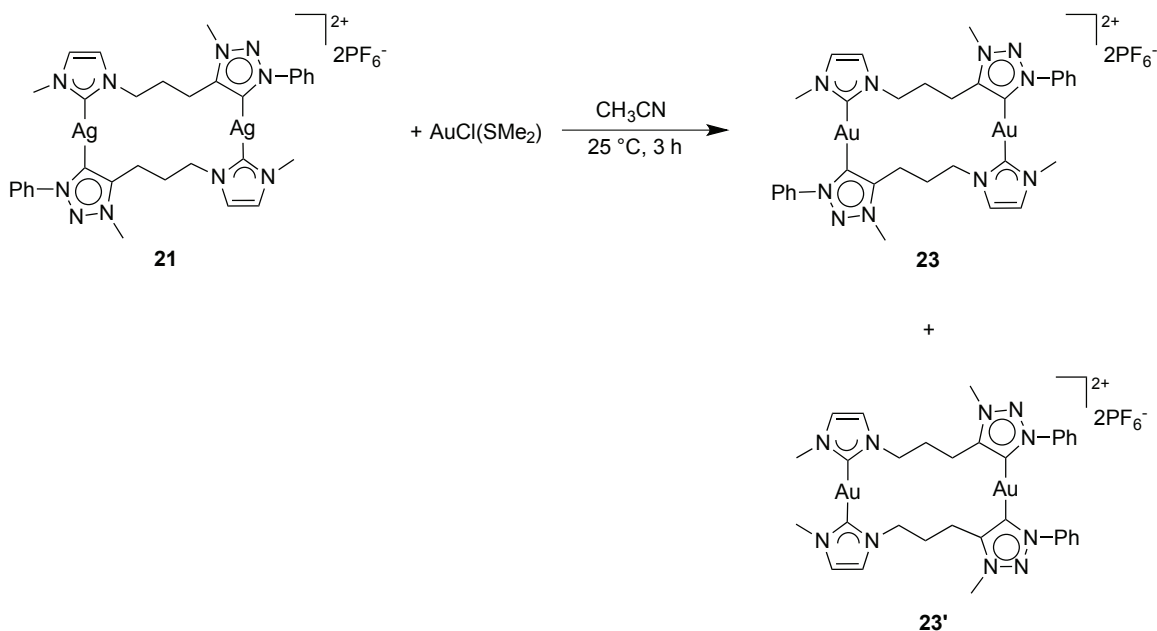
For the synthesis of the gold(I) complex with benzyl as substituent on the triazole moieties, the silver(I) complex **20**, obtained reacting proligand **p** with silver(I) oxide in acetonitrile (see previous section), was not isolated. The reaction mixture was filtered through a Celite plug and a solution of AuCl(SMe₂) in acetonitrile (in 1:1 ratio between the metal precursor and the proligand) was added (Scheme 4.14). The reaction mixture obtained in this way was left at room temperature under stirring for three hours, then

filtered to remove the formed AgCl; after concentration of the solvent and recrystallization, a solid was isolated (complexes **22** and **22'**).



Scheme 4.14: syntheses of gold(I) complexes **22** and **22'**

The gold(I) complex with phenyl substituents to the triazole ring was obtained starting from the pre-isolated silver(I) complex **21** dissolved in acetonitrile followed by addition of the gold(I) precursor AuCl(SMe₂) in 1:1 Ag: Au ratio (Scheme 4.15).



Scheme 4.15: syntheses of gold(I) complexes **23** and **23'**

Interestingly, the NMR spectra of the isolated solids show two sets of signals both in the ¹H and in ¹³C{¹H}-NMR, probably due to the presence of two isomers in solution, resulting from the isomers. As can be clearly observed in Figure 4.3 only one isomer is observed for the silver(I) complex. This is in contrast with the gold(I) complex, whose ¹H NMR spectrum shows two sets of signals.

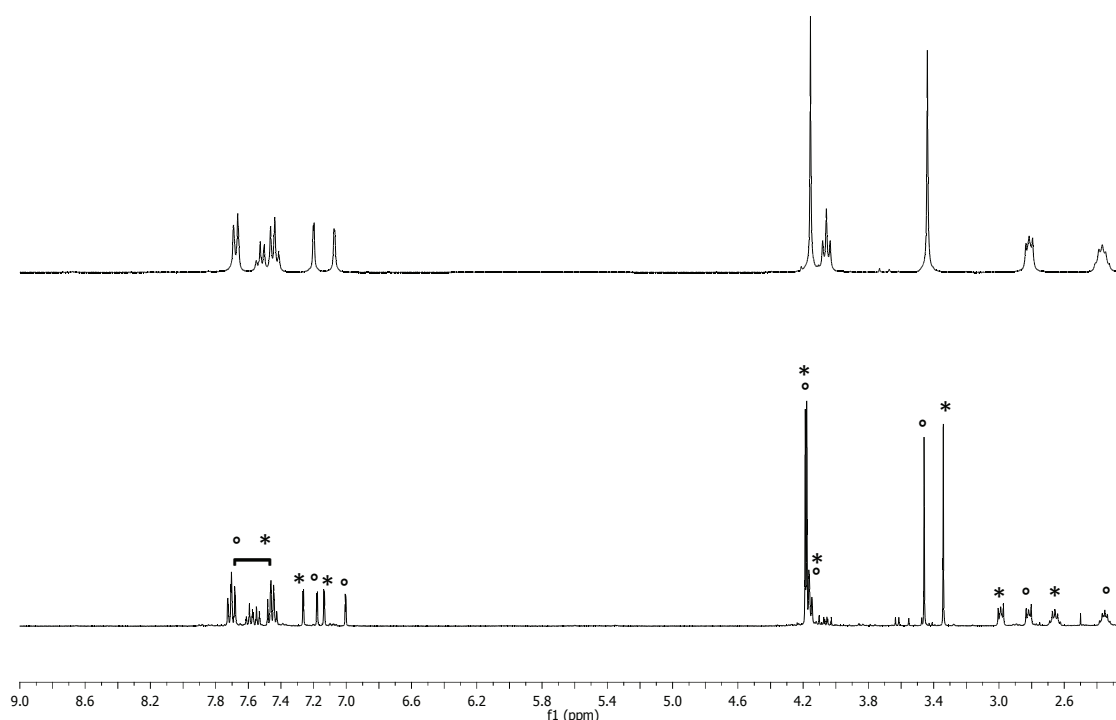


Figure 4.3: comparison between the ^1H -NMR spectra of the silver(I) complex **21** (top) and gold(I) complexes **23** (◉) and **23'** (*) (bottom) in CD_3CN

The two sets of signals could not be associated to two different conformational isomers. In fact, the ^1H NMR spectra registered after heating the solution of the mixture **23/23'** at $70\text{ }^\circ\text{C}$ in a NMR tube remains unchanged and also the relative ratio of the two set of signals remains constant.

As described for the silver complexes in the previous section, the heteroditopic nature of the ligand allows the formation of two isomers: as reported in Figure 4.4, after coordination, each five member ring can be faced to a ring of the same nature belonging to the another ligand ($n\text{NHC-Au-}n\text{NHC}$ and $tz\text{NHC-Au-}tz\text{NHC}$) or faced to the different heterocyclic ring ($n\text{NHC-Au-}tz\text{NHC}$ and $tz\text{NHC-Au-}n\text{NHC}$).

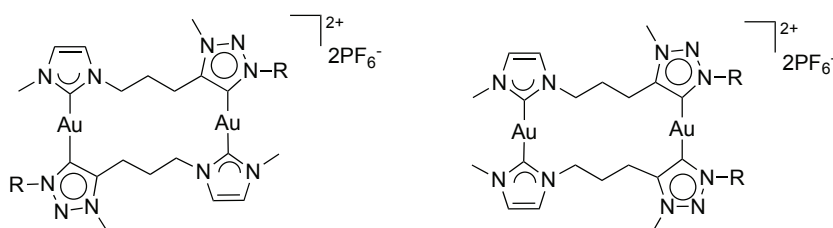


Figure 4.4: representation of the two different ways of coordination of the ligands on the gold(I) centers

The ratio between the two isomers is close to 1:1 for both the substituents on the nitrogen in position 1 of the triazole rings, despite their different nature and steric hindrance (phenyl vs. benzyl). In general, concerning the $^1\text{H-NMR}$ spectra, all the signals associable to the proposed structure of complexes **22/22'** and **23/23'** can be identified and assigned.

The transmetalation to gold(I) centers can be confirmed by the presence of signals at ca. δ 169 and 185 ppm concerning the carbene carbons in position 2 and 5 of the *n*NHC and *tz*NHC respectively, slightly downfield shifted from those observed for the related silver(I) complexes and in the range of ppm reported in the literature for *n*NHC and *tz*NHC gold(I) complexes.¹³⁹

The dinuclear dicationic structure of complexes **22/22'** and **23/23'** was confirmed by ESI-MS spectra which present a signal attributed to the species $[\text{Au}_2\text{L}_2\text{PF}_6]^+$ with $\text{L} = \textit{n}\text{NHC-}t\textit{z}\text{NHC}$ dicarbene ligand.

By slow diffusion of diethyl ether into a solution of the mixture containing complexes **23** and **23'** in acetonitrile, few crystals were obtained and the molecular structure of the crystallized compound has been determined by X-ray diffraction.

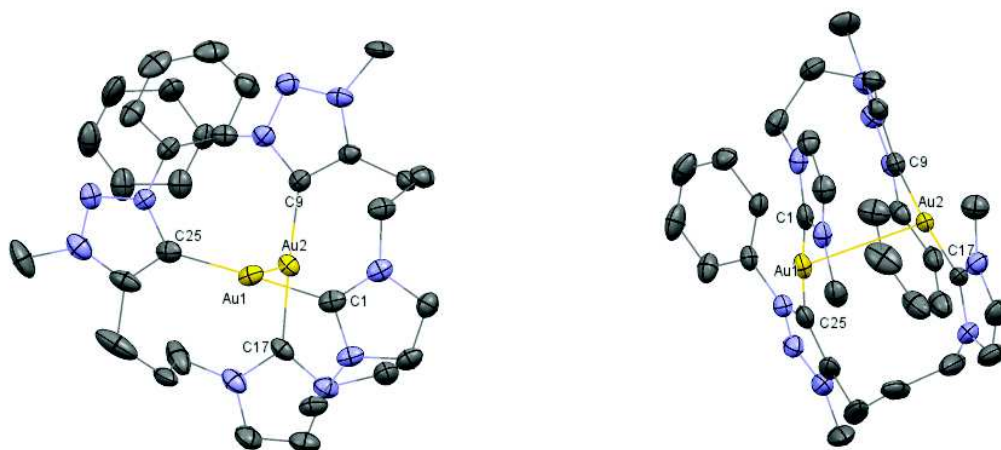


Figure 4.5: ORTEP view of the cationic unit of complex **23**. Ellipsoids are drawn at their 30 % probability. Hydrogen atoms, CH_3CN and PF_6^- anions have been omitted for clarity. Selected bond distances (\AA) and angles (deg): Au1-C1 2.021(10), Au1-C25 2.042(10), Au2-C9 2.021(9), Au2-C17 2.012(9), Au1-Au2 3.068(5), C1-Au1-C25 176.7(3), C9-Au2-C17 175.6(3)

The crystal structure confirms that the complex has a dinuclear dicationic nature with two dicarbene ligands bridging the two gold atoms. In particular, the analyzed crystals show the presence of only one species, complex **23**, in which both the gold(I) centers bind one *tz*NHC and one *n*NHC (Figure 4.5).

The two gold(I) centers are coordinated together, as expected for a metal center having a d^{10} electronic configuration. The bond angles C1-Au1-C25 and C9-Au2-C17 are respectively 176.7(3) and 175.6(3) Å, close to the linearity. The bond distances between the metals and the carbene carbons in position 2 of the *n*NHC are 2.021(10) and 2.012(9) Å (Au1-C1 and Au2-C17 respectively) and the distances between the gold centers and the carbene of the *tz*NHC are 2.042(10) and 2.021(9) Å (Au1-C25 and Au2-C9 distances), comparable to those reported for analogous complexes.^{139,141,142,143}

In complex **23** the bridging ligands form a 16-member ring, and the planes passing through the two different rings (imidazole-2-ylidene and triazol-5-ylidene) have dihedral angles that span from 17.7° to 18.5°. The angle between the planes formed by C1-Au1-C25-Au2 atoms and C17-Au2-C9-Au1 atoms is 81°, in a twisted conformation. The conformation of the complex has a great influence on the distances between the metal centers: interestingly, the Au...Au interatomic separation 3.068(5) Å observed in the complex **23** is slightly shorter than the sum of the Van der Waals radii for gold, thus suggesting the presence of aurophilic interaction between the two metals.¹³⁹

Moreover, considering the phenyl ring labeled by atoms C11, C12, C13, C14, C15, C16 and the triazole ring defined by atoms N8, N9, N10, C24, C25 (evidenced in Figure 4.6 by the *ball and stick* drawing), they lie on almost parallel planes (dihedral angle of 8°) at a distance between the centroids of the rings of 3.763 Å (Figure 4.6).

The bridging coordination mode of the dicarbene ligands imposes coordination chirality to the complex. Nevertheless, the complex crystallizes in *C2/c* spatial group and so both enantiomers are present in the crystals.

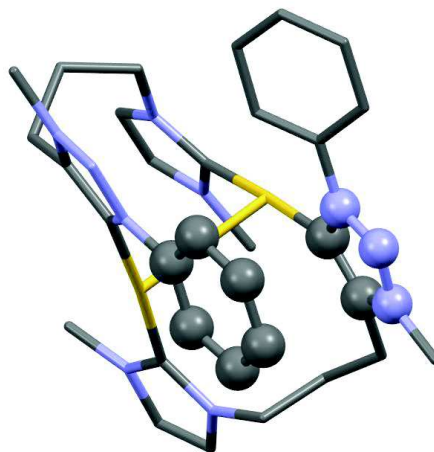


Figure 4.6: view of the cationic part of complex **23**, emphasizing the parallel planes of the phenyl ring the triazole one

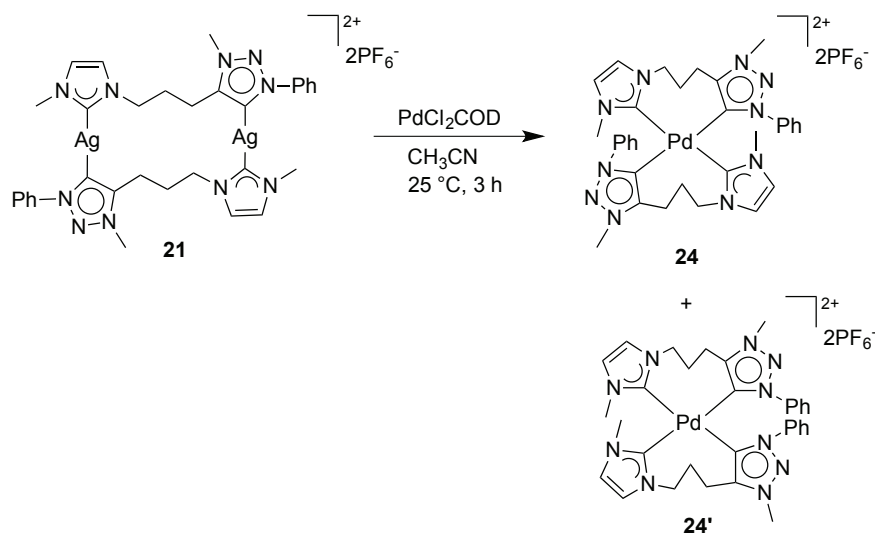
In the crystal packing of the compound no strong intermolecular interactions are present.

The solution in which the crystals have been grown, was also analyzed. After removal of the volatiles and dissolution of the residue in deuterated acetonitrile a $^1\text{H-NMR}$ spectrum was registered. An enhancement in the ratio **23'**:**23** was observed which is coherent with the expectations, considering that the crystals contained only complex **23**.

4.5 Syntheses of palladium(II) complexes

The transmetalation procedure was adopted also for the syntheses of palladium(II) complexes, starting from the silver(I) complex **21**.

$[\text{PdCl}_2\text{COD}]$ was used as palladium(II) precursor due to the labile nature of the diene ligand. The reaction was performed under very mild conditions (three hours at room temperature) working in acetonitrile as solvent with 1:1 molar ratio between the silver(I) complex **21** and the palladium precursor $[\text{PdCl}_2\text{COD}]$. A solid was obtained after filtration of the reaction mixture through a Celite plug and removal of the solvent (Scheme 4.16).

Scheme 4.16: syntheses of the complexes **24** and **24'**

The d^8 electronic configuration of the palladium(II) center suggests a square planar geometry around the metal centers with two dicarbene ligands bonded in a chelate fashion to the same metal.

The ESI-MS spectra confirm the coordination of two ligands on the same metal center due to the presence of a signal at m/z 813.1957 referred to the fragment $[\text{PdL}_2\text{PF}_6]^+$ with $L = n\text{NHC-tzNHC}$ dicarbene ligand.

In contrast with the silver(I) complex **21** in which the coordination of the ligands is in a bridging fashion, complexes **24** and **24'** show the chelation of the ligand on the metal center. This is associated in the shift of the signals and in the change of the pattern in the $^1\text{H-NMR}$ spectra, as can be clearly observed in Figure 4.7. In particular, the CH_2 protons of the bridge give very complicated multiplets, as a consequence of the formation of a rigid 8 member metallacycle. Due to the slow interconversion between the possible conformations of this chelate ring, all the protons of the bridge are not equivalent; they can be however assigned on the basis of 2D experiments.

As observed in the case of gold(I) complexes, two sets of signals can be observed in both the $^1\text{H-NMR}$ and $^{13}\text{C}\{^1\text{H}\}\text{-NMR}$ spectra due to the presence of the two isomers **24** and **24'** (Figure 4.7).

The molar ratio between the two complex **24** and **24'** is 3:2 (referred to the CH_3 signals). This is probably due to the different stability of the species, related to the

different steric hindrance around the metal center. In fact, complex **24'** should involve the close proximity of two phenyl rings.

The $^{13}\text{C}\{^1\text{H}\}$ -NMR spectrum confirms the coordination of the dicarbene ligand to the palladium(II) center: the *n*NHC carbene carbon signal is observed at δ ca. 171 ppm, coherent with the literature.^{144,145} Unfortunately, due to the low concentration of the complex in solution, the signal for the carbene carbon of the *tz*NHC was not detected.

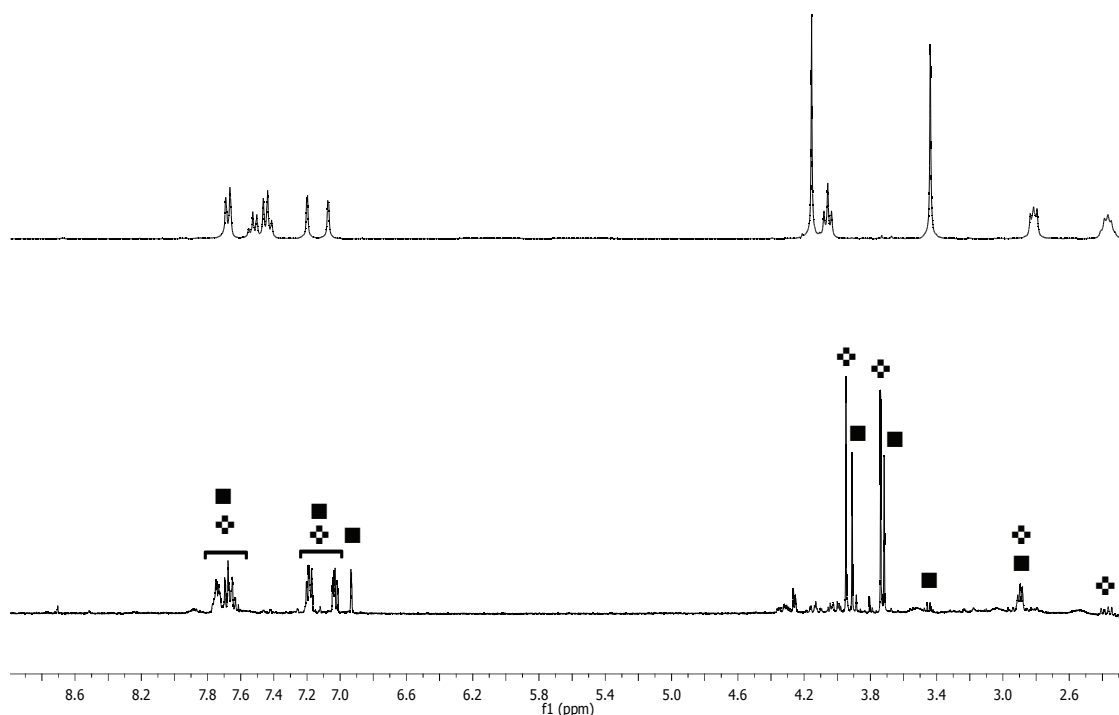


Figure 4.7: comparison between the ^1H -NMR spectra of the silver(I) complex **21** (top) and palladium(II) complexes **24** (✚) and **24'** (■) (bottom)

By slow diffusion of diethyl ether into an acetonitrile solution of complexes **24** and **24'**, single crystals were obtained; the crystal structure was solved by X-ray diffraction studies and it confirmed the proposed structure for complex **24**. Figure 4.8 displays the molecular structure of the palladium complex.

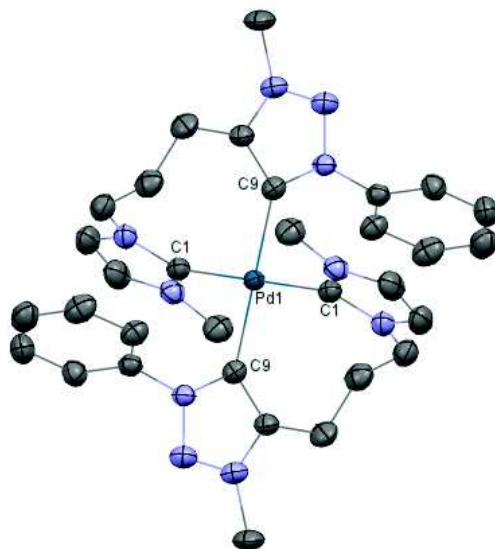


Figure 4.8: ORTEP view of the cationic unit of complex **24**. Ellipsoids are drawn at their 30% probability. Hydrogen atoms, CH₃CN and PF₆⁻ anions have been omitted for clarity. Selected bond distances (Å) and angles (deg): Pd1-C1 2.062(6), Pd1-C9 2.058(5), C1-Pd1-C1 180.0, C9-Pd1-C9 180.0, C1-Pd1-C9 92.4(2), C9-Pd1-C1 87.6(2)

The crystal structure confirms the dicationic nature of the complex with two dicarbene ligands chelating the palladium center. The structure is centrosymmetric, with the metal atom located on an inversion center. The palladium(II) presents, as expected, a square planar configuration: the C1-Pd1-C9 and C9-Pd1-C1 deviated slightly from the ideal 90° value (92.4(2) and 87.6(2) degree). The ligand forms an 8 membered chelating ring, with a boat conformation.

The distances between the palladium(II) center and the carbene carbon atoms are 2.062(6) Å (*n*NHC) and 2.058(5) Å (*tz*NHC), in the expected range of distances for this type of compounds.^{48,145,146,147,148} In order to minimize the steric hindrance the dihedral angle between the phenyl substituent and the triazole ring is twisted of 71.5°.

An interesting feature is observed in the crystal packing of the compound in which it can be observed that the cationic palladium compounds tend to dispose in layers developing in the *bc* crystallographic planes while the solvent molecules and the anionic PF₆⁻ moieties are disposed between the layers.

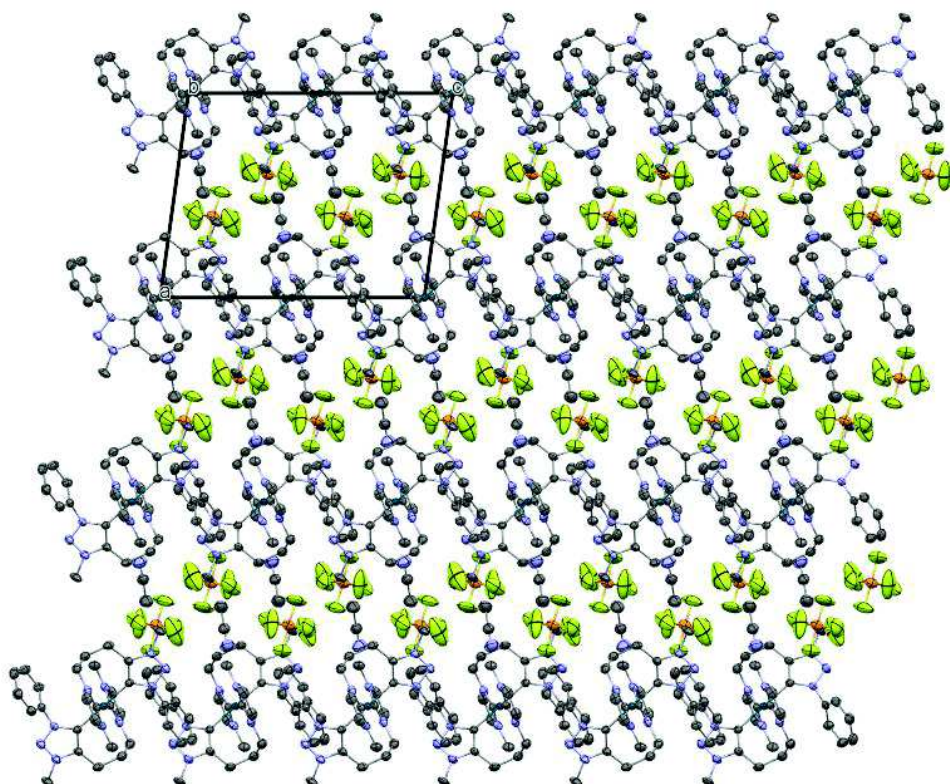


Figure 4.9: layers developing of the complex 24

In conclusion, different transition metal complexes have been obtained with these *n*NHC-*tz*NHC dicarbene ligands. The most promising results are those regarding the gold(I) complexes: the Au-Au distance is in fact very short and indicates the presence of aurophilic interaction, so that these complexes should present interesting luminescence properties. However, since the gold(I) complexes have been obtained as a mixture of two isomers, in the future it will be necessary to separate the two species by crystallization, in order to obtain a reasonable amount of each isomer.

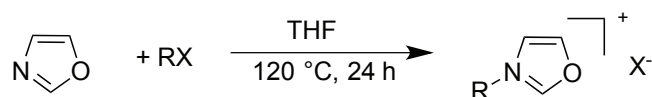
Chapter 5: RESULTS AND DISCUSSION

Bis(benzoxazolium) proligands and attempted synthesis of related transition metal complexes

5.1 Introduction

The Section 1.4 in Chapter 1 was focused on the different procedures for the synthesis of azolium salts. In this section we briefly describe the procedures used for the synthesis of oxazolium or benzoxazolium salts and their corresponding oxazol- or benzoxazol-2-ylidene metal complexes.

The simplest way for the synthesis of oxazolium salts is the direct functionalization of the nitrogen atom of the oxazole (or benzoxazole) ring with an alkylating agent; however, this method presents some limitations, due to the low nucleophilicity of the oxazole nitrogen atom and the procedure is successful only with highly activated electrophilic reagents, as for example methyl iodide and benzyl bromide derivatives.¹⁴⁹ The required experimental reaction conditions are usually strong (high temperatures and long reaction times), especially with benzyl bromide derivatives. Tubaro *et al.*¹⁴⁹ used this approach (Scheme 5.1) for obtaining several oxazolium proligands (Figure 5.1).



Scheme 5.1: general synthesis of the proligands

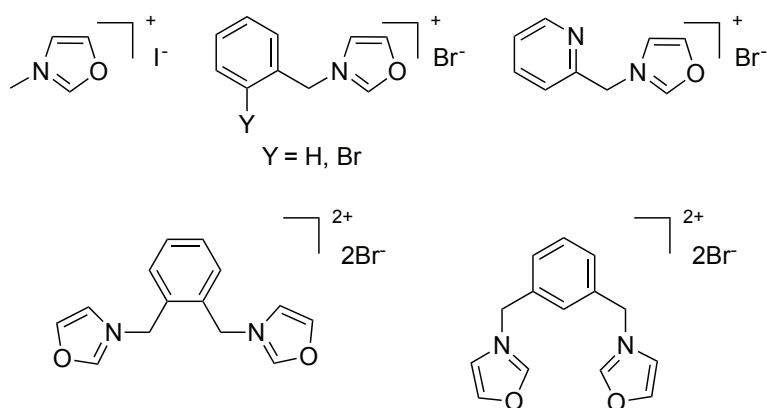
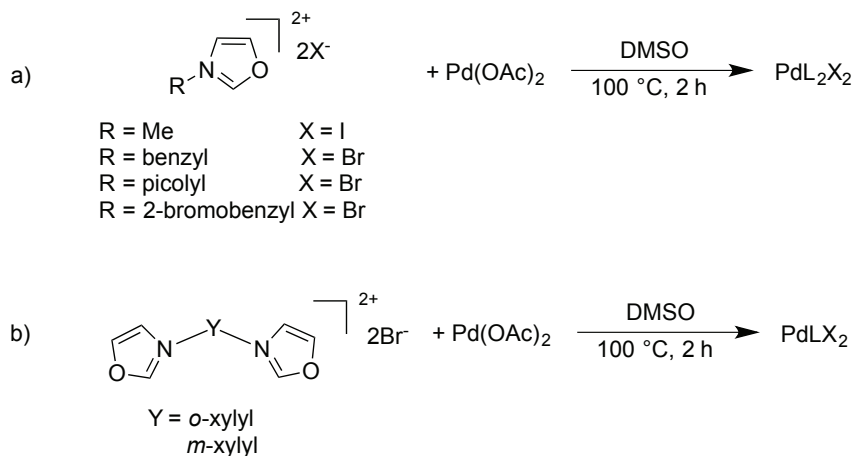


Figure 5.1: Example of proligands synthesized with the procedure reported in Scheme 5.1

The reaction between these oxazolium or bis(oxazolium) salts with palladium(II) acetate afforded stable neutral palladium(II) complexes (Scheme 5.2 and Figure 5.2).



Scheme 5.2: general procedure for the syntheses of palladium(II) complexes with a) oxazol-2-ylidene ligands or b) bis(oxazol-2-ylidene) ligands

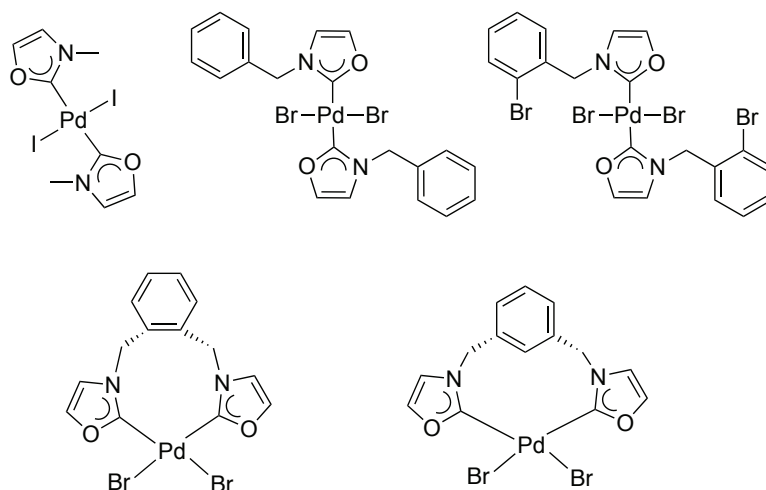
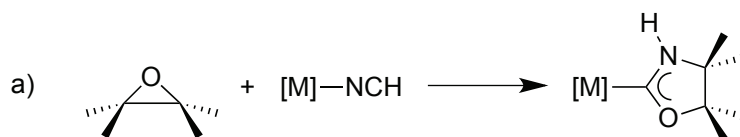
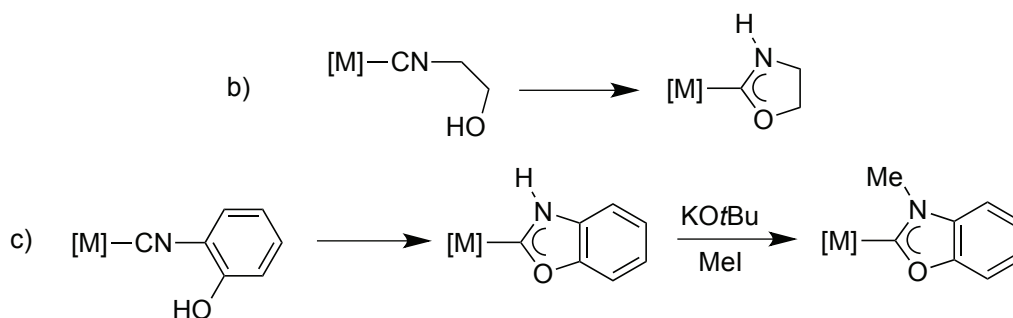


Figure 5.2: palladium(II) complexes synthesized according to the procedure reported in Scheme 5.2

Other procedures that can be adopted for the synthesis of oxazol-2-ylidene complexes are the reaction between epoxide and hydrogen-isocyanide complex (Scheme 5.3 a) or the intramolecular cyclization of functionalized hydroxyisocyanide (Scheme 5.3 b and c).^{150,151,152,153,154,155,156}

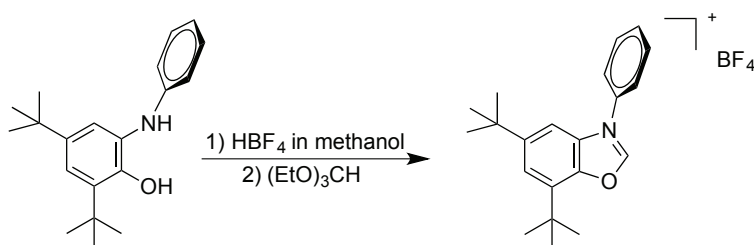




Scheme 5.3: different reactions for the synthesis of oxazol-2-ylidene complexes

These reaction pathways display some limitations mainly related to the synthesis of the functionalized isonitrile compounds and corresponding metal complexes. Furthermore, the nature of the metal is a key parameter for the activation of the coordinated isocyanide and therefore for the synthesis of the oxazol-2-ylidene ligand. In this context the preferred metal centers are usually metals on the left of periodic table and in high oxidation state, capable to activate isonitrile carbon atom towards the nucleophilic attack of the oxygen.^{157,158}

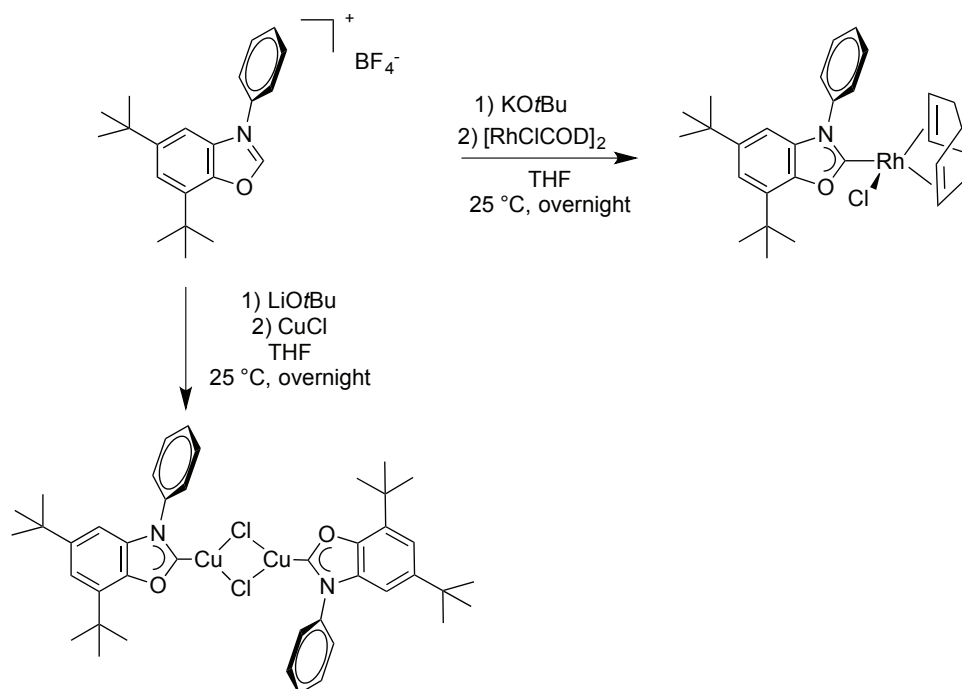
A different pathway, recently proposed by Bellemin-Laponnaz¹⁵⁹ for the synthesis of benzoxazolium salts, is depicted in Scheme 5.4.



Scheme 5.4: strategy for the synthesis of benzoxazolium proligand

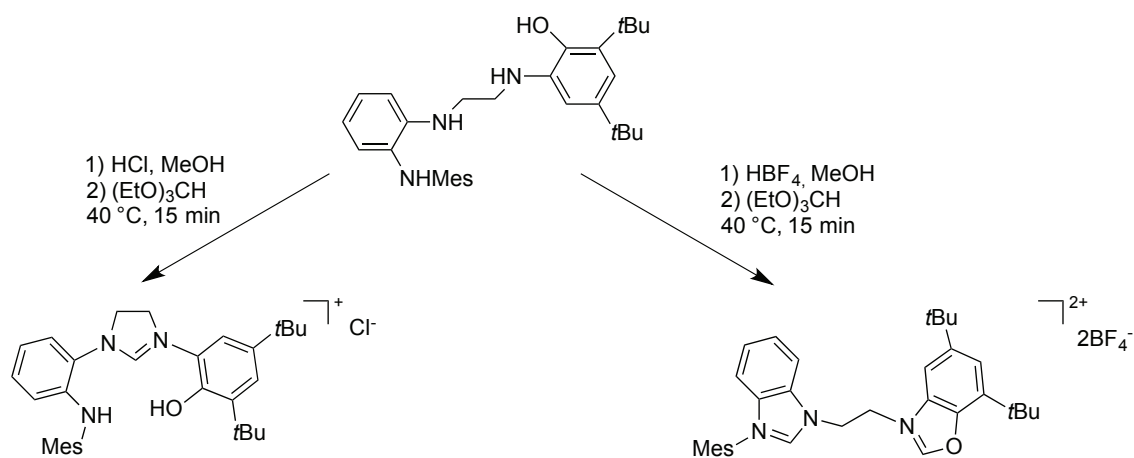
In this procedure 3,5-di-*tert*-butyl-2-hydroxy-*N*-phenylaniline was treated with HBF_4 in order to protonate the amine, and then the subsequent reaction with triethylorthoformate, $(\text{EtO})_3\text{CH}$, afforded the benzoxazole proligand in quantitative yield.

Rhodium(I) and copper(I) carbene complexes (Scheme 5.5) were synthesized starting from the above described benzoxazolium proligand in the presence of an external base and the proper metal source, under very mild conditions.



Scheme 5.5: synthesis of rhodium(I) and copper(I) complexes starting from the benzoxazolium proligand

The group of Bercaw¹⁶⁰ adopted a synthetic pathway similar to that described by Bellemin-Laponnaz for the synthesis of different scaffolds (Scheme 5.6): the nature of the formed heterocycle depends on the nature of the acid used during the cyclization step. Working with HCl, the ring closure was obtained between the two aminic positions giving an imidazolium salt (compound on the left of Scheme 5.6). In contrast, with HBF₄ the ring closure was observed between both the vicinal NH/OH and NH/NHMe groups, thus giving a dicationic moiety containing an imidazolium and a benzoxazolium (compound on the right of Scheme 5.6).



Scheme 5.6: effect of counter ion (Cl⁻ vs. BF₄⁻) on the formation of azolium salts

5.2 Synthesis and characterization of the oxazolium proligands

In this thesis we wanted to investigate the possibility of synthesizing metal complexes with bis(benzoxazol-2-ylidene) ligands derived from bis(benzoxazolium) precursors, obtained with a modified experimental procedure reported by Bellemin-Laponnaz.

Different bis(benzoxazolium) proligands characterized by an aliphatic or aromatic bridge between the heterocyclic rings (Figure 5.3) have been successfully synthesized with a two step procedure.

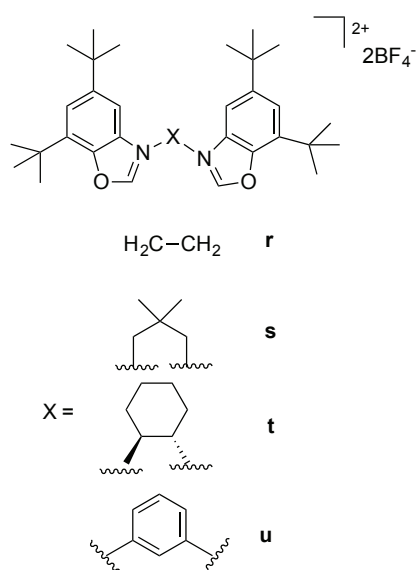
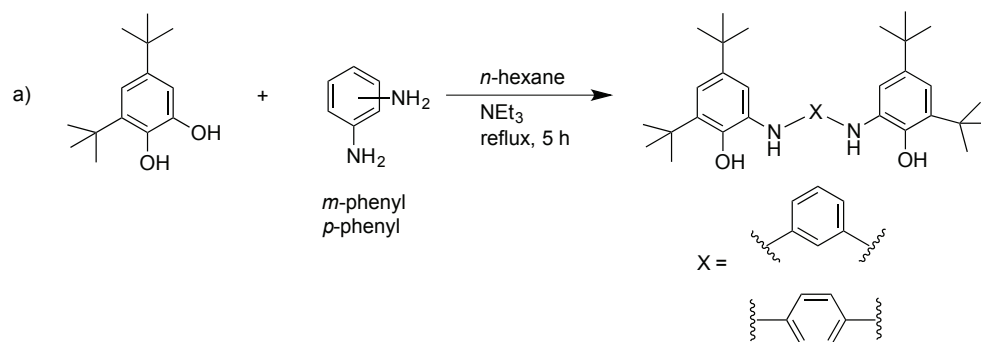
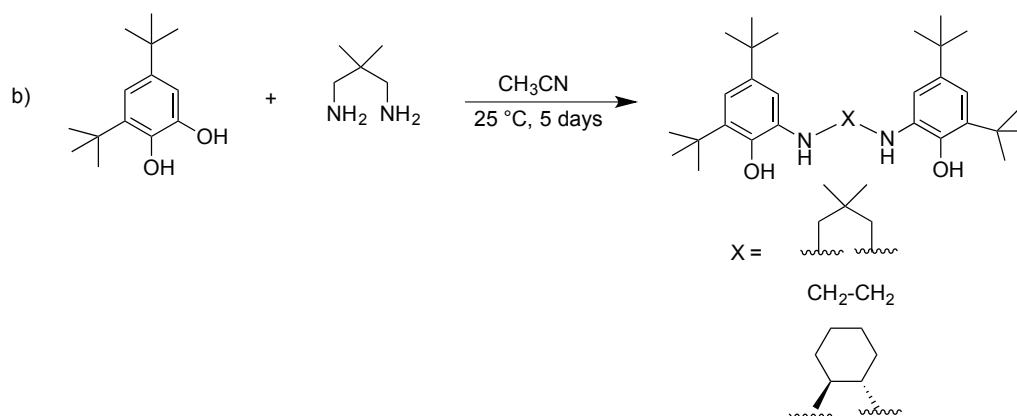


Figure 5.3: general structure of the bis(benzoxazolium) proligands synthesized in this work

The first step is the linkage between two 3,5-di-*tert*-butylcatechol units with the opportune diamino-compound: this reaction has been carried out in *n*-hexane under reflux for 5 hours in the case of an aromatic diamine¹⁶¹ (Scheme 5.7 reaction a) or in acetonitrile at room temperature for a longer period when using aliphatic diamine compounds (Scheme 5.7 reaction b).^{160,162,163}



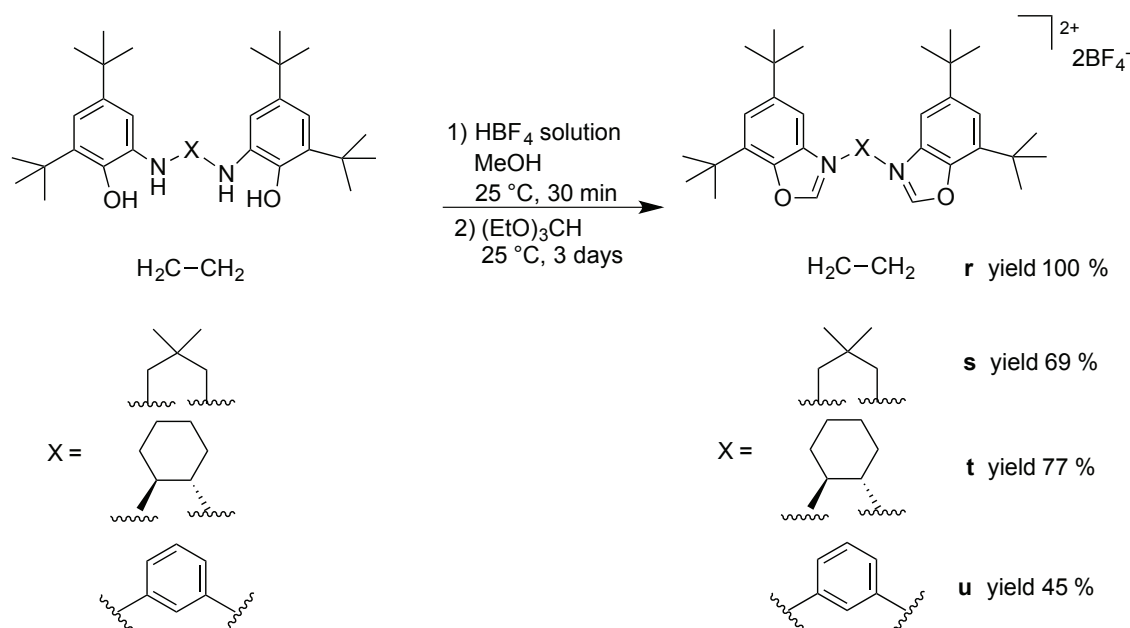


Scheme 5.7: synthesis of N, N'-bis(3,5-di-*tert*-butyl-2-hydroxyphenyl)-R-diamine derivatives.

The syntheses are straightforward, affording almost pure products, isolated as white solids. The $^1\text{H-NMR}$ spectra confirmed the structure of the products with the diagnostic signals for the protons of the bridges, slightly shifted from those of the reagents. The signals for the NH and OH groups were not always observed probably due to exchange processes occurring with traces of water present in the deuterated solvent.

The second step of the synthesis is the formation of the two oxazole moieties by ring closure. As described in the Section 5.1, the Brønsted acid used in this reaction is a key parameter for the formation of the rings.¹⁶⁰

In order to obtain the bis(benzoxazolium) proligands, a solution of tetrafluoroboric acid (in water) was added to a solution of the N, N'-bis(3,5-di-*tert*-butyl-2-hydroxyphenyl)-(substituted)-diamine in methanol to obtain the bis-ammonium salts. After the removal of the solvent, the crude off-white solids/oily residues were directly dissolved in $(\text{EtO})_3\text{CH}$ and left at room temperature under stirring for three days. The products precipitated directly in the reaction media; they were filtered off and washed with cold *n*-pentane, obtaining solid species in good yields and excellent purities (Scheme 5.8).



Scheme 5.8: syntheses of the bis(benzoxazolium) proligands

All compounds were soluble both in polar and in halogenated solvents (DMSO, CH_3CN , CHCl_3 , CH_2Cl_2) and they were fully characterized by $^1\text{H-NMR}$, $^{13}\text{C-NMR}$ and mass spectrometry.

The formation of the oxazolium moieties was confirmed by $^1\text{H-NMR}$ by the presence of a signal at ca. 10 ppm, concerning the protons in position 2 of the heterocyclic rings. The $^{13}\text{C-NMR}$ spectra show the diagnostic signal at ca. 157 ppm for the carbon in position 2 of the oxazole rings, together with all the signals of the functional groups present in the molecule.

As example, the comparison between the $^1\text{H-NMR}$ spectra of the compound $\text{N,N}'$ -bis(3,5-di-*tert*-butyl-2-hydroxyphenyl)-1,3-phenylenediamine and the proligand **u** can be done (Figure 5.4). The main difference in the $^1\text{H-NMR}$ spectra of the two compounds is the shift to higher chemical shift for all the signals of the product **u**. This can be attributed to the different global charge of the involved species: compound **u** is a dicationic species while the precursor is neutral. Furthermore, in compound **u** the aromatic signals of the 3,5-di-*tert*-butyl-phenyl ring could be downfield shifted, because of the formation of a second condensed aromatic ring. Finally, another confirmation for the formation of the benzoxazole ring is the absence of NH and OH proton signals, respectively at δ 4.94 and 6.34 ppm.

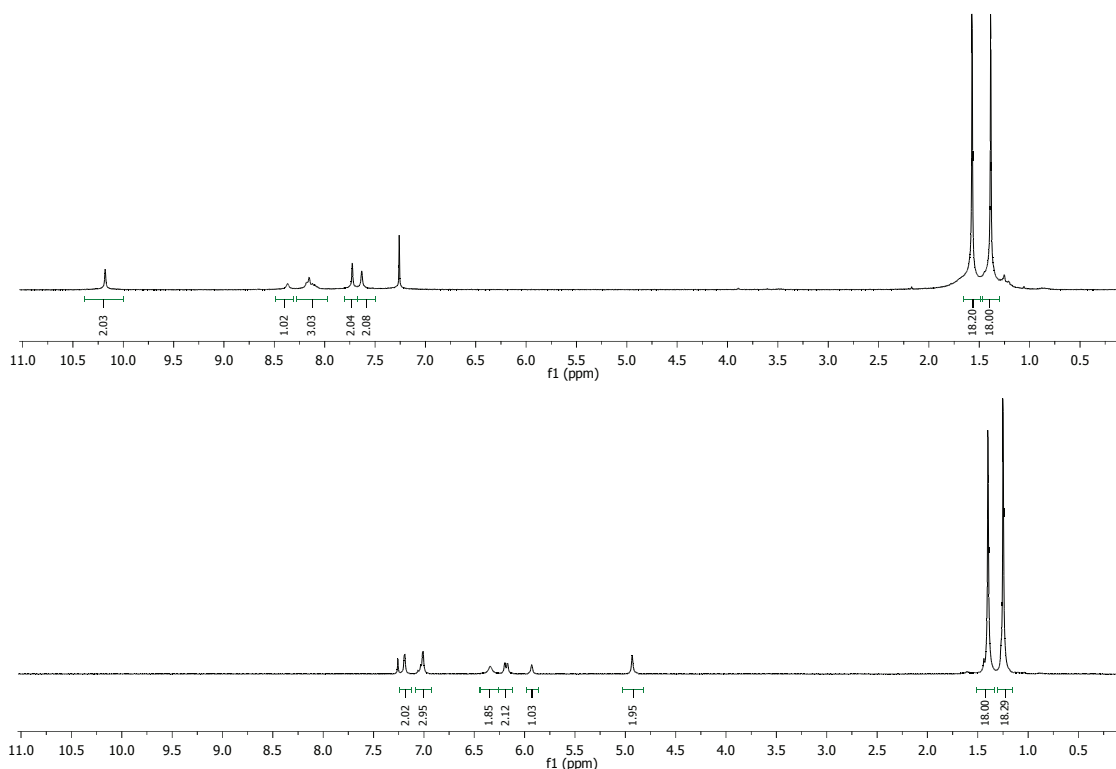
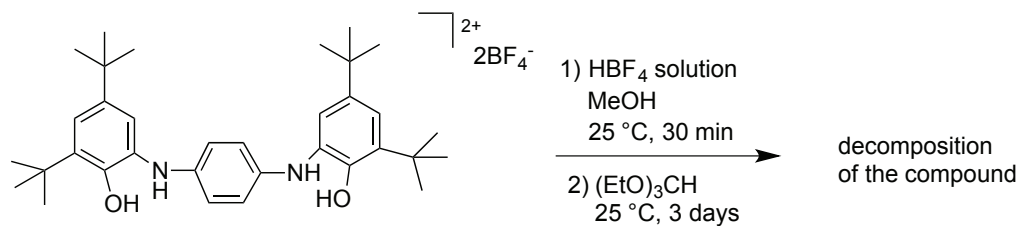


Figure 5.4: ¹H-NMR spectra of compound **u** (top) and *N,N'*-bis(3,5-di-*tert*-butyl-2-hydroxyphenyl)-1,3-phenylenediamine (bottom)

The mass spectra confirmed the formation of the proligands with signals concerning the cationic fragments plus an OH group $[M+OH]^+$. This can be probably caused by the presence of traces of water in the solvent used to solubilize the compounds, that can interact with the molecule to form some adduct during the MS analysis.

In the synthesis of the proligand with a *para*-phenylene linker, the addition of HBF_4 to the solution of the *N,N'*-bis(3,5-di-*tert*-butyl-2-hydroxyphenyl)-1,4-phenylenediamine led to the formation of a dark solution and the second step did not provide any desired product. This may probably due to the decomposition of the *N,N'*-bis(3,5-di-*tert*-butyl-2-hydroxyphenyl)-1,4-phenylenediamine compound upon addition of the acid, as evidenced by the ¹H-NMR spectra in which several new signals can be observed (Scheme 5.9).



Scheme 5.9: attempts to synthesize the bis(benzoxazolium) proligand with *para*-phenylene bridge

5.3 Attempts to synthesize transition metal complexes bearing bis(benzoxazol-2-ylidene) ligands

Different reaction procedures were investigated for the synthesis of transition metal complexes containing bis(benzoxazol-2-ylidene) ligands; in particular both the synthesis of NHC silver(I) complexes followed by transmetalation of the ligand to a second metal center or the deprotonation of the proligand with a strong base, followed by coordination to a metal center, have been attempted. However, it can be anticipated that no metal complexes have been obtained.

Regarding silver(I) complexes, several attempts were carried out using different solvents (chloroform, acetonitrile or dichloromethane) and reaction temperatures (25 °C or 60 °C) for 24 hours.

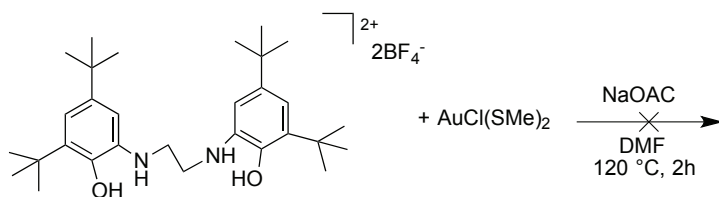
Precursor **r** with a CH₂CH₂ between the benzoxazolium moieties is stable in the presence of silver(I) oxide both in CDCl₃ at room temperature or in CD₃CN at 60 °C; the ¹H-NMR spectra showed in fact the presence of the unreacted proligand.

By contrast, when precursor **u** was reacted with Ag₂O in dichloromethane at room temperature under strictly inert atmosphere and the ¹H-NMR spectrum of the crude product (isolated after filtration on Celite plug and precipitation with diethyl ether) showed several signals that are consistent with the decomposition of the substrate.

So we decided to use the deprotonation procedure in the presence of different metal sources.

At beginning, we used a classical procedure for the synthesis of gold(I) complexes, i.e. the deprotonation in dimethylformamide of the azolium salt with sodium acetate in the presence of the gold precursor AuCl(SMe₂).³¹ The ¹H-NMR spectrum of the isolated solid starting from salt **r** with this procedure showed the presence of a various sets of signals, mostly in the aromatic region. No signals were observed in the region 5 - 6

ppm, characteristic of the CH₂ groups of the bridge, thus suggesting decomposition of the proligand during the reaction (Scheme 5.10).

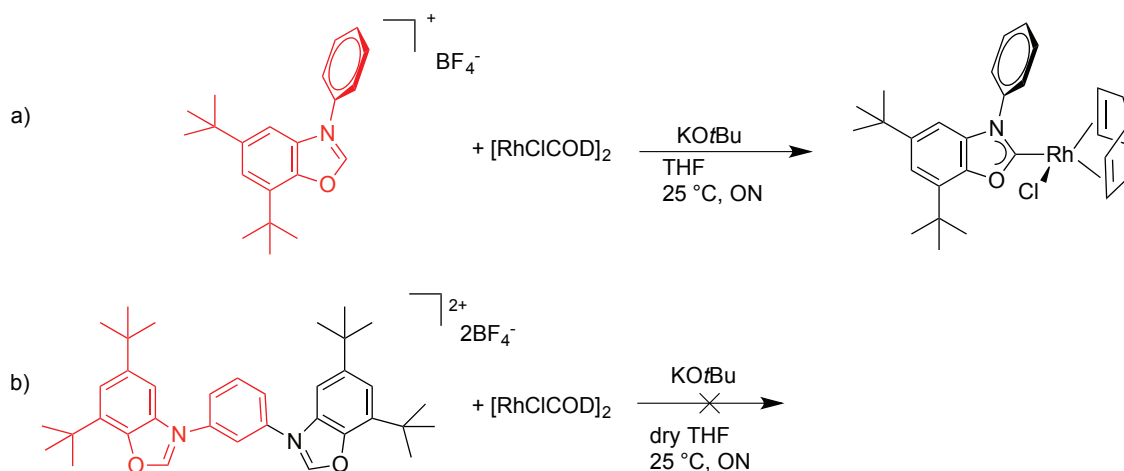


Scheme 5.10: attempts for the synthesis of gold(I) complex

The use of a stronger base (KO^{*t*}Bu) was also attempted. The reactions were performed adding the base to a solution of the proligand **r**, **s** or **t** and the metal salt ([PdCl₂COD]) in dry THF under inert atmosphere. After filtration on Celite plug and removal of the solvent, a yellow-brown oil was obtained. The ¹H-NMR spectra of the crude product present a complex pattern of signals, most of them very large, so that it is difficult to understand the nature of the product.

Finally, the same procedure reported by Bellemin-Laponnaz¹⁵⁹ for the synthesis of rhodium(I) complexes with monocarbene ligands, was adopted. The reaction was performed with proligand **u** in the presence of KO^{*t*}Bu as base and [RhCl(COD)]₂ as metal precursor, in the same way used above for palladium(II). Unfortunately, in the ¹H-NMR spectrum it was impossible to identify signals attributable to a rhodium complex. The same reaction was performed in dry-box under strictly anaerobic conditions, in order to minimize all the possible factors that could decompose the complexes however, also in this case, decomposition was observed as indicated by the presence of several peaks in the ¹H-NMR spectrum.

According to the results presented in this chapter, the presence of a second benzoxazolium moiety seems to prevent the formation of metal complexes, probably for the instability of the intermediate species formed during the synthesis.



Scheme 5.11: comparison between the reaction pathways for the synthesis of mono and bis(benzoxal-2-ylidene) complexes

For example it is possible to compare with the results reported in Scheme 5.11, in which the benzoxazole moiety has very similar substituents in the mono and bis-derivative (phenyl ring). In the case of the monobenzoxazolium proligand, the reaction afforded a stable complex both in solid and in solution, while with the bisbenzoxazolium species, it was not possible to identify metal complexation.

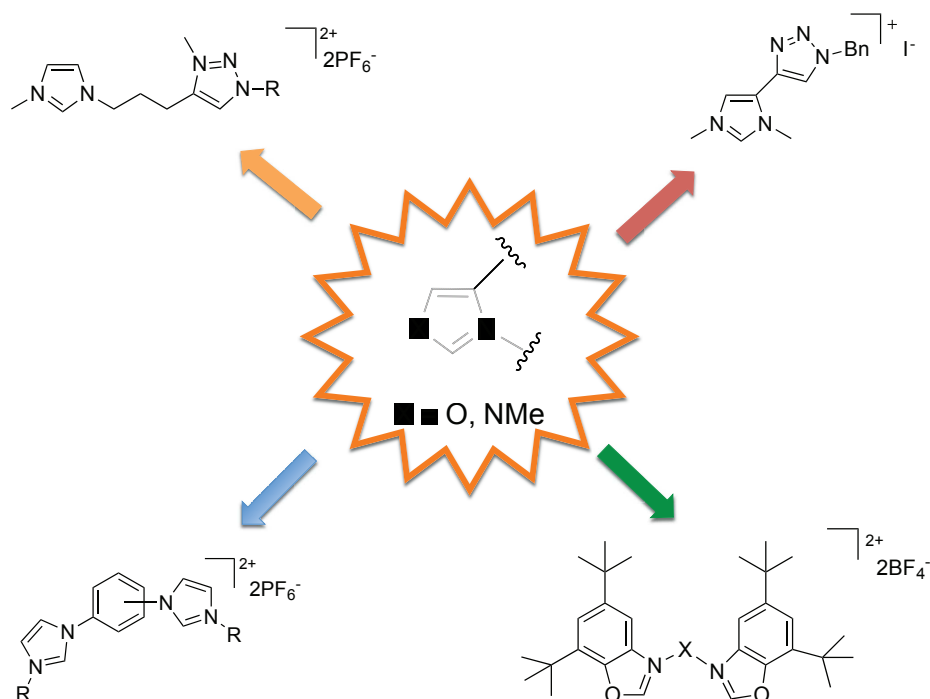
Chapter 6: CONCLUSIONS

The research activity of this project was focused on the synthesis of transition metal complexes bearing different N-heterocyclic carbene ligands.

This class of ligands has been demonstrated to be very easily to functionalize, thus changing the sterical and the electronical properties.

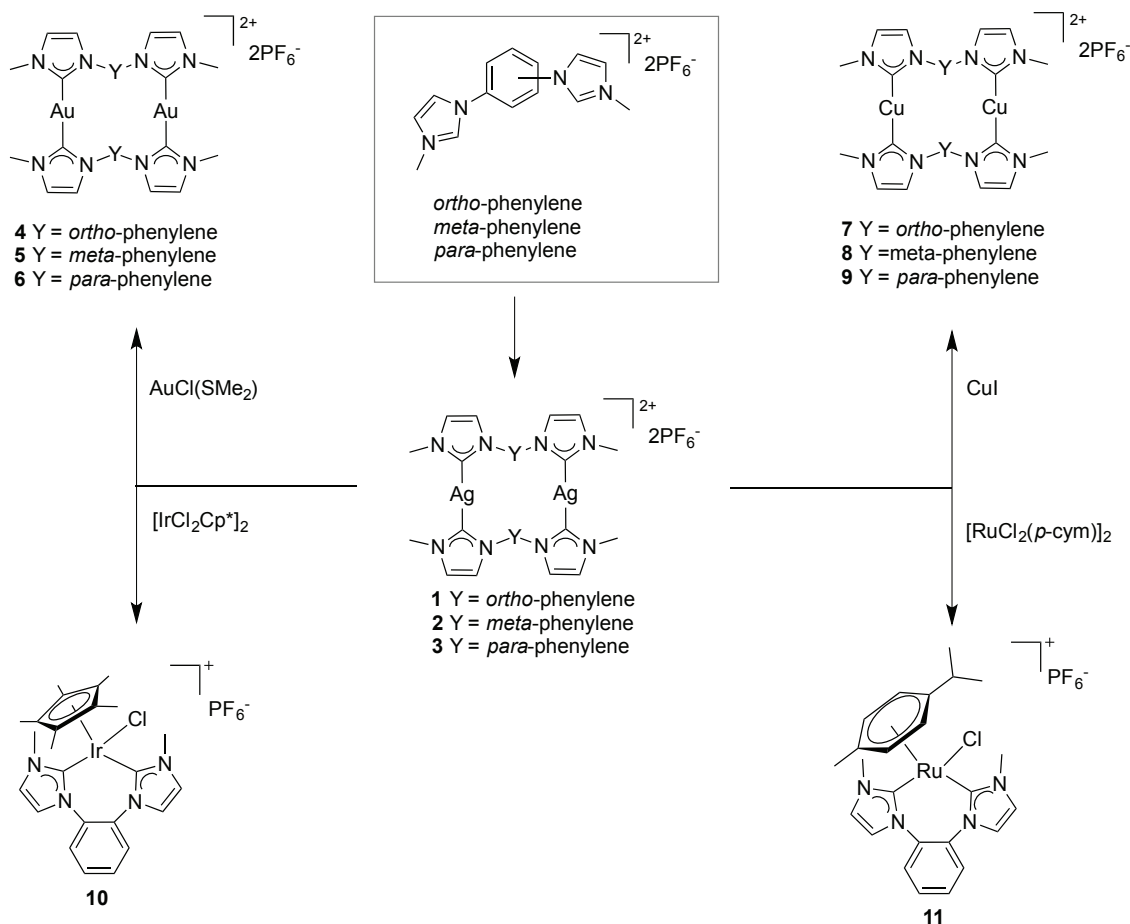
The different azolium salts synthesized in this thesis are:

- bis-imidazolium salts having a rigid phenylene bridge between the imidazolium moieties;
- imidazolium salt functionalized with a triazole in the 5 position of the backbone;
- mixed imidazolium/triazolium salts bridged by a propylene linker;
- bis-benzoxazolium salts.



In general, the best way for the obtainment of transition metal complexes starting from these proligands, is the transmetalation reaction. This procedure implies the pre-formation of the silver(I) complexes and subsequent transmetalation of the ligand to different metal centers.

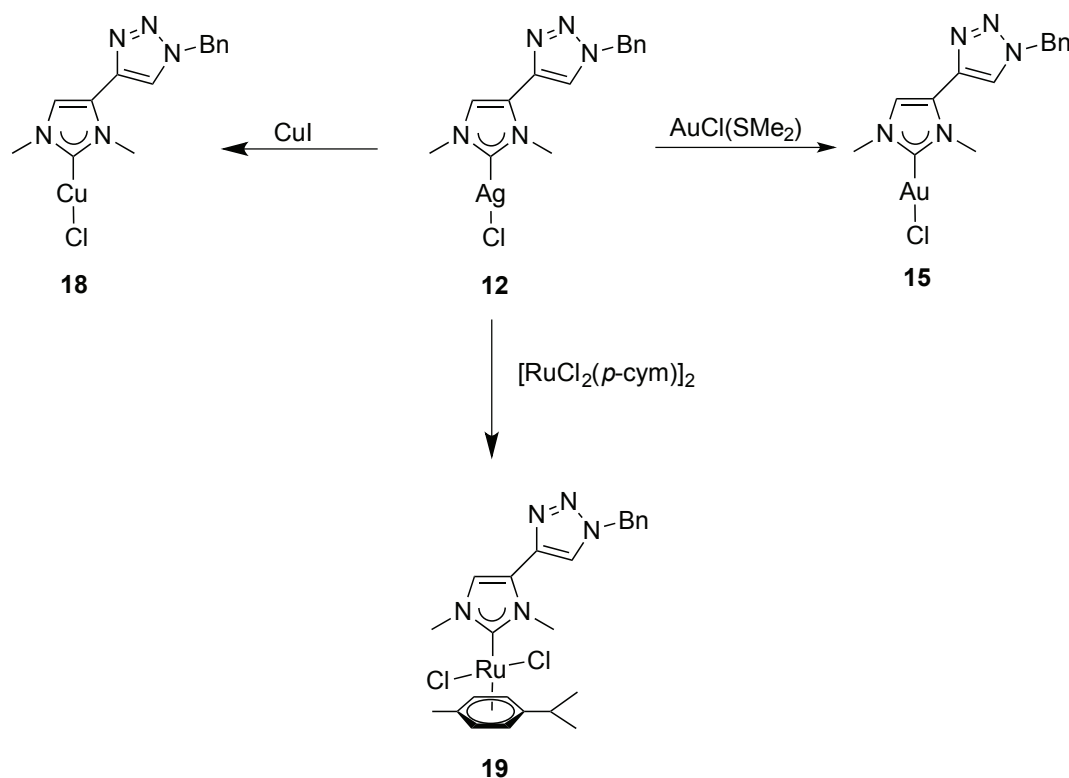
With this procedure silver(I), gold(I), copper(I), ruthenium(II) and iridium(III) complexes bearing di(N-heterocyclic carbene) ligands with rigid phenylene bridge have been synthesized and fully characterized. The solid state crystal structure of some complexes have also been obtained.



The gold(I) complexes possess interesting photoluminescence properties, superior to those of the silver(I) ones. These features depend on several factors and not only on the aurophilic interaction, i.e. on the Au⋯Au distance.

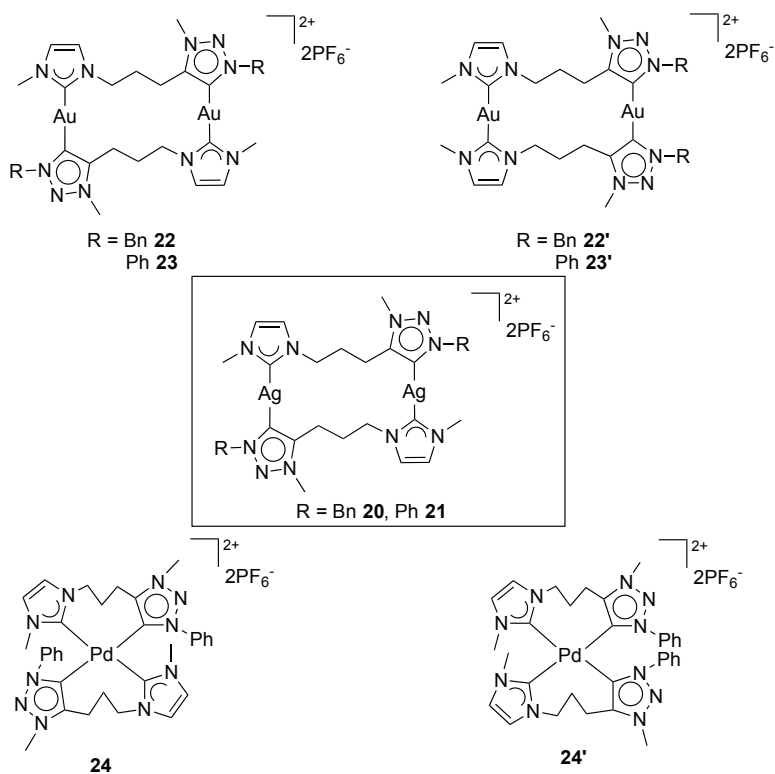
For example, comparing complexes **4** and **5** (having the same LC emission), the first has a smaller Au⋯Au distance (3.657 Å) with respect to complex **5** (7.140 Å). Interestingly, the photoluminescence quantum yield of the gold(I) complex with *meta*-phenylene bridge is higher than the one observed for the complex with *ortho*-phenylene bridge. This is due to important π⋯π crystal stacking, that influences the optical properties of the dinuclear gold(I) complexes.

Another part of the work has concerned the use of triazole-functionalized imidazole-2-ylidene as ligands for various metal centers. Also in this case, the transmetalation has been used for the synthesis of the complexes. Interestingly, the structure of the silver(I) complex is different from the expected one, observing the coordination of a chloride anion, derived from the solvent CHCl_3 .



The Ag(I), Au(I) and Ru(II) complexes have been studied as anticancer molecules against different tumoral cell lines showing a difference in the performances depending on the metal.

Finally, silver(I), gold(I) and palladium(II) complexes with mixed imidazole-2-ylidene/triazole-5-ylidene ligands connected by a propylene bridge have been synthesized. The dinuclear dicationic silver(I) complexes are characterized by a unique species in solution while the gold(I) and palladium(II) complexes show in the NMR spectra two sets of signals, assignable to two isomers, whose formation is justifiable considering the heteroditopic nature of the ligand.



In the case of gold(I) and palladium(II), the crystal structure of one of the two isomers has been characterized by X-ray diffraction. The distance between the gold(I) centers is ca. 3 Å and this supports the presence of aurophilic interactions. It will be interesting to study the luminescence properties of the complexes, but it will be necessary to find a way to separate the two species.

Finally, concerning the bis(benzoxazolium) salts, we have demonstrated that they are rather unstable species and for this reason the attempts to obtain transition metal complexes starting from these proligands have been unsuccessful.

Chapter 7: EXPERIMENTAL SECTION

7.1 Materials and methods

Unless otherwise stated, all the synthesis and manipulations have been carried out using standard Schlenk techniques under an atmosphere of argon. Some syntheses have been carried out in a MBraun Labmaster sp dry box, working under an atmosphere of dinitrogen. The reagents were purchased by Aldrich as high purity compounds and used without any further purification and all the solvent have been used as received as technical grade solvents.

Elemental analysis

The elemental analysis were carried out by the microanalytical laboratory in the Department of Chemical Sciences (University of Padova) with a Fisons EA 1108 CHNS-O apparatus.

Mass Spectra

ESI-MS spectra have been carried out with an Agilent LC/MSD Trap SL spectrometer at a capillary potential of 1500 V or using a LCQ-Duo (Thermo-Finnigan) operating in positive ion mode. Instrumental parameters for the LCQ-Duo: capillary voltage 10 V, spray voltage 4.5 kV; capillary temperature 200 °C; mass scan range from 150 to 2000 amu; dinitrogen was used as sheath gas; the He pressure inside the trap was kept constant. The pressure directly read by an ion gauge (in the absence of the N₂ stream) was 1.33×10^{-5} Torr. All the samples have been dissolved in acetonitrile and directly injected into the ESI source by a syringe pump at 8 μ L/min flow rate.

HR-MS experiments were performed on a Bruker Daltonics microTOF spectrometer (Bruker Daltonik GmbH, Bremen, Germany) equipped with an orthogonal electrospray (ESI) interface. Calibration was performed using Tunning mix (Agilent Technologies). Sample solutions were introduced into the spectrometer source with a syringe pump (Harvard type 55 1111: Harvard Apparatus Inc., South Natick, MA, USA) with a flow rate of 5 μ L/min.

MALDI experiments were done using a time-of-flight mass spectrometer (MALDI-TOF-TOF Autoflex II TOF-TOF, Bruker Daltonics, Bremen, Germany) equipped with a nitrogen laser ($\lambda = 337$ nm). An external multi-point calibration was carried out before each measurement. Scan accumulation and data processing were performed with

FlexAnalysis 3.0 software. 1,8,9-anthracenetriol (dithranol) was used as matrix without any further purification (from Alfa Aesar Karlsruhe, Germany) and the relative solution was prepared by dissolution of dithranol in THF to obtain a 20 mg/mL solution. 0.5 μ L of a mixture containing the sample solution and the matrix (1/1) was deposited on the stainless steel plate.

NMR Spectra

NMR spectra were recorded generally on a Bruker Avance 300 MHz (300.1 MHz for ^1H , 75.5 MHz for ^{13}C , 282.2 MHz for ^{19}F and 121.5 MHz for ^{31}P) spectrometer.

Other measurements have been carried out Bruker DMX - 600 (599.98 MHz for ^1H and 150.07 MHz for ^{13}C , using a cryomagnet of 14.1 T and an inverse probe TX - 1 equipped by field gradients on X, Y, and Z axis) and Bruker DRX - 400 (400.13 MHz for ^1H and 100.62 MHz for ^{13}C equipped by cryomagnet of 9.4 T and an inversebroad-band probe VSQ - 400 with a gradients on x axis).

Unless otherwise stated, all the spectra have been recorded at 298 K. The chemical shift values (δ) are reported in units of ppm relative to the residual of the deuterated solvent and all the coupling constants (J) are reported in Hertz. The multiplicity of the signals are reported using these abbreviations: singlet (s), doublet (d), triplet (t), multiplet (m) and broad (br).

The complete characterization of the transition metal complexes have been carried out using different experiments: ^1H -NMR, $^{13}\text{C}\{^1\text{H}\}$ -NMR, $^{31}\text{P}\{^1\text{H}\}$ -NMR, $^{19}\text{F}\{^1\text{H}\}$ -NMR, HMQC (*Heteronuclear Multiple Quantum Coherence*), HMBC (*Heteronuclear Multiple Bond Coherence*) and, if necessary, NOESY (*Nuclear Overhauser Enhancement Spectroscopy*).

X-ray crystal structure determination

The crystallographic data for all complexes were collected on a Bruker Smart Apex II single-crystal diffractometer working with monochromatic Mo-K α radiation and equipped with an area detector.¹⁶⁴ The structures were solved by direct methods and refined against F^2 with SHELXL-2014/7¹⁶⁵ with anisotropic thermal parameters for all non-hydrogen atoms. Idealized geometries were assigned to the hydrogen atoms. Details for the X-ray data collection are reported in Sections 7.2.9, 7.3.15 and 7.4.10.

X-ray diffraction studies of complex **12** were carried out at the Institut de Chimie X-ray Facility of the University of Strasbourg. Crystal data were collected at 173 K using a Mo-K α graphite-monochromated ($\lambda = 0.71073 \text{ \AA}$) radiation with a Nonius KappaCCD

diffractometer. The structures were solved by direct methods with SHELXS97 and refined against F2 using the SHELXL97 software. Non-hydrogen atoms were refined anisotropically. Hydrogen atoms were generated according to stereochemistry and refined using a riding model in SHELXL97.

Photophysical measurements

Uncorrected emission spectra were obtained with an Edinburgh FLS980 spectrometer equipped with a peltier-cooled Hamamatsu R928 photomultiplier tube (185 - 850 nm). An Edinburgh Xe900 450 W Xenon arc lamp was used as exciting light source. Corrected spectra were obtained via a calibration curve supplied with the instrument. Emission lifetimes in the ns- μ s range were determined with the single photon counting technique by means of the same Edinburgh FLS980 spectrometer using pulsed NanoLED excitation sources at 330 nm, (pulse width \leq 0.3 ns). Solid samples, Φ_{em} have been calculated by corrected emission spectra obtained from an apparatus consisting of a barium sulphate coated integrating sphere (4 or 6 inches), a 450W Xe lamp and a R928 photomultiplier tube signal detectors, following the procedure described by De Mello *et al.*¹⁶⁶ Experimental uncertainties are estimated to be \pm 8% for lifetime determinations, \pm 20% for emission quantum yields.

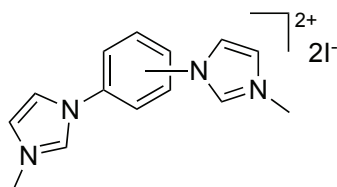
In vitro cytotoxic measurements

Samples were prepared by dissolution of the compounds in DMSO at stock concentration of 10 mM. Cells were plated in 96-well tissue culture plates in 200 μ L complete medium at a density of 1000 - 2500 cells per well and treated 24 hours later with 2 μ L of compounds using a Biomek 3000 automation workstation (Beckman-Coulter). Controls received the same volume of the appropriate vehicle (DMSO, 1% final volume). After 72 hours exposure, MTS reagent (CellTiter 96 Aqueous One, Promega) was added and incubated for 3 hours at 37 °C: the absorbance was monitored at 490 nm and results expressed as the inhibition of cell proliferation calculated as the ratio $[(1 - (\text{OD}_{490} \text{ treated}/\text{OD}_{490} \text{ control})) \times 100]$ in triplicate experiments after subtraction of the blank without cells.

Positive controls (cells incubated with a reference drug at its IC₅₀ concentration) were routinely added to check the responsiveness of cells. For IC₅₀ determination [50% inhibition of cell proliferation], cells were incubated for 72 hours following the same protocol with compound concentrations ranging 5 nM to 100 μ M in separate duplicate experiments.

7.2 Metal complexes with di(N-heterocyclic carbene) ligands bearing a rigid phenylene bridge

7.2.1 General procedure for the synthesis of 1,1'-dimethyl-3,3'-phenylene-bis(imidazolium) diiodide a - c



a = *ortho*-phenylene
b = *meta*-phenylene
c = *para*-phenylene

CH₃I (120 μ L, 1.9 mmol) was added to a solution of the appropriate 1,1'-phenylene-bis(imidazole) (synthesized according to the literature⁸⁵ (0.55 g, 0.74 mmol) in DMSO (1 mL). The reaction mixture was kept under stirring for 24 hours at room temperature obtaining an orange solution. Addition of CH₂Cl₂ (35 mL) affords the product as an off-white solid, which was filtered and dried under vacuum.

a.

White solid, yield 94 %. ¹H-NMR (DMSO-d₆, 300 MHz): δ = 3.92 (s, 6H, CH₃), 7.74 (s, 2H, CH), 7.85 (s, 2H, CH), 7.93 (s, 4H, CH Ar), 9.45 (s, 2H, NCHN).

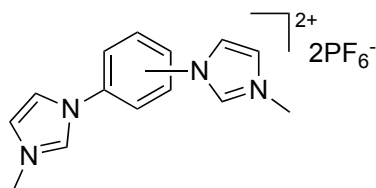
b.

White solid, yield 95 %. ¹H-NMR (DMSO-d₆, 300 MHz): δ = 3.99 (s, 6H, CH₃), 7.99 (s, 3H, CH Ar), 8.02 (s, 2H, CH), 8.29 (s, 1H, CH Ar), 8.36 (s, 2H, CH), 9.86 (s, 2H, NCHN).

c.

White solid, yield 91 %. ¹H-NMR (DMSO-d₆, 300 MHz): δ = 3.97 (s, 6H, CH₃), 8.00 (s, 2H, CH), 8.09 (s, 4H, CH Ar) 8.38 (s, 2H, CH), 9.87 (s, 2H, NCHN).

7.2.2 General procedure for the synthesis of the 1,1'-dimethyl-3,3'-phenylene bis(imidazolium) bis(hexafluorophosphate) salts d - f



d = *ortho*-phenylene
e = *meta*-phenylene
f = *para*-phenylene

A solution of NH_4PF_6 (0.28 g, 1.7 mmol) in MeOH (1 mL) was added to a solution of 1,1'-dimethyl-3,3'-phenylene-bis(imidazolium) diiodide (0.30 g, 0.61 mmol) in MeOH (4 mL). The mixture was stirred for two hours at room temperature giving a solid that was filtered and dried under vacuum.

d.

White solid, yield 76 %. $^1\text{H-NMR}$ (CD_3CN , 300 MHz): $\delta = 3.90$ (s, 6H, CH_3), 7.35 (d, $^3J_{\text{HH}} = 1.8$ Hz, 2H, CH), 7.46 (d, $^3J_{\text{HH}} = 1.8$ Hz, 2H, CH), 7.75 (m, 2H, CH Ar), 7.89 (m, 2H, CH Ar), 8.66 (s, 2H, NCHN).

$^{31}\text{P}\{^1\text{H}\}$ -NMR (CD_3CN , 121 MHz): $\delta = -144.6$ (heptet, PF_6).

e.

White solid, yield 76 %. $^1\text{H-NMR}$ (CD_3CN , 300 MHz): $\delta = 3.98$ (s, 6H, CH_3), 7.60 (s, 2H, CH), 7.84 (m, 3H, CH Ar), 7.91 (s, 2H, CH), 8.03 (m, 1H, CH Ar), 9.25 (s, 2H, NCHN).

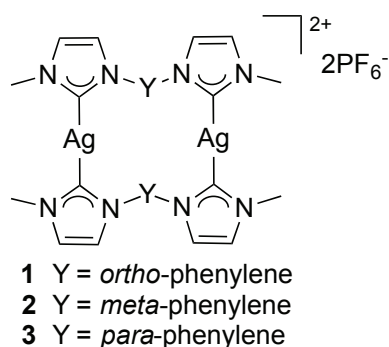
$^{31}\text{P}\{^1\text{H}\}$ -NMR (CD_3CN , 121 MHz): $\delta = -144.6$ (heptet, PF_6).

f.

White solid, yield 80 %; $^1\text{H-NMR}$ (CD_3CN , 300 MHz): $\delta = 3.96$ (s, 6H, CH_3), 7.58 (s, 2H, CH), 7.82 (s, 2H, CH), 7.85 (s, 4H, CH Ar), 8.96 (s, 2H, NCHN).

$^{31}\text{P}\{^1\text{H}\}$ -NMR (CD_3CN , 121 MHz): $\delta = -144.6$ (heptet, PF_6).

7.2.3 General procedure for the syntheses of the silver(I) complexes 1 - 3



A mixture of the proper proligand **d** – **f** (0.10 g, 0.19 mmol) and Ag₂O (0.12 g, 0.52 mmol) was placed in a two neck round bottom flask. Subsequently, CH₃CN (10 mL) was added and the reaction mixture was left under stirring for 24 hours at 65 °C with the exclusion of light. Afterwards, it was filtered on Celite and the filtrate was concentrated at low pressure. Addition of diethyl ether (10 mL) affords the product as a light grey solid, which was filtered and dried under vacuum.

1.

Light grey solid, yield 40 %.

¹H-NMR (CD₃CN, 300 MHz): δ = 3.81 (s, 6H, CH₃), 7.04 (s, 2H, CH), 7.20 (s, 2H, CH), 7.37 (m, 2H, CH Ar), 7.47 (m, 2H, CH Ar).

¹³C{¹H}-NMR (CD₃CN, 75 MHz): δ = 39.1 (CH₃), 123.6 (CH), 124.2 (CH), 128.7 (CH Ar), 131.3 (CH Ar), 135.8 (C Ar), 186.7 (C Ag).

ESI-MS (positive-ions, CH₃CN): *m/z* 836.88 (100 %, [Ag₂L₂PF₆]⁺), 690.97 (20 %, [Ag₂L₂]⁺), 346.09 (50 %, [Ag₂L₂]²⁺) with L = diNHC.

Crystals of complex **1** were obtained by slow diffusion of diethyl ether into an acetonitrile solution of the complex.

2.

Light grey solid, yield 32 %.

¹H-NMR (CD₃CN, 300 MHz): δ = 3.97 (s, 6H, CH₃), 7.31 (m, 1H, CH Ar), 7.38 (d, ³J_{HH} = 1.8 Hz, 2H, CH), 7.48 (d, ³J_{HH} = 1.8 Hz, 2H, CH), 7.56 (m, 3H, CH Ar).

¹³C{¹H}-NMR (CD₃CN, 75 MHz): δ = 39.2 (CH₃), 120.5 (CH Ar), 122.7 (CH), 124.5 (CH), 124.9 (CH Ar), 131.0 (CH Ar), 141.5 (C Ar), 181.7 (C Ag).

ESI-MS (positive-ions, CH₃CN): m/z 836.88 (100 %, [Ag₂L₂PF₆]⁺), 691.04 (20 %, [Ag₂L₂]⁺), 346.19 (50 %, [Ag₂L₂]²⁺) with L = diNHC.

Crystals of complex **2** were obtained by slow diffusion of diethyl ether into an acetonitrile solution of the complex.

3.

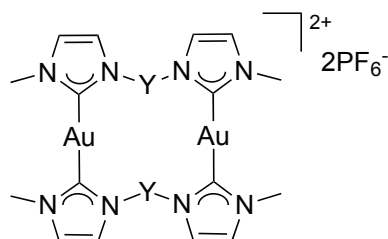
Light grey solid, yield 40 %.

¹H-NMR (CD₃CN, 300 MHz): δ = 3.98 (s, 6H, CH₃), 7.39 (s, 2H, CH), 7.54 (s, 2H, CH), 7.65 (s, 4H, CH Ar).

¹³C{¹H}-NMR (CD₃CN, 75 MHz): δ = 39.7 (CH₃), 122.3 (CH), 124.4 (CH), 125.4 (CH Ar), 141.0 (C Ar), 180.0 (CAg).

ESI-MS (positive-ions, CH₃CN): m/z 836.89 (100 %, [Ag₂L₂PF₆]⁺), 691.04 (20 %, [Ag₂L₂]⁺), 346.22 (55 %, [Ag₂L₂]²⁺) with L = diNHC.

7.2.4 General procedure for the syntheses of gold(I) complexes 4 - 6



4 Y = *ortho*-phenylene

5 Y = *meta*-phenylene

6 Y = *para*-phenylene

A solution of AuCl(SMe₂) (0.031 g, 0.105 mmol) in acetonitrile (5 mL) was added to a solution of the proper silver(I) complex **1** – **3** (0.051 g, 0.052 mmol) in the same solvent (5 mL). The reaction mixture was left under stirring for 2 hours at room temperature. Afterwards, it was filtered on Celite and the filtrate was concentrated at low pressure. Addition of diethyl ether (15 mL) affords the product as a white solid, which was filtered and dried under vacuum.

4.

White solid, yield 30 %. Anal. Calcd for C₂₈H₂₈N₈Au₂F₁₂P₂: C, 28.98; H, 2.43; N, 9.66%. Found: C, 29.09; H, 2.40; N, 9.36%.

$^1\text{H-NMR}$ (CD_3CN , 300 MHz): $\delta = 3.82$ (s, 6H, CH_3), 7.03 (d, $^3J_{\text{HH}} = 1.5$ Hz, 2H, CH), 7.21 (d, $^3J_{\text{HH}} = 1.5$ Hz, 2H, CH), 7.42 (m, 2H, CH Ar), 7.51 (m, 2H, CH Ar).

$^{13}\text{C}\{^1\text{H}\}$ -NMR (CD_3CN , 75 MHz): $\delta = 38.0$ (CH_3), 123.9 (CH), 124.5 (CH), 129.1 (CH Ar), 131.9 (CH Ar), 135.5 (C Ar), 185.3 (CAu).

ESI-MS (positive-ions, CH_3CN): m/z 1015.08 (100 %, $[\text{Au}_2\text{L}_2\text{PF}_6]^+$), 435.42 (27 %, $[\text{Au}_2\text{L}_2]^{2+}$) with L = diNHC.

Crystals of complex **4** were obtained by slow diffusion of diethyl ether into an acetonitrile solution of the complex.

5.

White solid, yield 38 %. Anal. Calcd for $\text{C}_{28}\text{H}_{28}\text{N}_8\text{Au}_2\text{F}_{12}\text{P}_2$: C, 28.98; H, 2.43; N, 9.66%. Found: C, 28.75; H, 2.49; N, 10.06%.

$^1\text{H-NMR}$ (CD_3CN , 300 MHz): $\delta = 3.98$ (s, 6H, CH_3), 7.40 (m, 6H, CH + CH Ar), 7.64 (m, 2H, CH Ar).

$^{13}\text{C}\{^1\text{H}\}$ -NMR (CD_3CN , 75 MHz): $\delta = 38.5$ (CH_3), 122.4 (CH Ar), 123.3 (CH), 124.5 (CH), 126.6 (CH Ar), 131.2 (CH Ar), 140.3 (C Ar), 183.2 (CAu).

ESI-MS (positive-ions, CH_3CN): m/z 1015.09 (100 %, $[\text{Au}_2\text{L}_2\text{PF}_6]^+$), 435.40 (27 %, $[\text{Au}_2\text{L}_2]^{2+}$) with L = diNHC.

Crystals of complex **5** were obtained by slow diffusion of diethyl ether into an acetonitrile solution of the complex.

6.

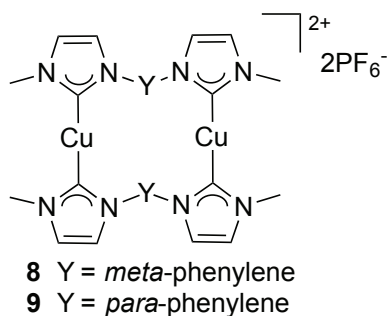
White solid, yield 46 %. Anal. Calcd for $\text{C}_{30}\text{H}_{31}\text{N}_9\text{Au}_2\text{F}_{12}\text{P}_2$ ($[\text{Au}_2\text{L}_2](\text{PF}_6)_2 \cdot \text{CH}_3\text{CN}$) C, 29.99; H, 2.60; N, 10.49%. Found: C, 30.97; H, 2.65; N, 10.19%.

$^1\text{H-NMR}$ (CD_3CN , 300 MHz): $\delta = 4.00$ (s, 6H, CH_3), 7.40 (s, 2H, CH), 7.52 (s, 2H, CH), 7.74 (s, 4H, CH Ar).

$^{13}\text{C}\{^1\text{H}\}$ -NMR (CD_3CN , 75 MHz): $\delta = 39.2$ (CH_3), 122.5 (CH), 124.6 (CH), 126.1 (CH Ar), 139.8 (C Ar), 183.8 (CAu).

ESI-MS (positive-ions, CH_3CN): m/z 1015.07 (100 %, $[\text{Au}_2\text{L}_2\text{PF}_6]^+$), 435.33 (25 %, $[\text{Au}_2\text{L}_2]^{2+}$) with L = diNHC.

7.2.5 General procedure for the syntheses of the copper(I) complexes 8 - 9



CuI (0.032 g, 0.017 mmol) was added to a solution of the proper silver(I) complex **2** or **3** (0.041 g, 0.042 mmol) in acetonitrile (5 mL). The reaction mixture was left under stirring for one hour at room temperature. Afterwards, it was filtered on Celite and the filtrate was concentrated at low pressure. Addition of diethyl ether (10 mL) affords the product as a solid, which was filtered and dried under vacuum. Unfortunately, the instability of the products does not allow to obtain good elemental analyses. For this reason, the products were characterized only by means of spectroscopic techniques

8.

Off-white solid, yield 29 %.

$^1\text{H-NMR}$ (CD_3CN , 300 MHz): δ = 4.00 (s, 6H, CH_3), 7.09 (m, 1H, CH Ar), 7.35 (d, $^3J_{\text{HH}} = 1.8$ Hz, 2H, CH), 7.49 (s, 1H, CH Ar), 7.52 (d, $^3J_{\text{HH}} = 1.8$ Hz, 2H, CH), 7.58 (m, 2H, CH Ar).

$^{13}\text{C}\{^1\text{H}\}$ -NMR (CD_3CN , 75 MHz): δ = 39.2 (CH_3), 122.1 (CH), 122.2 (CH Ar), 124.1 (CH Ar), 124.2 (CH Ar), 124.7 (CH), 177.7 (CCu), C Ar not detected.

ESI-MS (positive-ions, CH_3CN): m/z 746.95 (100 %, $[\text{Cu}_2\text{L}_2\text{PF}_6]^+$), 601.25 (45 %, $[\text{Cu}_2\text{L}_2]^+$), 301.33 (35 %, $[\text{Cu}_2\text{L}_2]^{2+}$) with L = diNHC.

9.

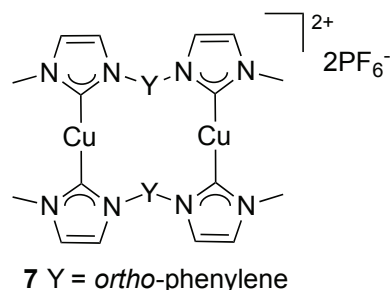
Off-white solid, yield 30 %.

$^1\text{H-NMR}$ (CD_3CN , 300 MHz): δ = 3.99 (s, 6H, CH_3), 7.34 (d, $^3J_{\text{HH}} = 1.8$ Hz, 2H, CH), 7.47 (d, $^3J_{\text{HH}} = 1.8$ Hz, 2H, CH) 7.61 (s, 4H, CH Ar).

$^{13}\text{C}\{^1\text{H}\}$ -NMR (CD_3CN , 75 MHz): δ = 39.1 (CH_3), 122.2 (CH), 124.7 (CH), 125.9 (CH Ar), 137.2 (C Ar), 177.2 (CCu).

ESI-MS (positive-ions, CH₃CN): *m/z* 747.05 (100 %, [Cu₂L₂PF₆]⁺), 601.13 (28 %, [Cu₂L₂]⁺), 301.22 (35 %, [Cu₂L₂]²⁺) with L = diNHC.

7.2.6 *In situ* synthesis of the copper complex 7



This compound was prepared *in situ* using the same procedure described in the previous section, however the reaction was carried out in a dry box in deuterated acetonitrile starting from the silver(I) complex **1** and the colorless solution was directly analyzed.

¹H-NMR (CD₃CN, 300 MHz): δ = 3.75 (s, 6H, CH₃), 7.01 (d, ³J_{HH} = 1.8 Hz, 2H, CH), 7.05 (d, ³J_{HH} = 1.8 Hz, 2H, CH), 7.56 (m, 2H, CH Ar), 7.64 (m, 2H, CH Ar).

¹³C{¹H}-NMR (CD₃CN, 75 MHz): δ = 38.8 (CH₃), 123.2 (CH), 123.3 (CH), 129.3 (CH Ar), 131.0 (CH Ar), 137.4 (C Ar), 180.1 (CCu).

Upon standing 12 hours on air, the colour of the solution turned yellow and a new spectrum was recorded. The main signals are assigned to species **7***.

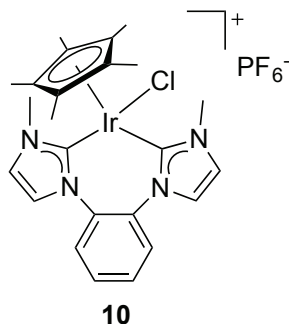
¹H-NMR (CD₃CN, 300 MHz): δ = 4.51 (s, 6H, CH₃), 8.08 (m, 2H, CH Ar), 8.19 (d, ³J_{HH} = 2.1 Hz, 2H, CH), 8.49 (m, 2H, CH Ar), 8.65 (d, ³J_{HH} = 2.1 Hz, 2H, CH).

¹³C{¹H}-NMR (CD₃CN, 75 MHz): δ = 42.6 (CH₃), 119.3 (CH), 119.5 (CH Ar), 123.7 (C Ar), 127.4 (NCN), 131.7 (CH), 132.7 (C Ar).

¹H-NMR (DMSO-d₆, 600 MHz): δ = 4.60 (s, 6H, CH₃), 8.12 (m, 2H, CH Ar), 8.67 (bs, 2H, CH), 8.80 (m, 2H, CH Ar), 9.50 (bs, 2H, CH).

¹³C{¹H}-NMR (DMSO-d₆, 150 MHz): δ = 41.7 (CH₃), 118.3 (CH), 118.9 (CH Ar), 123.2 (C Ar), 127.4 (NCN), 130.8 (CH), 131.7 (C Ar).

7.2.7 Synthesis of the iridium(III) complex **10** and characterization of the species **10***



A solution of $[\text{IrCl}_2\text{Cp}^*]_2$ (0.026 g, 0.033 mmol) in CH_3CN (7 mL) was added to a solution of the silver complex **1** (0.031 g, 0.031 mmol) in the same solvent (7 mL). The reaction mixture was left under stirring for 5 hours at room temperature. Afterwards, it was filtered on Celite and the filtrate was concentrated at low pressure. Addition of diethyl ether (15 mL) affords the product as a yellow solid, which was filtered and dried under vacuum.

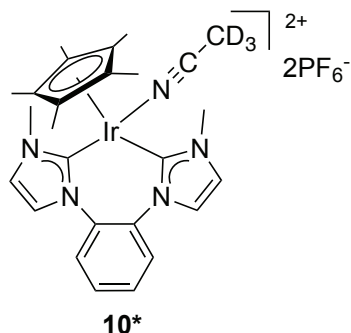
Yield 20 %. Anal. Calcd for $\text{C}_{24}\text{H}_{29}\text{N}_4\text{ClIrP}$: C, 38.60; H, 3.92; N, 7.51 %. Found: C, 36.34; H, 3.71; N, 6.61 %. The elemental analysis confirms the expected C/H/N ratio, however the values are lower than the estimated ones probably because of a small amount of silver salt.

$^1\text{H-NMR}$ (CD_3CN , 300 MHz): $\delta = 1.42$ (s, 15H, CH_3), 3.92 (s, 6H, CH_3), 7.38 (d, $^3J_{\text{HH}} = 2.1$ Hz, 2H, CH), 7.49 (d, $^3J_{\text{HH}} = 2.1$ Hz, 2H, CH), 7.52 (m, 2H, CH Ar), 7.62 (m, 2H, CH Ar).

$^{13}\text{C}\{^1\text{H}\}$ -NMR (CD_3CN , 75 MHz): $\delta = 9.1$ (CH_3), 40.1 (NCH_3), 94.0 (CCp^*), 124.7 (CH), 127.3 (CH), 129.6 (CH Ar), 130.7 (CH Ar), 134.2 (C Ar), 157.0 (C Ir).

ESI-MS (positive-ions, CH_3CN): m/z 601.26 (90 %, $[\text{IrClCp}^*\text{L}]^+$), 363.19 (31 %, $[\text{IrClCp}^*]^{2+}$) with L = diNHC.

The NMR solution of complex **10** slowly evolves and in ca. 10 days a second similar set of signals emerges. The new signals can be attributed to the dicationic species **10**^{*}, in which the chloride ligand has been substituted by a deuterated acetonitrile solvent molecule.



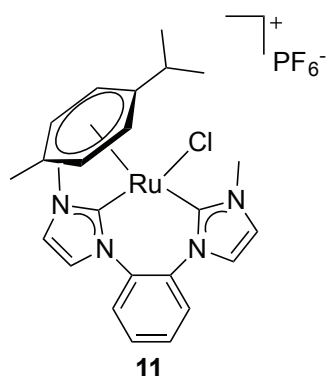
To confirm this, complex **10** (5.5 mg, 0.0074 mmol) and AgPF₆ (7.5 mg, 0.013 mmol, 3.5 eq.) were placed in a vial. Afterwards CD₃CN (1 ml) was added and the solution was heated at 50 °C for two hours, giving complete conversion of complex **10** in **10***.

¹H-NMR (CD₃CN, 300 MHz): δ = 1.50 (s, 15H, CH₃), 3.77 (s, 6H, CH₃), 7.50 (d, ³J_{HH} = 2.1 Hz, 2H, CH), 7.58 (m, 4H, CH + CH Ar), 7.68 (m, 2H, CH Ar).

¹³C{¹H}-NMR (CD₃CN, 75 MHz): δ = 9.3 (CH₃), 39.8 (NCH₃), 96.4 (CCp*), 125.8 (CH), 127.3 (CH), 129.8 (CH Ar), 131.3 (CH Ar), 133.2 (C Ar), 150.3 (CIr).

ESI-MS (positive-ions, CH₃CN): *m/z* 585.17 (60 %, [IrCp*L(HDO)]⁺), 565.34 (68 %, [IrCp*L]⁺), 303.38 (100 %, [IrCp*LCD₃CN]²⁺), 283.32 (31 %, [IrCp*L]²⁺) with L = diNHC.

7.2.8 Synthesis of the ruthenium(II) complex **11**



Complex **1** (0.042 g, 0.043 mmol) and [RuCl₂(*p*-cymene)]₂ (0.053 g, 0.086 mmol) were placed in a two neck round bottom flask. Subsequently, CH₃CN (5 mL) was added and the reaction mixture was left under stirring for one hour at room temperature. Afterwards, it was filtered on Celite and the filtrate was concentrated at low pressure. Addition of diethyl ether (10 mL) affords the product as an orange solid, which was filtered and dried under vacuum.

Yield 23 %. Anal. Calcd for $C_{24}H_{28}N_4ClF_6PRu \cdot CH_3CN$: C, 44.93; H, 4.50; N, 10.08 %. Found: C, 43.98; H, 4.25; N, 10.30 %.

1H -NMR (CD_3CN , 300 MHz): δ = 0.85 (d, $^3J_{HH}$ = 6.9 Hz, 6H, $CH(CH_3)_2$), 1.65 (heptet, 1H, $CH(CH_3)_2$), 1.94 (s superimposed to the deuterated solvent signal, 3H, CH_3 *p*-cym), 4.04 (s, 6H, NCH_3), 5.20 (d, $^3J_{HH}$ = 6.3 Hz, 2H, CH Ar *p*-cym), 5.32 (d, $^3J_{HH}$ = 6.3 Hz, 2H, CH Ar *p*-cym), 7.39 (s, 2H, CH), 7.48 (m, 4H, CH Ar + CH), 7.62 (m, 2H, CH Ar).

$^{13}C\{^1H\}$ -NMR (CD_3CN , 75 MHz): δ = 18.7 (CH_3 *p*-cym), 22.7 ($CH(CH_3)_2$), 31.8 ($CH(CH_3)_2$), 40.8 (NCH_3), 86.1 (CH Ar *p*-cym), 91.6 (CH Ar *p*-cym), 106.0 (C *p*-cym), 112.2 (C *p*-cym), 124.5 (CH), 127.2 (CH), 128.9 (CH Ar), 130.2 (CH Ar), 134.4 (C Ar), 179.5 (CRu).

ESI-MS (positive-ions, CH_3CN): m/z 509.05 (100 %, $[RuClL(p\text{-cym})]^+$), 415.82 (38 %, $[RuCl(p\text{-cym})PF_6]^+$), 375.01 (20 %, $[RuClL]^+$), 311.86 (34%, $[RuCl(CH_3CN)(p\text{-cym})]^+$) with L = diNHC.

Crystals of complex **11** were obtained by slow diffusion of diethyl ether into a solution of the complex in acetonitrile.

7.2.9 X-ray crystal structure details of compounds 1, [Ag₂(ortho-diNHC)(CH₃CO₂)](PF₆), 2, 4, 5 and 11

	1	[Ag ₂ (ortho-diNHC)(CH ₃ CO ₂)](PF ₆)	2
Formula	C ₂₈ H ₂₈ Ag ₂ F ₁₂ N ₈ P ₂	C ₁₆ H ₁₇ Ag ₂ F ₆ N ₄ O ₂ P	C ₂₈ H ₂₈ Ag ₂ F ₁₂ N ₈ P ₂
Molecular weight	982.26	658.05	982.26
Crystal system	monoclinic	orthorhombic	triclinic
Space group	<i>C2/c</i>	<i>Pmcn</i>	<i>P-1</i>
<i>a</i> /Å	31.211(7)	11.051(2)	8.468(1)
<i>b</i> /Å	30.103(7)	11.852(2)	9.693(2)
<i>c</i> /Å	17.385(4)	16.403(3)	12.056(2)
α /°	90.00	90.00	87.014(3)
β /°	118.71(4)	90.00	84.837(3)
γ /°	90.00	90.00	67.882(3)
Volume, Å ³	14326(7)	2148.5(7)	912.8(3)
T/K	293(2)	173(2)	298(2)
Z	16	4	1
D _{calc} /g cm ⁻³	1.822	2.034	1.787
F(000)	7744	1280	484
μ (Mo-K)/mm ⁻¹	1.279	1.969	1.255
Reflection collected	88506	23142	13214
Unique reflection	14894 [R _{int} = 0.0655]	2163 [R _{int} = 0.0578]	4684 [R _{int} = 0.0334]
Observed reflection [<i>I</i> > 2 σ (<i>I</i>)]	10462	1745	3741
Final R index [<i>I</i> > 2 σ (<i>I</i>)]	R1 = 0.0490, wR2 = 0.1189	R1 = 0.0325, wR2 = 0.0777	R1 = 0.0440, wR2 = 0.1174
Final R index [all data]	R1 = 0.0767, wR2 = 0.1361	R1 = 0.0434, wR2 = 0.0830	R1 = 0.0571, wR2 = 0.1273
CCDC number	1433307	1433308	1433309
$R1 = \frac{\sum F_o - F_c }{\sum (F_o)}$ $wR2 = \frac{[\sum [w(F_o^2 - F_c^2)^2]}{[\sum [w(F_o^2)^2]]}^{1/2}$			

	4	5	11
Formula	C ₃₀ H ₃₁ Au ₂ F ₁₂ N ₉ P ₂	C ₂₈ H ₂₈ Au ₂ F ₁₂ N ₈ P ₂	C ₂₆ H ₃₁ ClF ₆ N ₅ PRu
Molecular weight	1201.51	1160.46	695.05
Crystal system	orthorhombic	triclinic	orthorhombic
Space group	<i>Cmcm</i>	<i>P</i> -1	<i>P</i> 2 ₁ nb
<i>a</i> /Å	12.899(3)	8.437(1)	8.687 (1)
<i>b</i> /Å	17.022(5)	9.906(1)	12.641(2)
<i>c</i> /Å	17.781(5)	11.951(2)	26.391(3)
α /°	90.00	86.876(2)	90.00
β /°	90.00	84.808(2)	90.00
γ /°	90.00	66.637(2)	90.00
Volume, Å ³	3904.2(18)	913.0(2)	2898.0(6)
T/K	293(2)	293(2)	293(2)
Z	4	1	4
D _{calc} /g cm ⁻³	2.044	2.111	1.593
F(000)	2280	548	1408
μ (Mo-K)/mm ⁻¹	7.682	8.208	0.753
Reflection collected	30846	13770	44263
Unique reflection	3213 [R _{int} = 0.0618]	5589 [R _{int} = 0.0422]	8478 [R _{int} = 0.0525]
Observed reflection [<i>I</i> > 2 σ (<i>I</i>)]	2638	4743	7016
Final R index [<i>I</i> > 2 σ (<i>I</i>)]	R1 = 0.0304, wR2 = 0.0805	R1 = 0.0348, wR2 = 0.0901	R1 = 0.0414, wR2 = 0.1036
Final R index [all data]	R1 = 0.0391, wR2 = 0.0845	R1 = 0.0441, wR2 = 0.0962	R1 = 0.0548, wR2 = 0.1151
CCDC number	1433310	1433311	1433312
$R1 = \sum F_o - F_c / \sum (F_o)$ $wR2 = [\sum [w(F_o^2 - F_c^2)^2] / \sum [w(F_o^2)^2]]^{1/2}$			

7.3 Metal complexes with an imidazole based NHC ligand functionalised with a triazole in the 5 position of the backbone

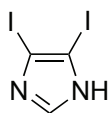
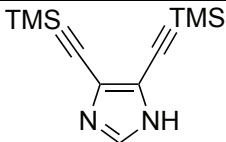
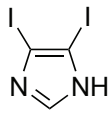
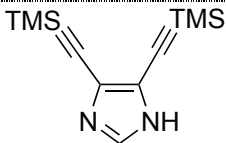
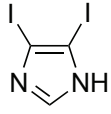
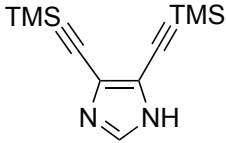
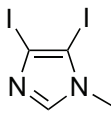
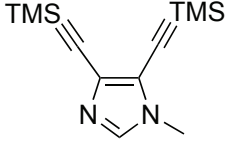
7.3.1 Synthesis of halogen - functionalized imidazoles

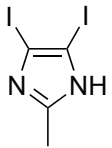
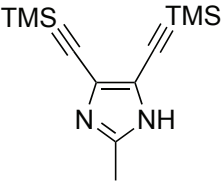
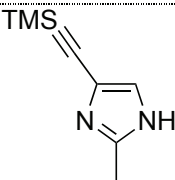
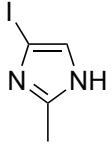
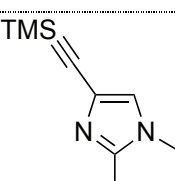
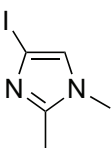
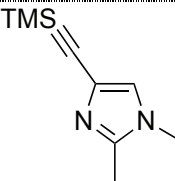
The organic compounds 4,5-diiodoimidazole¹⁶⁷, 4,5-diiodo-1-methylimidazole, 4,5-diiodo-2-methylimidazole, 4-iodo-2-methylimidazole and 4-iodo-1,2-dimethylimidazole¹⁶⁸ were synthesized according to the literature.

7.3.2 Attempts for the synthesis of different (ethynyl)imidazoles¹⁶⁹

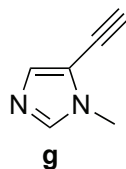
Different attempts have been carried out in order to obtain functionalized imidazoles with (trimethylsilyl)ethynyl groups in position 4 and/or 5 of the backbone, although without the obtainment of the expected products. The reaction conditions are reported in Table 7.1.

Table 7.1: attempts for the syntheses of functionalized imidazoles with (trimethylsilyl)ethynyl groups

Imidazole precursor	Reaction condition	Expected compound
 1 eq.	(trimethylsilyl)acetylene (4 eq.) CuI (10 mol%), PdCl ₂ (PPh ₃) ₂ (5 mol%) THF/diisopropylamine (1:1 v/v), 50 °C, 18 h	
 1 eq.	(trimethylsilyl)acetylene (4 eq.) CuI (5 mol%), PdCl ₂ (PPh ₃) ₂ (5 mol%) THF/triethylamine (3:2 v/v) 25 °C, 18 h	
 1 eq.	(trimethylsilyl)acetylene (4 eq.) CuI (10 mol%), Pd(PPh ₃) ₄ (5 mol%) DMF/triethylamine (9:1 v/v) 25 °C, 18 h	
 1 eq.	(trimethylsilyl)acetylene (4 eq.) CuI (5 mol%), PdCl ₂ (PPh ₃) ₂ (5 mol%)	

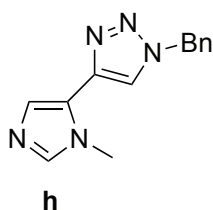
1 eq.	THF/triethylamine (3:2 v/v) 25 °C, 18 h	
	(trimethylsilyl)acetylene (4 eq.) CuI (5 mol%), PdCl ₂ (PPh ₃) ₂ (5 mol%) THF/triethylamine (3:2 v/v) 25 °C, 18 h	
1 eq.	(trimethylsilyl)acetylene (4 eq.) CuI (5 mol%), PdCl ₂ (PPh ₃) ₂ (5 mol%) THF/triethylamine (3:2 v/v) 25 °C, 18 h	
	(trimethylsilyl)acetylene (4 eq.) CuI (5 mol%), PdCl ₂ (PPh ₃) ₂ (5 mol%) THF/triethylamine (3:2 v/v) 25 °C, 18 h	
	(trimethylsilyl)acetylene (4 eq.) CuI (5 mol%), PdCl ₂ (PPh ₃) ₂ (5 mol%) THF/triethylamine (3:2 v/v) 25 °C, 18 h	

7.3.3 Synthesis of 5-ethynyl-1-methylimidazole **g**



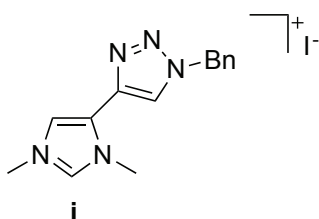
[5-(trimethylsilyl)ethynyl]-1-methylimidazole (0.39 g, 2.19 mmol) and K₂CO₃ (0.92 g, 6.65 mmol) were placed in a two neck round bottom flask and dissolved in MeOH (3 mL). The reaction mixture was left under stirring for 2 hours at 25 °C. Afterwards, the mixture was filtered and concentrated in vacuo. The residue was dissolved in CH₂Cl₂ (5 mL), filtered on a Celite plug and then the filtrate dried under vacuum to obtain a yellow oil (yield 100 %).

¹H-NMR (CDCl₃, 300 MHz) δ = 3.46 (s, 1H, C≡CH), 3.68 (s, 3H, CH₃), 7.29 (s, 1H, CH), 7.42 (s, 1H, CH *im*).

7.3.4 Syntheses of **h**¹⁰⁸

5-ethynyl-1-methylimidazole (0.088 g, 0.82 mmol), sodium-L-ascorbate (0.18 g, 0.88 mmol) and copper(II) sulfate pentahydrate (0.21 g, 0.86 mmol) were placed in a two neck round bottom flask. Subsequently, a mixture of H₂O/THF 1:1 v/v (30 mL) was added. Finally, benzyl azide (0.13 mL, 1.04 mmol) was introduced and the reaction mixture was left under stirring for 48 hours at 25 °C. After removal of THF under reduced pressure, the residue was extracted with CHCl₃ (3 × 20 mL) and the combined organic layers were dried with Na₂SO₄; the organic solvent was then evaporated, obtaining the desired compound as a yellow oil (yield 52 %).

¹H-NMR (CDCl₃, 300 MHz) δ = 3.89 (s, 3H, CH₃), 5.54 (s, 2H, CH₂), 7.41 (m, 7H, CH + CH Ar + CH tz), 7.52 (s, 1H, CH *im*).

7.3.5 Synthesis of the proligand **i**

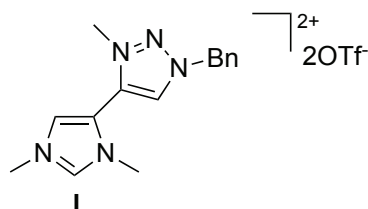
CH₃I (0.09 mL, 1.45 mmol) was added to a solution of **h** (0.12 g, 0.47 mmol) in CHCl₃ (3 mL). The reaction mixture was kept under stirring for 18 hours at 45 °C obtaining an orange solution. Addition of diethyl ether (10 mL) affords the desired product as an orange solid, which was filtered and dried under vacuum (yield 50 %).

¹H-NMR (CDCl₃, 300 MHz) δ = 4.04 (s, 3H, CH₃), 4.14 (s, 3H, CH₃), 5.60 (s, 2H, CH₂), 7.36 (s, 5H, CH Ar), 7.68 (s, 1H, CH), 8.26 (s, 1H, CH *tz*), 9.80 (s, 1H, CH *im*).

$^{13}\text{C}\{^1\text{H}\}$ -NMR (CDCl_3 , 75 MHz): $\delta = 36.7$ (CH_3), 37.3 (CH_3), 54.7 (CH_2), 121.3 (CH), 124.3 (C), 126.8 (C), 128.5 (CH Ar), 129.1 (CH Ar), 129.3 (CH Ar), 133.7 (CH tz), 137.8 (CH im) (C Ar not detected).

ESI-MS (positive-ions, CHCl_3): m/z 254.07 (100 %, $[\text{M-I}]^+$).

7.3.6 Synthesis of the proligand **1**



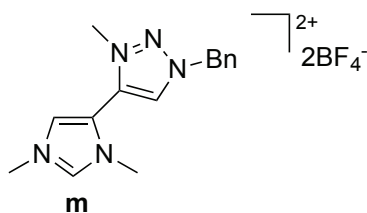
A solution of **h** (0.086 g, 0.36 mmol) in CH_2Cl_2 (6 mL) was cooled at $-78\text{ }^\circ\text{C}$ and then MeOTf (0.12 mL, 1.09 mmol) was added dropwise. The mixture was allowed to warm to room temperature and further kept under stirring for 18 hours. The solvent was removed under vacuum and the oily residue was washed with diethyl ether (3 mL), giving an oil (yield 39 %).

^1H -NMR (DMSO-d_6 , 300 MHz) $\delta = 3.85$ (s, 3H, CH_3), 3.97 (s, 3H, CH_3), 4.27 (s, 3H, CH_3), 6.00 (s, 2H, CH_2), 7.50 (m, 5H, CH Ar), 8.27 (s, 1H, CH), 9.40 (s, 1H, CH tz), 9.46 (s, 1H, CH im).

^1H -NMR (CD_3CN , 300 MHz) $\delta = 3.76$ (s, 3H, CH_3), 3.93 (s, 3H, CH_3), 4.17 (s, 3H, CH_3), 5.83 (s, 2H, CH_2), 7.51 (m, 5H, CH Ar), 7.87 (s, 1H, CH), 8.77 (s, 1H, CCHN), 8.78 (s, 1H, NCHN).

$^{13}\text{C}\{^1\text{H}\}$ -NMR (DMSO-d_6 , 75 MHz): $\delta = 36.5$ (CH_3), 36.6 (CH_3), 38.4 (CH_3), 58.6 (CH_2), 118.9 (CH), 129.3 (C), 130.9 (CH Ar), 131.0 (CH Ar), 131.2 (CH Ar), 131.3 (C Ar), 133.5 (C), 134.5 (CH tz), 141.8 (CH im).

ESI-MS (positive-ions, CH_3CN): m/z 178.11 (100 %, $[\text{M-2OTf-C}_6\text{H}_5]^+$), 254.14 (15 %, $[\text{M-2OTf-CH}_3]^+$), 418.11 (15 %, $[\text{M-OTf}]^+$).

7.3.7 *Synthesis of the proligand m*

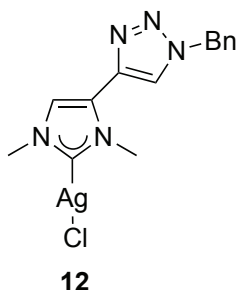
In a two neck round bottom flask, proligand **h** (0.22 g, 0.92 mmol) and Me_3OBF_4 (0.42 g, 2.81 mmol) were dissolved in a mixture of $\text{CHCl}_3/\text{CH}_2\text{Cl}_2$ 1:1 v/v (10 mL). The reaction mixture was kept under stirring for 24 hours at room temperature. The solution was dried under vacuum, washed with diethyl ether giving a brown solid (yield 56 %).

$^1\text{H-NMR}$ (DMSO-d_6 , 300 MHz) $\delta = 3.83$ (s, 3H, CH_3), 3.96 (s, 3H, CH_3), 4.25 (s, 3H, CH_3), 5.99 (s, 2H, CH_2), 7.51 (m, 5H, CH Ar), 8.25 (s, 1H, CH), 9.39 (s, 1H, CH *tz*) 9.46 (s, 1H, CH *im*).

$^1\text{H-NMR}$ (CD_3CN , 300 MHz) $\delta = 3.76$ (s, 3H, CH_3), 3.93 (s, 3H, CH_3), 4.18 (s, 3H, CH_3), 5.83 (s, 2H, CH_2), 7.51 (m, 5H, CH Ar), 7.91 (s, 1H, CH), 8.77 (s, 2H, CH *tz* + CH *im*).

$^{13}\text{C}\{^1\text{H}\}$ -NMR (CD_3CN , 75 MHz): $\delta = 35.7$ (CH_3), 37.3 (CH_3), 39.7 (CH_3), 58.5 (CH_2), 128.4 (CH), 129.8 (C), 130.0 (CH Ar), 130.2 (CH Ar), 130.6 (CH Ar), 130.9 (C Ar), 132.3 (C), 132.6 (CH *tz*), 140.5 (CH *im*).

ESI-MS (positive-ions, CH_3CN): m/z 178.11 (100 %, $[\text{M}-2\text{BF}_4\text{-Bn}]^+$), 268.16 (80 %, $[\text{M}-2\text{BF}_4\text{-H}]^+$) 356.17 (30 %, $[\text{M}-\text{BF}_4]^+$).

7.3.8 *Synthesis of the silver(I) complex 12*

Proligand **i** (0.10 g, 0.27 mmol) and Ag_2O (0.17 g, 0.72 mmol) were placed in a two neck round bottom flask. Subsequently, CHCl_3 (10 mL) was added and the reaction

mixture was left under stirring for 2 hours at 45 °C. Afterwards, it was filtered on Celite and the filtrate was concentrated at low pressure; addition of diethyl ether (20 mL) affords the product as a yellow solid, that was filtered and dried under vacuum (yield 62 %).

Anal. Calcd for $C_{14}H_{15}N_5AgCl$: C, 42.40; H, 3.81; N, 17.66 %. Found: C, 42.22; H, 3.85; N, 17.36 %.

1H -NMR ($CDCl_3$, 300 MHz) δ = 3.82 (s, 3H, CH_3), 3.95 (s, 3H, CH_3), 5.60 (s, 2H, CH_2), 7.17 (s, 1H, CH), 7.34 (m, 2H, CH Ar), 7.40 (m, 3H, CH Ar), 7.58 (s, 1H, CH *tz*).
 $^{13}C\{^1H\}$ -NMR ($CDCl_3$, 75 MHz): δ = 38.2 (CH_3), 38.9 (CH_3), 54.5 (CH_2), 120.9 (CH), 122.1 (CH *tz*), 126.1 (C), 128.3 (CH Ar), 129.1 (CH Ar), 129.3 (CH Ar), 134.0 (C Ar), 136.3 (C), 182.0 (CAg).

ESI-MS (positive-ions, $CHCl_3$): m/z 613.13 (100 %, $[AgL_2]^+$) with L = NHC.

Crystals of complex **12** were obtained by slow diffusion of diethyl ether into a solution of the complex in chloroform.

7.3.9 Synthesis of the silver(I) complex 13

Proligand **1** (0.069 g, 0.12 mmol) and Ag_2O (0.072 g, 0.31 mmol) were placed in a two neck round bottom flask. Subsequently, CH_3CN (10 mL) was added and the reaction mixture was left under stirring for 24 hours at 50 °C. Afterwards, it was filtered on Celite and the filtrate was concentrated at low pressure; addition of diethyl ether (15 mL) affords the product as a brown oil. The solution was removed with a syringe and the oil dried under vacuum and analyzed without further purifications.

1H -NMR (CD_3CN , 300 MHz) δ = 3.63 (s, 3H, CH_3), 3.68 (s, 3H, CH_3), 4.06 (s, 3H, CH_3), 5.75 (s, 2H, CH_2), 7.39 (m, 5H, CH Ar), 7.50 (s, 1H, CH).

$^{13}C\{^1H\}$ -NMR (CD_3CN , 75 MHz): δ = 38.2 (CH_3), 38.3 (CH_3), 39.4 (CH_3), 59.8 (CH_2), 121.8 (CH), 126.5 (C), 129.5 (CH Ar), 129.8 (CH Ar), 130.0 (CH Ar), 135.9 (C Ar), 137.5 (C), 168.6 (CAg *tz*NHC), 184.5 (CAg *n*NHC).

MALDI-TOF (Dithranol): 899.17 (50 %, $[Ag_2L_2OTf]^+$), 1049.09 (20 %, $[Ag_2L_2(OTf)_2H]^+$) with L = *n*NHC-*tz*NHC dicarbene ligand.

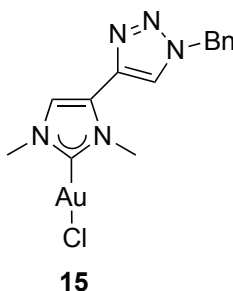
7.3.10 Synthesis of the silver(I) complex 14

Proligand **m** (0.23 g, 0.52 mmol) and Ag₂O (0.30 g, 1.30 mmol) were placed in a two neck round bottom flask. Subsequently, CH₃CN (20 mL) was added and the reaction mixture was left under stirring for 24 hours at 60 °C. Afterwards, it was filtered on Celite and the filtrate was evaporated to dryness, giving a dark brown solid, which was analyzed without further purifications.

¹H-NMR (CD₃CN, 300 MHz) δ = 3.59 (s, 3H, CH₃), 3.69 (s, 3H, CH₃), 4.03 (s, 3H, CH₃), 5.73 (s, 2H, CH₂), 7.39 (m, 5H, CH Ar), 7.47 (s, 1H, CH).

¹³C{¹H}-NMR (CD₃CN, 75 MHz): δ = 38.0 (CH₃), 38.3 (CH₃), 39.5 (CH₃), 59.8 (CH₂), 121.8 (CH), 126.5 (C), 129.3 (CH Ar), 129.8 (CH Ar), 130.0 (CH Ar), 135.8 (C Ar), 137.4 (C), 168.3 (CAg *tz*NHC), 184.2 (CAg *n*NHC).

7.3.11 Synthesis of the gold(I) complex 15



A solution of AuCl(SMe₂) (0.041 g, 0.14 mmol) in chloroform (5 mL) was added to a solution of silver(I) complex **12** (0.052 g, 0.13 mmol) in the same solvent (10 mL). The reaction mixture was left under stirring for 2 hours at room temperature; afterwards, it was filtered on Celite and the filtrate was concentrated at low pressure. Addition of diethyl ether (30 mL) affords the product as a white solid. The solvent was decanted and removed with a syringe and the solid was dried under vacuo (yield 51 %).

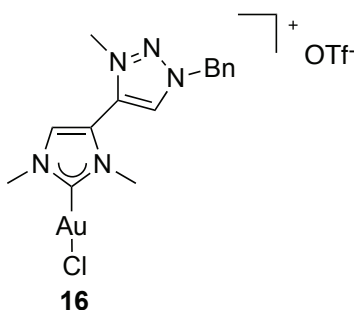
Anal. Calcd for C₁₄H₁₅N₅AuCl: C, 34.62; H, 3.11; N, 14.42 %. Found: C, 35.72; H, 3.43; N, 14.29 %.

¹H-NMR (CDCl₃, 300 MHz) δ = 3.83 (s, 3H, CH₃), 3.97 (s, 3H, CH₃), 5.60 (s, 2H, CH₂), 7.14 (s, 1H, CH), 7.35 (m, 2H, CH Ar), 7.46 (m, 3H, CH Ar), 7.64 (s, 1H, CH *tz*).

$^{13}\text{C}\{^1\text{H}\}$ -NMR (CDCl_3 , 75 MHz): $\delta = 37.3$ (CH_3), 38.4 (CH_3), 54.6 (CH_2), 120.2 (CH), 121.9 (CH tz), 125.4 (C) 128.3 (CH Ar), 129.2 (CH Ar), 129.4 (CH Ar), 133.8 (C Ar), 136.1 (C), 173.2 (CAu).

HR-MS (positive-ions, CHCl_3): m/z calcd for $\text{C}_{14}\text{H}_{16}\text{N}_5$ (80 %, $[\text{L}]^+$) 254.1406, found 254.1387, m/z calcd for $\text{C}_{16}\text{H}_{18}\text{N}_6\text{Au}$ (100 %, $[\text{AuL}(\text{CH}_3\text{CN})]^+$) 491.1259, found 491.1280, m/z calcd for $\text{C}_{16}\text{H}_{19}\text{AuClNa}$ (10 %, $[\text{AuClL}(\text{CH}_3\text{CN})\text{Na}]^+$) 549.0822, found 549.0839 with $\text{L} = \text{NHC}$.

7.3.12 Synthesis of gold(I) complex 16 via post-methylation of complex 15 and conversion to complex 17



Gold(I) complex **15** (0.0054 g, 0.011 mmol) was dissolved in CDCl_3 (1 mL) and MeOTf (4.0 μL , 0.036 mmol) was added. The mixture was left in the NMR tube for 3 days, observing the progressive formation of crystals; after this period, the NMR spectra of the solution showed only the signals associable to the deuterated solvent. Therefore CDCl_3 was removed, the crystals were dried at low pressure and redissolved in CD_3CN .

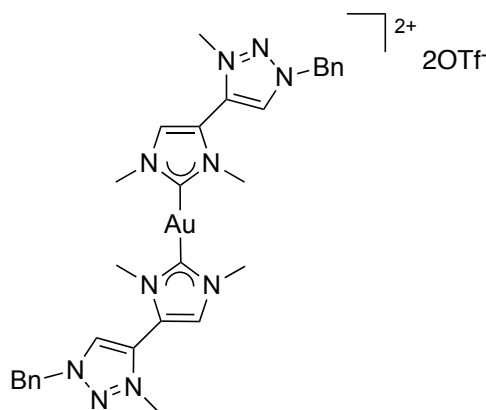
^1H -NMR (CD_3CN , 300 MHz) $\delta = 3.73$ (s, 3H, CH_3), 3.87 (s, 3H, CH_3), 4.12 (s, 3H, CH_3), 5.78 (s, 2H, CH_2), 7.50 (m, 5H, CH Ar), 7.62 (s, 1H, CH), 8.61 (s, 1H, CH tz).

$^{13}\text{C}\{^1\text{H}\}$ -NMR (CD_3CN , 75 MHz): $\delta = 37.6$ (CH_3), 39.4 (CH_3), 39.7 (CH_3), 58.5 (CH_2), 127.9 (CH), 128.6 (C) 130.2 (CH Ar), 130.3 (CH Ar), 130.7 (CH Ar), 131.8 (CH tz), 132.6 (C Ar), 132.8 (C), 175.8 (CAu).

ESI-MS (positive-ions, CHCl_3): m/z 500.00 (100 %, $[\text{AuLCl}]^+$), 1148.87 (70 %, $[\text{Au}_2\text{L}_2\text{ClOTf}]^+$) with $\text{L} = \text{NHC}$ ligand.

Complex **16** evolves in solution, as demonstrated by the NMR spectra registered after 72 hours in which a new set of signal appears. The new set of signals is associable to

complex **17** and its formation can be accelerated by the addition of Ag_2O (3 eq.) and heating the solution at $60\text{ }^\circ\text{C}$ for eight hours.

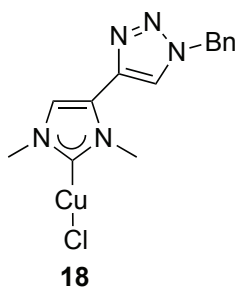
**17**

$^1\text{H-NMR}$ (CD_3CN , 300 MHz) $\delta = 3.82$ (s, 3H, CH_3), 3.97 (s, 3H, CH_3), 4.16 (s, 3H, CH_3), 5.82 (s, 2H, CH_2), 7.50 (m, 5H, CH Ar), 7.74 (s, 1H, CH), 8.72 (s, 1H, CH *tz*).

$^{13}\text{C}\{^1\text{H}\}$ -NMR (CD_3CN , 75 MHz): $\delta = 37.3$ (CH_3), 39.2 (CH_3), 39.6 (CH_3), 58.4 (CH_2), 128.4 (CH), 129.9 (C) 130.2 (CH Ar), 130.4 (CH Ar), 130.8 (CH Ar), 131.8 (CH *tz*), 132.2 (C Ar), 132.6 (C), 188.6 (CAu).

ESI-MS (positive-ions, CHCl_3): m/z 791.08 (20 %, $[\text{AuL}_2\text{ClNa}]^+$, 1031.05 (100 %, $[\text{AuL}_2(\text{OTf})_2]^+$) with L = NHC.

7.3.13 Synthesis of copper(I) complex **18**

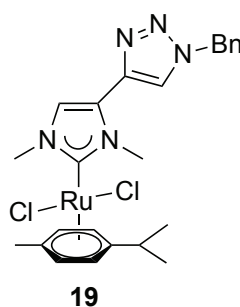
**18**

A solution of CuI (0.018 g, 0.088 mmol) in chloroform (5 mL) was added to a solution of the silver(I) complex **12** (0.031 g, 0.077 mmol) in the same solvent (5 mL). The reaction mixture was left under stirring for 1 hour at room temperature; afterwards, it was filtered on Celite and the filtrate was concentrated at low pressure. Addition of diethyl ether (30 mL) affords the product as a white solid. The solvent was removed with a syringe and the solid was dried (yield 51 %). The copper complex is not stable and tends to evolve both in solution and in the solid state, as evidenced by the darkening

of the solid with time and by the appearance of a brown/dark precipitate from the NMR solutions.

$^1\text{H-NMR}$ (CDCl_3 , 300 MHz) δ = 3.83 (s, 3H, CH_3), 3.97 (s, 3H, CH_3), 5.60 (s, 2H, CH_2), 7.14 (s, 1H, CH), 7.33 (m, 2H, CH Ar), 7.43 (m, 3H, CH Ar), 7.61 (s, 1H, CH *tz*). $^{13}\text{C}\{^1\text{H}\}$ -NMR (CDCl_3 , 75 MHz): δ = 37.8 (CH_3), 38.3 (CH_3), 54.0 (CH_2), 120.4 (CH), 121.7 (CH *tz*), 125.7 (C), 128.4 (CH Ar), 128.7 (CH Ar), 129.0 (CH Ar), 133.6 (C Ar), 136.6 (C), 179.8 (CCu).

7.3.14 Synthesis of ruthenium(II) complex 19



Silver(I) complex **12** (0.027 g, 0.068 mmol) and $[\text{RuCl}_2(p\text{-cymene})]_2$ (0.023 g, 0.038 mmol) were placed in a two neck round bottom flask. Subsequently, dry CH_2Cl_2 (5 mL) was added and the reaction mixture was left under stirring for 3 hours at 25 °C. Afterwards, it was filtered on Celite and the filtrate was concentrated at low pressure; addition of diethyl ether (15 mL) affords the product as a brown-orange solid, that was filtered and dried under vacuum (yield 61 %).

Anal. Calcd for $\text{C}_{24}\text{H}_{29}\text{N}_5\text{RuCl}_2 \cdot \text{CH}_2\text{Cl}_2$: C, 46.59; H, 4.85; N, 10.87 %. Found: C, 46.02; H, 4.67; N, 10.78 %.

$^1\text{H-NMR}$ (CDCl_3 , 300 MHz) δ = 1.27 (d, $^3J_{\text{HH}} = 6.9$ Hz, 6H, $\text{CH}(\text{CH}_3)_2$), 2.08 (s, 3H, CH_3 *p*-cym), 2.96 (heptet, 1H, $\text{CH}(\text{CH}_3)_2$), 3.94 (s, 3H, NCH_3), 3.97 (s, 3H, NCH_3), 5.13 (d, $^3J_{\text{HH}} = 6.0$ Hz, 2H, CH Ar *p*-cymene), 5.42 (d, $^3J_{\text{HH}} = 6.0$ Hz, 2H, CH Ar *p*-cymene), 5.59 (s, 2H, CH_2), 7.21 (s, 1H, CH), 7.30 (m, 5H, CH Ar), 7.68 (s, 1H, CH *tz*). $^{13}\text{C}\{^1\text{H}\}$ -NMR (CDCl_3 , 75 MHz): δ = 18.8 ($\text{CH}(\text{CH}_3)_2$), 22.5 (CH_3 *p*-cym), 31.0 ($\text{CH}(\text{CH}_3)_2$), 38.2 (NCH_3), 39.7 (NCH_3), 54.5 (CH_2), 82.2 (CH *p*-cym), 85.4 (CH *p*-cym), 99.0 (C *p*-cym), 109.5 (C *p*-cym), 122.8 (CH *tz*), 123.3 (CH), 126.9 (C), 128.2 (CH Ar), 129.1 (CH Ar), 129.3 (CH Ar), 134.6 (C Ar) 136.7 (C), 175.7 (CRu).

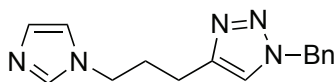
HR-MS (positive-ions, CHCl₃): *m/z* calcd for C₂₄H₂₉N₅ClRu (100 %, [RuCl(L)(*p*-cym)]⁺ with L = NHC) 524.1153, found 542.1148.

7.3.15 X-ray crystal structure details of complexes 12 and 15

	12	15
Formula	C ₁₄ H ₁₅ AgClN ₅	C ₁₄ H ₁₅ AuClN ₅
Molecular weight	396.63	485.73
Crystal system	Monoclinic	triclinic
Space group	P 2 ₁ /c	P -1
<i>a</i> /Å	14.1778(10)	6.1232(3)
<i>b</i> /Å	8.6340(3)	9.0459(5)
<i>c</i> /Å	13.6404(10)	14.7389(7)
α /°	90	99.134(4)
β /°	114.866(2)	99.238(4)
γ /°	90	97.041(4)
Volume, Å ³	1514.70(16)	786.34(7)
T/K	173.2	296.9(8)
<i>Z</i>	4	2
D _{calc} /g cm ⁻³	1.739	2.051
F(000)	792	460
μ (Mo-K)/mm ⁻¹	1.507	19.145
Reflection collected	8619	7079
Unique reflection	3470 [R _{int} = 0.0724]	3118 [R _{int} = 0.0331]
Observed reflection [<i>I</i> > 2 σ (<i>I</i>)]	2424	2843
Final R index [<i>I</i> > 2 σ (<i>I</i>)]	R1 = 0.0756, wR2 = 0.1261	R1 = 0.0401, wR2 = 0.0765
Final R index [all data]	R1 = 0.0874, wR2 = 0.1507	R1 = 0.0346, wR2 = 0.0794
CCDC number		
$R1 = \sum F_o - F_c / \sum (F_o)$ $wR2 = [\sum [w(F_o^2 - F_c^2)^2] / \sum [w(F_o^2)^2]]^{1/2}$		

7.4 Metal complexes with heteroditopic ligands based on imidazol-2-ylidene and 1,2,3-triazol-5-ylidene moieties connected with a propylene bridge

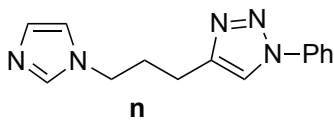
7.4.1 Synthesis of 4-[3-(1H-imidazol-1-yl)propyl]-1-benzyl-1H-1,2,3-triazole



The compound has been synthesized according to the literature.¹³⁷

Yield 78 %. ¹H-NMR (CDCl₃, 300 MHz) δ = 2.22 (s br, 2H, CH₂), 2.65 (s br, 2H, CH₂), 4.08 (s br, 2H, CH₂), 5.49 (s, 2H, CH₂), 7.30 – 7.40 (m, 9H, CH + CH Ar + CH *tz* + CH *im*).

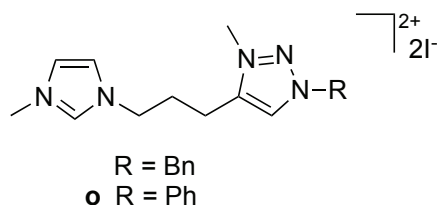
7.4.2 Synthesis of 4-[3-(1H-Imidazol-1-yl)propyl]-1-phenyl-1H-1,2,3-triazole *n*



1-(pent-4-ynyl)-1H-imidazole (0.30 g, 2.25 mmol), sodium-L-ascorbate (0.24 g, 1.18 mmol) and copper(II) sulfate pentahydrate (0.29 g, 1.16 mmol) were placed in a two neck round bottom flask. Subsequently, MeOH (10 mL) and a solution of phenyl azide (0.5 M in tert-butyl-methyl-ether, 4.5 mL, 2.25 mmol) were added and the reaction mixture was left under stirring for 72 hours at 25 °C. Afterwards, methanol was removed under vacuum; the residue was dissolved in CH₂Cl₂ (50 mL) and washed with water (3 × 50 mL). The organic phase was dried with Na₂SO₄ and the solvent was then removed in order to obtain the desired compound as a yellow oil, that was further washed with diethyl ether (3 × 5 mL) (yield 33 %).

¹H-NMR (CDCl₃, 300 MHz) δ = 2.30 (s br, 2H, CH₂), 2.65 (s br, 2H, CH₂), 4.10 (s br, 2H, CH₂), 7.26 – 7.42 (m, 9H, CH + CH Ar + CH *tz* + CH *im*).

7.4.3 Synthesis of 3-(benzyl)-1-methyl-5-[3-(3-methyl-1H-imidazol-3-ium-1-yl)propyl]-3H-1,2,3-triazol-1-ium diiodide and 3-(phenyl)-1-methyl-5-[3-(3-methyl-1H-imidazol-3-ium-1-yl)propyl]-3H-1,2,3-triazol-1-ium diiodide o



The compound 3-(benzyl)-1-methyl-5-[3-(3-methyl-1H-imidazol-3-ium-1-yl)propyl]-3H-1,2,3-triazol-1-ium diiodide was synthesized according to the literature.¹³⁷

Brown solid, yield 90 %. ¹H-NMR (CDCl₃, 300 MHz) $\delta = 2.64$ (t, ³J_{HH} = 7.5 Hz, 2H, CH₂), 3.35 (t, ³J_{HH} = 7.5 Hz, 2H, CH₂), 3.99 (s, 3H, CH₃), 4.43 (s, 3H, CH₃), 4.77 (t, ³J_{HH} = 7.5 Hz, 2H, CH₂), 5.76 (s, 2H, CH₂), 7.43 (m, 3H, CH Ar), 7.54 (m, 2H, CH Ar), 8.16 (s, 2H, CH), 9.41 (s, 1H, CH *tz*), 9.93 (s, 1H, CH *im*).

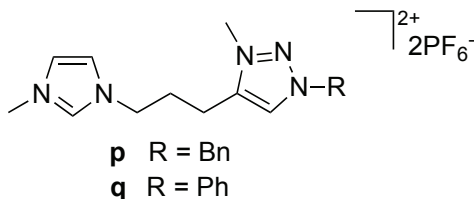
In analogy with the literature¹³⁷ CH₃I (4.80 mmol) was added to a solution of 4-[3-(1H-imidazol-1-yl)propyl]-1-(phenyl)-1H-1,2,3-triazole **n** (0.45 mmol) in CH₃CN (5 mL). The reaction mixture was kept under stirring for 18 hours under reflux, obtaining an orange solution. The solvent was removed under vacuum and the orange oil was washed with diethyl ether and dried in order to obtain a solid.

o.

Orange/brown solid, yield 82 %. ¹H-NMR (CD₃CN, 300 MHz) $\delta = 2.50$ (t, ³J_{HH} = 7.5 Hz, 2H, CH₂), 3.13 (t, ³J_{HH} = 7.5 Hz, 2H, CH₂), 3.89 (s, 3H, CH₃), 4.44 (s, 3H, CH₃), 4.48 (t, ³J_{HH} = 7.5 Hz, 2H, CH₂), 7.45 (s, 1H, CH), 7.69 (m, 3H, CH Ar), 7.76 (s, 1H, CH), 7.99 (m, 2H, CH Ar), 9.24 (CH *tz*), 9.44 (CH *im*).

¹³C{¹H}-NMR (CD₃CN, 75 MHz): $\delta = 14.9$ (CH₂), 20.4 (CH₂), 36.4 (CH₃), 39.0 (CH₃), 48.3 (CH₂), 122.3 (CH), 123.9 (CH), 128.2 (CH *tz*), 129.2 (CH Ar), 129.3 (CH Ar), 129.7 (CH Ar), 132.1 (C Ar), 136.3 (CH *im*), 144.0 (C).

7.4.4 General synthesis of 3-(substituted)-1-methyl-5-[3-(3-methyl-1*H*-imidazol-3-ium-1-yl)propyl]-3*H*-1,2,3-triazol-1-ium bis(hexafluorophosphate) *p* and *q*



A solution of KPF_6 (1.96 mmol) in H_2O (3 mL) was added to a solution of 3-(substituted)-1-methyl-5-[3-(3-methyl-1*H*-imidazol-3-ium-1-yl)propyl]-3*H*-1,2,3-triazol-1-ium diiodide (0.37 mmol) in MeOH (3 mL). The mixture was stirred for 24 hours at room temperature, giving a solid that was filtered and dried under vacuum.

p.

Light brown solid, yield 100 %. $^1\text{H-NMR}$ (CD_3CN , 300 MHz) δ = 2.17 (t, $^3J_{\text{HH}} = 7.5$ Hz, 2H, CH_2), 2.78 (t, $^3J_{\text{HH}} = 7.5$ Hz, 2H, CH_2), 3.84 (s, 3H, CH_3), 4.10 (s, 3H, CH_3), 4.21, (t, $^3J_{\text{HH}} = 7.5$ Hz, 2H, CH_2), 5.68 (s, 2H, CH_2), 7.36 (s, 1H, CH), 7.39 (s, 1H, CH), 7.46 (s, 5H, CH Ar), 8.17 (s, 1H, CH *tz*), 8.43 (s, 1H, CH *im*).

$^{13}\text{C}\{^1\text{H}\}$ -NMR (CD_3CN , 75 MHz): δ = 19.8 (CH_2), 29.9 (CH_2), 36.0 (CH_3), 37.7 (CH_3), 48.1 (CH_2), 56.9 (CH_2), 122.3 (CH), 123.9 (CH), 128.2 (CH *tz*), 129.2 (CH Ar), 129.3 (CH Ar), 129.7 (CH Ar), 132.1 (C Ar), 136.3 (CH *im*), 143.4 (C).

$^{31}\text{P}\{^1\text{H}\}$ -NMR (CD_3CN , 121 MHz): δ = -144.6 (heptet, PF_6).

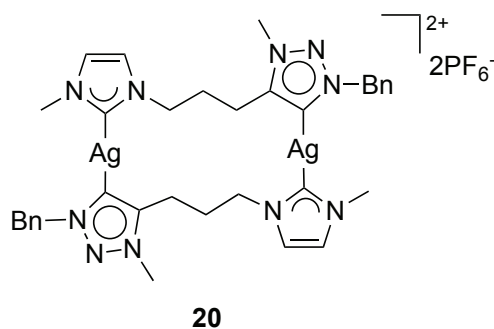
q.

Off-white solid, yield 81 %. $^1\text{H-NMR}$ (CD_3CN , 300 MHz) δ = 2.31 (t, $^3J_{\text{HH}} = 7.5$ Hz, 2H, CH_2), 2.93 (t, $^3J_{\text{HH}} = 7.5$ Hz, 2H, CH_2), 3.86 (s, 3H, CH_3), 4.24 (s, 3H, CH_3), 4.29 (t, $^3J_{\text{HH}} = 7.5$ Hz, 2H, CH_2), 7.39 (s br, 1H, CH), 7.46 (s br, 1H, CH), 7.72 (m, 3H, CH Ar), 7.84 (m, 2H, CH Ar), 8.54 (s, 1H, CH *tz*), 8.74 (s, 1H, CH *im*).

$^{13}\text{C}\{^1\text{H}\}$ -NMR (CD_3CN , 75 MHz): δ = 19.8 (CH_2), 26.9 (CH_2), 36.0 (CH_3), 38.0 (CH_3), 48.1 (CH_2), 121.6 (CH), 122.3 (CH), 124.0 (CH *tz*), 126.7 (CH Ar), 130.5 (CH Ar), 132.0 (CH Ar), 135.0 (C Ar), 136.3 (CH *im*), 144.0 (C).

$^{31}\text{P}\{^1\text{H}\}$ -NMR (CD_3CN , 121 MHz): δ = -144.7 (heptet, PF_6).

7.4.5 Synthesis of silver(I) complex 20



Proligand **p** (0.10 g, 0.17 mmol) and Ag₂O (0.20 g, 0.87 mmol) were placed in a two neck round bottom flask. Subsequently, CH₃CN (15 mL) was added and the reaction mixture was left under stirring for 48 hours at 85 °C. Afterwards, it was filtered on Celite and the solvent was removed in order to obtain an oil.

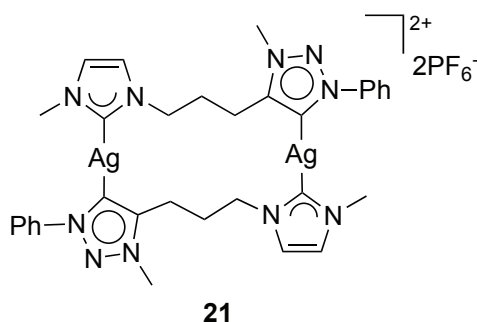
Due to the oily nature of the product it was not possible to correctly estimate the yield.

¹H-NMR (CD₃CN, 300 MHz) δ = 2.39 (t, ³J_{HH} = 6.6 Hz, 2H, CH₂), 2.77 (t, ³J_{HH} = 6.6 Hz, 2H, CH₂), 3.51 (s, 3H, CH₃), 4.07 (s, 3H, CH₃), 4.11 (m, 2H, CH₂), 5.40 (s, 2H, CH₂), 7.23 (m, 6H, CH + CH Ar), 7.45 (s, 1H, CH).

¹³C{¹H}-NMR (CD₃CN, 75 MHz): δ = 22.1 (CH₂), 29.2 (CH₂), 37.1 (CH₃), 38.8 (CH₃), 50.5 (CH₂), 59.6 (CH₂), 121.8 (CH), 124.2 (CH), 128.9 (CH Ar), 129.6 (CH Ar), 129.8 (CH Ar), 135.9 (C Ar), 148.5 (C), 164.18 (CAg *tz*NHC), 182.1 (CAg *n*NHC). Traces of acetic acid are present (as indicated by the signals at ca. 20 and 173 ppm) probably due to the hydrolysis of the acetonitrile solvent.

HR-MS (positive-ions, CD₃CN): *m/z* calcd for C₁₇H₂₁AgN₅ (25 %, [AgL]⁺) 402.0842, found 402.0958, *m/z* calcd for C₃₄H₄₂Ag₂F₆N₁₀P (100 %, [Ag₂L₂PF₆]⁺) 951.1331, found 951.1356; with L = *n*NHC-*tz*NHC dicarbene ligand.

7.4.6 Synthesis of silver(I) complex 21

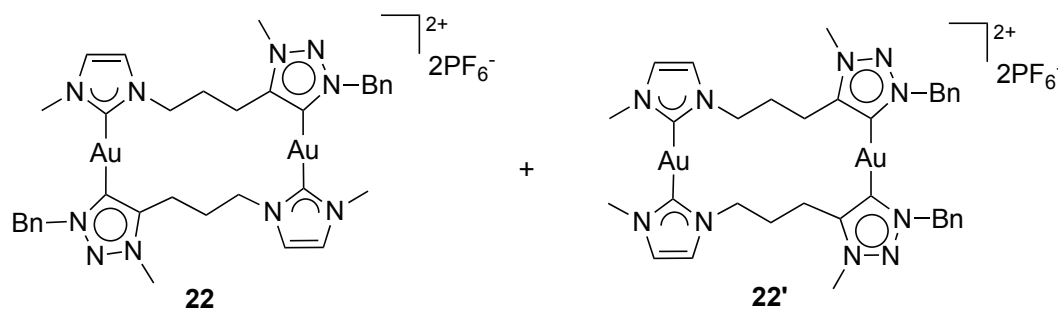


Proligand **q** (0.051 g, 0.089 mmol) and Ag₂O (0.12 g, 0.50 mmol) were placed in a two neck round bottom flask. Subsequently, CH₃CN (7 mL) was added and the reaction mixture was left under stirring for 48 hours at 85 °C. Afterwards, it was filtered on Celite and the filtrate was concentrated at low pressure; addition of diethyl ether (20 mL) affords the formation of an off-white solid, that was filtered and dried under vacuum (yield 78 %).

¹H-NMR (CD₃CN, 300 MHz) δ = 2.39 (m, 2H, CH₂), 2.82 (m, 2H, CH₂), 3.39 (s, 3H, CH₃), 4.11 (t, ³J_{HH} = 6.6 Hz, 2H, CH₂), 4.17 (s, 3H, CH₃), 7.06 (s, 1H, CH), 7.20 (s, 1H, CH), 7.42, (m, 3H, CH Ar), 7.64 (m, 2H, CH Ar).

¹³C{¹H}-NMR (CD₃CN, 75 MHz): δ = 20.9 (CH₂), 27.4 (CH₂), 36.5 (CH₃), 37.7 (CH₃), 49.1 (CH₂), 120.35 (CH), 122.8 (CH), 123.6 (CH Ar), 129.6 (CH Ar), 130.3 (CH Ar), 139.8 (C Ar), 147.2 (C), 167.0 (CAg *tz*NHC), 180.0 (CAg *n*NHC).

HR-MS (positive-ions, CD₃CN): *m/z* calcd for C₃₂H₃₈Ag₂F₆N₁₀P (100 %, [Ag₂L₂PF₆]⁺) 923.1021, found 923.1026; with L = *n*NHC-*tz*NHC dicarbene ligand.

7.4.7 Synthesis of gold(I) complexes **22** and **22'**

Due to the oily nature of the silver(I) complex **20** its instability both in solid state and solution, we decided to not isolate it but to carry out directly the transmetalation reaction with the gold(I) precursor.

Proligand **p** (0.049 g, 0.086 mmol) and Ag₂O (0.10 g, 0.44 mmol) were placed in a two neck round bottom flask. Subsequently, CH₃CN (10 mL) was added and the reaction mixture was left under stirring for 48 hours at 85 °C. Afterwards, it was filtered on Celite and a solution of AuCl(SMe₂) (0.026 g, 0.088 mmol) in acetonitrile (5 mL) was added. The reaction mixture was left under stirring for 3 hours at room temperature; afterwards, it was filtered on Celite and the solvent was removed under vacuum in order to obtain an oil. Recrystallization by CH₃CN/Et₂O affords the product as an off-white solid (global yield 78 %).

ESI-MS (positive-ions, CH₃CN): *m/z* 1129.27 [100 %, Au₂L₂PF₆]⁺; with L = *n*NHC-*tz*NHC dicarbene ligand.

The ¹H-NMR spectra show two set of signals, attributable to the complexes **22** and **22'**, in a 1:1 ratio.

22.

¹H-NMR (CD₃CN, 600 MHz,) δ = 2.55 (m, 2H, CH₂), 2.89 (m, 2H, CH₂), 3.42 (s, 3H, CH₃), 4.10 (s, 3H, CH₃), 4.22 (m, 2H, CH₂), 5.44 (s, 2H, CH₂), 7.13 (s, 1H, CH), 7.29 (s, 1H, CH), 7.38 (m, 5H, CH Ar).

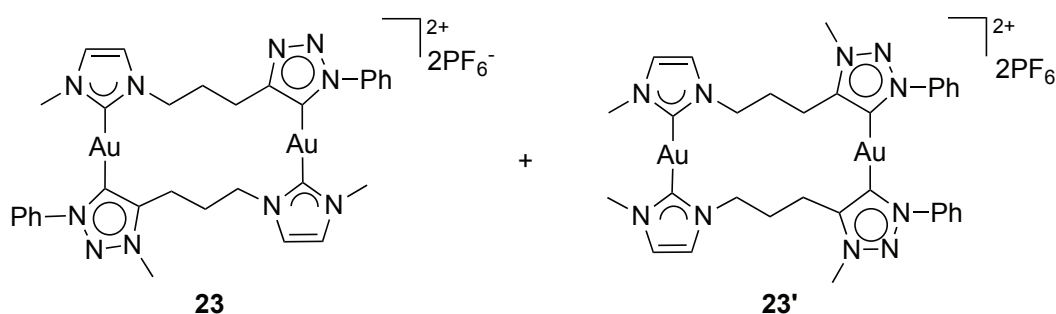
¹³C{¹H}-NMR (CD₃CN, 150 MHz): δ = 20.5 (CH₂), 26.2 (CH₂), 36.4 (CH₃), 36.7 (CH₃), 48.5.2 (CH₂), 57.9 (CH₂), 120.2 (CH), 123.4 (CH), 128.1 (CH Ar), 128.7 (CH Ar), 128.9 (CH Ar), 135.0 (C Ar), 148.2 (C), 170.1 (CAu *tz*NHC), 185.9 (CAu *n*NHC).

22'.

$^1\text{H-NMR}$ (CD_3CN , 600 MHz,) $\delta = 2.52$ (m, 2H, CH_2), 2.89 (m, 2H, CH_2), 3.62 (s, 3H, CH_3), 4.06 (s, 3H, CH_3), 4.26 (m, 2H, CH_2), 5.32 (s, 2H, CH_2), 7.24 (s, 1H, CH), 7.33 (s, 1H, CH), 7.38 (m, 5H, CH Ar).

$^{13}\text{C}\{^1\text{H}\}\text{-NMR}$ (CD_3CN , 150 MHz): $\delta = 21.2$ (CH_2), 27.8 (CH_2), 36.9 (CH_3), 37.3 (CH_3), 49.2 (CH_2), 58.2 (CH_2), 120.9 (CH), 123.7 (CH), 127.6 (CH Ar), 128.8 (CH Ar), 128.9 (CH Ar), 134.5 (C Ar), 146.9 (C), 169.0 (CAu *tz*NHC), 183.5 (CAu *n*NHC).

7.4.8 Synthesis of gold(I) complexes **23** and **23'**



A solution of $\text{AuCl}(\text{SMe}_2)$ (0.033 g, 0.113 mmol) in acetonitrile (5 mL) was added to a solution of silver(I) complex **21** (0.060 g, 0.0561 mmol) in the same solvent (5 mL). The reaction mixture was left under stirring for 3 hours at room temperature; afterwards, it was filtered on Celite and the solvent was removed under vacuum in order to obtain a white solid (yield 75 %).

Anal. Calcd for $\text{C}_{32}\text{H}_{38}\text{N}_{10}\text{Au}_2\text{P}_2\text{F}_{12}$: C, 30.83; H, 3.07; N, 11.24 %. Found: C, 30.40; H, 3.15; N, 10.86 %.

ESI-MS (positive-ions, CH_3CN): m/z 1101.23 [100 %, $\text{Au}_2\text{L}_2\text{PF}_6$] $^+$. L = *n*NHC-*tz*NHC dicarbene ligand.

The $^1\text{H-NMR}$ spectra show two set of signals, attributable to the complexes **23** and **23'**, in a 1:1 ratio.

23.

$^1\text{H-NMR}$ (CD_3CN , 400 MHz) $\delta = 2.35$ (m, 2H, CH_2), 2.83 (m, 2H, CH_2), 3.46 (s, 3H, CH_3), 4.16 (m, 2H, CH_2), 4.18 (s, 3H, CH_3), 7.00 (d, $^3J_{\text{HH}} = 2.0$ Hz, 1H, CH), 7.18 (d,

$^3J_{HH} = 2.0$ Hz, 1H, CH), 7.45 (m, 2H, CH Ar), 7.57 (m, 1H, CH Ar), 7.70 (m, 2H, CH Ar).

$^{13}\text{C}\{^1\text{H}\}$ -NMR (CD_3CN , 100 MHz): $\delta = 21.3$ (CH_2), 27.2 (CH_2), 37.6 (CH_3), 37.8 (CH_3), 48.9 (CH_2), 120.7 (CH) 123.9 (CH), 124.2 (CH Ar), 130.1 (CH Ar), 131.1 (CH Ar), 139.6 (C Ar), 147.0 (C), 169.3 (CAu *tz*NHC), 183.6 (CAu *n*NHC).

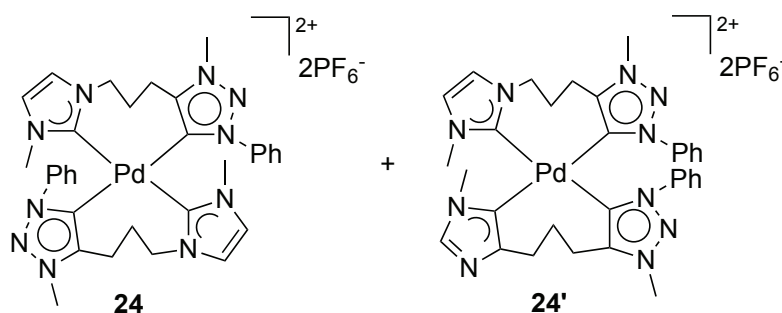
Crystals of complex **23** were obtained by slow diffusion of diethyl ether into a solution of the complexes **23** and **23'** in acetonitrile.

23'

^1H -NMR (CD_3CN , 400 MHz) $\delta = 2.65$ (m, 2H, CH_2), 2.97 (m, 2H, CH_2), 3.34 (s, 3H, CH_3), 4.16 (m, 2H, CH_2), 4.19 (s, 3H, CH_3), 7.13 (d, $^3J_{HH} = 2.0$ Hz, 1H, CH), 7.27 (d, $^3J_{HH} = 2.0$ Hz, 1H, CH), 7.47 (m, 2H, CH Ar), 7.54 (m, 1H, CH Ar), 7.70 (m, 2H, CH Ar).

$^{13}\text{C}\{^1\text{H}\}$ -NMR (CD_3CN , 100 MHz): $\delta = 22.0$ (CH_2), 27.5 (CH_2), 37.7 (CH_3), 37.8 (CH_3), 49.6 (CH_2), 120.9 (CH), 124.0 (CH), 124.4 (CH Ar), 130.3 (CH Ar), 131.2 (CH Ar), 139.6 (C Ar), 147.7 (C), 169.3 (CAu *tz*NHC), 184.3 (CAu *n*NHC).

7.4.9 Synthesis of palladium(II) complexes **24** and **24'**



A solution of $[\text{PdCl}_2\text{COD}]$ (0.014 g, 0.049 mmol) in acetonitrile (5 mL) was added to a solution of silver(I) complex **21** (0.0519 g, 0.0486 mmol) in the same solvent (5 mL). The reaction mixture was left under stirring for 3 hours at room temperature; afterwards, it was filtered on Celite and the solvent was removed under vacuum, giving a white solid (yield 74 %).

HR-MS (positive-ions, CD_3CN): m/z calcd for $\text{C}_{32}\text{H}_{38}\text{N}_{10}\text{PdPF}_6$ (100 %, $[\text{PdL}_2\text{PF}_6]^+$) 813.1957, found 813.2056. L = *n*NHC-*tz*NHC dicarbene ligand.

The ^1H -NMR spectrum shows two set of signals, attributable to the complexes **24** and **24'**, in a 3:2 ratio.

24.

^1H -NMR (CD_3CN , 400 MHz) δ = 2.35 (m, 2H, CH_2), 2.89 (m, 2H, CH_2), 3.73 (s, 3H, CH_3), 3.95 (s, 3H, CH_3), 4.24 (m, 2H, CH_2), 7.01 (d, $^3J_{\text{HH}} = 1.35$ Hz, 1H, CH), 7.04 (d, $^3J_{\text{HH}} = 1.35$ Hz, 1H, CH), 7.17 (m, 2H, CH Ar), 7.70 (m, 3H, CH Ar).

$^{13}\text{C}\{^1\text{H}\}$ -NMR (CD_3CN , 400 MHz): δ = 23.5 (CH_2), 25.7 (CH_2), 36.7 (CH_3), 39.0 (CH_3), 53.2 (CH_2), 123.6 (CH), 125.0 (CH), 126.7 (CH Ar), 130.6 (CH Ar), 131.7 (CH Ar), 140.7 (C Ar), 145.9 (C), 171.6 (CPd *n*NHC). (CPd *tz*NHC not detected).

Crystals of complex **24** were obtained by slow diffusion of diethyl ether into a solution of the complexes **24** and **24'** in acetonitrile.

24'.

^1H -NMR (CD_3CN , 400 MHz) δ = 2.89 (m, 2H, CH_2), 3.40 (m, 2H, CH_2), 3.72 (s, 3H, CH_3), 3.91 (s, 3H, CH_3), 4.14 (m, 2H, CH_2), 6.93 (d, $^3J_{\text{HH}} = 1.35$ Hz, 1H, CH), 7.03 (d, $^3J_{\text{HH}} = 1.35$ Hz, 1H, CH), 7.21 (m, 2H, CH Ar), 7.70 (m, 3H, CH Ar).

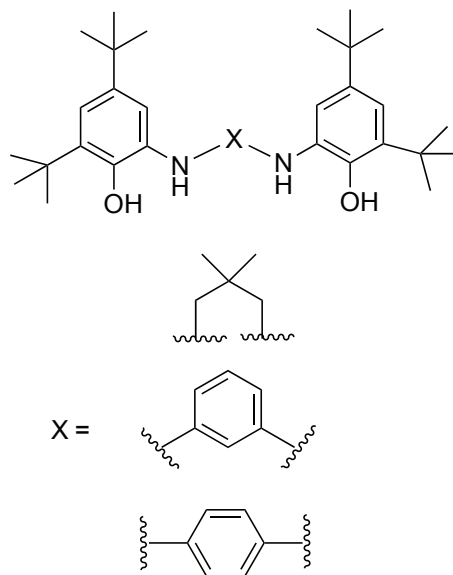
$^{13}\text{C}\{^1\text{H}\}$ -NMR (CD_3CN , 400 MHz): δ = 25.4 (CH_2), 27.0 (CH_2), 36.9 (CH_3), 38.9 (CH_3), 53.2 (CH_2), 123.7 (CH), 124.0 (CH), 126.8 (CH Ar), 130.7 (CH Ar), 131.8 (CH Ar), 140.6 (C Ar), 147.1 (C), 171.5 (CPd *n*NHC). (CPd *tz*NHC not detected).

7.4.10 X-ray crystal structure details of complex 23 and 24.

	23 · CH ₃ CN	24 · CH ₃ CN
Formula	C ₃₄ H ₄₁ Au ₂ F ₁₂ N ₁₁ P ₂	C ₃₆ H ₄₁ Au ₂ F ₁₂ N ₁₁ P ₂
Molecular weight	1287.65	1041.17
Crystal system	Monoclinic	Monoclinic
Space group	C 2/c	P 2 ₁ /c
<i>a</i> /Å	24.845(2)	11.917(3)
<i>b</i> /Å	14.7302(12)	12.117(3)
<i>c</i> /Å	24.302(2)	15.264(4)
α /°	90	90
β /°	105.8310(10)	97.905(5)
γ /°	90	90
Volume, Å ³	8556.8(12)	2183.0(10)
T/K	173.2	173(2)
Z	8	2
D _{calc} /g cm ⁻³	1.999	1.584
F(000)	4944	1056
μ (Mo-K)/mm ⁻¹	7.019	0.593
Reflection collected	55629	23253
Unique reflection	10024 [R _{int} = 0.0571]	3843 [R _{int} = 0.0618]
Observed reflection [<i>I</i> > 2 σ (<i>I</i>)]	8133	2915
Final R index [<i>I</i> > 2 σ (<i>I</i>)]	R1 = 0.0439, wR2 = 0.1106	R1 = 0.0408, wR2 = 0.1610
Final R index [all data]	R1 = 0.0704, wR2 = 0.1162	R1 = 0.0785, wR2 = 0.1814
CCDC number		
$R1 = \sum F_o - F_c / \sum (F_o)$ $wR2 = [\sum [w(F_o^2 - F_c^2)^2] / \sum [w(F_o^2)^2]]^{1/2}$		

7.5 bis(benzoxazole) proligands and attempts for the synthesis of transition metal complexes

7.5.1 Syntheses of the precursors *N,N'*-bis(3,5-di-*tert*-butyl-2-hydroxyphenyl)-(substituted)diamine



For the synthesis of the compounds with 2,2-dimethylpropyl bridge¹⁷⁰ and with the *meta*- and *para*-phenylene bridges¹⁷¹ the experimental procedures, already reported in the literature, have been adopted.

***N,N'*-bis(3,5-di-*tert*-butyl-2-hydroxyphenyl)-2,2-dimethylpropylenediamine.**

In a round bottom flask, 3,5-di-*tert*-butylcatechol (5.10 g, 22.9 mmol) and 2,2-dimethylpropylenediamine (1.11 g, 10.8 mmol) were dissolved in CH₃CN (30 mL) and the mixture was left under stirring at room temperature for 5 days; the formed white solid was filtered and washed with cold *n*-pentane (yield 72 %).

¹H-NMR (CDCl₃, 300 MHz) δ = 1.15 (s, 6H, CH₃), 1.31 (s, 18H, CH₃), 1.42 (s, 18H, CH₃), 2.99 (s, 4H, CH₂), 6.85 (s, 2H, CH), 6.98 (s, 2H, CH) (NH and OH not detected).

***N,N'*-bis(3,5-di-*tert*-butyl-2-hydroxyphenyl)-1,3-phenylenediamine.**

In a round bottom flask, 3,5-di-*tert*-butylcatechol (4.44 g, 20 mmol) and 1,3-phenylenediamine (1.08 g, 10 mmol) were dissolved in *n*-hexane (50 mL) and triethylamine (1.0

mL) was added. The mixture was left under stirring at reflux for 5 hours to obtain a an off white solid that was filtered and washed with cold *n*-pentane (yield 51 %).

¹H-NMR (CDCl₃, 300 MHz) δ = 1.25 (s, 18H, CH₃), 1.40 (s, 18H, CH₃), 4.93 (s, 2H, NH), 5.92 (s, 1H, CH Ar), 6.17 (d, ³J_{HH} = 9 Hz, 2H, CH Ar), 6.34 (s, 2H, OH) 7.03 (s, 3H, CH Ar), 7.20 (s, 2H, CH Ar).

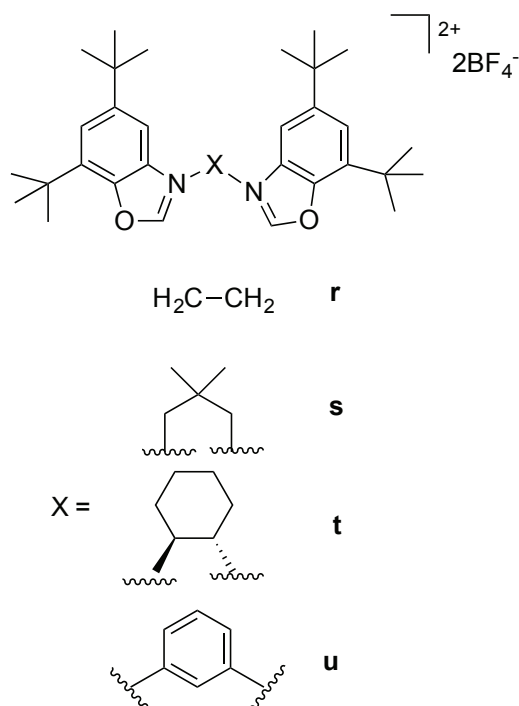
N,N'-bis(3,5-di-*tert*-butyl-2-hydroxyphenyl)-1,4-phenylenediamine.

Same procedure reported for compound N,N'-bis(3,5-di-*tert*-butyl-2-hydroxyphenyl)-1,3-phenylenediamine, but using 1,4-phenylenediamine obtaining a light brown solid (yield 84 %).

¹H-NMR (CDCl₃, 300 MHz) δ = 1.25 (s, 18H, CH₃), 1.41 (s, 18H, CH₃), 6.58 (s, 4H, CH Ar), 6.71 (d, ³J_{HH} = 2.1 Hz, 2H, CH Ar), 6.87 (d, ³J_{HH} = 9 Hz, 2H, CH Ar) (NH and OH not detected).

Compounds N,N'-bis(3,5-di-*tert*-butyl-2-hydroxyphenyl)ethylenediamine and N,N'-bis(3,5-di-*tert*-butyl-2-hydroxyphenyl)(1*S*,2*S*)cyclohexanediamine were already available in the laboratory and were used without any further purification.

7.5.2 Syntheses of N,N'-(substituted)bis(5,7-di-*tert*-butyl-3*H*-benzooxazol-1-ium) bis(tetrafluoroborate)



In a round bottom flask, the *N,N'*-bis(3,5-di-*tert*-butyl-2-hydroxyphenyl)-(substituted)diamine (0.96 mmol) was dissolved in methanol (50 mL) and a solution of HBF_4 (50 % in water) (2.41 mmol) was added. The mixture was left under stirring at room temperature for 30 minutes. The solvent was then removed and the residue was dissolved in $(\text{EtO})_3\text{CH}$ (50 mL); the mixture was stirred at room temperature for three days, giving a solid that was filtered and washed with cold *n*-pentane.

Attempts for the syntheses of the proligand *N,N'*-(1,4-phenylene)bis(5,7-di-*tert*-butyl-3*H*-benzooxazol-1-ium) bis(tetrafluoroborate) have been carried out, but without appreciable results, probably due to the decomposition of the precursor after the addition of the HBF_4 solution.

r.

Off-white solid, yield 100 %.

$^1\text{H-NMR}$ (CDCl_3 , 300 MHz) δ = 1.17 (s, 18H, CH_3), 1.49 (s, 18H, CH_3), 5.69 (s, 4H, CH_2), 7.42 (s, 2H, CH Ar), 7.55 (s, 2H, CH Ar), 10.1 (s, 2H, NCHO).

$^{13}\text{C}\{^1\text{H}\}$ -NMR (CDCl_3 , 75 MHz): δ = 29.8 (CH_3), 31.2 (CH_3), 34.9 (C), 35.8 (C), 46.3 (CH_2), 111.2 (CH Ar), 124.8 (CH Ar), 128.4 (C Ar), 137.8 (C Ar), 145.8 (C Ar), 153.8 (C Ar), 157.7 (NCHO).

$^1\text{H-NMR}$ (CD_3CN , 300 MHz) δ = 1.31 (s, 18H, CH_3), 1.52 (s, 18H, CH_3), 5.24 (s, 4H, CH_2), 7.57 (s, 2H, CH Ar), 7.77 (s, 2H, CH Ar), 9.75 (s, 2H, NCHO).

$^{13}\text{C}\{^1\text{H}\}$ -NMR (CD_3CN , 75 MHz): δ = 29.9 (CH_3), 31.5 (CH_3), 35.6 (C), 36.7 (C), 46.2 (CH_2), 109.4 (CH Ar), 126.4 (CH Ar), 129.6 (C Ar), 138.4 (C Ar), 146.8 (C Ar), 154.7 (C Ar), 157.9 (NCHO).

ESI-MS (positive-ions, CH_3CN): m/z 507.22 (100 %, $\text{M-2BF}_4+\text{OH}]^+$).

s.

Light brown solid, yield 69 %.

$^1\text{H-NMR}$ (CDCl_3 , 300 MHz) δ = 1.31 (s, 6H, CH_3), 1.41 (s, 18H, CH_3), 1.50 (s, 18H, CH_3), 5.04 (s, 4H, CH_2), 7.66 (s, 2H, CH Ar), 8.08 (s, 2H, CH Ar), 9.99 (s, 2H, NCHO).

$^{13}\text{C}\{^1\text{H}\}$ -NMR (CDCl_3 , 75 MHz): δ = 29.8 (CH_3), 30.9 (CH_3), 31.5 (CH_3), 34.8 (C), 36.0 (C), 38.0 (C), 53.6 (CH_2), 109.7 (CH Ar), 124.9 (CH Ar), 129.7 (C Ar), 137.2 (C Ar), 146.0 (C Ar), 154.2 (C Ar), 156.1 (NCHO).

$^1\text{H-NMR}$ (CD_3CN , 400 MHz) δ = 1.28 (s, 6H, CH_3), 1.47 (s, 18H, CH_3), 1.57 (s, 18H, CH_3), 4.77 (s, 4H, CH_2), 7.82 (d, $^3J_{\text{HH}} = 1.6$ Hz, 2H, CH Ar), 7.94 (d, $^3J_{\text{HH}} = 1.6$ Hz, 2H, CH Ar), 9.76 (s, 2H, NCHO).

$^{13}\text{C}\{^1\text{H}\}$ -NMR (CD_3CN , 100 MHz): δ = 22.0 (CH_3), 29.6 (CH_3), 31.2 (CH_3), 35.2 (C), 36.4 (C), 36.7 (C), 54.6 (CH_2), 109.4 (CH Ar), 125.4 (CH Ar), 130.7 (C Ar), 137.7 (C Ar), 146.6 (C Ar), 154.7 (C Ar), 157.2 (NCHO).

ESI-MS (positive-ions, CH_3CN): m/z 531.22 (100 %, $\text{M-2BF}_4\text{-H}^+$), 549.20 (20 %, $\text{M-2BF}_4\text{+OH}^+$).

t.

Off-white solid, yield 77 %.

$^1\text{H-NMR}$ (CDCl_3 , 300 MHz) δ = 1.36 (s, 36H, CH_3), 2.13 (s br, 4H, CH_2), 2.66 (s br, 4H, CH_2), 5.94 (s, 2H, CH), 7.57 (s, 2H, CH Ar), 8.00 (s br, 2H, CH Ar), 10.55 (s br, 2H, NCHO).

$^{13}\text{C}\{^1\text{H}\}$ -NMR (CDCl_3 , 75 MHz): δ = 23.4 (CH_2), 29.8 (CH_3), 31.3 (CH_3), 31.9 (CH_2), 34.8 (C), 36.2 (C), 62.6 (CH), 108.5 (CH Ar), 125.7 (CH Ar), 128.0 (C Ar), 137.5 (C Ar), 145.1 (C Ar), 156.1 (NCHO). (C Ar not detected)

$^1\text{H-NMR}$ (CD_3CN , 300 MHz) δ = 1.39 (s, 36H, CH_3), 2.15 (s br, 4H, CH_2), 2.60 (s br, 4H, CH_2) 5.70 (s br, 2H, CH), 7.70 (s, 2H, CH Ar), 7.76 (s br, 2H, CH Ar), 9.90 (s, 2H, NCHO).

$^{13}\text{C}\{^1\text{H}\}$ -NMR (CD_3CN , 75 MHz): δ = 24.2 (CH_2), 29.6 (CH_3), 31.4 (CH_3), 32.7 (CH_2), 35.3 (C), 35.6 (C), 61.9 (CH), 111.0 (CH Ar), 126.3 (CH Ar), 128.8 (C Ar), 138.2 (C Ar), 148.3 (C Ar), 154.7 (C Ar), 156.1 (NCHO).

ESI-MS (positive-ions, CH_3CN): m/z 561.40 (100 %, $\text{M-2BF}_4\text{+OH}^+$), 579.42 (100 %, $\text{M-2BF}_4\text{+2OH}^+$).

u.

Grey solid, yield 45 %.

$^1\text{H-NMR}$ (CDCl_3 , 300 MHz) δ = 1.38 (s, 18H, CH_3), 1.57 (s, 18H, CH_3), 7.63 (s, 2H, CH Ar), 7.72 (s, 2H, CH Ar), 8.17 (m br, 3H, CH Ar), 8.36 (s br, 1H, CH Ar), 10.18 (s br, 2H, NCHO).

$^{13}\text{C}\{^1\text{H}\}$ -NMR (CDCl_3 , 75 MHz): $\delta = 29.9$ (CH_3), 31.4 (CH_3), 34.9 (C), 36.0 (C), 108.5 (CH Ar), 123.9 (CH Ar), 125.3 (CH Ar), 128.9 (C Ar), 129.1 (C Ar), 131.7 (CH Ar), 133.0 (CH Ar), 137.8 (C Ar), 146.0 (C Ar), 154.4 (C Ar), 156.0 (NCHO).

^1H -NMR (CD_3CN , 400 MHz) $\delta = 1.42$ (s, 18H, CH_3), 1.62 (s, 18H, CH_3), 7.65 (d, $^3J_{\text{HH}} = 2.0$ Hz, 2H, CH Ar), 7.88 (d, $^3J_{\text{HH}} = 2.0$ Hz, 2H, CH Ar), 8.20 (m br, 1H, CH Ar), 8.22 (s, 3H, CH Ar), 10.07 (s br, 2H, NCHO).

$^{13}\text{C}\{^1\text{H}\}$ -NMR (CD_3CN , 100 MHz): $\delta = 29.5$ (CH_3), 31.2 (CH_3), 35.3 (C), 36.4 (C), 109.2 (CH Ar), 123.9 (CH Ar), 125.9 (CH Ar), 130.2 (CH Ar), 130.3 (C Ar), 132.4 (C Ar), 134.1 (CH Ar), 138.0 (C Ar), 146.5.8 (C Ar), 154.7 (C Ar), 156.4 (NCHO).

ESI-MS (positive-ions, CH_3CN): m/z 555.09 (100 %, $\text{M}-2\text{BF}_4+\text{OH}]^+$).

7.5.3 Attempts for the syntheses of metal complexes with 3,3'-(substituted)bis(5,7-di-tert-butyl-3H-benzoxazol-1-ium)bistetrafluoroborate proligands

Different attempts have been done in order to obtain transition metal complexes with carbene ligands deriving from the proligands **r** – **u**; however, all these attempts have been unsuccessful. The reaction conditions are reported in Table 7.2.

Table 7.2: reaction between bis(benzoxazolium) salts **r** – **u** and different metal precursors

salt	Reaction condition	observation
r (1 eq.)	2 eq. $\text{AuCl}(\text{SMe}_2)$, NaOAc DMF, 120 °C, 2 h	Several signals in the ^1H -NMR spectrum
r (1 eq.)	2.5 eq Ag_2O , CDCl_3 25 °C, 24 h	No reaction
r (1 eq.)	2.5 eq Ag_2O , CD_3CN , 60 °C, 24 h	No reaction
r (1 eq.)	1.0 eq $[\text{PdCl}_2\text{COD}]$, KO t Bu THF, 25 °C, 18 h	Several signals in the ^1H -NMR spectrum, decomposition
s (1 eq.)	1.0 eq $[\text{PdCl}_2\text{COD}]$, KO t Bu THF, 25 °C, 18 h	Several signals in the ^1H -NMR spectrum, decomposition
t (1 eq.)	1.0 eq $[\text{PdCl}_2\text{COD}]$, KO t Bu THF, 25 °C, 18 h	Several signals in the ^1H -NMR spectrum, decomposition
u (1 eq.)	2.5 eq Ag_2O , CH_2Cl_2 , 25 °C, 24 h	Several signals in the ^1H -NMR spectrum, decomposition

Chapter 7: EXPERIMENTAL SECTION

u (1 eq.)	0.5 eq [RhClCOD] ₂ , KO ^t Bu THF, 25 °C, 18 h	Several signals in the ¹ H-NMR spectrum, decomposition
---------------------	--	--

Publications

“Metal complexes with di(N-heterocyclic carbene) ligands bearing a rigid *ortho*-, *meta* or *para*-phenylene bridge.”

M. Monticelli, C. Tubaro, M. Baron, M. Basato, P. Sgarbossa, C. Graiff, G. Accorsi, T. P. Pell, D. J. D. Wilson, P. J. Barnard, *Dalton Trans.* **2016**, 45, 9540.

Communications to congresses

10th International School of Organometallic Chemistry, Camerino (Italy) 5 – 9 September 2015, Flash and poster presentation: “Metal Complexes with di(N-Heterocyclic carbene) ligands bearing an *ortho*-, *meta*- or *para*-phenylene bridge” M. Monticelli, C. Tubaro, C. Graiff, G. Accorsi.

XLIII National Conference of the Inorganic chemistry division of the Italian Chemical Society, Camerino (Italy) 9 – 12 September 2015, Oral presentation: “Metal Complexes with di(N-Heterocyclic carbene) ligands bearing an *ortho*-, *meta*- or *para*-phenylene Bridge” M. Monticelli, C. Tubaro, C. Graiff, G. Accorsi.

XLIII National Conference of the Inorganic chemistry division of the Italian Chemical Society, Camerino (Italy) 9 – 12 September 2015, Poster presentation: “Bidentate heteroditopic diNHCs: an original class of ligands for transition metal complexes” M. Monticelli, C. Tubaro, S. Bellemin-Lapponnaz.

National Conference of Interdivisional Group of Organometallic Chemistry of the Italian Chemical Society, Genova (Italy) 5 – 8 June 2016, Poster presentation “Heteroditopic diNHCs as novel ligands for transition metal centers” M. Monticelli, C. Tubaro, S. Bellemin-Lapponnaz.

XLIV National Conference of the Inorganic Chemistry Division of the Italian Chemical Society, Padova (Italy) 14 – 17 September 2016, Poster presentation “Heteroditopic diNHCs as novel ligands for transition metal centers” M. Monticelli, C. Tubaro, S. Bellemin-Lapponnaz.

Chapter 8: REFERENCES

- ¹ a) S. Díez-González, N. Marion, S. P. Nolan, *Chem. Rev.* **2009**, *109*, 3612. b) J. C. Garrison, W. J. Youngs, *Chem. Rev.* **2005**, *105*, 3978.
- ² see for example (a) S. P. Nolan, *N-Heterocyclic Carbenes, Effective Tools for Organometallic Synthesis* **2014**, Weinheim: Wiley-VCH. (b) S. Díez-González, *N-Heterocyclic Carbenes: From Laboratory Curiosities to Efficient Synthetic Tools* **2010**, Cambridge: RSC Catalysis Series, RSC. (c) C. S. J. Cazin, *N-Heterocyclic Carbenes in Transition Metal Catalysis and Organocatalysis*, in *Catalysis by Metal Complexes*. **2010**, vol. 32, Heidelberg: Springer. (d) O. Köhl, *Functionalised N-heterocyclic carbene complexes* **2010**, John Wiley and Sons. (e) F. Glorius, *N-Heterocyclic Carbenes in Transition Metal Catalysis*, in *Topics in Organometallic Chemistry*, **2007**, vol. 21, Heidelberg: Springer.
- ³ H. Olivier-Bourbigou, L. Magna, D. Morvan, *Applied Catalysis A: General* **2010**, *373*, 1.
- ⁴ K. Goossens, P. Nockemann, K. Driesen, B. Goderis, C. Görrler-Walrand, K. Van Hecke, L. Van Meervelt, E. Pouzet, K. Binnemans, T. Cardinaels, *Chem. Mater.* **2008**, *20*, 157.
- ⁵ a) J.-W. Wang, F.-H. Meng, L.-F. Zhang, *Organometallics* **2009**, *28*, 2334. b) H. Zhou, Y. Zhao, G. Gao, S. Li, J. Lan, J. You, *J. Am. Chem. Soc.* **2013**, *135*, 14908. c) H. Zhou, Z. Wang, C. Gao, J. You, G. Gao, *Chem. Commun.* **2013**, *49*, 1832. d) C. Gao, H. Zhou, S. Wei, Y. Zhao, J. You, G. Gao, *Chem. Commun.* **2013**, *49*, 1127.
- ⁶ (a) K. Öfele, *J. Organomet. Chem.* **1968**, *12*, 42. (b) H.-W. Wanzlick, H.-J. Schönherr, *Angew. Chem. Int. Ed. Engl.* **1968**, *7*, 141.
- ⁷ (a) A. J. Arduengo III, R. L. Harlow, M. Kline, *J. Am. Chem. Soc.* **1991**, *113*, 361. (b) D. A. Dixon, A. J. Arduengo III, *J. Phys. Chem.* **1991**, *95*, 4180. (c) A. J. Arduengo III, H. V. R. Dias, R. L. Harlow, M. Kline, *J. Am. Chem. Soc.* **1992**, *114*, 5530.
- ⁸ V. César, S. Bellemin-Lapponnaz, L. H. Gade, *Chem. Soc. Rev.* **2004**, *33*, 619.
- ⁹ See for example: (a) M. Scholl, T. M. Trnka, J. P. Morgan, R. H. Grubbs, *Tetrahedron Lett.* **1999**, *40*, 2247. (b) M. S. Sanford, M. Ulman, R. H. Grubbs, *J. Am. Chem. Soc.* **2001**, *123*, 749.
- ¹⁰ R. R. Schrock, *Angew. Chem. Int. Ed.* **2006**, *45*, 3748.

- ¹¹ D. Bourissou, O. Guerret, F. P. Gabbaï, G. Bertrand, *Chem. Rev.* **2000**, *100*, 39.
- ¹² W. A. Herrmann, T. Weskamp, V. P. W. Böhm, *Adv. Organomet. Chem.* **2001**, *48*, 1.
- ¹³ S. Fantasia, J. L. Petersen, H. Jacobsen, L. Cavallo, S. P. Nolan, *Organometallics* **2007**, *26*, 5880.
- ¹⁴ X. Hu, I. Castro-Rodriguez, K. Olsen, K. Meyer, *Organometallics* **2004**, *23*, 755.
- ¹⁵ D. Nemcsok, K. Wichmann, G. Frenking, *Organometallics* **2004**, *23*, 3640.
- ¹⁶ W. A. Herrmann, C. Köcher, *Angew. Chem. Int. Ed. Engl.* **1997**, *36*, 2162.
- ¹⁷ M. Baron, S. Bellemin-Laponnaz, C. Tubaro, B. Heinrich, M. Basato, G. Accorsi, *J. Organomet. Chem.* **2016**, *801*, 60.
- ¹⁸ L.-A. Schaper, S. J. Hock, W. A. Herrmann, F. E. Kühn, *Angew. Chem. Int. Ed.* **2013**, *52*, 270.
- ¹⁹ A. Marchenko, H. Koidan, A. Hurieva, O. Kurpiieva, Y. Vlasenko, A. Kostyuk, C. Tubaro, A. Lenarda, A. Biffis, C. Graiff, *J. Organomet. Chem.* **2014**, *771*, 14.
- ²⁰ A. A. Danopoulos, N. Tsoureas, S. A. Macgregor, C. Smith, *Organometallics* **2007**, *26*, 253.
- ²¹ Y. Unger, D. Meyer, O. Molt, C. Schildknecht, I. Münster, G. Wagenblast, T. Strassner, *Angew. Chem. Int. Ed.* **2010**, *49*, 10214.
- ²² O. Schuster, L. Yang, H. G. Raubenheimer, M. Albrecht, *Chem. Rev.* **2009**, *109*, 3445.
- ²³ (a) M. Albrecht, *Adv Organomet Chem.* **2014**, *62*, 111. (b) M. Albrecht, *Chem. Commun.* **2008**, 3601 c) K. F. Donnelly, A. Petronilho, M. Albrecht, *Chem. Commun.* **2013**, *49*, 1145.
- ²⁴ D. J. Debon, S. P. Nolan, *Chem. Soc. Rev.* **2013**, *42*, 6723.
- ²⁵ A. Marchenko, H. Koidan, A. Hurieva, O. Kurpiieva, Y. Vlasenko, A. Kostyuk, A. Biffis, *Organometallics* **2016**, *35*, 762.
- ²⁶ a) F. E. Hahn, M. C. Jahnke, *Angew. Chem. Int. Ed.* **2008**, *47*, 3122. b) C. Tubaro, M. Baron, M. Costante, M. Basato, A. Biffis, A. Gennaro, A. A. Isse, C. Graiff, G. Accorsi, *Dalton Trans.* **2013**, *42*, 10952.
- ²⁷ K. F. Donnelly, A. Petronilho, M. Albrecht, *Chem. Commun.* **2013**, *49*, 1145.
- ²⁸ a) B. Schulze, U. S. Schubert, *Chem. Soc. Rev.* **2014**, *43*, 2522. b) G. Guisado-Barrios, J. Bouffard, B. Donnadiou, G. Bertrand, *Angew. Chem. Int. Ed.* **2010**, *49*, 4759.
- ²⁹ J. Li, W. Shen, X. Li, *Current Organic Chemistry* **2012**, *16*, 2879.

- ³⁰ a) J. W. Ogle, S. A. Miller, *Chem. Commun.* **2009**, 5728. b) S. Würtz, F. Glorius, *Acc. Chem. Res.* **2008**, *41*, 1523. c) C. Präsang, B. Donnadieu, G. Bertrand, *J. Am. Chem. Soc.* **2005**, *127*, 10182. d) A. Fürstner, M. Alcarazo, K. Radkowski, C. W. Lehmann, *Angew. Chem. Int. Ed.* **2008**, *47*, 8302.
- ³¹ M. Baron, C. Tubaro, A. Biffis, M. Basato, C. Graiff, A. Poater, L. Cavallo, N. Armaroli, G. Accorsi, *Inorg. Chem.* **2012**, *51*, 1778.
- ³² A. Pöethig, T. Strassner, *Organometallics* **2011**, *30*, 6674.
- ³³ S. N. Sluijter, C. J. Elsevier, *Organometallics* **2014**, *33*, 6389.
- ³⁴ A. J. Arduengo, U.S. Patent No. 5077414, 1991.
- ³⁵ L. Benhamou, E. Chardon, G. Lavigne, S. Bellemin-Laponnaz, V. César, *Chem. Rev.* **2011**, *111*, 2705.
- ³⁶ generale
- ³⁷ A. S. K. Hashmi, C. Lothschütz, C. Böhlting, F. Rominger, *Organometallics* **2011**, *30*, 2411.
- ³⁸ C.-Y. Liu, D.-Y. Chen, G.-H. Lee, S.-M. Peng, S.-T. Liu, *Organometallics* **1996**, *15*, 1055.
- ³⁹ F. E. Hahn, M. C. Jahnke, *Angew. Chem. Int. Ed.* **2008**, *47*, 3122.
- ⁴⁰ a) B. Çetinkaya, P. B. Hitchcock, M. F. Lappert, D. B. Shaw, K. Spyropoulos, N. J. W. Warhurst, *J. Organomet. Chem.* **1993**, *459*, 311. b) I. Özdemir, B. Yiğit, B. Çetinkaya, D. Ülkü, M. N. Tahir, C. Arici, *J. Organomet. Chem.* **2001**, *633*, 27.
- ⁴¹ I. J. B. Lin, C. S. Vasam, *Coord. Chem. Rev.* **2007**, *251*, 642.
- ⁴² H. M. J. Wang, I. J. B. Lin, *Organometallics* **2008**, *17*, 972.
- ⁴³ P. J. Barnard, M. V. Baker, S. J. Berners-Price, B. W. Skelton, A. H. White, *Dalton Trans.* **2004**, 1038.
- ⁴⁴ A. Collado, A. Gómez-Suárez, A. R. Martin, A. M. Z. Slawin, S. P. Nolan, *Chem. Commun.* **2013**, *49*, 5541.
- ⁴⁵ R. Visbal, A. Laguna, M. C. Gimeno, *Chem. Commun.* **2013**, *49*, 5642.
- ⁴⁶ L. Mercks, M. Albrecht, *Chem. Soc. Rev.* **2010**, *39*, 1903.
- ⁴⁷ a) M. K. Whittlesey, E. Peris, *ACS Catal.* **2014**, *4*, 3152. b) F. Lazreg, F. Nagra, C. S. J. Cazin, *Coord. Chem. Rev.* **2015**, *293-294*, 48. c) S. Gaillard, C. S. J. Cazin, S. P. Nolan, *Acc. Chem. Res.* **2012**, *45*, 778. d) S. P. Nolan, *Acc. Chem. Res.* **2011**, *44*, 91. e) A. Biffis, C. Tubaro, M. Baron, *Chem. Rec.* **2016**, *16*, 1742. f) C. S. J. Cazin, N-

- Heterocyclic Carbenes in Transition Metal Catalysis and Organocatalysis, in *Catalysis by Metal Complexes*. vol. 32, Heidelberg: Springer; 2010. g) Glorius F. N-Heterocyclic Carbenes in Transition Metal Catalysis, in *Topics in Organometallic Chemistry*. vol. 21, Springer: Heidelberg; 2007. h) S. Bellemin-Laponnaz, S. Dagorne, *Chem. Rev.* 2014, 114, 8747.
- ⁴⁸ a) J. A. Mata, F. E. Hahn, E. Peris, *Chem. Sci.* **2014**, 5, 1723. b) M. T. Zamora, M. J. Ferguson, R. McDonald, M. Cowie, *Organometallics* **2012**, 31, 5463.
- ⁴⁹ H. Schmidbaur, A. Schier, *Chem. Soc. Rev.* **2008**, 37, 1931.
- ⁵⁰ P. Pyykkö, *Chem. Rev.* **1997**, 97, 597.
- ⁵¹ V. W.-W. Yam, E. C.-C. Cheng, *Chem. Soc. Rev.* **2008**, 37, 1806.
- ⁵² A. Vogler, H. Kunkely, *Chem. Phys. Lett.* **1988**, 150, 135.
- ⁵³ P. Pyykkö, *Angew. Chem. Int. Ed.* **2004**, 43, 4412.
- ⁵⁴ P. Schwerdtfeger, A. E. Bruce, M. R. M. Bruce, *J. Am. Chem. Soc.* **1998**, 120, 6587.
- ⁵⁵ A. Juris, V. Balzani, F. Barigelletti, S. Campagna, P. Belser, A. von Zelewsky, *Coord. Chem. Rev.* **1988**, 84, 85.
- ⁵⁶ S. U. Son, K. H. Park, Y.-S. Lee, B. Y. Kim, C. H. Choi, M. S. Lah, Y. H. Jang, D.-J. Jang, Y. K. Chung, *Inorg. Chem.* **2004**, 43, 6896.
- ⁵⁷ R. H. Magnuson, H. Taube, *J. Am. Chem. Soc.* **1975**, 97, 5129.
- ⁵⁸ T. Sajoto, P. I. Djurovich, A. Tamayo, M. Yousufuddin, R. Bau, M. E. Thompson, *Inorg. Chem.* **2005**, 44, 7792.
- ⁵⁹ Y. Unger, A. Zeller, S. Ahrensy, T. Strassner, *Chem. Commun.* **2008**, 3263.
- ⁶⁰ a) B. Rosenberg, L.V. Camp, *Nature* **1965**, 205, 698. b) B. Rosenberg, L.V. Camp, J. E. Trosko, V. H. Mansour, *Nature* **1969**, 222, 385. c) J B. Rosenberg, L.V. Camp, *Canc. Res.* **1970**, 30, 1799.
- ⁶¹ T. W. Hambley, *Coord. Chem. Rev.* **1997**, 166, 181.
- ⁶² M. L. Teyssot, A. S. Jarrousse, M. Manin, A. Chevy, S. Roche, F. Norre, C. Beaudoin, L. Morel, D. Boyer, R. Mahiou, A. Gautier, *Dalton Trans.* **2009**, 6894.
- ⁶³ W. Liu, R. Gust, *Chem. Soc. Rev.* **2013**, 42, 755.
- ⁶⁴ a) S. Das Adhikary, D. Bose, P. Mitra, K. Das Saha, V. Bertolasi, J. Dinda, *New J. Chem.* **2012**, 36, 759. b) E. Chardon, G. L. Puleo, G. Dahm, G. Guichard, S. Bellemin-Laponnaz, *Chem. Commun.* **2011**, 47, 5864. c) O. Ciftci, I. Ozdemir, N. Vardi, N. Gurbuz, *Hum. Exp. Toxicol.* **2011**, 30, 1342. d) O. Ciftci, A. Beytur, O. Cakir, N.

- Gurbuz, N. Vardi, *Basic Clin. Pharmacol. Toxicol.* **2011**, *109*, 328. e) M. Skander, P. Retailleau, B. Bourrie, L. Schio, P. Mailliet, A. Marinetti, *J. Med. Chem.* **2010**, *53*, 2146. f) G. Alves, L. Morel, M. El-Ghozzi, D. Avignant, B. Legeret, L. Nauton, F. Cisnetti, A. Gautier, *Chem. Commun.* **2011**, *47*, 7830. g) R. W. Y. Sun, A. L. F. Chow, X. H. Li, J. J. Yan, S. S. Y. Chui, C. M. Che, *Chem. Sci.* **2011**, *2*, 728.
- ⁶⁵ M. Bouché, G. Dahm, M. Wantz, S. Fournel, T. Achard, S. Bellemin-Lapponnaz, *Dalton Trans.* **2016**, *45*, 11362.
- ⁶⁶ a) C. G. Hartinger, P. J. Dyson, *Chem. Soc. Rev.* **2009**, *38*, 391. b) K. M. Hindi, M. J. Panzner, C. A. Tessier, C. L. Cannon, W. J. Youngs, *Chem. Rev.* **2009**, *109*, 3859. c) M. Patra, G. Gasser, N. Metzler-Nolte, *Dalton Trans.* **2012**, *41*, 6350.
- ⁶⁷ a) S. Ray, R. Mohan, J. K. Singh, M. K. Samantaray, M. M. Shaikh, D. Panda, P. Ghosh, *J. Am. Chem. Soc.* **2007**, *129*, 15042. b) D. A. Medvetz, K. M. Hindi, M. J. Panzner, A. J. Ditto, Y. H. Yun, W. J. Youngs, *Met.-Based Drugs*, **2008**, *2008*, 384010. c) S. Roland, C. Jolivald, T. Cresteil, L. Eloy, P. Bouhours, A. Hequet, V. Mansuy, C. Vanucci, J. M. Paris, *Chem. Eur. J.* **2011**, *17*, 1442. d) C. H. Wang, W. C. Shih, H. C. Chang, Y. Y. Kuo, W. C. Hung, T. G. Ong, W. S. Li, *J. Med. Chem.* **2011**, *54*, 5245. e) L. Kaps, B. Biersack, H. Müller-Bunz, K. Mahal, J. Munzner, M. Tacke, T. Mueller, R. Schobert, *J. Inorg. Biochem.* **2012**, *106*, 52.
- ⁶⁸ A. Bindoli, M. P. Rigobello, G. Scutari, C. Gabbiani, A. Casini, L. Messori, *Coord. Chem. Rev.* **2009**, *253*, 1692.
- ⁶⁹ a) S. Patil, A. Deally, F. Hackenberg, L. Kaps, H. Müller-Bunz, R. Schobert, M. Tacke, *Helv. Chim. Acta*, **2011**, *94*, 1551. b) J. L. Hickey, R. A. Ruhayel, P. J. Barnard, M. V. Baker, S. J. Berners-Price, A. Filipovska, *J. Am. Chem. Soc.* **2008**, *130*, 12570. c) P. J. Barnard, L. E. Wedlock, M. V. Baker, S. J. Berners-Price, D. A. Joyce, B. W. Skelton, J. H. Steer, *Angew. Chem. Int. Ed.* **2006**, *45*, 5966. d) S. Urig, K. Fritz-Wolf, R. Reau, C. Herold-Mende, K. Toth, E. Davioud-Charvet, K. Becker, *Angew. Chem. Int. Ed.* **2006**, *45*, 1881. e) R. Rubbiani, I. Kitanovic, H. Alborzinia, S. Can, A. Kitanovic, L. A. Onambele, M. Stefanopoulou, Y. Geldmacher, W. S. Sheldrick, G. Wolber, A. Prokop, S. Wölfl, I. Ott, *J. Med. Chem.* **2010**, *53*, 8608. f) R. Rubbiani, S. Can, I. Kitanovic, H. Alborzinia, M. Stefanopoulou, M. Kokoschka, S. Monchgesang, W. S. Sheldrick, S. Wölfl, I. Ott, *J. Med. Chem.* **2011**, *54*, 8646.
- ⁷⁰ a) F. Tisato, C. Marzano, M. Porchia, M. Pellei, C. Santini, *Med. Res. Rev.* **2010**, *30*,

708. b) L. Ruiz-Azuara, M. E. Bravo-Gomez, *Curr. Med. Chem.* **2010**, *17*, 3606. c) R. J. Bowen, M. Navarro, A. M. Shearwood, P. C. Healy, B. W. Skelton, A. Filipovska, S. J. Berners-Price, *Dalton Trans.* **2009**, 10861.

⁷¹ a) T. Wang, Z. Guo, *Curr. Med. Chem.* **2006**, *13*, 525. b) C. Marzano, M. Pellei, F. Tisato, C. Santini, *Anti-Cancer Agents Med. Chem.* **2009**, *9*, 185. c) M. L. Teysot, A. S. Jarrousse, A. Chevy, A. De Haze, C. Beaudoin, M. Manin, S. P. Nolan, S. Diez-Gonzalez, L. Morel, A. Gautier, *Chem. Eur. J.* **2009**, *15*, 314.

⁷² S. Ray, J. Asthana, J. M. Tanski, M. M. Shaikh, D. Panda, P. Ghosh, *J. Organomet. Chem.* **2009**, *694*, 2328.

⁷³ a) A. Bergamo, G. Sava, *Dalton Trans.* **2011**, *40*, 7817. b) A. Casini, C. Gabbiani, F. Sorrentino, M. P. Rigobello, A. Bindoli, T. J. Geldbach, A. Marrone, N. Re, C. G. Hartinger, P. J. Dyson, L. Messori, *J. Med. Chem.* **2008**, *51*, 6773. c) P. Mura, M. Camalli, A. Bindoli, F. Sorrentino, A. Casini, C. Gabbiani, M. Corsini, P. Zanello, M. P. Rigobello, L. Messori, *J. Med. Chem.* **2007**, *50*, 5871. d) R. G. de Lima, A. B. P. Lever, I. Y. Ito, R. S. da Silva, *Transition Met. Chem.* **2003**, *28*, 272. e) W. H. Ang, A. Casini, G. Sava, P. J. Dyson, *J. Organomet. Chem.* **2011**, *696*, 989. f) N. P. Barry, P. J. Sadler, *Chem. Soc. Rev.* **2012**, *41*, 3264. g) Y. K. Yan, M. Melchart, A. Habtemariam, P. J. Sadler, *Chem. Commun.* **2005**, 4764. h) O. Ciftci, I. Ozdemir, O. Cakir, S. Demir, *Toxicol. Ind. Health*, **2011**, *27*, 735. i) J. Lemke, N. Metzler-Nolte, *Eur. J. Inorg. Chem.* **2008**, 3359. j) P. Nowak-Sliwinska, J. R. van Beijnum, A. Casini, A. A. Nazarov, G. Wagnieres, H. van den Bergh, P. J. Dyson, A. W. Griffioen, *J. Med. Chem.* **2011**, *54*, 3895. k) M. Alfaro, A. Prades, M. D. Ramos, E. Peris, J. Ripoll- Gomez, M. Poyatos, J. S. Burgos, *Zebrafish*, **2010**, *7*, 13. l) G. C. Vougioukalakis, R. H. Grubbs, *Chem. Rev.* **2010**, *110*, 1746. m) L. Oehninger, H. Alborzinia, S. Ludewig, K. Baumann, S. Wölfl, I. Ott, *ChemMedChem*. **2011**, *6*, 2142.

⁷⁴ a) G. T. S. Andavan, E. B. Bauer, C. S. Letko, T. K. Hollis, F. S. Tham, *J. Organomet. Chem.* **2005**, *690*, 5938. b) J. Cho, T. K. Hollis, T. R. Helgerta, E. J. Valente, *Chem. Commun.* **2008**, 5001. c) J. Cho, T. K. Hollis, E. J. Valente, J. M. Trate, *J. Organomet. Chem.* **2011**, *696*, 373. d) X. Zhang, A. M. Wright, N. J. DeYonker, T. K. Hollis, N. I. Hammer, C. E. Webster, E. J. Valente, *Organometallics* **2012**, *31*, 1664. e) T. R. Helgert, T. K. Hollis, E. J. Valente, *Organometallics* **2012**, *31*, 3002. f) A. J. Huckaba, T. K. Hollis, T. O. Howell, H. U. Valle, Y. Wu, *Organometallics* **2013**, *32*,

63. g) X. Zhang, B. Cao, E. J. Valente, T. K. Hollis, *Organometallics* **2013**, *32*, 752. h) R. J. Rubio, G. T. S. Andavan, E. B. Bauer, T. K. Hollis, J. Cho, F. S. Tham, B. Donnadieu, *J. Organomet. Chem.* **2005**, *690*, 5353.
- ⁷⁵ a) Y. Canac, C. Lepetit, M. Abdalilah, C. Duhayon, R. Chauvin, *J. Am. Chem. Soc.* **2008**, *130*, 8406. b) B. K. Rana, V. Bertolasi, S. Pal, P. Mitra, J. Dinda, *J. Mol. Struct.* **2013**, *1049*, 458.
- ⁷⁶ a) W. Zuo, P. Braunstein, *Organometallics* **2010**, *29*, 5535. b) W. Zuo, P. Braunstein, *Dalton Trans.* **2012**, *41*, 636. c) N. Darmawan, C.-H. Yang, M. Mauro, M. Raynal, S. Heun, J. Pan, H. Buchholz, P. Braunstein, L. De Cola, L. *Inorg. Chem.* **2013**, *52*, 10756. d) M. Raynal, R. Pattacini, C. S. J. Cazin, C. Vallee, H. Olivier-Bourbigou, P. Braunstein, *Organometallics* **2009**, *28*, 4028.
- ⁷⁷ a) A. R. Chianese, A. Mo, N. L. Lampland, R. L. Swartz, P. T. Bremer, *Organometallics* **2010**, *29*, 3019. b) A. R. Chianese, S. E. Shaner, J. A. Tandler, D. M. Pudalov, D. Y. Shopov, D. Kim, S. L. Rogers, A. Mo, *Organometallics* **2012**, *31*, 7359. c) A. R. Chianese, M. J. Drance, K. H. Jensen, S. P. McCollom, N. Yusufova, S. E. Shaner, D. Y. Shopov, J. A. Tandler, *Organometallics* **2014**, *33*, 457.
- ⁷⁸ a) A. Rit, T. Pape, F. E. Hahn, *J. Am. Chem. Soc.* **2010**, *132*, 4572. b) A. Rit, T. Pape, A. Hepp, F. E. Hahn, *Organometallics* **2011**, *30*, 334. c) Y. F. Han, G. X. Jin, F. E. Hahn, *J. Am. Chem. Soc.* **2013**, *135*, 9263. d) R. Maity, C. Schulte to Brinke, F. E. Hahn, *Dalton Trans.* **2013**, *42*, 12857. e) R. Maity, H. Koppetz, A. Hepp, F. E. Hahn, *J. Am. Chem. Soc.* **2013**, *135*, 4966. f) R. Maity, A. Rit, C. Schulte to Brinke, C. G. Daniliuc, F. E. Hahn, *Chem. Commun.* **2013**, *49*, 1011.
- ⁷⁹ S. Zlatogorsky, C. A. Muryn, F. Tuna, D. J. Evans, M. J. Ingleson, *Organometallics* **2011**, *30*, 4974.
- ⁸⁰ Y.-M. Zhang, J.-Y. Shao, C.-J. Yoa, Y.-W. Zhong, *Dalton Trans.* **2012**, *41*, 9280.
- ⁸¹ M. Albrecht, R. H. Crabtree, J. Mata. E. Peris, *Chem. Commun.* **2002**, 32.
- ⁸² D. Munz, A. Poethig, A. Tronnier, T. Strassner, *Dalton Trans.* **2013**, *42*, 7297.
- ⁸³ A. Tronnier, T. Strassner, *Dalton Trans.* **2013**, *42*, 9847.
- ⁸⁴ L. Mercs, A. Neels, H. Stoeckli-Evans, M. Albrecht, *Inorg. Chem.* **2011**, *50*, 8188.
- ⁸⁵ Y.-H. So, *Macromolecules* **1992**, *25*, 516.
- ⁸⁶ C. Tubaro, A. Biffis, R. Gava, E. Scattolin, A. Volpe, M. Basato, M. M. Díaz-Requejo, P. J. Perez, *Eur. J. Org. Chem.* **2012**, 1367.

- ⁸⁷ A. Rit, T. Pape, F. E. Hahn, *Organometallics* **2011**, *30*, 6393.
- ⁸⁸ R. Zhong, A. Pöthig, D. C. Mayer, C. Jandl, P.- J. Altmann, W. A. Herrmann, F. E. Kühn, *Organometallics* **2015**, *34*, 2573.
- ⁸⁹ P. de Fremont, P. R. Singh, E. D. Stevens, J. L. Petersen, S. P. Nolan, *Organometallics* **2007**, *26*, 1376.
- ⁹⁰ S. Saito, M. Saika, R. Yamasaki, I. Azumaya, H. Masu, *Organometallics* **2011**, *30*, 1366.
- ⁹¹ (a) A. Herbst, C. Bronner, P. Dechambenoit, O. S. Wenger, *Organometallics* **2013**, *32*, 1807. (b) J. Vaughan, D. J. Carter, A. L. Rohl, M. I. Ogden, B. W. Skelton, P. V. Simpson, D. H. Brown, *Dalton Trans.* **2016**, *45*, 1484. (c) T. P. Pell, B. D. Stringer, C. F. Hogan, D. J. D. Wilson, P. J. Barnard, unpublished results.
- ⁹² (a) D. H. Brown, G. L. Nealon, P. V. Simpson, B. W. Skelton, Z. Wang, *Organometallics* **2009**, *28*, 1965. (b) J. C. C. Chen, I. J. B. Lin, *J. Chem. Soc., Dalton Trans.* **2000**, 839. (c) A. Caballero, E. Díez-Barra, F. A. Jalón, S. Merino, A. M. Rodríguez, J. Tejada, *J. Organomet. Chem.* **2001**, *627*, 263.
- ⁹³ F. Jean-Baptiste dit Dominique, H. Gornitzka, A. Sournia-Saquet, C. Hemmert, *Dalton Trans.* **2009**, 340.
- ⁹⁴ R. Maity, A. Rit, C. Schulte to Brinke, J. Kösters, F. E. Hahn, *Organometallics* **2013**, *32*, 6174.
- ⁹⁵ J. Garnier, D. W. Thomson, S. Zhou, P. I. Jolly, L. E. A. Berlouis, J. A. Murphy, *Beilstein J. Org. Chem.* **2012**, *8*, 994.
- ⁹⁶ A. Volpe, A. Sartorel, C. Tubaro, L. Meneghini, M. Di Valentin, C. Graiff, M. Bonchio, *Eur. J. Inorg. Chem.* **2014**, 665.
- ⁹⁷ G. Buscemi, M. Basato, A. Biffis, A. Gennaro, A. A. Isse, M. M. Natile, C. Tubaro, C. *J. Organomet. Chem.* **2010**, *695*, 2359.
- ⁹⁸ J. DePasquale, M. Kumar, M. Zeller, E. T. Papish, *Organometallics* **2013**, *32*, 966.
- ⁹⁹ M. Poyatos, E. Mas-Marzá, M. Sanaú, E. Peris, *Inorg. Chem.* **2004**, *43*, 1793.
- ¹⁰⁰ R. Huisgen, 1,3-Dipolar Cycloaddition Chemistry (Ed.: A. Padwa), Wiley, New York, **1984**, 1.
- ¹⁰¹ a) R. Huisgen, *Pure Appl. Chem.* **1989**, *61*, 613. b) R. Huisgen, G. Szeimies, L. Moebius, L. *Chem. Ber.* **1967**, *100*, 2494. c) W. Lwowski, 1,3-Dipolar Cycloaddition Chemistry, (Ed.: A. Padwa), Wiley, New York, **1984**, vol 1, chap. 5; d) J. Bastide, J.

- Hamelin, F. Texier, V. Q. Ven, *Bull. Soc. Chim. Fr.* **1973**, 2555. e) J. Bastide, J. Hamelin, F. Texier, V. Q. Ven, *Bull. Soc. Chim. Fr.* **1973**, 2871.
- ¹⁰² a) O. Henri-Rousseau, *Bull. Chim. Soc. Fr.* **1973**, 2294. b) N. P. Stepanova, N. A. Orlova, V. A. Galishev, A. Turbanova, A. Petrov, *Zh. Org. Khim.* **1985**, *21*, 979. c) N. P. Stepanova, V. A. Galishev, E. S. Turbanova, A. V. Maleev, K. A. Potekhin, E. N. Kurkutova, T. Yu, A. Struchkov, A. Petrov, *Zh. Org. Khim.* **1989**, *25*, 1613. d) D. Clarke, R. W. Mares, H. McNab, *J. Chem. Soc. Perkin Trans.* **1997**, *1*, 1799.
- ¹⁰³ V. V. Rostovtsev, L. G. Green, V. V. Fokin, K. B. Sharpless, *Angew. Chem. Int. Ed.* **2002**, 2596.
- ¹⁰⁴ M. Meldal, C. W. Tornøe, *Chem. Rev.* **2008**, *108*, 2952.
- ¹⁰⁵ a) E. Chardon, G. L. Puleo, G. Dahm, H. Guichard, E. Bellemin-Lapponnaz, *Chem. Commun.* **2011**, *47*, 5864. b) E. Chardon, G. L. Puleo, G. Dahm, S. Fournel, G. Guichard, S. Bellemin-Lapponnaz, *ChemPlusChem* **2012**, *77*, 1028.
- ¹⁰⁶ A. K. Renfrew, L. Juillerat-Jeanneret, P.J. Dyson, *J. Organomet. Chem.* **2011**, *696*, 772.
- ¹⁰⁷ W. H. Ang, E. Daldini, C. Scolaro, R. Scopelliti, L. Juillerat-Jeanneret, P. J. Dyson, *Inorg. Chem.* **2006**, *45*, 9006.
- ¹⁰⁸ M. Baron, S. Bellemin-Lapponnaz, C. Tubaro, M. Basato, S. Bogialli, A. Dolmella, *J. Inorg. Biochem.* **2014**, *141*, 94.
- ¹⁰⁹ (a) L. Zhang, X. Chen, P. Xue, H. H. Y. Sun, I. D. Williams, K. B. Sharpless, V. V. Fokin, G. Jia, *J. Am. Chem. Soc.* **2005**, *127*, 15998. (b) L. K. Rasmussen, B. C. Boren, V. V. Fokin, *Org. Lett.* **2007**, *9*, 5337. (c) B. C. Boren, S. Narayan, L. K. Rasmussen, L. Zhang, H. Zhao, Z. Lin, G. Jia, V. V. Fokin, *J. Am. Chem. Soc.* **2008**, *130*, 8923.
- ¹¹⁰ G. Kim, S. Kang, R. Keum, M. J. Seo, *Synth. Commun.* **1999**, *29*, 507.
- ¹¹¹ Z. Zhao, Y. Peng, N. Kent Dalley, J. F. Cannon, M. A. Peterson, *Tetrahedron Lett.* **2004**, *45*, 3621.
- ¹¹² K. J. Kilpin, U. S. D. Paul, A.-L. Lee, J. D. Crowley, *Chem. Commun.* **2011**, *47*, 328.
- ¹¹³ C. Tubaro, D. Bertinazzo, M. Monticelli, O. Saoncella, A. Volpe, M. Basato, D. Badocco, P. Pastore, C. Graiff, A. Venzo, *Eur. J. Inorg. Chem.* **2014**, 1524.
- ¹¹⁴ A. A. D Tulloch, A. A. Danapoulos, S. Winston, S. Kleinhenz, G. Eastham, *G. J. Chem. Soc., Dalton Trans.* **2000**, 4499.

- ¹¹⁵ J. Berding, H. Kooijman, A. L. Spek, E. Bouwman, *J. Organomet. Chem.* **2009**, 694, 2217.
- ¹¹⁶ P. De Fremont, N. M. Scott, E. D. Stevens, T. Ramnial, O. C. Lightbody, C. L. B. Macdonald, J. A. C. Clyburne, C. D. Abernethy, S. P. Nolan, *Organometallics* **2005**, 24, 6301.
- ¹¹⁷ M. Monticelli, C. Tubaro, M. Baron, M. Basato, P. Sgarbossa, C. Graiff, G. Accorsi, T. P. Pell, D. J. D. Wilson, P. J. Barnard, *Dalton Trans.* **2016**, 45, 9540.
- ¹¹⁸ Y. Zhang, C. Chen, S. C. Ghosh, Y. Li, S. H. Hong, *Organometallics* **2010**, 29, 1374.
- ¹¹⁹ a) E. Mas-Marzá, J. A. Mata, E. Peris, *Angew. Chem. Int. Ed.* **2007**, 46, 3729. c) M. T. Zamora, M. J. Ferguson, R. McDonald, M. Cowie, *Organometallics* **2012**, 31, 5463.
- ¹²⁰ M. V. Baker, P. J. Barnard, S. J. Berners-Price, S. K. Brayshaw, J. L. Hickey, B. W. Skelton, A. H. White, *Dalton Trans.* **2006**, 3708.
- ¹²¹ G. Dahm, C. Bailly, L. Karmazin, S. Bellemin-Laponnaz, *J. Organomet. Chem.* **2015**, 794, 115.
- ¹²² W. Liu, R. Gust, *Coord. Chem. Rev.* **2016**, 329, 191.
- ¹²³ a) M. L. Teyssot, A. S. Jarrouse, M. Manin, A. Chevry, S. Roche, F. Norre, C. Beaudoin, L. Morel, D. Boyer, R. Mahiou, A. Gautier, *Dalton Trans.* **2009**, 6894. b) L. Eloy, A.-S. Jarrouse, M.-L. Teyssot, A. Gautier, L. Morel, C. Jolival, T. Cresteil, S. Roland, *ChemMedChem*. **2012**, 7, 805.
- ¹²⁴ M. Skander, P. Retailleau, B. Bourri, L. Schio, P. Mailliet, A. Marinetti, *A. J. Med. Chem.* **2010**, 53, 2146.
- ¹²⁵ S. J. Tan, Y. K. Yan, P. P. Lee, K. H. Lim, *Future Med. Chem.* **2010**, 2, 1591.
- ¹²⁶ M. V. Baker, P. J. Barnard, S. J. Berners-Price, S. K. Brayshaw, J. L. Hickey, B. W. Skelton, A. H. White, *J. Organomet. Chem.* **2005**, 690, 5625.
- ¹²⁷ H. J. Lhasen, *Burns*, **2000**, 26, 117.
- ¹²⁸ Y. Li, G.-F. Liu, C.-P. Tan, L.-N. Ji, Z.-W. Mao, *Metallomics* **2014**, 6, 1460.
- ¹²⁹ A. Levina, A. Mitra, P. A. Lay, *Metallomics* **2009**, 1, 458.
- ¹³⁰ F. Schmitt, K. Donnelly, J. K. Muenzner, T. Rehm, V. Novohradsky, V. Brabec, J. Kasparkova, M. Albrecht, R. Schobert, T. Mueller, *J. Inorg. Biochem.* **2016**, 163, 221.
- ¹³¹ D. C. F. Monteiro, R. M. Phillips, B. D. Crossley, J. Fielden, C. E. Willans, *Dalton Trans.* **2012**, 41, 3720.

- ¹³² F. Hackenberg, H. Müller, R. Smith, W. Streciwilk, X. Zhu, M. Tacke, *Organometallics* **2013**, *32*, 5551.
- ¹³³ P. J. Barnard, S. J. Berners-Price, *Coord. Chem. Rev.* **2007**, *251*, 1889.
- ¹³⁴ I. Ott, *Coord. Chem. Rev.* **2009**, *253*, 1670.
- ¹³⁵ a) S. Gu, H. Xu, N. Zhang, W. Chen, *Chem. Asian J.* **2010**, *5*, 1677. b) A. Hospital, C. Gibard, C. Gaulier, L. Nauton, V. Théry, M. El-Ghozzi, D. Avignat, F. Cisnetti, A. Gautier, *Dalton Trans.* **2012**, *41*, 6803. c) D. Yuan, H. V. Huynh *Organometallics*, **2014**, *33*, 6033. d) M. Hollering, M. Albrecht, F. E. Kühn *Organometallics* **2016**, *35*, 2980.
- ¹³⁶ S. Warsink, R. M. Drost, M. Lutz, A. L. Spek, C. J. Elsevier, *Organometallics* **2010**, *29*, 3109.
- ¹³⁷ S. S. Khan, J. Liebscher, *Synthesis* **2010**, *15*, 2609.
- ¹³⁸ a) A. Poulain, D. Canseco-Gonzalez, R. Hynes-Roche, H. Müller- Bunz, O. Schuster, H. Stoeckli-Evans, A. Neels, M. Albrecht, *Organometallics* **2011**, *30*, 1021. b) A. Prades, E. Peris, M. Albrecht, *Organometallics* **2011**, *30*, 1162. c) P. Mathew, A. Neels, M. Albrecht, *J. Am. Chem. Soc.* **2008**, *130*, 13534. d) T. Karthikeyan, S. Sankararaman, *Tetrahedron Lett.* **2009**, *50*, 5834. e) S. Hohloch, C.-Y. Su, B. Sarkar, *Eur. J. Inorg. Chem.* **2011**, 3067. f) R. Saravanakumar, V. Ramkumar, S. Sankararaman, *Organometallics* **2011**, *30*, 1689.
- ¹³⁹ C. Mejuto, G. Guisado-Barrios, D. Gusev, E. Peris, *Chem. Commun.* **2015**, *51*, 13914.
- ¹⁴⁰ S. Sluijter, Multidentate di-N-heterocyclic carbene ligands for transition metal catalyzed hydrogenation reactions, PhD thesis, University of Amsterdam, 18th September 2015.
- ¹⁴¹ P. J. Barnard, M. V. Baker, S. J. Berners-Price, B. W. Skelton, A. H. White, *Dalton Trans.* **2004**, 1038.
- ¹⁴² (a) A. Liu, X. Zhang, W. Chen, H. Qiu, *Inorg. Chem. Commun.* **2008**, *11*, 1128. (b) R. Frañkel, J. Kniczek, W. Ponikwar, H. Nöth, K. Polborn, W. P. Fehlhammer, *Inorg. Chim. Acta* **2001**, *312*, 235.
- ¹⁴³ a) J. R. Wright, P. C. Young, N. T. Lucas, A.-L. Lee, J. D. Crowley, *Organometallics* **2013**, *32*, 7065. b) D. Canseco-Gonzalez, A. Petronilho, H. Mueller-Bunz, K. Ohmatsu, T. Ooi, M. Albrecht, *J. Am. Chem. Soc.* **2013**, *135*, 13193.

- ¹⁴⁴ (a) G. Buscemi, M. Basato, A. Biffis, A. Gennaro, A. A. Isse, M. M. Natile, C. Tubaro, *J. Organomet. Chem.* **2010**, 695, 2359. (b) S. Ahrens, A. Zeller, M. Taige, T. Strassner, *Organometallics* **2006**, 25, 5409. (c) A. M. Magill, D. S. McGuinness, K. J. G. Cavell, J. P. Britovsek, V. C. Gibson, A. J. P. White, D. J. Williams, A. H. White, B. W. Skelton, *J. Organomet. Chem.* **2001**, 617–618, 546.
- ¹⁴⁵ a) P. Pinter, A. Biffis, C. Tubaro, M. Tenne, M. Kaliner, T. Strassner, *Dalton Trans.* **2015**, 44, 9391. b) D. Munz, A. Poethig, A. Tronnier, T. Strassner, *Dalton Trans* **2013**, 42, 7297.
- ¹⁴⁶ R. Saravanakumar, V. Ramkumar, S. Sankararaman, *Organometallics* **2011**, 30, 1689.
- ¹⁴⁷ H. V. Huynh, R. Jothibas, *J. Organomet. Chem.* **2011**, 696, 3369.
- ¹⁴⁸ J. R. Wright, P. C. Young, N. T. Lucas, A.-L. Lee, J. D. Crowley, *Organometallics* **2013**, 32, 7065.
- ¹⁴⁹ C. Tubaro, A. Biffis, M. Basato, F. Benetollo, K. J. Cavell, L.-I. Ooi, *Organometallics* **2005**, 24, 4153
- ¹⁵⁰ U. Plaia, H. Stolzenberg, W.P. Fehlhammer, *J. Am. Chem. Soc.* **1985**, 107, 2171.
- ¹⁵¹ F. E. Hahn, M. Tamm, *J. Organomet. Chem.* **1993**, 456, 11.
- ¹⁵² F. E. Hahn, M. Tamm, T. Lügger, *Angew. Chem. Int. Ed. Engl.* **1994**, 33, 1356.
- ¹⁵³ F. E. Hahn, M. Tamm, *Chem. Commun.* **1995**, 569.
- ¹⁵⁴ F. E. Hahn, M. Tamm, *Organometallics* **1995**, 14, 2597.
- ¹⁵⁵ U. Kernbach, T. Lügger, F. E. Hahn, W.P. Fehlhammer, *J. Organomet. Chem.* **1997**, 541, 51.
- ¹⁵⁶ M. Tamm, F. E. Hahn, *Coord. Chem. Rev.* **1999**, 182, 175.
- ¹⁵⁷ R. Fränkel, U. Kernbach, M. Bakola-Christianopoulou, U. Plaia, M. Suter, W. Ponikwar, H. Nöth, C. Moinet, W. P. Fehlhammer, *J. Organomet. Chem.* **2001**, 617-618, 530.
- ¹⁵⁸ W. P. Fehlhammer, M. Fritz, *Chem. Rev.* **1993**, 93, 1243.
- ¹⁵⁹ S. Bellemin-Lapponnaz, *Polyedron* **2010**, 29, 30.
- ¹⁶⁰ E. Despagnet-Ayoub, K. Miqueu, J.-M. Sotiropoulos, L. M. Henling, M. W. Day, J. A. Labinger, J. E. Bercaw, *Chem. Sci.* **2013**, 4, 2117.
- ¹⁶¹ A. Dei, D. Gatteschi, C. Sangregorio, L. Sorace, M. G. F. Vaz, *Inorg. Chem.* **2003**, 42, 1701.

- ¹⁶² K. S. Min, T. Weyhermuller, E. Bothe, K. Wieghardt, *Inorg. Chem.* **2004**, *43*, 2922.
- ¹⁶³ P. Steffanut, C. Romain, S. Dagorne, S. Bellemin-Laponnaz, EP., 794041, 2011.
- ¹⁶⁴ SMART Software User Guide, Version 5.1, Bruker Analytical X-ray Systems, Madison, WI, **1999**; SAINT Software User Guide, Version 6.0, Bruker Analytical X-ray Systems, Madison, WI, **1999**; G. M. Sheldrick, SADABS, Bruker Analytical X-ray Systems, Madison, WI, **1999**; APEX II Software User Guide, SAINT, version 7.06a, SADABS, version 2.01, Bruker AXS Inc., Madison, WI, **2008**.
- ¹⁶⁵ G. M. Sheldrick, *Acta Crystallogr., Sect. A: Found. Crystallogr.* **2008**, *64*, 112.
- ¹⁶⁶ J. C. De Mello, H. F. Wittmann, R. H. Friend, *Adv. Mat.* **1997**, *9*, 230.
- ¹⁶⁷ H. Jin, T. S. Y. Tan, F. E. Hahn, *Angew. Chem. Int. Ed.* **2015**, *54*, 13811.
- ¹⁶⁸ (a) A. A. Tolmachev, A.A. Yurchenko, A. S. Merculov, M. G. Semenova, E. V. Zarudnitskii, V. V. Ivanov, A. M. Pinchuk, *Heteroat. Chem.* **1999**, *10*, 585. b) P. C. Kunz, G. J. Reiß, W. Frank, W. Kläui, *Eur. J. Inorg. Chem.* **2003**, 3945.
- ¹⁶⁹ G. Kim, S. Kang, R. Keum, M. J. Seo, *Synth. Commun.* **1999**, *29*, 507.
- ¹⁷⁰ K. S. Min, T. Weyhermuller, E. Bothe, K. Wieghardt, *Inorg. Chem.* **2004**, *43*, 2922.
- ¹⁷¹ a) A. Dei, D. Gatteschi, C. Sangregorio, L. Sorace, M. G. F. Vaz, *Inorg. Chem.* **2003**, *42*, 1701. b) S. Mukherjee, T. Weyhermüller, E. Bothe, K. Wieghardt, P. Chaudhuri, *Dalton Trans.* **2004**, 3842.

NOVEL DI(N-HETEROCYCLIC CARBENE)
LIGANDS AND RELATED TRANSITION METAL
COMPLEXES

Résumé

Le travail de thèse, en co-tutelle entre l'Université de Padoue et l'Université de Strasbourg, se concentre sur la chimie des carbènes bis-(N-hétérocycliques) et peut être divisé en quatre familles de ligands qui constituent les quatre chapitres du manuscrit:

- i) complexes métalliques de Cu(I), Ag(I), Au(I), Ir(III) et Ru(II) avec des ligands di(carbène N-hétérocyclique) portant un pont phénylène rigide entre les unités carbéniques;
- ii) complexes métalliques de Cu(I), Ag(I), Au(I) et Ru(II) combinant un ligand NHC fonctionnalisé avec un triazole dans la position 5 du squelette;
- iii) complexes métalliques d'Ag(I), Au(I) et Pd(II) avec des ligands hétéroditopiques à base d'un imidazol-2-ylidène et d'un 1,2,3-triazol-5-ylidène reliés par un pont propylène;
- iv) proligands bis (benzoxazoles) et les tentatives de complexation sur des métaux de transition.

Mots-clés: Chimie organométallique, réactivité, Carbène N-Hétérocyclique, métaux de transition, application en luminescence.

Résumé en anglais

The PhD, a collaboration between the University of Padova and the University of Strasbourg, is focused on the chemistry of di(N-heterocyclic carbene) ligands and can be divided in four families of ligands that constitute the four chapters:

- i) metal complexes (Cu(I), Ag(I), Au(I), Ir(III), Ru(II)) with di(N-heterocyclic carbene) ligands bearing a rigid phenylene bridge between the carbene units;
- ii) metal complexes (Cu(I), Ag(I), Au(I), Ru(II)) combining an imidazole-based NHC ligand functionalized with a triazole in the 5 position of the backbone;
- iii) metal complexes (Ag(I), Au(I), Pd(II)) with heteroditopic ligands based on imidazol-2-ylidene and 1,2,3-triazol-5-ylidene moieties connected with a propylene bridge;
- iv) bis(benzoxazolium) proligands and attempted synthesis of related transition metal complex

Keywords: organometallic chemistry, reactivity, N-Heterocyclic carbenes, transition metals, applications in luminescence.